I, Nerida Fay Ellerton, nee Gersch, hereby give my consent to make available for loan one copy of my thesis (submitted for the degree of Doctor of Phil which is deposited in the Library. I also consent my thesis to be available for photocopying.

26th June, 1966.

THE INTERACTION OF AMINOACRIDINES AND AMINOBENZACRIDINES WITH DNA.

29-11-66

MERIDA FAY GERSCH, B.Sc.

[Elliston]

THE INTERACTION OF AMINOACRIDINES AND AMINOBENZACRIDINES WITH DNA.

- - - - - - - - - - -

Thesis for the degree of Doctor of Philosophy

in

The University of Adelaide

Department of Physical and Inorganic Chemistry.

- - - - - - - - - - -

Typewritten ms.

Adelaide

1966

CONTENTS.

SUMMARY.

The thesis is concerned with the mechanism and extent of binding of heterocyclic bases (aminoacridines and aminobenzacridines) to DNA and with the extent and cause of the consequential stabilisation of the DNA double helix.

The binding curves for several DNA-aminoacridine and DNA-aminobenzacridine systems have been found using the techniques of spectrophotometry and equilibrium dialysis. It is evident that the equilibrium constant for the reaction DNA + dye → DNA-dye depends on the nature of the dye. The binding is also markedly dependent on ionic strength and temperature. The thermal denaturation of several DNA-aminoacridine and DNA-aminobenzacridine systems has been studied, the increase in the thermal denaturation temperature depending on the system under consideration for a given amount of heterocyclic base bound. The viscosities of several such systems have also been found to increase above that of native DNA.

The observed properties of the DNA-dye systems are discussed in terms of both the intercalated model involving the intercalation of a dye molecule

between two base pairs of the DNA, and the model involving external edgewise attachment of the dye to DNA.

Free energy calculations have been made on the basis of these two models for the DNA-proflavine complex. The total free energy thus found is less (i.e. more negative) for both models than that found by De Voe and Tinoco for native DNA.

In order to extend these calculations to the interaction of other related dyes with DNA, LCAO molecular orbital calculations were carried out for both the charged and uncharged forms of aminobenz[a]-, [b]-, and [c]-acridine and for the charged aminoacridines. From the charge distribution of these molecules it was possible to find their theoretical dipole moment vectors. Correlations of several physical properties of these molecules with various calculated quantities are presented.

It is concluded that the observed properties of the various DNA-aminoacridine and DNA-aminobenzacridine complexes are best explained in terms of the intercalated model.

To the best of my knowledge and belief, this thesis contains no material previously published or written by another person, nor any material previously submitted for a degree or diploma in any University, except where due reference is made in the text.

ACKNOWLEDGEMENTS.

I wish to express my appreciation to my supervisor, Professor D. O. Jordan, for his guidance and assistance throughout the course of this work. On several occasions, I have also been indebted to Dr. T. Kurucsev and Mr. M. L. Martin, as well as to Mrs. R. E. O. Kelly, for helpful discussions and suggestions.

In addition I would like to thank Mr. P.Rapp for performing the sedimentation runs, and the glass-blowing and workshop staffs for constructing several pieces of apparatus used in this work.

The gift of aminoacridines and aminobenzacridines from Professor A. Albert of the Department of Medical Chemistry, the Australian National University, and the gift of 3-aminoacridine from Dr. G. Chandler of the Organic Chemistry Department of the University of Adelaide, are gratefully acknowledged.

I would like to thank my fiancé, David, for his help in preparing the thesis diagrams and tables, and for convincing me that I should continue working although others were publishing concurrently in the same field.

I gratefully acknowledge the financial assistance provided by a Commonwealth Scientific and Industrial Research Organization Senior Postgraduate Studentship.

N. F. G.

Department of Physical and
Inorganic Chemistry,
University of Adelaide.

February, 1966

LIBRARY OF THE UNIVERSITY OF ADELAIDE

CHAPTER 1.

INTRODUCTION. *

One of the first discoveries in the field of the interaction of nucleic acids with basic heterocyclic dyes was that of histological staining as performed by Ehrlich over eighty years ago. With toluidine blue for example, the nucleic acid of the cytoplasm stained blue while certain substances such as chrondoitin sulphate in the tissue stained purple.[1] The change in colour from blue to purple was termed 'metachromasia'. The techniques of differential tissue staining using the metachromatic effect with acridine orange, for example, have wide applications today.[2,3]

Before the Watson and Crick structure for DNA [4] had been proposed, many difficulties were encountered in the interpretation of the interaction of basic dyes with nucleic acids both *in vivo* and *in vitro*. The pH effects of proflavine binding to DNA [5] and the different spectral properties of the RNA-dye

---

* The structures of the various dyes mentioned in this thesis are shown (in alphabetical order) in Appendix 1.

complex compared with those of the DNA-dye complex[5] may now be easily interpreted in terms of the denaturation of DNA and the different tertiary structures, respectively. It was hoped to elucidate the structure of the nucleic acid by means of dye binding studies[6]. From spectrophotometric studies, Michaelis concluded that nucleic acid destroyed the dye aggregates thought to exist in solution.[6] Although for such a conclusion, his studies were not extended over a sufficient concentration range of nucleic acid and dye, it is of considerable interest to quote his suggestion as to the structure of the nucleic acid-dye complex, written in 1947.

"Nucleic acid, whether of high or low molecular weight, may be imagined to consist of strings or bundles of nucleotides arranged in such a way that the pyrimidine and purine rings lie parallel to each other, connected by phosphate groups; the dye molecules attached to the negatively charged end of the phosphate group. Each dye cation combined with one phosphate group must lie in the space between the planes of the pyrimidine or purine rings, and so they are prevented from approaching each other in such a way as to interfere optically

with each other and from exhibiting the spectrum of a higher dyestuff aggregate."

In 1951, Oster suggested that the flat acridine ring of acriflavine may fit between the purine and pyrimidine rings of the DNA molecule, normal to the helix axis, with the quaternary nitrogen of the dye associated with the primary phosphoric acid groups of the DNA.[7] This model was also proposed by Heilweil and Van Winkle in 1955.[8] Two types of linkage, polar and non-polar, were postulated for the DNA-dye complex,[9] the non-polar linkages being responsible for the metachromatic effect observed.

In many studies, the interaction between DNA and basic dyes has been described in terms of two distinct binding processes[10] originally thought to arise from binding to primary and secondary phosphoric acid residues.[11,12] This possibility may be rejected, both on the grounds of the unrealistic relative numbers of the secondary sites[13] and of studies at several pH values.[14] The two binding processes, the first, a strong interaction up to a ratio, r , of dye bound per atom of nucleic acid phosphorus of about 0.2, and the second, a weaker interaction up to a value of r = 1.0,

in the case of DNA-proflavine, may be interpreted in terms of the binding of monomeric dye cations and aggregates of dye cations, respectively.[13] Van der Waals interactions between the planar purine bases and the dye cations are important, in addition to the electrostatic interactions.[8,13]

A statistical theory of aggregation of dye cations to DNA provides a simple explanation for the spectral effects observed.[15,16,17]

The models involving interaction between the planar bases of the DNA molecule and the planar dye cation[6,7,8] are not compatible with the Watson-Crick model for DNA as the bases in native DNA are in close Van der Waals contact. However, Lerman[18] suggested that if the DNA molecule was extended, the dye cations could be intercalated between successive base pairs. This change in configuration of DNA altered the viscosity[18,19], the sedimentation coefficient[18] as well as the X-ray diffraction pattern[20], the flow dichroism[21], the amino group reactivity of the aminoacridine[22], and the apparent length of the DNA-aminoacridine complex.[23] The observed modifications of these properties may be interpreted in terms of the intercalated model. However

this model does not appear to be completely compatible with the observed optical rotatory dispersion of the DNA-aminoacridine complex.[24,25] A model in which the acridine rings partially interact with the DNA base rings rather than complete intercalation of the cations between the base pairs may be more consistent with the observed properties of the complex.[26]

In view of the conflicting models of intercalation[18-22], of external edgewise binding[15-19, 24] and of the intermediate case of partial interaction[26] proposed, additional evidence supporting the first model, obtained from free energy calculations for several DNA-aminoacridine systems considering each of the models, and experimental data on the thermal denaturation, the viscosity and the sedimentation coefficients for DNA-aminoacridine and DNA-aminobenzacridine complexes will be presented.

The mutagenic action of several of the acridines[27,28] may be explained in terms of the intercalated model. The base pairing between two paired chromosomes will be out-of-register for some distance if intercalation of an acridine molecule occurs in one chromosome but not at the same place in the other.

This mechanism illustrates how insertion and deletion mutations may occur if the chromosomes break at the same position and reunite with exchange of partners.[21] This theory is a modification of that based on the intercalation of an acridine into a single strand of the DNA double helix.[27]

The antibacterial properties of the acridines[29] have also been studied with reference to the structure of the DNA-acridine complex, a loss of antibacterial activity being associated with a loss of ability to bind strongly with DNA when the planarity of one or more of the rings is destroyed by hydrogenation.[13,26]

As many benzacridines are known to be carcinogenic[30] and their structure is closely related to that of the carcinogenic polycyclic hydrocarbons, a study of the interaction between charged aminobenzacridines and DNA is significant, as it has been postulated that the reaction of polycyclic hydrocarbons such as benz[a]-anthracene with DNA may also involve intercalation as in the DNA-aminoacridine complex.[31]

References

1. Ehrlich, P., Arch.Anat.Physiol., Physiol.Abt.166 (1879).

2. Robbins, E. and Marcus, P.I., J.Cell Biol.18, 237 (1963).

3. Saunders, A.M., J.Histochem.Cytochem.12, 164 (1964).

4. Watson, J.D. and Crick, F.H.C., Nature 171, 737 (1953).

5. Northland, F.W., De Bruyn, P.P.H. and Smith, R.H., Exptl.Cell Research 7, 201 (1954).

6. Michaelis, L., Cold Spr.Harb.Symp.Quant.Biol.12, 131 (1947).

7. Oster, G., Trans.Faraday Soc.47, 660 (1951).

8. Heilweil, H.G. and Van Winkle, Q., J.Phys.Chem.59, 939 (1955).

9. Weismann, K., Carnes, W.H., Rubin, P.S. and Fisher,J., J.Am.Chem.Soc.74, 1423 (1952).

10. Steiner, R.F. and Beers, R.F., "Polynucleotides", Elsevier, Amsterdam (1961).

11. Cavalieri, L.F. and Angelos, A., J.Am.Chem.Soc.72, 4686 (1950).

12. Cavalieri, L.F., Angelos, A. and Balis, M.E., J.Am.Chem.Soc.73, 4902 (1951).

13. Peacocke, A.R. and Skerrett, J.N.H., Trans.Faraday Soc.52, 261 (1956).

14. Lawley, P.D., Biochim.Biophys.Acta 19, 160 (1956).

15. Bradley, D.F., Trans.N.Y.Acad.Sci.24, 64 (1961).

16. Bradley, D.F. and Felsenfeld, G., Nature 184, 1920 (1959).

17. Bradley, D.F. and Wolf, M.K., Proc.Nat.Acad.Sci., Wash.45, 944 (1959).

18. Lerman, L.S., J.Mol.Biol.3, 18 (1961).

19. Lerman, L.S., J.Cell.Comp.Physiol.Supp.1, 64, 1 (1964).

20. Luzzati, V., Masson, F. and Lerman, L.S., J.Mol.Biol. 3, 634 (1961).

21. Lerman, L.S., Proc.Nat.Acad.Sci., Wash.49, 94 (1963).

22. Lerman, L.S., J.Mol.Biol.10, 367 (1964).

23. Cairns, J., Cold Spr.Harb.Symp.Quant.Biol.27, 311 (1962).

24. Mason, S.F. and McCaffery, A.J., Nature 204, 468 (1964).

25. Blake, A. and Peacocke, A.R., Nature 206,1009 (1965).

26. Drummond, D.S., Simpson-Gildemeister, V.F.W. and Peacocke,A.R. Biopolymers 3, 135 (1965).

27. Brenner, S., Barnett, L., Crick, F.H.C. and Orgel, A., J.Mol.Biol.3, 121 (1961).

28. Orgel, A. and Brenner, S., J.Mol.Biol.3, 762 (1961).

29. Albert, A., "The Acridines", Edward Arnold and Co., London (1951).

30. Buu-Hoi, N.P., Zajdela, F., Roussel, O. and Petit,L. Bull. Cancer 52, 49 (1965).

31. Boyland, E., British Med.Bull.,20, 121 (1964).

CHAPTER 2.

THEORETICAL CONSIDERATIONS OF DNA.

2.1 Introduction.

The extinction coefficient for native DNA at 2600 Å is about 30 - 40 per cent less than that of denatured DNA or that of its constitutent nucleotides.[1-4] This is the hypochromic effect, and has been used to study the transition from a native to a denatured state for DNA and for other polynucleotides by following the increase in optical density with temperature,[5-7] with temporary extremes of pH,[1,2,6-8] with high concentrations of urea[9] and with decrease in the ionic strength of the solution.[6,7,10] In addition to the hypochromic effect, different optical rotatory dispersion curves are observed for native and denatured DNA[11] and for native and denatured RNA.[12]

It is evident that both of these effects may be associated with the tertiary structure of DNA which is partially disrupted by denaturation and completely destroyed when hydrolysed to nucleotides, the hypochromism partially disappearing on denaturation and fully disappearing on hydrolysis. The hypochromism exhibited by a single stranded polynucleotide may be attributed to the interaction between adjacent bases

along the randomly coiled chain. However a highly ordered structure such as that of native DNA permits greater interactions between bases along each of the polynucleotide chains, and, in addition, interactions occur between the bases of each base pair, perpendicular to the helix axis. In the ideal case of complete denaturation and strand separation of the DNA double helix, only the interactions between adjacent bases along the single chains remain, while those between the bases of each base pair are no longer present. Thus some hypochromism remains on denaturation of DNA. However, complete strand separation of DNA only occurs for certain types of DNA under specified conditions of denaturation. Therefore, in general, because some base pairs remain or are reformed after denaturation, interactions between the bases of some base pairs occur in denatured DNA, in addition to the interaction between adjacent bases, as in the ideal case above and both interactions give rise to the residual hypochromism observed.

The per-cent hypochromicity of a 1:1 helical complex of long lengths of polyriboadenylic acid and short lengths of polydeoxyribothymidylic acid may be

related to the chain length of the polydeoxyribothymidylic acid oligomers.[13] It is found experimentally that the smallest thymine polymer to exhibit hypochromism has 7 residues, but only shows the same per-cent hypochromicity as predicted for two set of base pairs. Similar results are obtained for longer polymers, implying that each polynucleotide has approximately 2 or 3 loose residues at each end which do not give rise to hypochromism.[13] That the interaction between adjacent base pairs in the DNA helix contributes to the hypochromic effect[14] is supported by evidence of a restricted rotation about the internucleotide linkages for the small polynucleotides di-, tri- and tetra-adenylic acids.[15] Such interactions between adjacent ring systems have been attributed to permanent dipole interactions[16] and to π-bonding[4,17]. The hyperchromic effect observed on the denaturation of DNA has also been attributed to an increase in the effective chromophoric area of the purine and pyrimidine ring systems.[18]

The first quantitative explanations to the phenomenon of hypochromism were given by Tinoco[19] and Rhodes[20] while the theory of optical rotatory

dispersion for a polymer was originally developed by Kirkwood.[21] These and other theories of hypochromism and optical rotatory dispersion will be discussed in section 2.2 .

In addition to the two optical problems already mentioned, some understanding of the forces which govern the stability of the configurations of DNA is desirable for an interpretation of the properties of DNA solutions. De Voe and Tinoco[22] have estimated the stability of a double stranded helical polynucleotide relative to constituent single strands in the random coil configuration by calculating the free energies of both the helix and the random coil. The problems of hypochromism and optical rotation, and stability of the helix of DNA are inter-related since the former two phenomena owe their occurrence to the latter.

2.2 Theory of Hypochromism and Optical Rotatory Dispersion.

Tinoco[19,23] has ascribed hypochromism in polynucleotides to the coulombic interactions between electrons of different bases, and has considered only induced dipole-induced dipole interactions, as also has Rhodes.[20] A conclusion from these calculations was that hypochromism in polynucleotides is mainly due to the 2600 Å band losing intensity to the 2000 Å band and to other $\pi \rightarrow \pi^*$ transitions. This is partly supported by the far ultraviolet spectra of native and denatured DNA which indicate that the integrated intensity of the 1850 Å band may increase only slightly or decrease upon denaturation of DNA.[24] As these spectra were measured to 1830 Å only, no definite conclusions about the integrated intensity of the 1850 Å band may be drawn until further experimental work is conducted below 1830 Å . In addition to the simple hypochromic effect at 2600 Å , there is a slight increase in intensity on the extreme long wavelength side between 2800 and 2900 Å where there is thought to be an $n \rightarrow \pi^*$ band.[25] In their calculations, Tinoco[19,23] and Rhodes[20] have included only the effect of mixing

the 2000 Å and 2600 Å $\pi \rightarrow \pi^*$ transitions. Rhodes[26] has extended his calculations by using third order perturbation theory in order to include $\pi \rightarrow \pi^*$ and $n \rightarrow \pi^*$ mixing. The importance of including the $n \rightarrow \pi^*$ transition has also been discussed by Kasha, El-Bayoumi and Rhodes[27] and by De Voe.[28]

A 'second quantization' technique may be used to calculate the hypochromic effect in polynucleotides.[29] For a perfect one-dimensional aggregate, the perturbation theory of Tinoco[19,23] and of Rhodes[20,26] and the results obtained from the 'second quantization' method[29] are in good agreement. However, both theories neglect net dipole moments and multiple dispersion forces. These assumptions are probably more serious than the differences between the theories.[30]

In the model adopted by Bolton and Weiss[31,32] to explain the hypochromism of polynucleotides, the transition moments were replaced by classical electron oscillators. This method of explaining the hypochromic effect has been criticized[33] on the grounds that it disobeys the Kuhn-Thomas sum rule[34] for oscillator strengths. However, a sum rule for integrated intensities does not seem to be generally true, and may be

proved only under well defined conditions including infinite dilution and identical finite or zero bandwidths.[35] In addition, it has been shown that the theory proposed by Bolton and Weiss[31] is that of the strong interaction case of a theory equivalent to semi-classical dispersion theory.[36] Although there are discrepancies between the static exciton theory proposed by Nesbet[37] and the theory put forward by Bolton and Weiss[31] and extended by Nesbet[36], when the case of a single absorption line is considered, the energy shift computed[36] corresponds to that predicted by the static exciton theory. Thus it appears that the latter theory[31,36] contains the more complete description of the intermolecular interactions. Furthermore, the latter theory predicts that there is no change in the position of the absorption maximum on denaturation of the polynucleotide, in agreement with experimental results.

By considering a single base pair, with no contributions from the remainder of the helix or from the solvent, large hypochromic effects may be predicted.[38] The calculations involved the use of self-consistent molecular orbital theory and have

the advantage that no dipole approximations are used. The off-resonance (static exciton) theories of Tinoco[19,23], of Rhodes[20] and of De Voe and Tinoco[39] and the on-resonance theory of Bolton and Weiss[31] can be shown to be complementary as they come from real and imaginary parts, respectively, of a complex polarizability function.[38,40]

It has been predicted[39] that the hypochromic effect would be greatest for DNA with a high guanine-cytosine content. However, experimental measurements indicate[4,9,41,42] that hypochromism increases with increasing adenine-thymine content. The calculations used for this prediction can only be refined by obtaining more information on the spectra of the bases below 2000 Å.[39]

To summarize the present position with regard to the theory of hypochromism, it seems that, although there appeared to be conflict between the original theory of hypochromism put forward by Tinoco[19,23] and by Rhodes,[20] and the formalism of Bolton and Weiss,[31] they are now regarded as compatible.[38,40,43] A more exact approach to the problem, including factors of dispersive refractive index and multiple scattering

terms, has recently been given,[35] and includes the original theories mentioned earlier as specific terms in a generalized treatment of the problem.

Although several features of the theory of hypochromism, including the residual hypochromism observed on denaturation of DNA and the contribution of the solvent to the hypochromism, have been discussed[28], they have not been analysed in detail. In particular, the latter effect warrants some attention, as the majority of theories of hypochromism to date refer only to conditions in *vacuo*, and do not take into account the fact that if the hypochromic effect is studied in solution, the macroions are surrounded by solvent molecules, and if studied in the solid state, water molecules are adsorbed by DNA to an extent depending on the relative humidity.[44] Some experimental solvent effects on the hypochromism of the 2600 Å band of isotactic polystyrene have indicated that a theoretical consideration of such effects is necessary for the interpretation of experimental data.[45]

In addition, it is evident that more experimental work in the far ultraviolet region below 1830 Å

is necessary to enable more complete comparisons between theory and experiment to be drawn. Further study of simple oligonucleotides would also be pertinent to the problem.

In contrast to hypochromism, no conflict between theories arises in the case of optical rotatory dispersion.[21,46-48] The rotational strength of a polymer may be interpreted on the basis of two terms, one from the intrinsic strengths of the individual residues and the other from the coupling between them. Circular dichroism of polypeptides[49] may be interpreted on the basis of the second term.

Theories which permit the calculation of any optical property of a polynucleotide[50-52] and which include the dependence of the optical properties on chain length[53] have been developed recently. As all optical properties of a polynucleotide are closely related, it would therefore seem desirable to find the correct electronic wave function for the molecule, thereby enabling any optical property to be calculated. However discretion must be used in this procedure, as the wave functions available from the use of present theories are, at best, approximations only.

2.3 The Stability of the Helical Configuration of DNA.

The original model for the structure of DNA[54] consists of two single, complementary polynucleotide chains held together by hydrogen bonds between the purine and pyrimidine bases. It is these hydrogen bonds between each base pair and Van der Waals forces between the adjacent base pairs that are generally considered to be responsible for the stability of the native DNA helical structure. Hence if the forces between the bases in the native DNA helix and the free energy of formation of the helix can be estimated, a basis is given for an understanding of the stability of the helical configuration of DNA.

Calculations for the free energy of nearest neighbour base-pair interactions indicate that different base sequences give rise to different free energies of interaction.[22] There are several approximations in this theory, including the neglecting of base-solvent interaction and the fact that the calculations are carried out for conditions in vacuo with a dielectric constant of unity whereas the effect of a solvent is such as to increase the dielectric constant depending upon the type of interaction under

consideration.[22] Further approximations are introduced by considering point dipole moments rather than point monopoles,[22,55,56] and by neglecting the entropy term produced by the solvation of the macro-ion.[56] However the comparison of the free energy of interaction for a given base sequence with that of another is acceptable to a first approximation for qualitative purposes.

The interaction of the charged planar amino-acridines with native DNA has been interpreted in terms of two models, one involving the intercalation of an aminoacridine ion between adjacent base pairs of the DNA helix[57,58] and the other involving external edgewise attachment of the dye to the phosphate groups.[59,60] The forces stabilizing these two models will differ according to the environment of the dye ions. In the former model, forces similar to those considered by De Voe and Tinoco[22] in their free energy calculations for DNA would be involved, while solvation effects on the externally attached dye ions will considerably reduce the interactions in the latter model.[61] Both models will include additional

forces arising from the charge on the dye ions. The free energy calculations for native DNA[22] have been extended to the DNA-aminoacridine complex[61] in order to determine which model has the more negative free energy and hence which model is more likely to represent the structure of the complex. As these extended calculations and their applications will be discussed in detail in Chapters 3 and 4, a description of the forces considered and the methods used by De Voe and Tinoco[22] will be given here. Only long range interactions have been considered in the free energy calculations.

The total free energy of interaction between two molecules, charged or uncharged, having permanent and induced dipole moments, is given by

$$F_{total} = F_{ES} + F_{L} \qquad (2.1)$$

where F_{ES} is the electrostatic free energy from interactions between charges, permanent and induced dipoles, and F_{L} is the London energy arising from fluctuation dipole-induced dipole interactions.

The electrostatic free energy of any distribution of charges, dipoles and polarizable groups, relative to infinite seperation, is equal to the work of reversibly discharging the infinitely separated charges and dipoles and reversibly charging them in the final distribution.

F_{ES} may be considered as a total of five interactions:

$$F_{\rho\rho},\ F_{\rho\mu},\ F_{\rho\alpha},\ F_{\mu\mu},\ \text{and}\ F_{\mu\alpha},$$

where ρ, μ and α represent charge, dipole moment and polarizability, respectively. These interactions are given by

$$F_{\rho\rho} = \sum_{i} \sum_{j>i} \frac{\rho_i \rho_j}{\epsilon_{ij} R_{ij}} \tag{2.2}$$

$$F_{\rho\mu} = \sum_{i} \sum_{j\neq i} \frac{1}{\epsilon_{ij}} \rho_i \mu_j C_{i,j} \tag{2.3}$$

$$F_{\mu\mu} = \sum_{i} \sum_{j>i} \frac{1}{\epsilon_{ij}} \mu_i \mu_j B_{i,j} \tag{2.4}$$

$$F_{\mu\alpha} = -\frac{1}{2} \sum_{i} \sum_{j\neq i} \sum_{l=1}^{3} \frac{1}{\epsilon_{ij}} \mu_i^2 \alpha_{jl} G^2_{i,jl} \tag{2.5}$$

$$F_{\rho\alpha} = -\frac{1}{2} \sum_{i} \sum_{j \neq i} \sum_{l=1}^{3} \epsilon_{ij}^{-1} \rho_i^2 \alpha_{jl} C_{i,jl}^2 \qquad (2.6)$$

where

$$C_{i,j} = \frac{1}{R_{ij}} \underline{e}_j \cdot \underline{R}_{ij} \qquad (2.7)$$

$$G_{i,j} = \frac{1}{R_{ij}^2} [\underline{e}_i \cdot \underline{e}_j - \frac{3}{R_{ij}^2} (\underline{e}_i \cdot \underline{R}_{ij}) (\underline{e}_j \cdot \underline{R}_{ij})] \qquad (2.8)$$

for two interacting molecules or ions i and j. The distance vector and the dielectric constant between i and j are denoted by $\underline{R}_{ij}$ and by ϵ_{ij} respectively. In their calculations, De Voe and Tinoco[22] assumed a value of unity for ϵ_{ij}.

In the above equations, α_{jl} is the component of the polarizability along the principal polarization axis l, and $C_{i,j}$ and $G_{i,j}$ (equations 2.7 and 2.8) are geometric factors involving the unit vectors $\underline{e}_i$ and $\underline{e}_j$ of the group dipoles μ_i and μ_j. The components of the molecular polarizability were taken as $\alpha_{11} = \alpha_{12} = 1.2\alpha_i$ along perpendicular directions in the base plane and $\alpha_{13} = 0.6\alpha_i$ in a direction normal to the plane of the molecule. Values of α_i were estimated from values of atomic refractions.[62]

The London energy is given by

$$F_L = -\frac{h}{4} \sum_{i} \sum_{j>i} \sum_{l=1}^{3} \sum_{m=1}^{3} \frac{\nu_i \nu_j}{\nu_i + \nu_j} \frac{\alpha_{il}\alpha_{jm} C^2_{il,jm}}{\epsilon_{ij}} \qquad (2.9)$$

where ν_i is the characteristic frequency. A value for the characteristic energy, $h\nu_i$, may be calculated from experimental values of the dispersion of the refractive index of group i .

Since these calculations require a knowledge of the dipole moment vectors of each molecule considered in the interaction, a method of calculating dipole moments, involving the separate contributions of σ- and π-electrons was developed.[22] A more detailed discussion of the methods of calculation of dipole moments is given in Chapter 3.

Application of equations 2.4, 2.5 and 2.9 to the native DNA helix indicates that the free energy of the helix depends on the base composition and on the sequence of the bases. The free energy calculations also show that London forces are important in determining the stability of the helix, which is found to be proportional to the guanine-cytosine content.[22]

References.

1. Blout, E.R. and Asadourian, A., Biochim.Biophys. Acta 13, 161 (1954).

2. Frick, G., Biochim.Biophys.Acta 8, 625 (1952).

3. Kurnick, N.B., Arch.Biochem. 29, 41 (1950).

4. Laland, S.G., Lee, W.A., Overend, W.G. and Peacocke, A.R., Biochim.Biophys.Acta 14,356 (1954).

5. Doty, P., Boedtker, H., Fresco, J.R., Haselkorn, R. and Litt, M., Proc.Nat.Acad.Sci., Wash. 45, 482 (1959).

6. Thomas, R., Trans.Faraday Soc. 50, 304 (1954).

7. Thomas, R., Biochim.Biophys.Acta 14, 231 (1954).

8. Shack, J. and Thompsett, J.M., J.Biol.Chem. 197, 17 (1952).

9. Warner, R.C., J.Biol.Chem. 229, 711 (1957).

10. Rich, A. and Davies, D.R., J.Am.Chem.Soc., 78, 3548 (1956).

11. Ts'o, P.O.P., Helmkamp, G.K. and Sander, C., Biochim.Biophys.Acta 55, 584 (1960).

12. Haschemeyer, R., Singer, B. and Fraenkel-Conrat, H., Proc.Nat.Acad.Sci.,Wash. 45, 313 (1959).

13. Rich, A. and Tinoco, I., J.Am.Chem.Soc. 82 6409 (1960).

14. Jordan, D.O., "The Chemistry of the Nucleic Acids", Butterworths, London (1960).

15. Michelson, A.M., Nature 182, 1502 (1958).

16. Thomas, R., Bull.Soc.Chim.Biol., Paris 35,609 (1953).

17. Ladik, J., Acta.Phys.Acad.Sci.Hung. 11, 239 (1960).

18. Lawley, P.D., Biochim.Biophys.Acta 21, 481 (1956).

19. Tinoco, I., J.Am.Chem.Soc. 82, 4785 (1960).

20. Rhodes, W., J.Am.Chem.Soc. 83, 3609 (1961).

21. Kirkwood, J.G., J.Chem.Phys. 5, 479 (1937).

22. De Voe, H. and Tinoco, I., J.Mol.Biol. 4, 500 (1962).

23. Tinoco, I., J.Chem.Phys. 33, 1332 (1960); and 34, 1067 (1961).

24. Falk, M., J.Am.Chem.Soc. 86, 1226 (1964).

25. Rich, A. and Kasha, M., J.Am.Chem.Soc. 82, 6197 (1960).

26. Rhodes, W., Radiation Res. 20, 120 (1963).

27. Kasha, M., El-Bayoumi, M.A. and Rhodes, W., J.Chim.Phys. 58, 916 (1961).

28. De Voe, H., Biopolymers Symp. No 1, 251 (1963).

29. Hoffmann, R., Radiation Res. 20, 140 (1963).

30. Sinanoğlu, O. Radiation Res. 20, 149 (1963).

31. Bolton, H.C. and Weiss, J.J., Nature 195, 666 (1962).

32. Weiss, J.J., Nature 197, 1296 (1963).

33. De Voe, H., Nature 197, 1295 (1963).

34. Kauzmann, W., "Quantum Chemistry", Academic Press, N.Y. p 630 (1957).

35. Bullough, R.K. J.Chem.Phys. 43, 1927 (1965).

36. Nesbet, R.K., Mol.Phys. 7, 211 (1963-64).

37. Nesbet, R.K., Mol.Phys. 5, 63 (1962).

38. Nesbet, R.K., Biopolymers Symp. No 1, 129 (1963).

39. De Voe, H. and Tinoco, I., J.Mol.Biol. 4, 518 (1962).

40. Fowler, G.N., Mol.Phys. 8, 383 (1964).

41. Marmur, J. and Doty, P., Nature 183, 1427 (1959).

42. Mahler, H.R., Kline, B. and Mehrotra, B.D., J.Mol.Biol. 9, 801 (1964).

43. McLachlan, A.D. and Ball, M.A., Mol.Phys. 8, 581 (1964).

44. Falk, M., Hartmann, K.A. and Lord, R.C., J.Am.Chem.Soc. 85, 387 (1963).

45. Vala, M.T. and Rice, S.A., J.Chem.Phys. 39, 2348 (1963).

46. Moffitt, W., J.Chem.Phys. 25, 467 (1956).

47. Moffitt, W., Proc.Nat.Acad.Sci.,Wash. 42, 736 (1956).

48. Moffitt, W., Fitts, D.D. and Kirkwood, J.G., Proc. Nat.Acad.Sci.,Wash.43,723 and 1046(1957).

49. Moffitt, W. and Yang, J.T., Proc.Nat.Acad.Sci., Wash. 42, 596 (1956).

50. Tinoco, I., Radiation Res. 20, 133 (1963).

51. Tinoco, I. and Woody, R.W., J.Chem.Phys. 40, 160 (1963).

52. Bradley, D.F., Tinoco, I. and Woody, R.W., Biopolymers 1, 239 (1963).

53. Tinoco, I., Woody, R.W. and Bradley, D.F., J.Chem.Phys. 38, 1317 (1963).

54. Watson, J.D. and Crick, F.H.C., Nature 171, 737 (1953).

55. Bradley, D.F., Lifson, S. and Honig, B., in "Electronic Aspects of Biochemistry", ed. B.Pullman, Academic Press,N.Y.(1964).

56. Sinanoğlu, O. and Abdulnur, S., Fed.Proc.24,S-12(1965).

57. Lerman, L.S., J.Mol.Biol. 3, 18 (1961).

58. Lerman, L.S., Proc.Nat.Acad.Sci.,Wash. 49, 94 (1963).

59. Bradley, D.F. and Wolf, M.K., Proc.Nat.Acad.Sci., Wash. 45, 944 (1959).

60. Mason, S.F. and McCaffery, A.J.,Nature 204,468(1964).

61. Gersch, M.F. and Jordan, D.O., J.Mol.Biol. 13 138 (1965).

62. Fajans, K., in "Techniques of Organic Chemistry", ed. A. Weissberger, Vol. 1, part 2, p 1169, Interscience N.Y. (1959).

CHAPTER 3.

MOLECULAR ORBITAL CALCULATIONS FOR AMINOACRIDINES AND FOR AMINOBENZACRIDINES.

3.1 Introduction.

The indices of electronic structure such as electronic charge, bond orders and energies of the highest filled and lowest empty molecular orbitals, have proved useful in the interpretation of certain physical and in particular, biochemical properties of molecules.[1] For the investigation of the free energy changes involved when charged dye molecules such as aminoacridines interact with DNA, a knowledge of the dipole moments of the dye molecules and of the nucleotides is required.[2,3] The π-dipole moment vector of a given molecule may be obtained from the electronic charge distribution of the molecule,[3,4] this method being particularly useful for charged molecules.

Although the symmetric and antisymmetric stretching frequencies of the aminoacridines and several aminobenzacridines have been reported[5], no correlation has been made between the theoretical bond orders of the C-N(amino) bond obtained from LCAO molecular orbital calculations and the antisymmetric stretching frequencies.

Molecular orbital calculations have therefore

been made for the eleven mono-amino-benz[a]-, -benz[b]- and -benz[c]-acridines both in the protonated and non-protonated forms, and for the protonated mono-amino-acridines, and will be described in this chapter.

3.2 Theory of the LCAO Molecular Orbital Calculations.

Each π-electron of the heterocyclic molecule may be described by an LCAO molecular orbital

$$\phi_i = \sum_r c_{ri} \phi_r \qquad (3.1)$$

giving a set of simultaneous equations

$$\sum_s c_{si}(H_{rs} - E_i S_{rs}) = 0 \qquad (3.2)$$

with one equation for each value of r in equation 3.1.

The solutions c_{si} may be found if E_i satisfies the condition

$$|H_{rs} - E_i S_{rs}| = 0 \qquad (3.3)$$

where

$$H_{rs} = \int \phi_r H \phi_s \, dv \qquad (3.4)$$

and

$$S_{rs} = \int \phi_r \phi_s \, dv \qquad (3.5)$$

and H is the Hamiltonian operator.

The Coulomb and exchange integrals are defined by

$$\alpha_r = \int \psi_r H \psi_r \, dv \qquad (3.6)$$

and

$$\beta_{rs} = \int \psi_r H \psi_s \, dv \qquad (3.7)$$

Using the Huckel approximation,[6] it is assumed that S_{rs} is zero between different atomic orbitals and H_{rs} is neglected for non-bonded atoms. It is also assumed that the atomic orbitals on different atoms are orthogonal.

Since the theory is required for a heterocyclic molecule, the Coulomb integrals, α_r, are given the same value, α, for all carbon atoms, but a different value for each non-carbon atom. Similarly, the resonance integrals, β_{rs}, are given a value, β, for all carbon-carbon bonds, but a different value for carbon-heteroatom bonds.

The Huckel approximation[6] as applied to a heterocyclic molecule gives the set of secular equations,

$$c_{ri}(y + \delta_r) + \sum_{\substack{s \text{ adjacent} \\ \text{to } r}} \eta_{rs} c_{si} = 0 \qquad (3.8)$$

for $r = 1,2,\ldots,n$, which gives the energy values and

the coefficients c_{ri} for each molecular orbital, ϕ_i, of a given conjugated heterocyclic molecule.

The values adopted[1] for the parameters η_{rs} and β_{rs} for the C=N-; C-N- and C$\overset{\oplus}{\text{N}}$- bonds were 1 and 0.4; 0.9 and 1; and 1 and 2, respectively. The eigenvalues and eigenvectors of the resulting matrices were found using Jacobi's diagonalization procedure. The eigenvalues represent the energies of the molecular orbitals and the eigenvectors of each eigenvalue are the coefficients c_{ri}. Thus the π-electronic charge, q_r, associated with the atom r is given by

$$q_r = \sum_i 2(c_{ri})^2 \qquad (3.9)$$

while the net charge on each aton is

$$q_{Net} = 1 - q_r \qquad (3.10)$$

for a one π-electron contributor and

$$q_{Net} = 2 - q_r \qquad (3.11)$$

for a two π-electron contributor.

The bond order, p_{rs}, of the bond rs may be computed from

$$p_{rs} = \sum_i 2c_{ri}c_{si} \qquad (3.12)$$

To compute the resonance energy of a conjugated heterocyclic molecule, three cases must be considered to compute the energy of the localised bonds.

(a) For each localised C=C bond, the energy contribution is

$$E_{Loc} = 2\alpha + 2\beta \qquad (3.13)$$

(b) For each localised C=X bond, the energy contribution is

$$E_{Loc} = 2\alpha + \beta\left[\delta_X + 2\sqrt{\eta_{C=X}^2 + \frac{\delta_X^2}{4}}\right] \qquad (3.14)$$

(c) For each atom Y with a localised lone pair, the energy contribution is

$$E_{Loc} = 2\alpha + 2\delta_Y\beta \qquad (3.15)$$

where η and δ have the values mentioned above for different atoms and bonds.

The resonance energy, R, may be found from the following expression:

$$R = E_{MO} - E_{Loc} \qquad (3.16)$$

where E_{MO} is the total energy found from the doubly occupied molecular orbitals and E_{Loc} is the total energy computed from equations 3.13, 3.14 and 3.15.

The CDC 3200 computer programme used[7] for the calculation of the eigenvalues, eigenvectors,

π-electronic charges, net charges and bond orders is given in Appendix 4.

3.3 Results and Discussion of the LCAO Molecular Orbital Calculations for Aminoacridines and Aminobenzacridines.

The results of the calculations are given in Appendix 2, the numbering of the atoms and bonds being indicated in Appendix 1. The resonance energies of the aminobenz[a]acridines (Table A2.3) are approximately equal to those of the aminobenz[c]acridines, (Table A2.9), while those of the aminobenz[b]acridines (Table A2.6) are lower. This may be accounted for in terms of the structural similarity of the former two series of molecules. The resonance energies of the aminobenzacridines are higher than those of their protonated analogues (Tables A2.12, A2.15 and A2.18), indicating that increased stability of the conjugated system due to the delocalized π-electrons is less for the protonated form.

The energies of the highest filled molecular orbitals of the aminobenz[b]acridine molecules (Table A2.6) are less than those of the aminobenz[a]acridine and aminobenz[c]acridine molecules (Tables A2.3 and A2.9, respectively), and hence the ionisation constants of the former

molecules are expected to be lower than those of the latter. However, the energies of the highest filled molecular orbitals for the series of aminobenzacridine ions (Tables A2.12, A2.15 and A2.18) are similar, these being lower than those for the aminobenz[a]acridine and aminobenz[c]acridine molecules (Tables A2.3 and A2.9, respectively) and higher than those for the aminobenz-[b]acridine molecules (Table A2.6). This implies that for aminobenz[a]acridine and aminobenz[c]acridine molecules the second ionization constant is smaller than the first, but for aminobenz[b]acridine molecules the second is greater than the first.

Fig. 3.1 indicates the correlation between pK_a [8,9] and the charge on the ring nitrogen atom (from Tables A2.4, A2.7 and A2.10) for several amino-benzacridines and all of the mono-aminoacridines.[1] It is evident that for tri- and tetra-N-heteroaromatic amines the correlation between basic strength and the electrical charge on the ring nitrogen is satisfactory, although this has not been found for rings containing several N-hetero atoms.[1]

For several aminobenzacridine and amino-acridine molecules the frequency of the longest wave-length band is a linear function of the difference in

FIG. 3.1. Values of the pK_a of several aminobenzacridines[9] and aminoacridines[8] as a function of the calculated charge on the ring nitrogen. The values for the charge on the ring nitrogen for the aminoacridines were obtained from reference 1. The points are numbered as follows:

1	1-aminoacridine
2	2-aminoacridine
3	3-aminoacridine
4	4-aminoacridine
5	9-aminoacridine
6	9-aminobenz[a]acridine
7	10-aminobenz[a]acridine
8	12-aminobenz[a]acridine
9	2-aminobenz[b]acridine
10	12-aminobenz[b]acridine
11	7-aminobenz[c]acridine
12	9-aminobenz[c]acridine
13	10-aminobenz[c]acridine

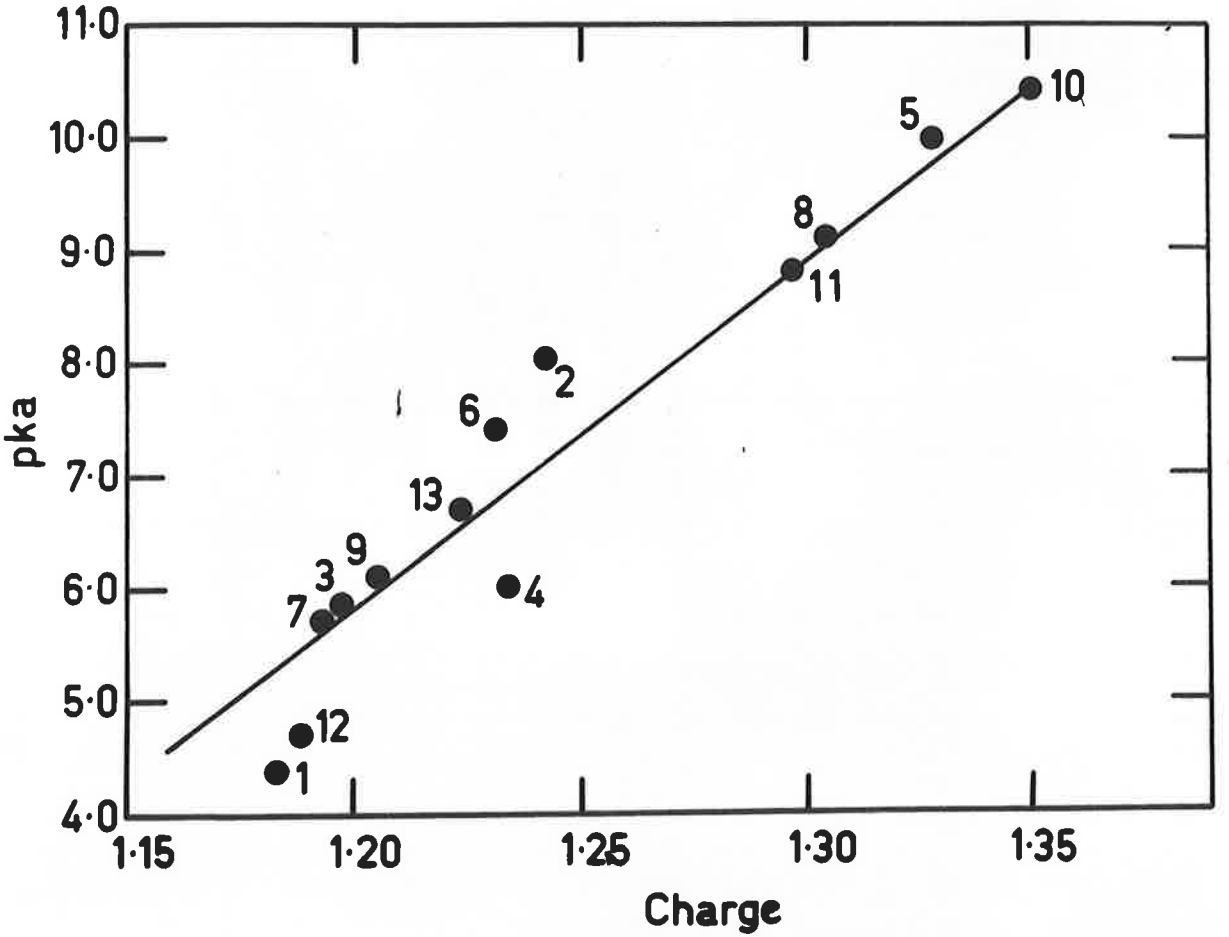
11·0
10·0
9·0
8·0
7·0
6·0
5·0
4·0
pka
1·15
1·20
1·25
1·30
1·35
Charge
10
5
8
11
2
6
13
9
3
7
4
12
1

energy between the highest filled and the lowest empty molecular orbitals, $\Delta\epsilon_1$ (Fig. 3.2). The spectra used to give Fig. 3.2 are presented in Appendix 3, the frequencies and $\log_e \varepsilon$ of the absorption maxima being listed in Table A3.1, and the spectra, obtained between 2200 Å and 6000 Å in dry ethanol solution, being shown in Figs. A3.1 to A3.12. In Fig. 3.3, the frequency of the β-band is plotted against the average difference in energy between the highest filled and lowest empty, and between the second highest filled and the second lowest empty molecular orbitals, $\Delta\epsilon_2$. Such linear relationships have previously been found to hold for several series of benzenoid hydrocarbons.[10,11]

By plotting the data of Mason[5] for the antisymmetric stretching frequencies against the calculated values for the bond order of the C-N(amino) bond of the aminobenzacridines (Tables A2.5, A2.8 and A2.11), and of the aminoacridines found by Pullman and Pullman,[1] a linear relationship is obtained for those molecules existing in the amino form (Fig. 3.4). There are three points which do not obey this relationship and these require additional comment.

12-Aminobenz[b]acridine has been found to assume mainly the imino form in carbon tetrachloride

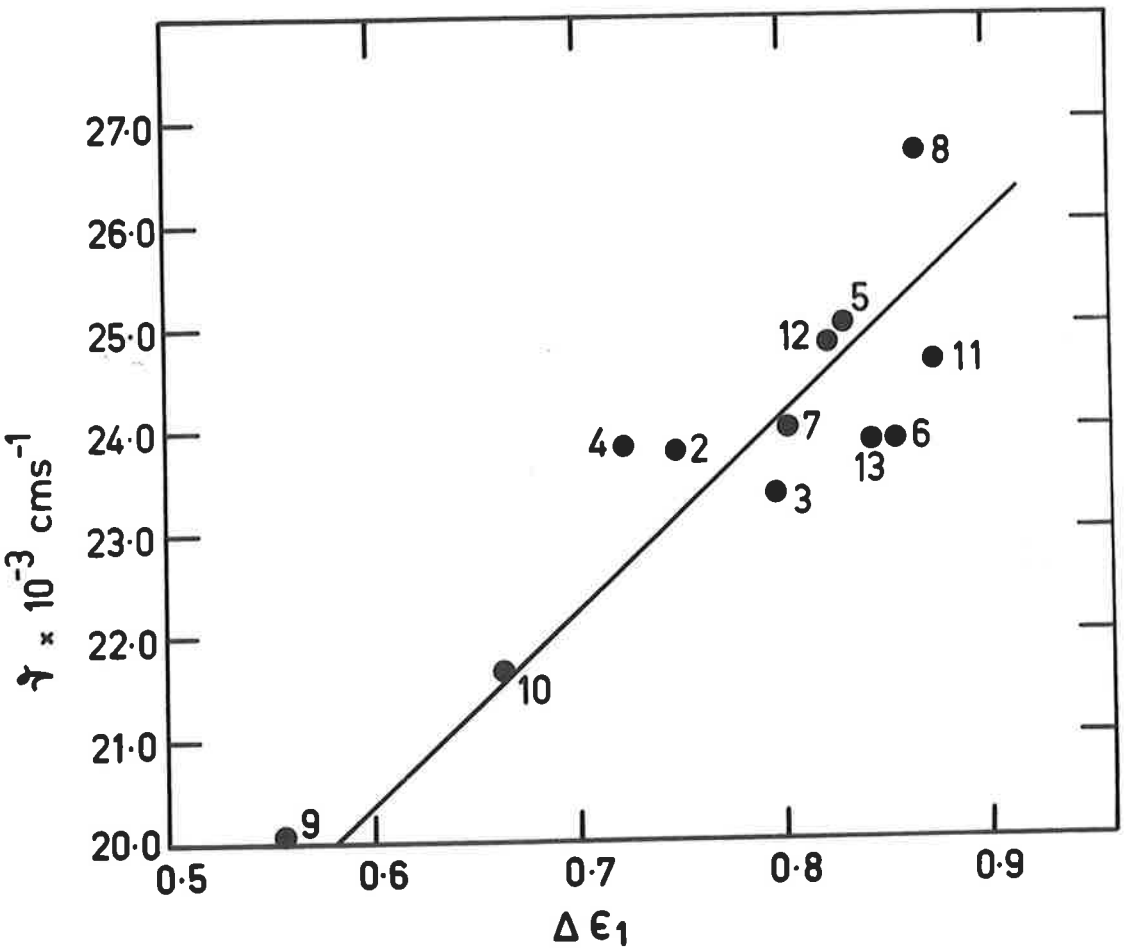

FIG. 3.2. Frequency of the longest wavelength band of several aminobenzacridines and aminoacridines as a function of the difference in energy between the highest filled and the lowest empty molecular orbitals, $\Delta\epsilon_1$. The points are numbered as in Fig. 3.1.

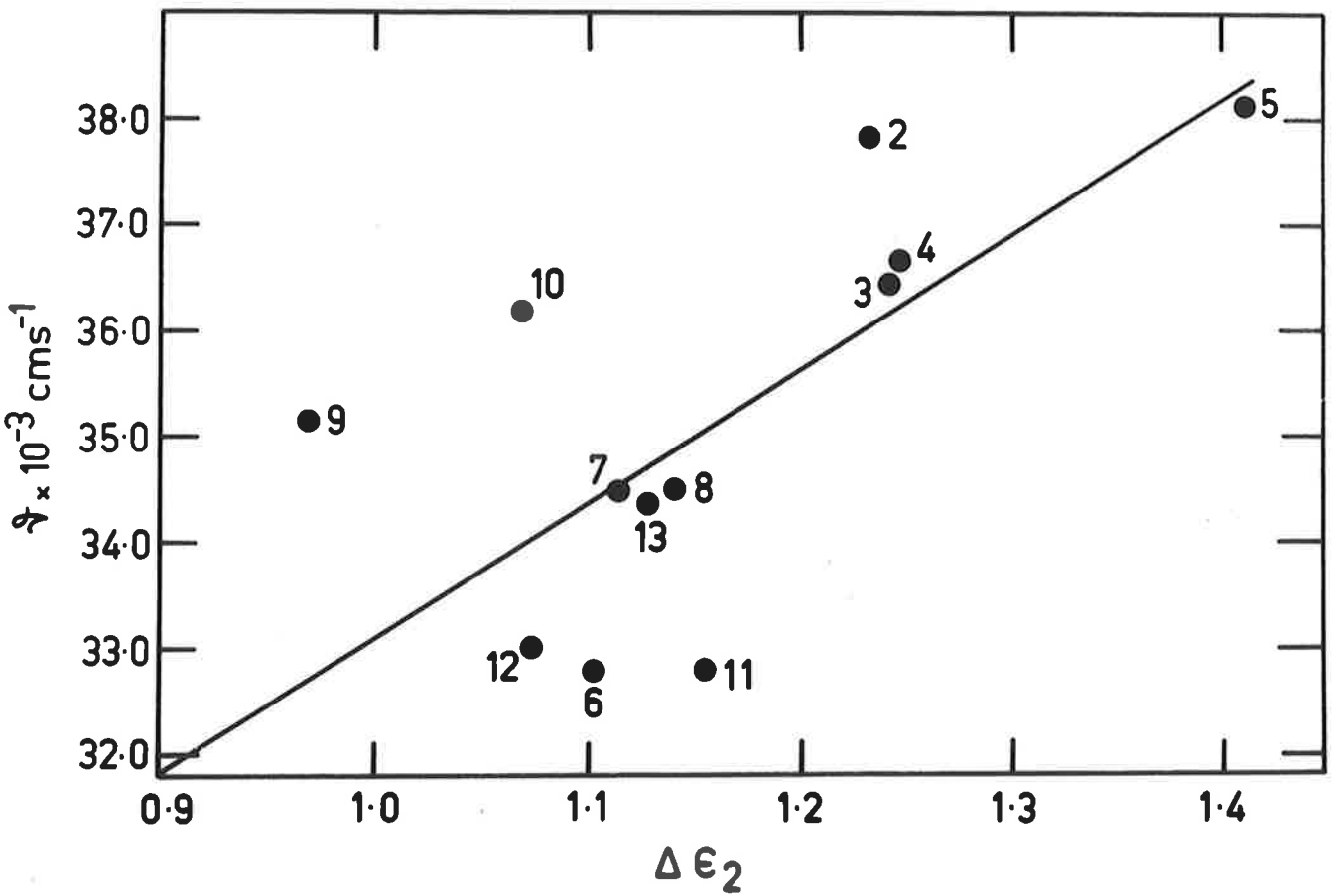

FIG. 3.3. Frequency of the β-band of several aminobenzacridines and aminoacridines as a function of the average difference in energy between the highest filled and lowest empty, and between the second highest filled and second lowest empty molecular orbitals, $\Delta\epsilon_2$. The points are numbered as in Fig. 3.1.

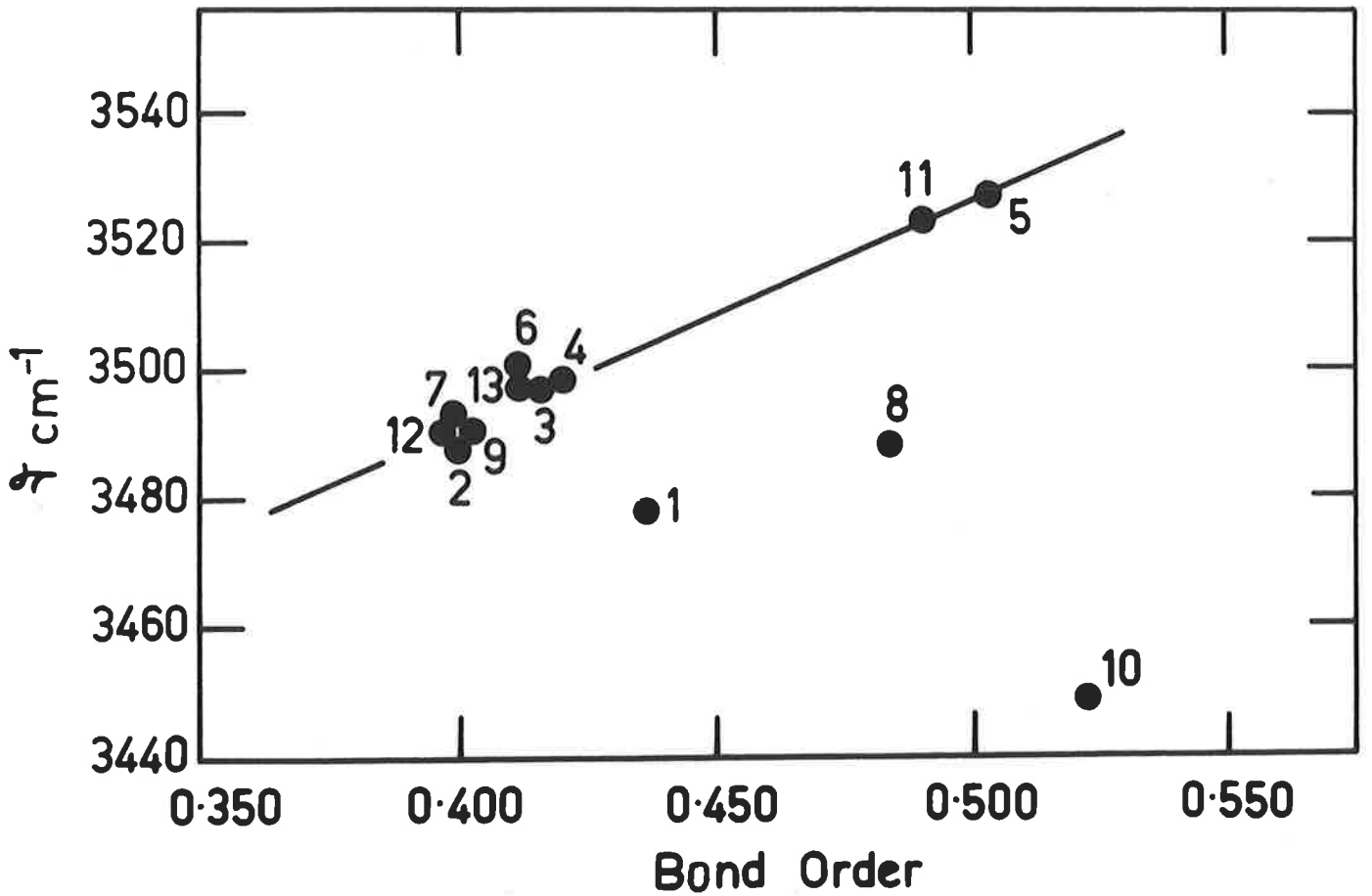

FIG. 3.4. Antisymmetric stretching frequencies[5] (ν cm^{-1}) of several aminobenzacridines and aminoacridines as a function of the calculated bond orders of the C-N (amino) bond. The bond orders of the aminoacridines were obtained from reference 1. The points are numbered as in Fig. 3.1.

solution.[5] Hence the bond length of the C-N(amino) bond is expected to be shorter than the normal C-N(amino) bond in other aminobenzacridines which exist in the amino form. Thus the bond order is expected to be larger. That this is so is shown in Table A2.8 and in Fig. 3.4, point 10, thus confirming that 12-aminobenz[b]-acridine assumes mainly the imino form in solution.

The observed antisymmetric stretching frequency of 12-aminobenz[a]acridine[5] (point 8 of Fig. 3.4) is 3488 cm^{-1}, whereas that expected from Fig. 3.4 for a bond order of 0.483 is about 3520 cm^{-1}, or approximately the same as that of 7-aminobenz[c]-acridine. However the amino group of the former molecule is subject to much steric hinderance to which this anomalous behaviour may be attributed.

1-Aminoacridine (point 1 of Fig. 3.4) is expected to have a higher force constant than observed[12] and therefore higher symetric and anti-symetric stretching frequencies. This conclusion may also be drawn from Fig. 3.4 from which it is expected that 1-aminoacridine would have an antisymetric stretching frequency of 3505 cm^{-1}. Furthermore the intensity of this transition for 1-aminoacridine is lower than that for other aminoacridines.[5] These

factors could indicate that 1-aminoacridine, although partly in the amino form, exists in the imino form to a greater extent than the other aminoacridines.

3.4 Theory of Dipole Moment Calculations.

The separate contributions of the σ- and π-electrons to the total dipole moment of a heterocyclic molecule are considered using the methods adopted by De Vos and Tinoco.[3]

The σ-bond dipole moment is given by

$$\mu_{rs} = 2e\left[\int x\psi_r\psi_s\,dv\right][1 + S_{rs}]^{-1}$$

$$+ 2\mu_p[-2(1 + \cos\theta_p)\cos\theta_p]^{\frac{1}{2}}[1 - \cos\theta_p]^{-1}$$

$$\times[S' - 0.5(S_{rs} + S_{rt} + 2)(1 + S_{rs})^{-1}(1 + S_{rt})^{-1}] \qquad (3.17)$$

where μ_p = 2.31D for carbon and 1.91D for nitrogen, [3] and x is the distance along the bond from the bond mid-point.

The first term in equation 3.17 gives the magnitude of the bond homopolar moment and the second gives the magnitude of the total hybrid moment.[13,3]

The ring bonds re and rt formed by ring atom r have overlap integrals S_{re} and S_{rt}, and the total hybrid moment is directed away from the ring along the bisection of the angle θ_r between bonds re and rt. The value of S' is taken as 2 if the atom r has a lone pair orbital and as $[1 + S_{ru}]^{-1}$ if an extra-annular bond ru is considered. The homopolar moments and the total hybrid moments used are given in Fig. 3.3.

The π-moment of each molecule was found from the electrical charges on the atoms and the position of each atom. The centre of gravity of a given molecule was chosen as the origin for the calculation described by Daudel, Le Febvre and Moser.[4] The π-moment vector of the molecule, μ_π, may then be found from

$$\mu_\pi = - \; e\sum_i (q_{Net})_i X_i - \; e\sum_i (q_{Net})_i Y_i \qquad (3.18)$$

where X_i and Y_i are the unit vectors along the positive OX and OY axes, respectively, and q_{Net} is the net charge calculated for each atom from equations 3.10 and 3.11. The minus signs in equation 3.18 take into account the direction of the dipole

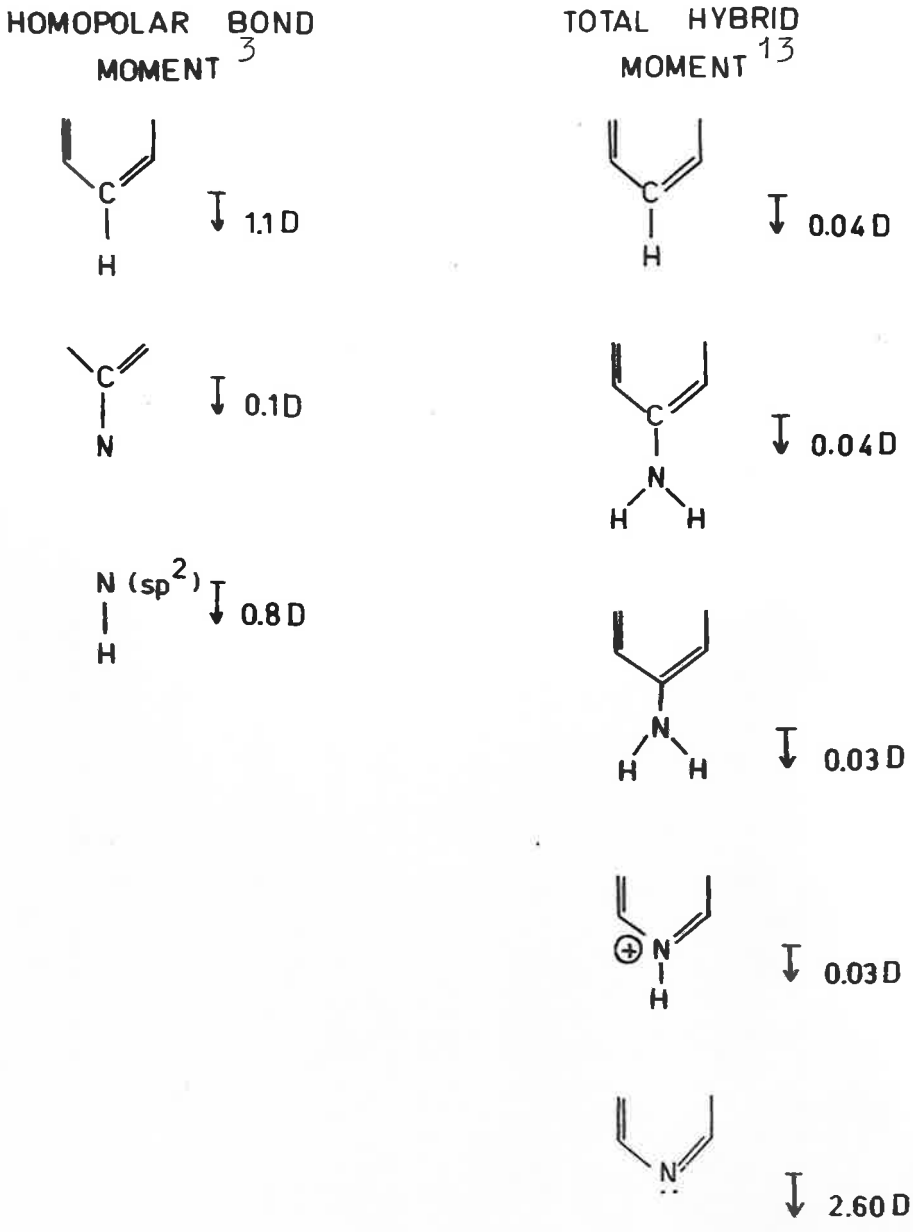

FIG. 3.5. The homopolar bond moments and total hybrid moments of σ-bonds.

moment so computed.

The total dipole moment is found from

$$\mu_{Tot} = \mu_{\psi} + \mu_{\sigma} \qquad (3.19)$$

The IBM 1620 computer programmes used for the calculation of the centre of gravity and the total dipole moment vectors of the molecules are given in Appendix 4.

It is important to note that the origin for a charged molecule must be carefully chosen as the dipole moment calculated depends on the origin. The centre of gravity of the molecule was therefore selected as the origin.

3.5 Results and Discussion of the Dipole Moment Calculations for Aminoacridines and Aminobenzacridines.

The dipole moments of the protonated form of the aminoacridines (Table A2.21) and of the aminobenzacridines (Tables A2.25, A2.26 and A2.27) are, in general larger in magnitude and different in direction from those of their uncharged analogues (Reference 14 for aminoacridines and Tables A2.22, A2.23 and A2.24 for aminobenzacridines).

The experimental dipole moment for acridine

has been reported as 2.1D,[15] 1.9±D,[16], 1.95D,[17] and 2.09D,[18] the latter two values being found by extrapolation of data for concentrations above about 10^{-2}M and 10^{-3}M, respectively. Using the above method of calculation, the dipole moment of acridine is found to be 3.4D,[2] and Pullman, who adopts different parameters for the σ-moment calculations, obtains a value of 2.71D.[14] Similarly, it is found that the experimental dipole moment of 9-aminoacridine is lower than the calculated dipole moment. The experimental dipole moment of 9-aminoacridine has been reported as 4.13D,[16] while the value calculated from equations 3.17, 3.18 and 3.19 is 8.06D and Pullman calculates a value of 7.64D.[14]

In the measurement of these dipole moments experimentally, no account has been taken of the fact that acridine and acridine derivatives have been found to associate in solutions more concentrated than about 10^{-4}M.[19-22] Furthermore, in the visible spectra of several acridine derivatives, a shift to shorter wavelengths is observed at concentrations above about 10^{-4}M [19-22], and this may be attributed to a 'card-pack' type of stacking in the dimer or aggregate.[23] For a favourable molecular orientation within a dimer, for

example, the overall dipole moment of the dimer will be considerably less than twice that of the monomer. This will therefore lead to a reduction of the experimental dipole moment in solutions where aggregation is occurring. It is evident, therefore, that more theoretical work to improve the calculated values of the dipole moments and more experimental work, at low concentrations to avoid any molecular association, for comparison with the calculated values are required.

The free energy of interaction between two molecules is different for molecules with different dipole moment vectors. Hence it is important to consider the molecule concerned in the correct form, either protonated or unprotonated, depending on the system under consideration. This is particularly important for theoretical studies on the free energy of interaction of DNA and either charged or uncharged tri- or tetra-N-heteroaromatic amines.[2]

The high dipole moments of some of the aminobenzacridines (Tables A2.25, A2.26 and A2.27 for the protonated forms and Tables A2.22, A2.23 and A2.24 for the non-protonated forms) indicate that considerable dipole-dipole interactions can occur in a given system

such as that mentioned above[2], while for 2-aminoacridine in the protonated form, with only a small dipole moment (Table A2.21), such interactions would be reduced. The results reported in Chapter 5 indicate that the protonated forms of 12-aminobenz[a]acridine and 7-aminobenz[c]acridine interact more strongly with DNA than does the protonated form of 2-aminoacridine.

References.

1. Pullman, B. and Pullman, A., "Quantum Biochemistry", Interscience, (1963).

2. Gersch, H.F. and Jordan, D.O., J.Mol.Biol. 13, 138 (1965).

3. De Vos, H. and Tinoco, I., J.Mol.Biol. 4, 500 (1962).

4. Daudel, R., Lefebvre, R. and Moser,C., "Quantum Chemistry", Interscience (1959).

5. Hasem, S.F., J.Chem.Soc. 1281 (1959).

6. Huckel, E., Z.Physik 70, 204 (1931); ibid, 72, 310 (1931); ibid, 76, 628 (1932); ibid,83, 632 (1933); and Z.Elektrochem. 43, 752 (1937).

7. The author gratefully acknowledges Dr. K.W.Mills of the Computing Science Department of the University of Adelaide for making available the 1620 programme for extracting eigen values and eigen vectors from an n x n symmetric matrix using Jacobi's diagonalization procedure.

8. Albert, A. and Goldacre, R., J.Chem.Soc. 706 (1946).

9. Albert, A., Rubbo, S.D. and Burvill, M.I., Brit.J. Exper.Path., 30, 159 (1949).

10. Zahradnik, R. and Koutecky, J., Coll.Czech.Chem.Comm. 28, 904 (1963).

11. Koutecky, J. and Zahradnick, R., Ibid., 28, 2089 (1963).

12. Short, L.N., J.Chem.Soc. 4584 (1952).

13. The values for the total hybrid moments were calculated from the second term of equation 3.17 using data for overlap integrals from I. Tinoco, personal communication (1965).

14. Pullman, B., In "Electronic Aspects of Biochemistry", Ed.B.Pullman, Academic Press,p559 (1964).

15. Acheson, R.M., "The Acridines", Interscience (1956).

16. Pushkareva, Z.V. and Kokoshko, Z.Yu., Doklady Akad. Nauk S.S.S.R. 93, 77 (1953).

17. Bergmann, E., Engel, L. and Meyer, H., Ber. 65 B, 446 (1932).

18. Cumper, C.W.N., Gimman, R.F.A. and Vogel, A.I., J.Chem.Soc. 4518 (1962).

19. Levshin, L.V., Zhur.Eksptl.i Teoret.Fiz. 28,213(1955).

20. Zanker, V., Z.Physik.Chem. 199, 225 (1952).

21. Haugen, G.R. and Melhuish, W.H., Trans.Faraday Soc. 60, 586 (1964).

22. Rabinowitch, E. and Epstein, L.F., J.Am.Chem.Soc. 63, 69 (1941).

23. Bradley, D.F., Trans.N.Y.Acad.Sci. 24, 64 (1961).

CHAPTER 4.

FREE ENERGY CALCULATIONS FOR DNA-AMINOACRIDINE AND DNA-AMINOBENZACRIDINE SYSTEMS.

4.1 Introduction.

The interaction of DNA with aminoacridines and other heterocyclic systems has been interpreted in terms of two models as previously described in Chapter 1. In the first, intercalation of an aminoacridine molecule or ion between adjacent base pairs occurs (model I), the DNA molecule consequently extending and the original right-handed helix becoming a left-handed helix in the process.[1,2] The principal forces stabilising this model arise from charge, permanent dipole and induced dipole interactions and London forces between the aminoacridine and the neighbouring base pairs. In the second model, the aminoacridine is associated with the phosphate group on the outside of the double helix, the helix dimensions remaining essentially unchanged. As originally described by Bradley and Wolf,[3] the dye molecules were stacked perpendicularly to the helix axis, but this model has recently been refined by Mason and McCaffery[4] who, on the basis of conclusions drawn from optical rotation measurements of streaming solutions, consider the amino-

acridine to be attached through the ring NH group to a phosphate group, the heterocyclic ring being oriented at an angle of between 45 and 90° to the helix axis (model II). Electrostatic and dye-dye interactions are involved in determining the stability of this model. In the intercalated model I, external attachment of the aminoacridine molecules, as in model II, is clearly also possible.

The results of calculations of the free energy of the interaction of DNA with aminoacridines according to both models I and II will be presented. The calculations[5] are based on the methods adopted by De Voe and Tinoco[6] for the determination of the free energy of the DNA double helix. This enables a comparison to be made of the relative stabilities of the two models, and also to predict the order of preference for dye interactions with the various base pairs. On the basis of fluorescence quenching measurements, Tubbs, Ditmars and Van Winkle[7] have already observed that adenine-thymine sites interact more strongly with acriflavine than guanine-cytosine sites.

4.2 General Principles.

The equations used for the free energy calculations have already been discussed in Chapter 2. The models adopted and the parameters chosen will be discussed using the DNA-proflavine system as an example. The results for this system, as well as those for other DNA-aminoacridine and DNA-aminobenzacridine systems will then be presented.

The characteristic energy, $h\nu_1$, for proflavine was estimated to be 200 Kcal $mole^{-1}$ from experimental values of the dispersion of benzene and pyridine, and a value of 20$(\text{Å})^3$ was obtained for the average group polarizability, α_1, from values of atomic refractions.[8] The total dipole moment of the proflavine ion was calculated as 4.5 D using the method outlined in Chapter 3. The angle which the dipole moment vector of the proflavine ion makes with the dipole moment vector of pyridine is 180°. The corresponding values of μ, α, and $h\nu$ for the bases of DNA were those given by De Voe and Tinoco.[6]

In these calculations, no charge-charge interactions have been estimated, and $V_{\rho\rho}$ has therefore been neglected. It has been assumed that the association of cosmions with DNA and dye is such as to neutralize the

charges. This would certainly be true in 0.1N sodium chloride. This assumption was, in effect, also made by De Voe and Tinoco.[6]

4.3 The Intercalated Model.

The model adopted for these calculations was that suggested by Lerman.[1,2] The native DNA helix (with orientations of base pairs with respect to helix and dyad axes as proposed by Langridge et al[9] in their model 3) is extended so that the distance between two adjacent base pairs is 6.72 Å and the angle between them, with a left-handed rotation, is 9° (Plate 4.1(a)). The aminoacridine (proflavine in Plate 4.1) is then considered to be inserted in such a way between the base pairs that the helix axis passes through the centre of the dye molecule (Plate 4.1(b)). The case considered is when one dye molecule is intercalated between each base pair and dye bonding by this mechanism is a maximum. For this situation, r, the amount of dye bound per mole of DNA phosphorus, is equal to 0.5. In Plate 4.1 the proflavine molecule is oriented at 4.5° in a left-handed rotation about the helix axis with respect to the lower base pair. Other orientations of the dye molecule are discussed later.

The IBM 1620 computer programme used for the calculation of the geometric factors $C_{i,j}$ and $\theta_{i,j}$, etc.,

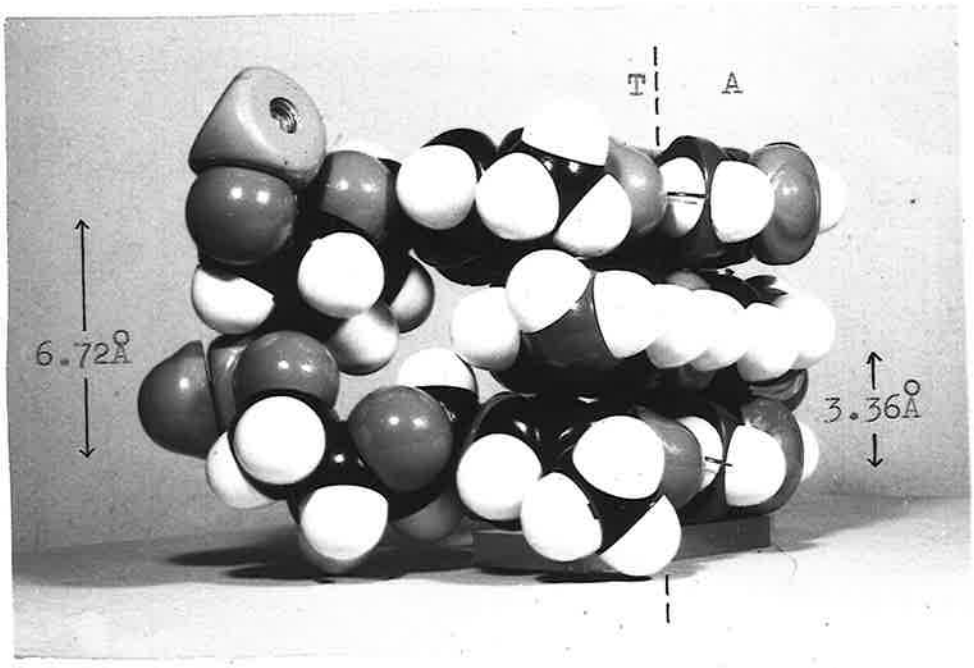

(a)

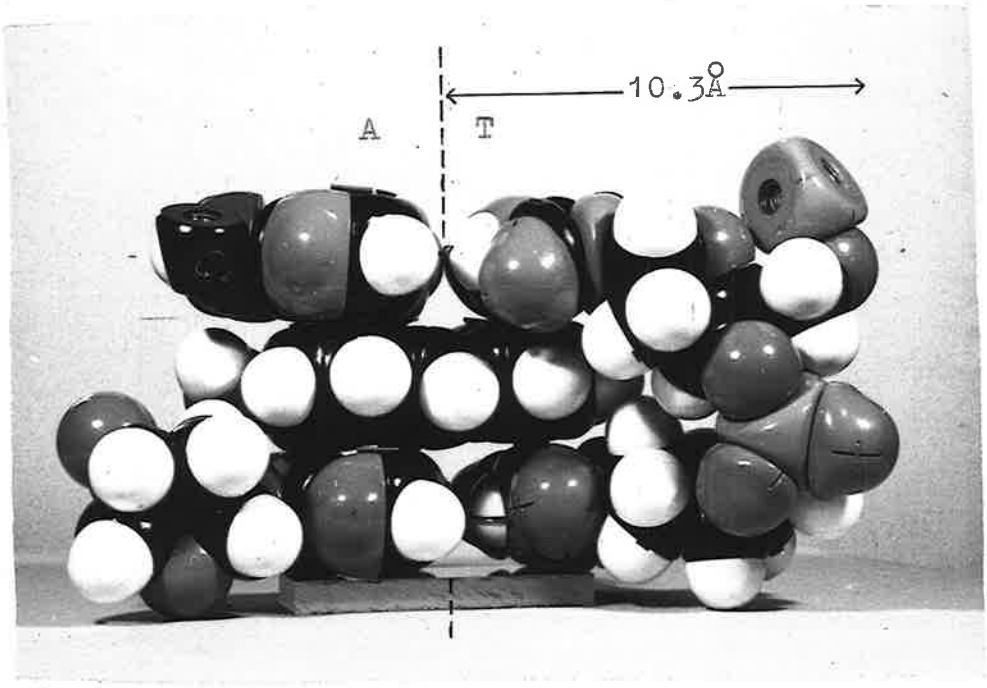

(b)

PLATE 4.1. Relative positions of a proflavine molecule between two A-T base pairs in model I. The helix axis is represented by a broken line. (a) and (b) are two different views of the same model.

defined by equations 2.7 and 2.8, at a number of angles of orientation of the dipole moment unit vector of the intercalated molecule (the angle θ in Fig. 4.1), is given in Appendix 5. The values of $F_{\rho\mu}$, $F_{\mu\mu}$, $F_{\mu\pi}$, $F_{\rho\pi}$ and F_L may then be found using equations 2.3 to 2.6 and 2.9, respectively. For proflavine, where the dipole moment vector is oriented at 180° with respect to the pyridine dipole moment vector, the possible values for θ are 175.5° and 355.5°. The former of these angles gives the positions of the molecules represented in Plate 4.1.

Calculations have also been made for the free energy of interaction between a given proflavine ion and the next intercalated dye ion 6.72 Å above and the base pair 10.08 Å above. The free energy arising from interactions between base pairs 6.72 Å apart in model I has not been included, since De Voe and Tinoco[6] found that the contribution to the free energy from interactions between base pairs more than 3.36 Å apart was small.

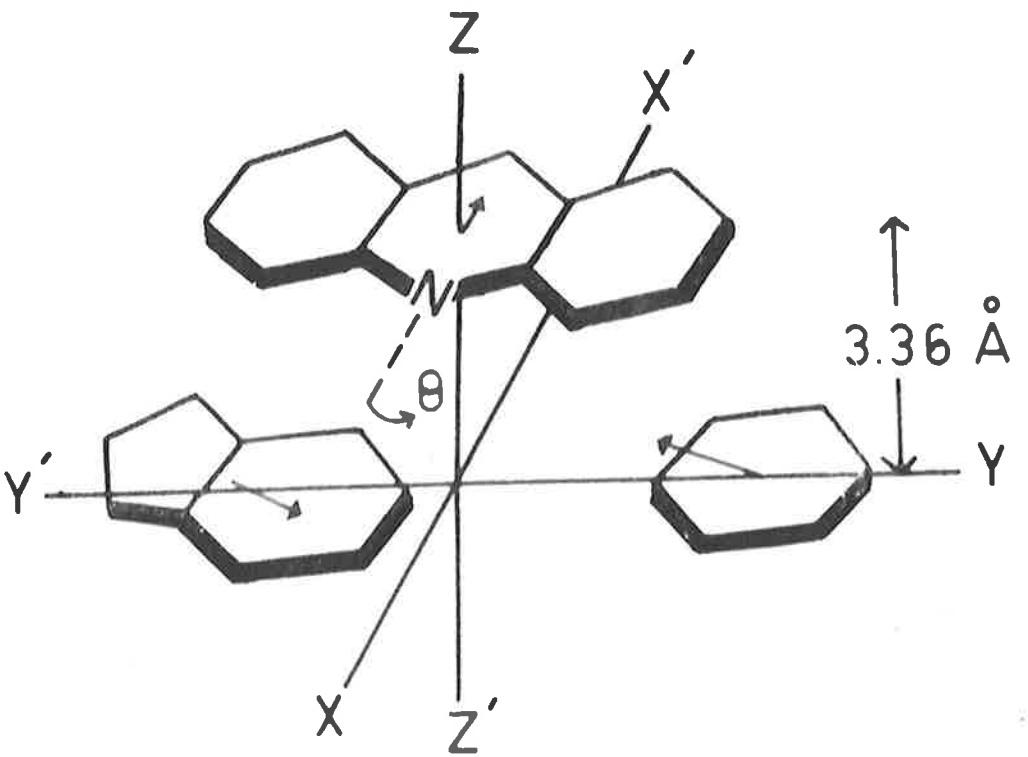

FIG. 4.1. Relative positions of an adenine-thymine base pair and an aminoacridine molecule, as used in the free energy calculations for the intercalated model (I). The skeletons of the molecules are shown and no amino or carboxyl groups are indicated, the ring nitrogen only of the dye being shown. The three dipole moments are represented by short arrows and are not drawn to scale.

4.4 The Model for External Edgewise Attachment of Dye Ions to DNA.

The model used for the calculation of the geometric factors for proflavine bound to the outside of the helix is shown as a projection on the XY plane in Fig. 4.2. If both the dye ions are oriented at the same angle to the helix axis but not perpendicular to it, as shown in Fig. 4.2, there will be no effect on the values of the free energy obtained provided that the angle between the dipole moment vectors remains at 36°. The energy calculations indicate that a variation in the angle of orientation of the two ions with respect to each other within the limits imposed by the model brings about a change in F_{total} of no more than ±0.5 Kcal per repeating unit.

Since only the situation for which r = 0.5 has been considered for the intercalated model, since this represents maximum binding, the case where r = 0.5 is also considered for the external edgewise binding model. This has the effect, since the maximum value of r in this case is 1.0, that a dye ion is bound to all the phosphate groups on one helix (model IIa), or, on the average, to every alternate phosphate group on both helices (model IIb). The former model (IIa) has been assumed in

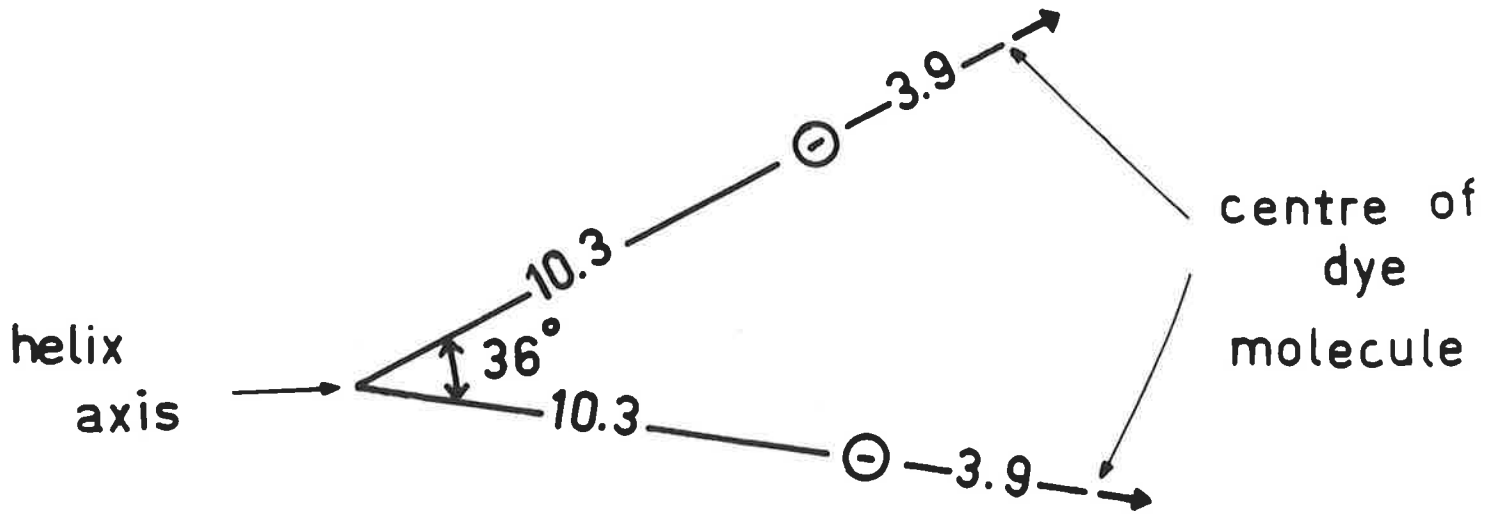

FIG. 4.2. Projection on the XY plane showing atomic distances used in the free energy calculations for model IIa, involving external edgewise attachment of the dye molecules to the phosphate groups. The arrows represent the dipole moment vectors of the charged dye molecules.

these calculations, since dye-dye interaction is greater for this model. However, calculations have also been made for the energy of interaction between a given proflavine ion and the proflavine ion in a plane 6.72 Å above it and with an angle of 72° between the dipole moment vectors of the two ions as in model IIb.

The charge on the phosphate group was considered to be a point charge 10.3 Å from the helix axis giving rise to charge-dipole and charge-polarizability interactions with the bound dye ions. These interactions are considered for model II where the dye ions are bound directly to the phosphate groups, whereas they are not considered for the intercalated model or for DNA alone. In model II the sodium ion formerly associated with the phosphate has been replaced by a bound dye ion and it is assumed that no marked change in charge distribution in the proflavine ion, due to the negative phosphate group, occurs by induction through the bonds and hence that the dipole moment of the ion in this case is the same as that used for the intercalated model. However, for the intercalated model no values of the charge-dipole and charge-polarizability interactions have been included in F_{total}. De Voe and Tinoco[6] made no estimate for these free energies for DNA alone. Such values cannot be calculated

with accuracy since there is a reduction of the effective charge of the phosphate groups due to gegenion association in the case of DNA and due also to intercalated dye ions for model I.

The geometric factors necessary for the calculation of the free energy of interaction for model IIa were found using the IBM 1620 computer programme given in Appendix 5.

4.5 Estimation of the Effective Dielectric Constant, ϵ_{ij}.

In the intercalated model (I) since the dye ions and the adjacent base pairs are effectively separated by a vacuum we have taken ϵ_{ij} as being 1.0, as did De Voe and Tinoco[6] for DNA. Helix solvation would reduce the contribution of the electrostatic interactions and, owing to the presence of the charged dye molecules within the helix for the intercalated model, this effect is likely to be larger than for DNA.

For external edgewise binding (model II) association of solvent molecules with bound dye ions will occur and thereby will increase the effective dielectric constant. Rice and Nagasawa[10] chose a value for ϵ_{ij} of 5.5 for calculations on the polymethacrylate ion where the charge separation is 2.5 Å. This value for ϵ_{ij} and those obtained here were found from the dependence of ϵ_{ij}

on the distance of a given point from an ion.[11] The charge separation between the negative phosphate and the positive bound dye in the DNA-dye complex is 3.9 Å (Fig. 4.2). The values of 35 and 10 for ϵ_{ij} were obtained by taking the average of ϵ_p and ϵ_g for the distance from an ion of 3.9/2 Å using the two models described by Hasted et al.[11] These are taken as limiting values for the effective dielectric constant, now denoted ϵ'_{ij}, used in the calculations of the interaction between the charge on the phosphate group and the dipole moment and polarisability of the bound dye ion (for model IIa). The charge separation is about 9.0 Å between adjacent bound dye positive charges (model IIa) and a value for ϵ_{ij} of 70 was chosen. For model IIb the corresponding charge separation is 11.7 Å, and ϵ_{ij} will have a value of about 78.

4.6 Method of Comparison of Free Energies.

For simplicity the values of free energy for DNA and for model I are quoted for ϵ_{ij}= 1.0. Comparison of these values is possible is account is taken of the following factors:

(i) the dipole-dipole, charge-dipole, etc. interactions will be reduced to a greater extent than will the London interactions for both DNA and model I,

by an increase in ϵ_{ij} due to helix solvation;

(ii) such reduction is expected to be slightly greater for model I than for DNA;

(iii) no account has been taken of the free energy required in the distortion of bond angles and alteration of bond lengths involved in the unwinding and extension of the helix to accommodate the dye molecule.

All of these factors will add a positive term to the calculated free energy for model I.

The free energy values corresponding to model II can be compared with those for DNA and model I only if account is taken of the above factors. Furthermore no account has been taken of base- solvent and dye-solvent interactions. It is evident that any such comparisons will be semi-quantitative, a more direct comparison only being possible if the calculations can be refined.

As previously stated, the value of r adopted for both models was 0.5. Thus for the intercalated model all possible intercalation sites are occupied, while for dye bound externally, half the total binding sites are occupied.

The repeating unit for DNA is one base pair. The energy calculations for a repeating unit may be considered in one of two ways. Either one half the sum

of the eight interactions between the given base pair and that above and that below together with the interaction energy between the bases of the given base pair is evaluated, or the sum of the four interactions between the given base pair and that above together with the average base pair energies of the two base pairs involved is taken. The latter definition involves less complications when base pair sequences are taken into account and is therefore the one used here.

The repeating unit for DNA is shown in Fig. 4.3 (a). For the purpose of comparison with the results obtained here, the method of quoting the values of the total free energies for the base pairs in DNA, F_{total}, found by De Voe and Tinoco[6] has been modified such that the free energies are quoted as Kcals. per repeating unit. For example, for TA above CG the sum of the four interactions above the CG plane, according to De Voe and Tinoco[6], is -18.6 Kcals., and the average interaction of the bases of each base pair is -1.9 Kcals.; this gives a value of -20.5 Kcals. for the total free energy per repeating unit. The difference between this value and that of -11.2 Kcals. per 2 moles of base quoted by De Voe and Tinoco[6] is a matter of definition only. This method of presenting F_{total} is necessary so as to permit

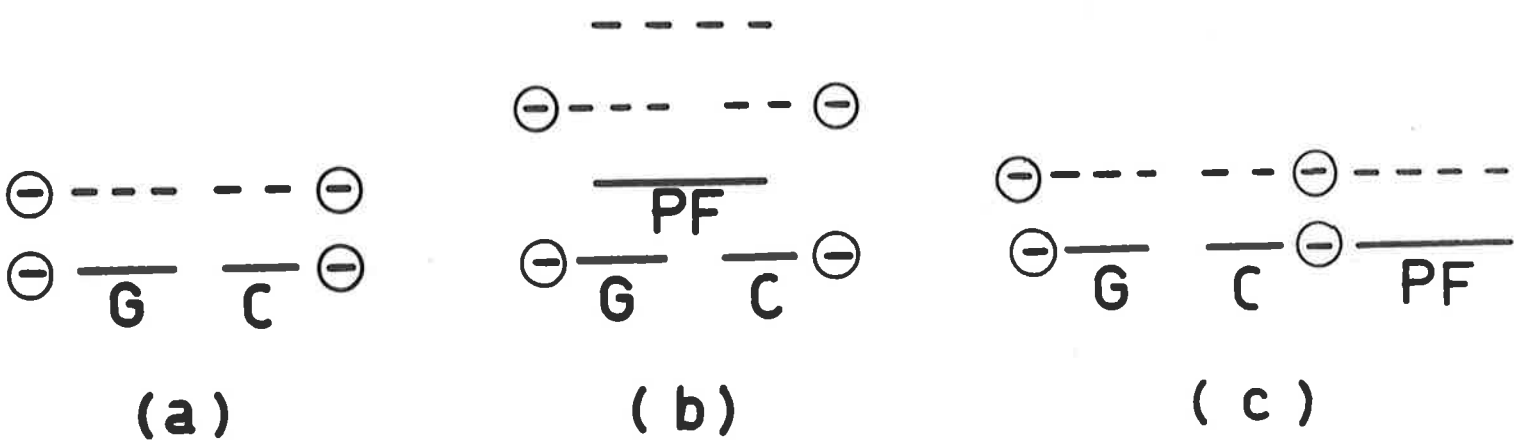

FIG. 4.3. A diagrammatic representation of the repeating units for (a) DNA; (b) model I; (c) model IIa. All interactions involving the molecules represented by a solid line with the molecules represented by a broken line are included in the total free energy calculations for one repeating unit. PF, proflavine.

comparison with values of F_{total} obtained for various aminoacridines and aminobenzacridines bound to DNA.

If there are n repeating units with one base pair each of the type shown in Fig. 4.3 (a) to make up one DNA molecule, and if the same molecule is allowed to bind dye until r = 0.5, then there will still be n repeating units with one base pair each, as indicated by Fig. 4.3 (b) and (c). Hence the free energies are quoted as Kcals. per repeating unit. However the energy per mole of repeating unit, which is found by dividing F_{total} by 2 or 3 as required, has no significance in a direct comparison of free energy. It is the total free energy of the DNA molecule as compared with that of the two different models for the DNA-dye complex which is important, but it is convenient to consider only 1/n th of the DNA molecule or the DNA-dye complex, i.e. one repeating unit. End effects have been neglected.

4.7 Results.

The values of $F_{\rho\mu}$ and $F_{\rho\alpha}$ for model I are invariant with respect to rotation and magnitude of the dye dipole moment and magnitude of the dye polarizability. $F_{\mu\mu}$ is directly proportional to the dipole moment of the intercalated molecule while $F_{\perp}$ and $F_{\rho\alpha}$ are directly proportional to the polarizability of the intercalated molecule.

Fig. 4.4 shows the variation of $F_{\mu\mu}$, $F_{\mu\pi}$ and $F_{\mu\mu} + F_{\mu\pi}$ with orientation of the dipole moment vector of the intercalated molecule for interaction with AT and GC base pairs. For convenience in presentation, the dipole moment of the intercalated molecule is taken as 1.0 D and α_i as $20(\text{Å})^3$. The values presented in Table 4.1 were obtained by combining the value of the dipole moment of the intercalated proflavine ion with the values of $F_{\mu\mu}$ and $F_{\mu\pi}$ obtained from Fig. 4.4 at the required angle. F_L, $F_{\rho\mu}$ and $F_{\rho\pi}$ are invariant with θ.

The values of the free energies were found to be essentially the same for GC, etc. above or below the intercalated molecule. The values of the interaction free energies between the bases of AT and GC base pairs were taken as 0.2 and -3.9 Kcals. as determined by De Voe and Tinoco.[6]

Table 4.1(a) indicates that the effect on F_{total} of a change in the dipole moment of the intercalated molecule is small since only $F_{\mu\mu}$ and $F_{\mu\pi}$ are affected. Values for the free energy of interaction of a proflavine ion with a neighbouring intercalated proflavine ion and an additional base pair are shown in Table 4.1 (b) and (c). Since the interactions of a given proflavine ion with the next intercalated ion 6.72 Å

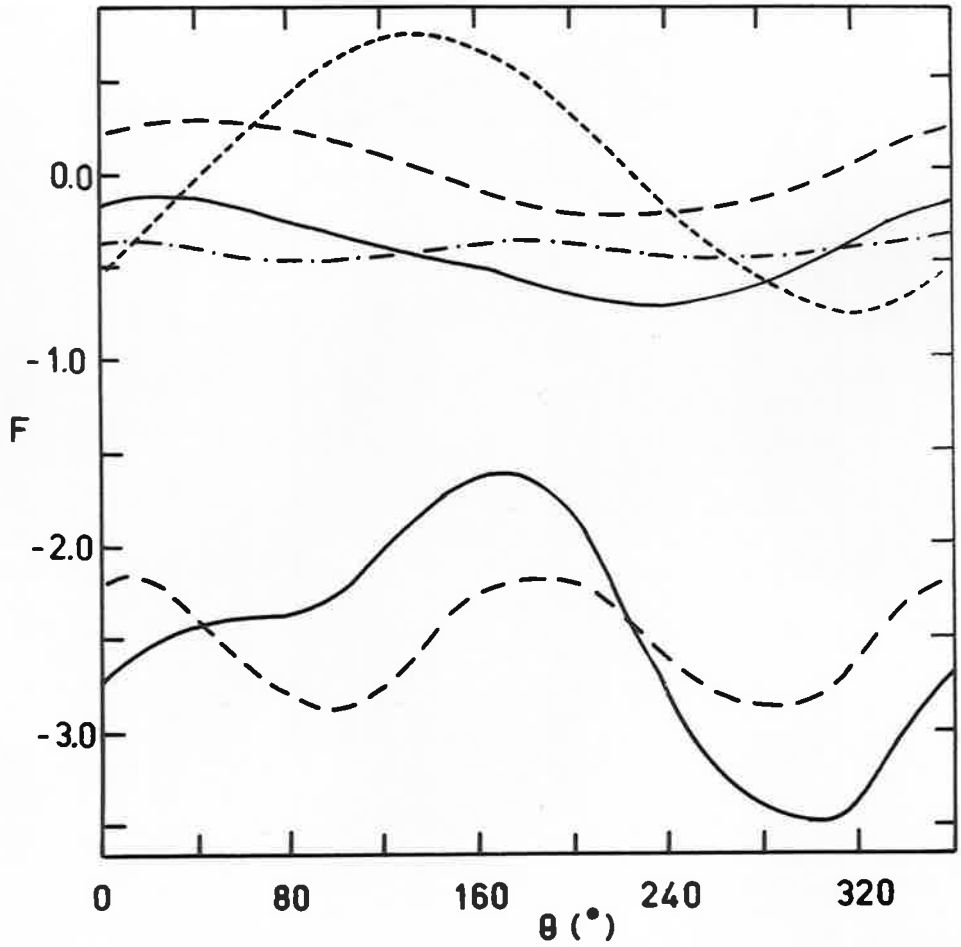

FIG. 4.4 F, the free energy of dipole-dipole and dipole-induced dipole interactions (in Kcal. per base pair) for the intercalated model as a function of θ, the angle of orientation of the dipole moment of the intercalated molecule. The values obtained are for the intercalated molecule above or below the base pair indicated in parentheses.

Upper curves: $F_{\mu\mu}$(AT), - - - -; $F_{\mu\alpha}$(AT), -·-·-·-·; $F_{\mu\mu} + F_{\mu\alpha}$(AT), ————; $F_{\mu\mu}$(GC), - - - -.

Lower curves: $F_{\mu\alpha}$(GC), - - - -; $F_{\mu\mu} + F_{\mu\alpha}$(GC), ————.

TABLE 4.1

CALCULATED FREE ENERGY VALUES (IN KCAL. PER REPEATING UNIT) FOR THE INTERCALATED MODEL I (ϵ_{ij}=1.0)

UNIT	$F_{\mu\mu}$	$F_{\mu\alpha}$	F_L	$F_{\rho\mu}$	$F_{\rho\alpha}$	F_{total}
(a) INTERACTION OF PROFLAVINE (PF) WITH NEAREST NEIGHBOUR BASE PAIRS						
G....C	5.4	-5.6	-13.8	-11.8	-16.6	-46.3
PF*	(-5.4)	(-5.6)	(-13.8)	(-11.8)	(-16.6)	(-57.1)
G....C						
A....T	-1.8	-2.0	-13.8	-26.6	-16.6	-60.6
PF*	(1.8)	(-2.0)	(-13.8)	(-26.6)	(-16.6)	(-57.0)
A....T						
C....G	4.5	-5.2	-13.8	-11.8	-16.6	-46.8
PF*	(-4.5)	(-5.2)	(-13.8)	(-11.8)	(-16.6)	(-55.8)
C....G						
T....A	-1.8	-2.0	-13.8	-26.6	-16.6	-60.6
PF*	(1.8)	(-2.0)	(-13.8)	(-26.6)	(-16.6)	(-57.0)
T....A						

THE VALUES IN PARENTHESES INDICATE VALUES AT θ =355.5°

* THE PROFLAVINE MOLECULE IS CONSIDERED TO INTERACT WITH ALL OTHER MOLECULES IN THE UNIT SHOWN

(b) INTERACTION OF ADJACENT PROFLAVINE MOLECULES						
PF*	.86	-.17	-.47	0.0	-.98	-.8
BASE PAIR	(-.86)	(-.17)	(-.47)	(0.0)	(-.98)	(-2.5)
PF*						

THE VALUES WITH AND WITHOUT BRACKETS REFER TO ANGLES OF 171° AND 351°, RESPECTIVELY, BETWEEN DYE DIPOLE MOMENT VECTORS

* ONLY INTERACTIONS BETWEEN THESE TWO MOLECULES ARE CONSIDERED

TABLE 4.1 (CONTINUED)

UNIT	$F_{\mu\mu}$	$F_{\mu\alpha}$	F_L	$F_{\rho\mu}$	$F_{\rho\alpha}$	F_{total}
(c) INTERACTION OF PROFLAVINE WITH BASE PAIR 10.08Å ABOVE OR BELOW						
PF BASE PAIR DYE G....C	.01	-.01	-.03	-.65	-.17	-.9
PF BASE PAIR DYE A....T	-.07	0.0	-.03	-1.01	-.17	-1.3
PF BASE PAIR DYE C....G	.06	-.01	-.03	-.65	-.17	-.8
PF BASE PAIR DYE T....A	0.0	0.0	-.03	-1.01	-.17	-1.2

THE INTERACTIONS ARE BETWEEN PROFLAVINE AND G AND C, A AND T, AS INDICATED. NO INTERACTIONS BETWEEN THE BASES OF A GIVEN BASE PAIR ARE INCLUDED AS THESE ARE ALREADY ACCOUNTED FOR IN F_{total} IN TABLE
THE VALUES ARE FOR θ =166.5 ONLY.

above are included in the repeating unit, an additional -0.8Kcals. per repeating unit is added to the value for $\phi = 175.5^{\circ}$ in Table 4.1 (a) to give the values of F_{total} for the intercalated model in Table 4.3. Also included in F_{total} is the free energy arising from the interaction of the lower base pair (the molecules represented by a solid line in Fig. 4.3 (b)) with the dye ion 10.0Å above. It should be noted that in Table 4.1 (a) and (c), rows one and three, and two and four, are not identical, since the interaction depends on the relative orientation of the dipole moments of the bases of the base pairs and of the proflavine ion.

Recently, free energy calculations similar to these have been reported for the association of purines and pyrimidines with polycyclic hydrocarbons.[12,13] The most important contribution to the free energy of interaction was shown to arise from the London dispersion forces which have also been found to be large for DNA-proflavine, as shown in Table 4.1. However, in the case of charged molecules, charge-dipole and charge-polarizability interactions contribute to the total free energy to as great an extent as do the London dispersion forces.

When other DNA-aminoacridine and DNA-aminobenzacridine systems are considered, and free energies

calculated for the intercalated model I, with the helix axis passing through the centre of gravity of the dye ion, the values of $F_{\mu\mu}$, and $F_{\mu\pi}$ are the same as those presented in Table 4.1 (a), while the value of F_L is directly proportional to the polarizability of the intercalated ion. However, small, but significant variations occur in $F_{\mu\mu}$ and $F_{\mu\pi}$, depending on the dye considered.

For the mono-aminoacridines and the monoaminobenzacridines, α_1 was estimated to be 18 and 21, respectively. The value of $h\nu_1$ was taken to be 200 Kcal. $mole^{-1}$ for all ions considered. The dipole moments used for the ions are given in Table A2.24 for the aminoacridines and in Tables A2.25, A2.26 and A2.27 for the aminobenzacridines. The acridine 'skeleton' (Fig. 4.1) of the various dye ions is, for these calculations, assumed to be oriented at -45° relative to the base pairs, as for proflavine in Plate 4.1, with the helix axis passing through the centre of gravity of the dye ion. Thus for each dye ion, two possible orientations, θ, are considered for the calculation of $F_{\mu\mu}$ and $F_{\mu\pi}$ in Table 4.2 where the values of θ depend on the direction of the dipole moment of the dye ion.

It is evident from Table 4.1 (a) and from Table 4.2 that $F_{\mu\mu}$ and $F_{\mu\pi}$ depend not only on the dye

TABLE 4.2

CALCULATED FREE ENERGIES (IN KCAL PER REPEATING UNIT) FOR THE INTERCALATED MODEL (ϵ_{ij}=1.0) FOR VARIOUS DYES.

	θ^{o}	$F_{\mu\mu}$	$F_{\mu\alpha}$		θ^{o}	$F_{\mu\mu}$	$F_{\mu\alpha}$
1-AMINOACRIDINIUM ION							
G....C	174.3	2.5	-4.2	C....G	174.3	2.4	-3.8
DYE	354.3	-2.5	-4.2	DYE	354.3	-2.4	-3.8
G....C				C....G			
A....T	174.3	-.8	-.9	T....A	174.3	-.9	-.8
DYE	354.3	.8	-.9	DYE	354.3	.9	-.8
A....T				T....A			
2-AMINOACRIDINIUM ION							
G....C	62.5	.5	-4.7	C....G	62.5	-1.5	-3.6
DYE	242.5	-.5	-4.7	DYE	242.5	1.5	-3.6
G....C				C....G			
A....T	62.5	.5	-.8	T....A	62.5	-.2	-.6
DYE	242.5	-.5	-.8	DYE	242.5	.2	-.6
A....T				T....A			
3-AMINOACRIDINIUM ION							
G....C	61.8	1.3	-5.1	C....G	61.8	-4.2	-4.0
DYE	241.8	-1.3	-5.1	DYE	241.8	4.2	-4.0
G....C				C....G			
A....T	61.8	1.4	-1.2	T....A	61.8	-.5	-1.0
DYE	241.8	-1.4	-1.2	DYE	241.8	.5	-1.0
A....T				T....A			
4-AMINOACRIDINIUM ION							
G....C	149.4	3.9	-4.5	C....G	149.4	-1.1	-3.9
DYE	329.4	-3.9	-4.7	DYE	329.4	1.1	-3.9
G....C				C....G			
A....T	149.4	-.5	-1.0	T....A	149.4	1.3	-.9
DYE	329.4	.5	-1.0	DYE	329.4	-1.3	-.9
A....T				T....A			

TABLE 4.2 (CONTINUED)

	θ^o	$F_{\mu\mu}$	$F_{\mu\alpha}$		θ^o	$F_{\mu\mu}$	$F_{\mu\alpha}$
9-AMINOACRIDINIUM ION							
G....C	175.5	3.5	-3.9	C....G	175.5	3.3	-3.6
DYE	355.5	-3.5	-3.9	DYE	355.5	-3.3	-3.6
G....C				C....G			
A....T	175.5	-1.1	-.7	T....A	175.5	-1.2	-.6
DYE	355.5	1.1	-.7	DYE	355.5	1.2	-.6
A....T				T....A			
12-AMINOBENZ(A)ACRIDINIUM ION							
G....C	88.9	3.0	-5.6	C....G	88.9	-2.3	-4.1
DYE	268.9	-3.0	-5.6	DYE	268.9	2.3	-4.1
G....C				C....G			
A....T	88.9	1.0	-1.3	T....A	88.9	-1.0	-1.1
DYE	268.9	-1.0	-1.3	DYE	268.9	1.0	-1.1
A....T				T....A			
2-AMINOBENZ(B)ACRIDINIUM ION							
G....C	91.6	6.6	-7.5	C....G	91.6	-6.9	-6.0
DYE	271.6	-6.6	-7.5	DYE	271.6	6.9	-6.0
G....C				C....G			
A....T	91.6	2.7	-3.2	T....A	91.6	2.3	-3.0
DYE	271.6	-2.7	-3.2	DYE	271.6	-2.3	-3.0
A....T				T....A			
7-AMINOBENZ(C)ACRIDINIUM ION							
G....C	35.2	-1.5	-6.2	C....G	35.2	-9.1	-5.8
DYE	215.2	1.5	-6.2	DYE	215.2	9.1	-5.8
G....C				C....G			
A....T	35.2	3.3	-2.6	T....A	35.2	.6	-2.6
DYE	215.2	-3.3	-2.6	DYE	215.2	-.6	-2.6
A....T				T....A			

considered, but also on the base pairs adjacent to the dye ion. Thus for 7-aminobenz[c]acridinium ion, the largest negative free energies for $F_{\mu\mu}$ and $F_{\mu\pi}$ are recorded for $\theta = 35.2^{\circ}$ with the dye ion between two C-G base pairs. On the other hand, the 2-aminoacridinium ion gives only small values for $F_{\mu\mu}$ and $F_{\mu\pi}$ with the dye ion between two A-T or T-A base pairs. It may therefore be expected that, since $F_{\mu\mu}$, $F_{\mu\pi}$ and F_{L} are essentially the same for all aminoacridinium and aminobenzacridinium ions, $F_{\mu\mu}$ and $F_{\mu\pi}$ will determine which dye, when intercalated in DNA, will give the highest free energy of interaction (i.e. the most negative value) and hence which dye may be expected to interact with DNA to give the most stable complex.

Liersch and Hartmann[14] concluded that electrostatic forces were responsible for the stability of the DNA-proflavine complex since the dissociation velocity of the complex during gel filtration on Sephadex is greatly increased by high ionic strength. The results in Table 4.1 show that although this is correct for model I, London forces also make a significant contribution to F_{total}. However London forces are less important for model II (Table 4.3).

The calculations for the free energies of

TABLE 4.3

CALCULATED FREE ENERGY VALUES (IN KCAL. PER REPEATING UNIT) FOR EXTERNAL EDGEWISE ATTACHMENT OF DYE (MODEL IIa)

UNIT	$F_{\mu\mu}$	$F_{\mu\alpha}$	F_L	$F_{\rho\mu}$	$F_{\rho\alpha}$	F_{total}
⊖ PF*	.06	-.02	-.10	-3.13	-.48	-.05
⊖ PF*						(ϵ_{ij}=70)
⊖ *				-2.43	-.54	-.04
⊖ PF*						(ϵ_{ij}=70)
⊖				20.4	-17.2	-3.8
⊖ *PF*						(ϵ_{ij}=10)
						-1.1
						(ϵ_{ij}=35)

⊖ REPRESENTS THE NEGATIVE PHOSPHATE GROUP.
* ONLY INTERACTIONS BETWEEN THESE MOLECULES ARE CONSIDERED.
ALL VALUES ARE FOR ϵ_{ij} =1.0 UNLESS STATED OTHERWISE.

interactions involved in the attachment of the dye ions to the phosphate groups in model II show a high degree of dependence on the value of the dipole moment of the attached ion, although the values of $F_{\mu\mu}$ and $F_{\mu\pi}$ are very small, as also is $F_{\rho\mu}$ when account is taken of ϵ'_{ij}, in direct contrast with the results for the intercalated model. The free energy arising from interactions between two dye ions in model IIa is -0.05 Kcals. per repeating unit while for model IIb these interactions are even smaller. The second rows of Table 4.3 are, however, still applicable for model IIb.

The distance between the centre of the dye ion and a base in model II, even if the dye ion is tilted inwards towards a base, is between about 7.5 and 10.5 Å. The maximum free energy for the interactions between the dye ion and the dipole moment and polarizability of the nearest base will be either about -0.6 or -1.0 Kcals., depending on the orientation of the dye ion and whether the base considered is A or T, or G or C, respectively. For this estimate ϵ_{ij} was taken as 10, since although the ion distance is large, not all of the volume between the bound dye and the base may be occupied by solvent molecules.

The free energy values for model IIa quoted

in Table 4.3 are the same for all base sequences. The total free energy with the value of ϵ'_{ij} equal to 10 is -3.9 Kcals. per repeating unit for model IIa and is only -0.05 Kcals. per repeating unit less for model IIb for which dye-dye interactions are not considered.

4.8 Discussion.

The decrease in the free energy, ΔF, for the reaction

DNA repeating unit + dye → DNA repeating unit-dye (4.1)

for different base sequences with proflavine for both models is given in Table 4.4. The results indicate that the free energy for both models is more negative than that of DNA alone, although that for model I is more negative than that for model IIa. For model I, the order of increased stabilization is AT:TA > AT:AT >TA:AT >TA:GC > AT:GC > AT:CG > GC:CG > TA:CG > GC:GC > CG:GC. Thus the base sequence with the most positive free energy in DNA alone is stabilized the most in the DNA-proflavine complex. However, for model IIa and $\epsilon'_{ij} = 10$, $\Delta F = -3.9$ Kcals. per repeating unit and does not depend on base sequence. If the bound dye ion is tilted inwards towards a base, ΔF becomes about -4.5 or -4.9 Kcals. per repeating unit, depending on whether the dye ion is

TABLE 4.4

COMPARISON OF CALCULATED FREE ENERGY VALUES (IN KCAL. PER REPEATING UNIT) FOR NATIVE DNA, MODEL I AND MODEL II a.

REPEATING UNIT	DE VOE AND TINOCO(1962) FOR NATIVE DNA $\epsilon_{ij}=1.0$	PROFLAVINE INTERCALATED (MODEL I) $\epsilon_{ij}=1.0$		EXTERNAL ATTACHMENT OF PROFLAVINE (MODEL II a) $\epsilon'_{ij}=10$		$\epsilon'_{ij}=35$	
	F_{total}	F_{total}	ΔF	F_{total}	ΔF	F_{total}	ΔF
CG GC	-35.7	-48.3	-12.6	-39.6	-3.9	-36.9	-1.2
GC GC	-19.9	-48.0	-28.1	-23.8	-3.9	-21.1	-1.2
TA CG	-20.5	-55.3	-34.8	-24.4	-3.9	-21.7	-1.2
AT CG	-13.7	-55.3	-41.6	-17.6	-3.9	-14.9	-1.2
AT GC	-12.9	-55.2	-42.3	-16.8	-3.9	-14.1	-1.2
TA GC	-12.5	-55.2	-42.7	-16.4	-3.9	-13.7	-1.2
GC CG	-7.5	-48.2	-40.7	-11.4	-3.9	-8.7	-1.2
TA AT	-10.6	-62.7	-52.5	-14.1	-3.9	-11.8	-1.2
AT AT	-10.2	-62.7	-52.5	-14.1	-3.9	-11.4	-1.2
AT TA	-3.4	-62.6	-59.2	-7.3	-3.9	-4.6	-1.2

THE REPEATING UNIT SHOWN IS FOR DNA. THOSE FOR THE DNA-PROFLAVINE COMPLEXES ARE THOSE INDICATED IN FIG. 4.3 WITH THE APPROPRIATE BASE PAIRS. SEE TEXT FOR EXPLANATION OF THE VALUES CHOSEN FOR ϵ_{ij} AND ϵ'_{ij}.

associated with an A or T base or a G or C base, respectively. The free energy for the modified version of model IIa therefore implies that GC sites bind dye slightly more strongly than AT sites. The experimental evidence obtained by Tubbs et al[7] from measurements of fluorescence quenching of DNA-acriflavine solutions suggested that the relative affinity of acriflavine for possible binding sites in DNA was AT:AT > AT:GC > GC:GC in agreement with the sequence predicted theoretically above for model I for the DNA-proflavine system. Hence only model I may be used to explain this relative affinity of binding sites.

The change in free energy, ΔF, which accompanies reaction 4.1 for other acridine dyes on intercalation is given in Table 4.5 for three typical selected base sequences. The free energy of interaction of adjacent dye ions has not been included. In this Table, ΔF has been quoted for both possible angles (θ and $180^\circ+\theta$ of Fig. 4.1), thus listing both the more favourable and less favourable values of ΔF obtained for each dye. However, in Table 4.4, only the values of ΔF corresponding to $\theta = 175.5^\circ$ were quoted, since this angle gave rise to the more positive and therefore less favourable values of F and hence of ΔF (see Table 4.1 (a)). The less

TABLE 4.5

THE DECREASE IN FREE ENERGY, ΔF, (IN KCAL PER REPEATING UNIT) WHICH ACCOMPANIES INTERCALATION OF A CHARGED DYE ION BETWEEN THE SELECTED BASE-PAIRS SHOWN.

	BASE SEQUENCE GC GC	AT GC	AT AT	θ^{o}
PROFLAVINE	-27.3	-41.5	-51.7	175.5
	-38.1	-45.1	-48.1	355.5
1-AMINOACRIDINE	-27.4	-39.8	-48.2	174.3
	-32.4	-41.5	-46.6	354.3
2-AMINOACRIDINE	-29.9	-40.3	-46.8	62.5
	-30.9	-41.3	-47.8	242.5
3-AMINOACRIDINE	-29.5	-39.9	-46.3	61.8
	-32.1	-42.6	-49.1	241.8
4-AMINOACRIDINE	-26.3	-39.1	-48.0	149.4
	-34.3	-42.6	-47.0	329.4
9-AMINOACRIDINE	-26.1	-39.2	-48.3	175.5
	-33.1	-41.6	-46.1	355.5
12-AMINOBENZ(A)ACRIDINE	-30.4	-41.6	-48.9	88.9
	-36.4	-45.6	-50.9	268.9
2-AMINOBENZ(B)ACRIDINE	-28.7	-40.9	-49.1	91.6
	-41.9	-50.2	-54.5	271.6
7-AMINOBENZ(C)ACRIDINE	-35.5	-43.7	-47.9	35.2
	-32.5	-45.5	-54.5	215.2

favourable values of ΔF were discussed for proflavine since the purpose of the results and discussion of this Chapter was to decide whether intercalation gave rise to a significantly more negative free energy of interaction than did external edgewise binding. Since these values of ΔF for the intercalated model were more negative than those for model IIa, then the more favourable ΔF values, listed in Table 4.5 but not in Table 4.4, would give rise to an even greater free energy of interaction.

The values of ΔF in Table 4.5 indicate that the relative values of ΔF for various base sequences with intercalation of other acridine dyes are similar to those with intercalation of proflavine. However, it is evident that several of the dyes (for example, 2-aminoacridine) have high values of ΔF and may therefore be expected to interact more strongly with DNA than other dyes with low values of ΔF (for example, 2-aminoacridine). The relative strength of binding of various dyes to DNA will be discussed with reference to this Table in later Chapters.

The values of the free energy of interaction between two adjacent intercalated dye ions were not included in the calculation of ΔF in Table 4.5 since,

when a comparison between dyes is involved, a knowledge of the exact base sequence of DNA is necessary before it is known whether the angle between dye dipole moments will be 171° or 351°, depending on which orientations are most favourable for a given base sequence and that adjacent to it. The values for F_{total} for the dye-dye interactions (corresponding to those in Table 4.1 (b)) are quoted in Table 4.6 for the different dyes, and for the two possible angles of orientation of one dye dipole moment relative to the other. It is evident that, for dyes which already have high ΔF values (Table 4.5), a high value of F_{total} is found in Table 4.6. The converse also appears to hold. This has the effect that, depending on the exact base sequence of the DNA, it is possible that the total change in free energy when intercalation occurs may become still more negative than already indicated in Table 4.5 to a greater extent for some dyes than for others.

The above calculations for the intercalated model apply only to $r = 0.5$, where all of the sites for intercalation have been used. Thus for $r > 0.5$, binding to the outside of the helix must also occur. Because of the left-handed helix formed for the intercalated model, two dye ions attached to the outside of the helix will be at an angle of 9° with respect to each other.

TABLE 4.6

VALUES OF F_{total} (IN KCAL PER REPEATING UNIT) FOR THE INTERACTION BETWEEN ADJACENT DYE IONS (SEPARATED BY A BASE PAIR) FOR THE INTERCALATED MODEL.

	ANGLE BETWEEN DYE DIPOLE MOMENTS	
	17°	35°
PROFLAVINE	-0.8	-2.5
1-AMINOACRIDINE	-1.2	-1.6
2-AMINOACRIDINE	-1.3	-1.4
3-AMINOACRIDINE	-1.0	-1.6
4-AMINOACRIDINE	-1.1	-1.7
9-AMINOACRIDINE	-1.0	-1.8
12-AMINOBENZ(A)ACRIDINE	-1.5	-2.0
2-AMINOBENZ(B)ACRIDINE	+0.9	-3.7
7-AMINOBENZ(C)ACRIDINE	-0.2	-3.4

The centres of the two ions are found to be about 7 Å apart, the plane of one dye being 6.72 Å above the plane of the other. However for native DNA with external attachment of the dye to adjacent phosphate groups on the one helix, owing to the larger angle of 36° between the two dye ions, the distance between the centre of these molecules is 9.4 Å. The distance between the centres of two externally bound dye ions is thus greater for native DNA than for DNA with the maximum number of intercalated dye ions. Thus the interaction forces will be smaller for dye bound to native DNA than for dye bound externally to DNA extended by the maximum amount of intercalated dye. Furthermore, because of the greater distance in native DNA, the amount of associated water will be increased and the value of ϵ_{ij} will be larger; this will also have the effect of decreasing the interactions. However these effects will be small, as it has already been shown (Table 4.3) that the contribution of dye-dye interactions to the stability of model IIa is very small.

The orientation of the dye ion in the intercalated model at 4.5° to both the adjacent base pairs (i.e. that above and that below the dye molecule, see Plate 4.1) favours the exclusion of water molecules and hence gives the maximum interaction. Other orientations

would allow water molecules to penetrate the helix; the effective dielectric constant would then be increased and the energies of interaction would become less negative.

From dye binding studies, Peacocke and Skerrett[15] obtained a value of 8 Kcal. per mole of bound dye for the standard free energy of association of herring sperm DNA and proflavine, and Chambron et al[16] obtained a value of 7.4 Kcal. per mole for calf thymus DNA and proflavine. Suter[17] deduced a value of 9.5 Kcal. per mole for the association of acriflavine and nucleic acids. From Table 4.4 the change in free energy calculated for the intercalated model varies between -12.6 and -39.2 Kcals. per repeating unit depending on the base sequence and is constant at -3.9 Kcals. per repeating unit for external attachment of the dye ions with $\epsilon'_{ij} = 10$. In view of the assumptions made the agreement between the calculated and the observed values, the latter being average values over all binding sites for the particular DNA studied, is regarded as satisfactory. It is to be emphasized that any refinements to the calculations for the intercalated model are likely to make the values of the interaction energies calculated less negative.

A value of -0.065 Kcals. per mole of dye for the attraction between two bound dye ions was found from the tendency of acridine orange ions to stack on native DNA[18] and represents an average value for this interaction. Tables 4.1 (b) and 4.3 yield values of either -0.8 or -2.5 Kcals. per mole of dye for the intercalated model for the interaction between two proflavine ions depending on the relative orientations of the two ions, and -0.05 Kcals. per mole for model IIa, respectively. Values for the interaction free energy between two intercalated dye ions for other acridine dyes are given in Table 4.6. For model IIa the agreement between the calculated and experimental values for the free energy of interaction between two dye ions, is good. However, for model I, extreme values of binding must be taken in order to compare the calculated and experimental values.

The above values calculated for the interaction between adjacent proflavine ions in model I will become about -0.16 or -0.5 Kcals. per mole of dye respectively if an average effective dielectric constant of 5 is chosen. If we consider for example, intercalation of the dye up to r = 0.22 with edgewise binding occurring at higher values of r, then for r < 0.22 the

free energy of interaction between two dye ions will be -0.16 or -0.5 Kcals. per mole of dye, but for r = 1.0 it will be -0.72 or -0.140 Kcals. per mole of dye, depending on the relative orientation of the dye ions. Since the value of -0.065 Kcals. per mole of dye obtained experimentally is an average for all methods of binding and all binding sites, the calculations indicate that the intercalated model is compatible with the experimental results. Although the intercalated model is being considered here, the free energy of interaction between two adjacent dye ions attached externally has been taken as -0.05 Kcals. per mole of dye, i.e. the value for model IIa. However, this is not a significant approximation.

For the above experimental value for the free energy of interaction between two dye ions bound to DNA, the values of the stacking coefficient, K, was taken as 1.25 [18] which is an average value obtained using several samples of DNA with varying GC contents. For calf thymus DNA (GC content = 42%) an average value of 1.14 was obtained for K, while for bacteriophage T4 DNA (GC content = 35%) a value of 1.33 was given. The values of the free energy of interaction between two dye ions corresponding to these values of K are -0.039 and -0.085 Kcals. per

mole of dye, respectively. The significant feature of these results for the interaction of two adjacent dye ions is that a decrease in free energy occurs with a decrease in GC content. In view of the interpretation suggested above in terms of model I for the strong mode of binding which occurs up to r = 0.22 for calf thymus DNA observed by Peacocke and Skerrett,[15] it is expected that for a given ionic strength and pH a higher value of r will be reached before the very weak binding predominates for DNA of lower GC content. Furthermore, the average free energy of association of dye with DNA will become more negative with decreasing GC content, and also, since more intercalation is possible because of the higher AT content, the experimental value for the free energy of interaction between adjacent dye ions will include a greater contribution from interactions between two intercalated dye ions. Thus the free energy for dye-dye interaction is expected to decrease (i.e. become more negative) with decreasing GC content. The above results for this free energy, calculated from values of K quoted by Stone and Bradley[18] for samples of DNA with different GC contents support this conclusion.

References.

1. Lerman, L.S., J.Mol.Biol. 3, 18 (1961).

2. Lerman, L.S., Proc.Nat.Acad.Sci.,Wash. 49, 94(1963).

3. Bradley, D.F. and Wolf, M.K., Proc.Nat.Acad.Sci., Wash. 45, 944 (1959).

4. Mason, S.F. and McCaffery, A.J., Nature 204, 468 (1964).

5. Gersch, M.F. and Jordan, D.O., J.Mol.Biol. 13, 138 (1965).

6. De Vos, H. and Tinoco, I., J.Mol.Biol. 4,500 (1962).

7. Tubbs, R.K., Ditmars, W.E. and Van Winkle, Q., J.Mol.Biol. 9, 545 (1964).

8. Fajans, K., In "Technique of Organic Chemistry", Ed. Weissberger, A., Vol.1, Part 2, p 1169 New York, Interscience (1959).

9. Langridge, R., Marvin, D.A., Seeds, W.E., Wilson, H., Hooper, C.W. and Wilkins, M.H.F., J.Mol.Biol. 2, 38 (1960).

10. Rice, S.A. and Nagasawa, M., "Polyelectrolyte Solutions", New York,Academic Press (1961).

11. Hasted, J.B., Ritson, D.M. and Collie, C.H., J.Chem.Phys. 16, 1 (1948).

12. Pullman, B., Claverie, P. and Caillet, J., Science 147, 1305 (1965).

13. Pullman, B., Claverie, P. and Caillet, J. C.R.Acad.Sci.,Paris 260, 5915 (1965).

14. Liersch, M. and Hartmann, G., Biochem.Z. 340, 390 (1964).

15. Peacocke, A.R. and Skerrett, J.N.H., Trans.Faraday Soc. 52, 261 (1956).

16. Chambron, J., Dunne, M. and Sadron, C., C.R.Acad.Sci.,Paris 258, 4867 (1964).

17. Oster, G., Trans.Faraday Soc. 47, 660 (1951).

18. Stone, A.L. and Bradley, D.F., J.Am.Chem.Soc. 83, 3627 (1961).

CHAPTER 5.

BINDING CURVES FOR DNA-DYE SYSTEMS.

5.1 Introduction.

The binding of small ions or molecules to a long polymer with n available homogeneous binding sites may be described by[1]

$$\frac{r}{c} = kn - kr \qquad (5.1)$$

where r is the number of occupied sites, c is the molar concentration of unbound small ions or molecules, and k is the intrinsic binding constant. When purely electrostatic interactions occur between bound ions or molecules, this becomes[2]

$$\frac{r}{c} e^{2wr} = kn - kr \qquad (5.2)$$

where w may be regarded as a parameter chosen by curve fitting for the system under consideration.

If p distinct types of binding sites are present, and n_i and k_i are the number of available binding sites and intrinsic binding constant, respectively, for each type of binding site, then equation 5.1 becomes

$$r = \sum_{i=1}^{p} \frac{n_i k_i c}{1+k_i c} \qquad (5.3)$$

In early quantitative studies of dye binding to DNA it was found that the data could not be analysed by using equation 5.2. [3] However, the experimental r/c against r curves could be fitted by assuming two different binding sites with binding constants k_1 and k_2 according to equation 5.3. Subsequent studies have added additional evidence for two distinct binding processes of aminoacridines to DNA.[4-6] One of these processes results in strong binding of the aminoacridine to DNA up to a value of r = 0.22 for proflavine, for example, and the other process results in weaker binding, predominant from r = 0.22 to r = 1.0. [5]

No binding studies of aminobenzacridines with DNA have been presented in the literature and, because of the similarity in structure between the aminobenzacridines and the aminoacridines on one hand, and the polycyclic hydrocarbons on the other, it was therefore of interest to extend the binding studies to DNA-

aminobenzacridine systems for comparison with other similar systems.

5.2 Spectral Changes in Dye Spectra on Binding to DNA.

An alteration of the spectrum of a dye in the presence of nucleic acids is well known, and has often been used to study the binding processes involved. The peaks and extinction coefficients of the visible spectra of several acridines with and without DNA have been listed in Table 5.1. As many acridines do not obey Beer's Law over certain concentration ranges,[7] the maximum concentration for which each dye obeys Beer's Law has been quoted where possible, or the maximum concentration tested is quoted. For example, in the Table, $> 12.3 \times 10^{-5}$M for 2-aminoacridine means that Beer's Law was found to hold up to this concentration, but may also be applicable at higher concentrations not studied in this work.

The main discrepancies between the values quoted in Table 5.1 appear in the extinction coefficients of the dyes in the absence of DNA. For the 357-359 mμ peak of 2-aminoacridine, for example, an extinction coefficient of 1.05×10^4 was found,

TABLE 5.1

SPECTRAL DATA FOR AMINOACRIDINES AND AMINOBENZACRIDINES WITH AND WITHOUT DNA.

	pH, SOLUTION†	CONC. DYE ($\times 10^5$ M)	CONC. DNA ($\times 10^5$ M)	POSITION OF PEAK *	($\lambda m\mu$)	ϵ $\times 10^{-4}$	BEERS LAW ($\times 10^5$ M)	REF.
2-AMINOACRIDINE	4.6, .001M	4.91	–	A	359	1.05	>12.3	THIS
	4.6, .001M	4.91	–	B	371	1.45	>12.3	THIS
	4.6, .001M	4.91	–	C	460	.68	>12.3	THIS
	7.0, .1MP	<3.0	–	A	357	.62	–	8
	3.0, Y		–		345	.40	–	10
	3.0, Y		–		414	.66	–	10
	4.6, .001M	4.73	2.32	B	371	1.35	–	THIS
	4.6, .001M	4.65	10.6	B	372	1.07	–	THIS
	5.0, .001M	4.62	20.7	B	373	.89	–	THIS
	4.6, .001M	4.73	2.32	C	465	.60	–	THIS
	4.6, .001M	4.65	10.6	C	470	.50	–	THIS
	5.0, .001M	4.62	20.7	C	493	.46	–	THIS
	7.0, .1MP	<3.0	0.5%	A	372	.37	–	8
	ISOBESTIC POINTS OCCUR AT 380, 400 AND 494 $m\mu$.							THIS

* THE PEAKS OF EACH SPECTRUM HAVE BEEN LABELLED A, B, AND C AS REQUIRED, FOR SIMPLICITY IN DETERMINING THE EFFECT OF DNA ON A PARTICULAR PEAK.

† THE CONCENTRATIONS .1M AND .001M REFER TO SODIUM CHLORIDE SOLUTION, WHILE P REFERS TO PHOSPHATE BUFFER, X TO ACETATE BUFFER, AND Y TO A SOLUTION OF POTASSIUM HYDROGEN PHTHALATE AND HCl IN 67% METHYL ALCOHOL.

TABLE 5.1 (CONTINUED)

	pH, SOLUTION	CONC. DYE ($\times 10^5$ M)	CONC. DNA ($\times 10^5$ M)	POSITION OF PEAK ($\lambda m\mu$)	ϵ $\times 10^{-4}$	BEERS LAW ($\times 10^5$ M)	REF.
3-AMINOACRIDINE	5.9, .1M	1.96	–	A 352	.89	>6.0	THIS
	5.9, .1M	1.96	–	B 367.6	1.20	>6.0	THIS
	5.9, .1M	1.96	–	C 456.6	1.11	>6.0	THIS
	7.0, .1MP	<3.0	–	B 366	1.40	–	8
	7.0, .1MP	<3.0	–	C 454	1.19	–	8
	4.0, –		–	–	–	7.5	7
	3.0, Y		–	349	.40	–	10
	3.0, Y		–	418	.71	–	10
	5.9, .1M	2.26	1.55	A 352	.85	–	THIS
	5.9, .1M	2.26	1.55	B 367.6	1.11	–	THIS
	5.9, .1M	1.65	13.7	B 367.6	.63	–	THIS
	5.9, .1M	3.02	46.5	B 370	.41	–	THIS
	5.9, .1M	2.26	1.55	C 456.6	1.00	–	THIS
	5.9, .1M	1.65	13.7	C 468	.78	–	THIS
	5.9, .1M	3.02	46.5	C 468	.68	–	THIS
	7.0, .1MP	<3.0	0.5%	B 373	.76	–	8
	7.0, .1MP	<3.0	0.5%	C 470	.92	–	8
	ISOBESTIC POINTS OCCUR AT 375 AND 483 $m\mu$.						THIS

TABLE 5.1 (CONTINUED)

	pH, SOLUTION	CONC. DYE ($\times 10^5$ M)	CONC. DNA ($\times 10^5$ M)	POSITION OF PEAK ($\lambda m\mu$)	ϵ $\times 10^{-4}$	BEERS LAW ($\times 10^5$ M)	REF.
9-AMINOACRIDINE	5.9, .1M	16.5	–	A 381	.65	24.0	THIS
	5.9, .1M	16.5	–	B 400.5	.98	24.0	THIS
	5.9, .1M	16.5	–	C 423	.78	24.0	THIS
	7.0, .1MP	<3.0	–	B 402	.97	–	8
	4.0, –	–	–	–	–	>13.5	7
	6.9, .1MP	9.34	–	A 382	.59	–	6
	6.9, .1MP	9.34	–	B 401	.89	–	6
	6.9, .1MP	9.34	–	C 423	.71	–	6
	3.0, Y		–	390	.71	–	10
	6.2, .001M	4.94	2.34	A 383	.49	–	THIS
	5.8, .001M	4.78	10.1	A 387.5	.42	–	THIS
	6.2, .001M	4.96	20.3	A 388	.34	–	THIS
	6.5, .001M	4.94	40.6	A 388	.33	–	THIS
	6.2, .001M	4.94	2.34	B 401	.72	–	THIS
	5.8, .001M	4.78	10.1	B 402	.60	–	THIS
	6.2, .001M	4.96	20.3	B 406.5	.49	–	THIS
	6.5, .001M	4.94	40.6	B 407.5	.50	–	THIS
	6.2, .001M	4.94	2.34	C 423	.58	–	THIS
	5.8, .001M	4.78	10.1	C 425	.48	–	THIS
	6.2, .001M	4.96	20.3	C 430	.40	–	THIS
	6.5, .001M	4.94	40.6	C 430	.43	–	THIS
	6.9, .1MP	9.34	50.0	A 387	.32	–	6
	6.9, .1MP	9.34	50.0	B 407	.48	–	6
	6.9, .1MP	9.34	50.0	C 430	.41	–	6
	7.0, .1MP	<3.0	0.5%	B 408	.49	–	8
	7.0, .1MP	<3.0	.05%	B 403	.70	–	8
	7.0, .1MP	<3.0	.005%	B 408	.52	–	8
	ISOBESTIC POINT OCCURS AT 429 $m\mu$.						THIS
	ISOBESTIC POINT OCCURS AT 428 $m\mu$.						6

TABLE 5.1 (CONTINUED)

	pH, SOLUTION	CONC. DYE ($\times 10^5$ M)	CONC. DNA ($\times 10^5$ M)	POSITION OF PEAK	($\lambda m\mu$)	ϵ $\times 10^{-4}$	BEERS LAW ($\times 10^5$ M)	REF.
3,6-DIAMINOACRIDINE	5.8, .1M	1.53	–	A	444	4.10	2.8	THIS
	4.0, –	–	–			–	>45.0	7
	4.0, .05MX	<5.0	–	A	444	4.10	5.0	11
	3.0, Y	–	–			2.80	–	10
	4.0, –	<6.0	–	A	444	3.34	6.0	9
	7.0, .1MP	<3.0	–	A	443	2.90	–	8
	6.2, .1MP	1.42	–	A	440	3.91	2.5	5
	6.2, .1M	1.61	1.55	A	448	3.23	–	THIS
	6.2, .1M	1.17	13.7	A	461	2.82	–	THIS
	6.2, .1M	1.28	46.5	A	463	2.75	–	THIS
	7.0, .1MP	<3.0	0.5%	A	464	2.91	–	8
	7.0, .1MP	<3.0	0.05%	A	462	2.60	–	8
	7.0, .1MP	<3.0	0.005%	A	456	2.89	–	8
	ISOBESTIC POINT OCCURS AT 456 $m\mu$.							THIS
	ISOBESTIC POINT OCCURS AT 454 $m\mu$.							5
12-AMINOBENZ(A)ACRIDINE	5.6, .001M	3.64	–	A	362.5	.96	14.5	THIS
	5.6, .001M	3.64	–	B	386	.91	14.5	THIS
	5.6, .001M	3.64	–	C	405	.76	10.0	THIS
	6.2, .001M	3.67	2.56	A	365	.71	–	THIS
	6.1, .001M	3.64	10.0	A	370	.71	–	THIS
	6.0, .001M	3.53	20.4	A	370	.71	–	THIS
	6.2, .001M	3.67	2.56	B	388	.62	–	THIS
	6.1, .001M	3.64	10.0	B	390	.60	–	THIS
	6.0, .001M	3.53	20.4	B	390	.59	–	THIS
	6.2, .001M	3.67	2.56	C	407	.52	–	THIS
	6.1, .001M	3.64	10.0	C	412	.46	–	THIS
	6.0, .001M	3.53	20.4	C	413	.45	–	THIS
	ISOBESTIC POINT OCCURS AT 415 $m\mu$.							THIS

TABLE 5.1 (CONTINUED)

	pH, SOLUTION	CONC. DYE ($\times 10^5$ M)	CONC. DNA ($\times 10^5$ M)	POSITION OF PEAK ($\lambda m\mu$)		ϵ $\times 10^{-4}$	BEERS LAW ($\times 10^5$ M)	REF.
2-AMINOBENZ(B)ACRIDINE	5.0, .001M	2.69	–	A	385	.75	13.3	THIS
	5.0, .001M	2.69	–	B	430	.61	13.3	THIS
	5.0, .001M	2.69	–	C	550	.41	13.3	THIS
	4.9, .001M	3.32	2.39	A	385	.65	–	THIS
	5.2, .001M	3.44	10.5	A	390	.66	–	THIS
	5.4, .001M	3.47	20.3	A	392.5	.67	–	THIS
	4.9, .001M	3.32	2.39	B	430	.53	–	THIS
	5.2, .001M	3.44	10.5	B	460	.51	–	THIS
	5.4, .001M	3.47	20.3	B	460	.51	–	THIS
	4.9, .001M	3.32	2.39	C	550	.38	–	THIS
	5.2, .001M	3.44	10.5	C	582	.33	–	THIS
	5.4, .001M	3.47	20.3	C	585	.33	–	THIS
	ISOBESTIC POINT OCCURS AT 440 $m\mu$.							
7-AMINOBENZ(C)ACRIDINE	6.1, .001M	3.36	–	A	376	.63	10.5	THIS
	6.1, .001M	3.36	–	B	393	1.09	10.5	THIS
	6.1, .001M	3.36	–	C	413	1.05	4.0	THIS
	6.1, .001M	3.60	2.29	A	376	.56	–	THIS
	6.5, .001M	3.56	10.1	A	381	.39	–	THIS
	6.6, .001M	3.60	19.9	A	381	.66	–	THIS
	6.1, .001M	3.60	2.29	B	394	.81	–	THIS
	6.5, .001M	3.56	10.1	B	400	.60	–	THIS
	6.6, .001M	3.60	19.9	B	399	.69	–	THIS
	6.1, .001M	3.60	2.29	C	413	.83	–	THIS
	6.5, .001M	3.56	10.1	C	422	.58	–	THIS
	6.6, .001M	3.60	19.9	C	421	.41	–	THIS
	ISOBESTIC POINT OCCURS AT 421 $m\mu$.							THIS

but Northland *et al*[8] quoted a value of 0.62×10^4 for the same extinction coefficient. For the single peak of proflavine at 444 nm, similar discrepancies are found in the extinction coefficient, the values varying from 2.80 to 4.10×10^4 (Table 5.1). The reasons for such discrepancies involve mainly the practical aspects of spectroscopy of these dyes. Proflavine (3,6-diaminoacridine) undergoes rapid photoreduction, although 2-, 3-, and 9-aminoacridine do not.[9] Thus if proflavine solutions are exposed to the light for unnecessarily long periods of time before measurements are made, the extinction coefficient is found to be too low. In addition, the dyes were found to be all readily adsorbed on the containing vessel, particularly if this was soft glass. It was also found that a small amount of dye was adsorbed on the silica cell used for spectrophotometry. Therefore the cells were well rinsed with dye solution before the spectral measurements were taken. The method of storing dye solutions is discussed in more detail in Chapter 8.

The magnitude of the alteration of the spectra of the various dyes in the presence of DNA found in the present study appears to be comparable to that observed

by other workers (Table 5.1). A red shift is observed, which may be attributed to the interactions of the ring system of the bound acridine with the bases of the DNA.[6,12] This is in contrast with a blue shift in the visible spectrum, observed, for example, with DNA-acridine orange[12] and DNA-resaniline[13] systems at low DNA/dye ratios. The blue shift may result from dye-dye interactions.[12] Experiments with DNA-proflavine systems have indicated that no blue shift is recorded at any DNA/dye ratio. However, for the polyanion heparin and proflavine, a blue shift of 13 mμ is observed for a heparin/dye ratio of about 2.5, indicating that under certain conditions (including closer inter-site spacing along the polyanion) dye-dye interactions leading to a blue shift in the spectrum may occur.[14]

The spectrum of 2-aminoacridine in the presence of different concentrations of DNA is shown in Fig. 5.1. Three isobestic points are observed at 380, 400 and 494 mμ, as well as a decrease in extinction coefficient and a red spectral shift. The presence of isobestic points implies that only one spectrally distinct DNA-dye complex has been formed.

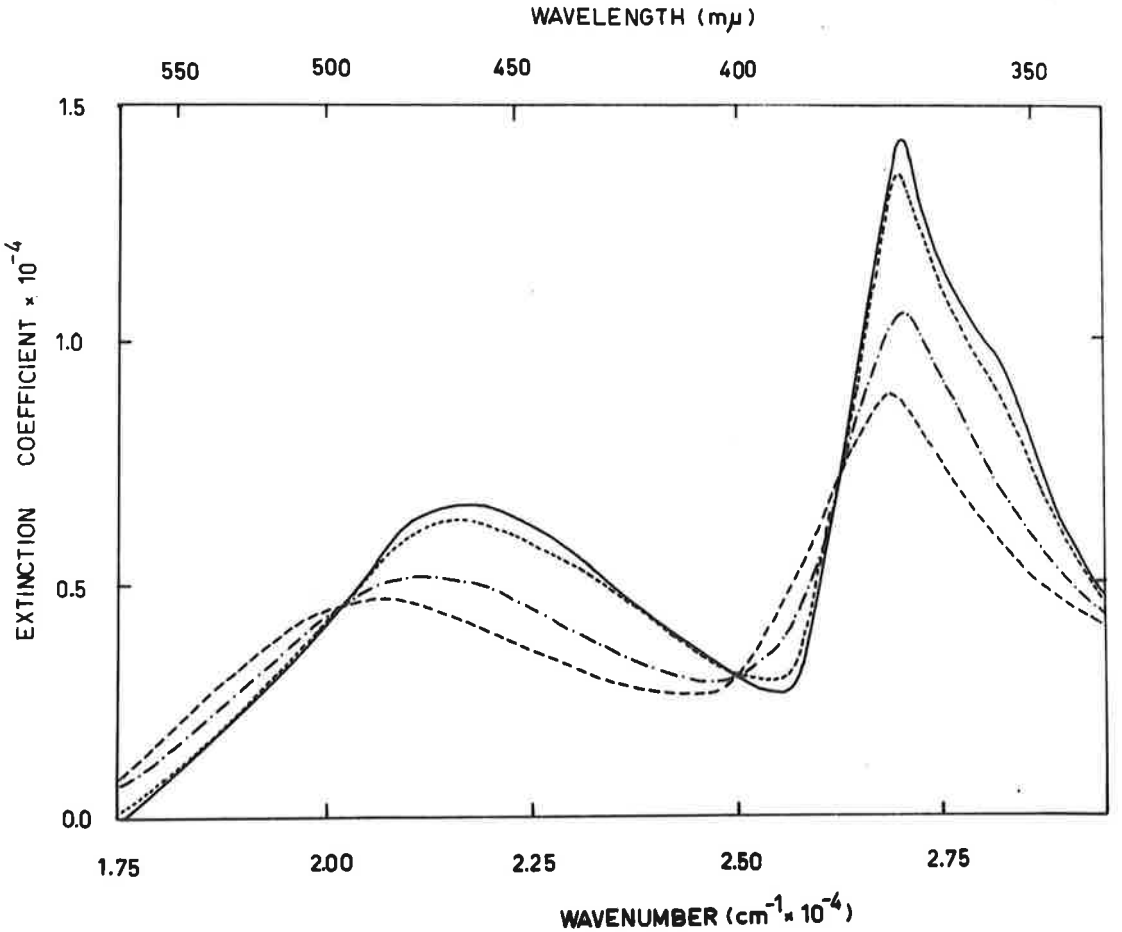

FIG. 5.1. The spectrum of 2-aminoacridine with and without DNA, at a dye concentration of 4.67×10^{-5}M in 0.001M NaCl and average pH of 4.8 at 20°C. ——, dye alone; - - -, with 2.32×10^{-5}M DNA; —·—·—·, with 10.6×10^{-5}M DNA; — — —, with 20.7×10^{-5}M DNA.

However, as the pH of the solutions used for these spectra was between 4.6 and 5.0, the results cannot be simply interpreted in terms of dye binding to native DNA, as denaturation of DNA begins at a pH below about 5.5 for 0.001M sodium chloride solutions.[15] The fact that isobestic points are still observed when native and partially denatured DNA are both present indicates that the binding process giving rise to the spectrally distinct species is the same for both native and partially denatured DNA.

A similar red spectral shift and decrease in extinction coefficient in the presence of DNA is observed with 12-aminobenz[a]acridine (Fig. 5.2) and with 7-aminobenz[c]acridine (Fig. 5.3). For simplicity only two spectra are drawn for each of these dyes. Isobestic points are also present at 415 mμ and 421 mμ, respectively.

5.3 Binding Curves for DNA-dye Systems.

Quantitative information about the binding of dyes to DNA may be obtained from spectral shifts by applying the following equation[16]

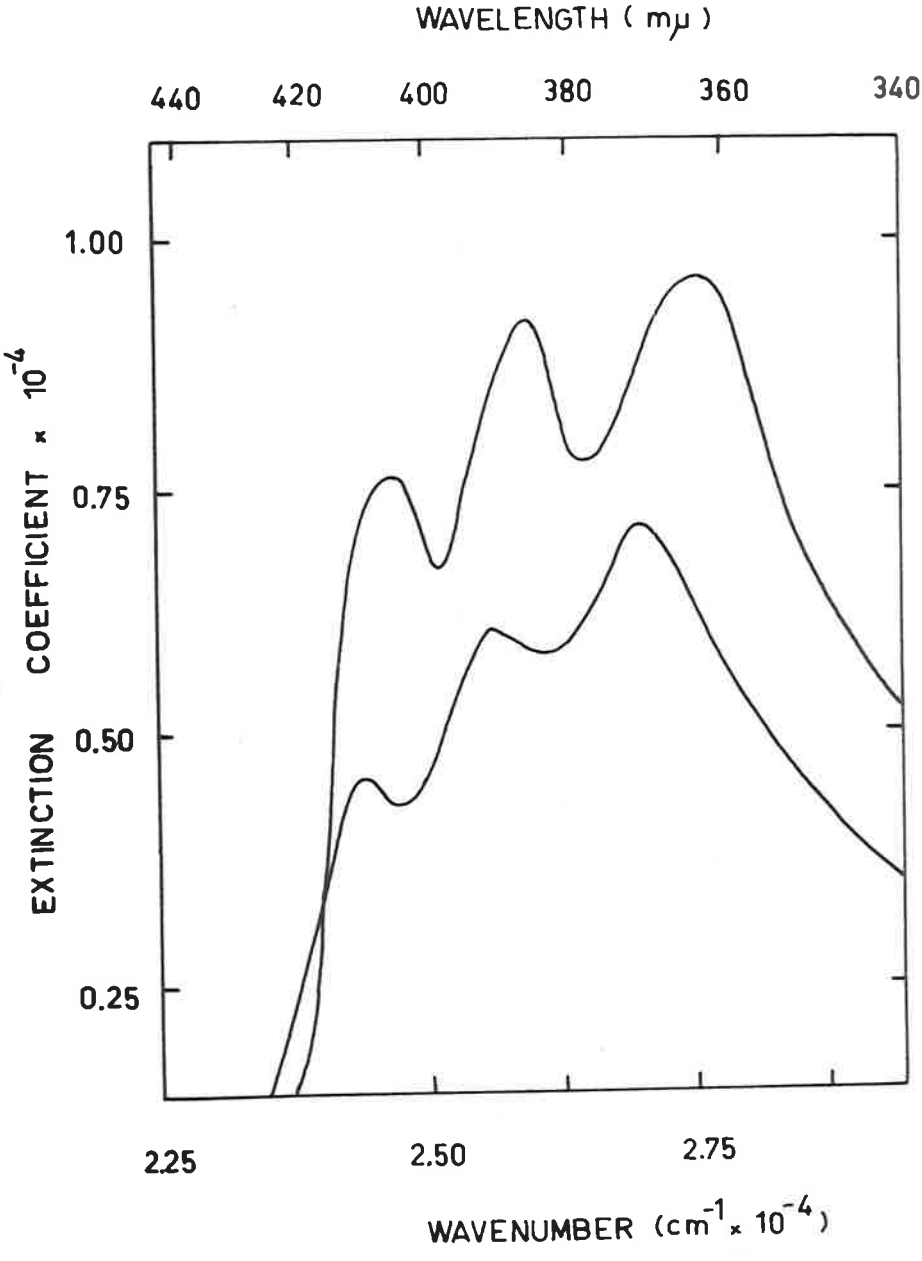

FIG. 5.2. The spectrum of 12-aminobenz[a]acridine with and without DNA, at a dye concentration of 3.64×10^{-5}M in 0.001M NaCl and average pH of 6.1 at 20°C. Upper curve: dye alone; lower curve: with 10.0×10^{-5}M DNA.

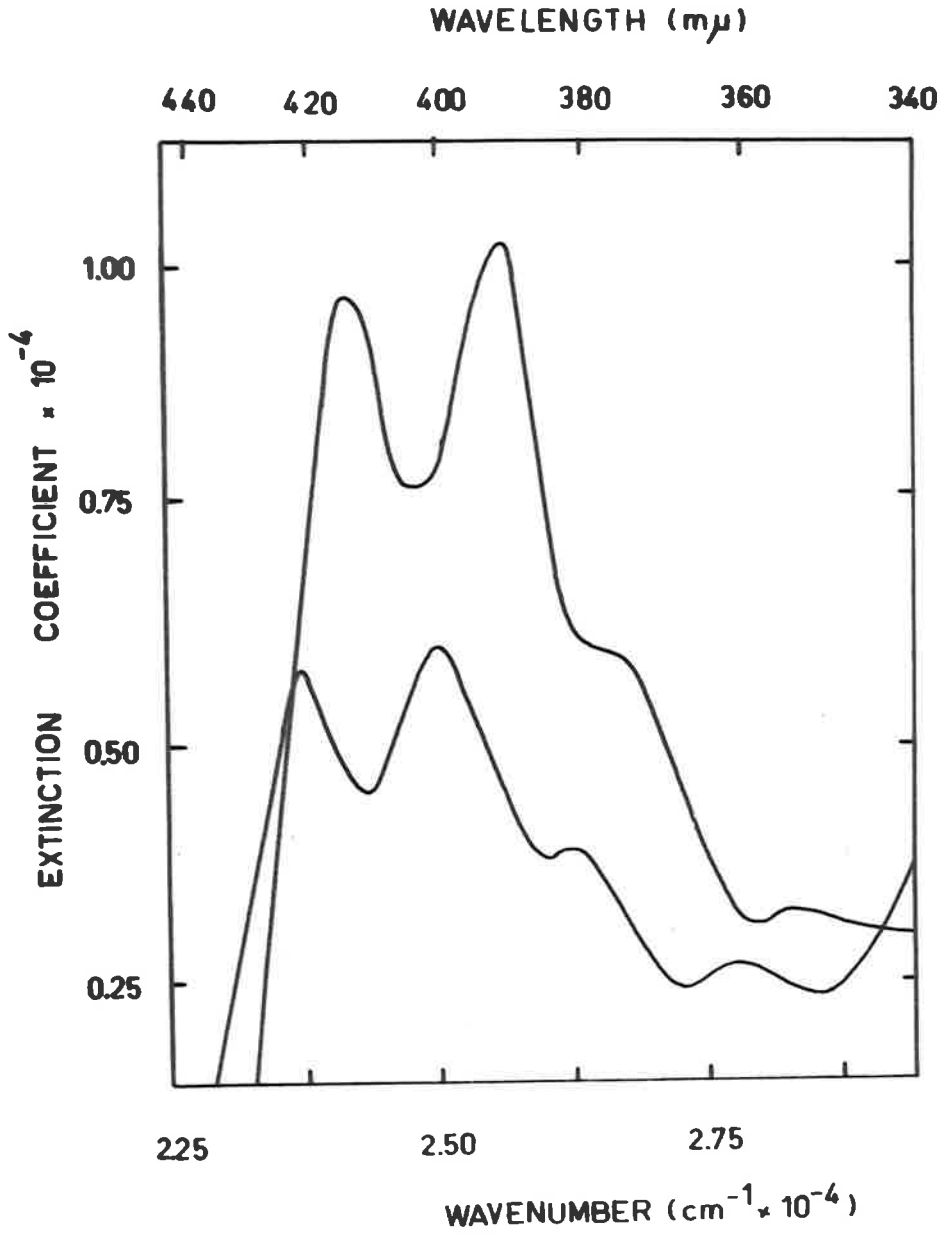

FIG. 5.3. The spectrum of 7-aminobenz[c]acridine with and without DNA, at a dye concentration of 3.55×10^{-5}M in 0.001M NaCl and average pH of 6.2 at 20°C. Upper curve: dye alone; lower curve, with 10.1 $\times 10^{-5}$M DNA.

$$r = \frac{T_L\ (D_1 - D)}{T_A\ (D_1 - D_2)} \qquad (5.4)$$

where T_L and T_A are the total concentrations of ligand and of DNA respectively, and D, D_1 and D_2 are the optical densities of the sample considered, of the dye in the absence of DNA, and of the dye in the presence of excess DNA, respectively, at a particular wavelength (usually at an absorption maximum of the dye).

For this equation to apply, the macromolecule must not absorb at the wavelength chosen, both free and bound ligand must obey Beer's Law over the concentration range considered, and it is assumed that the extinction coefficient of the bound ligand is constant and does not vary with r.[5]

The binding curves found spectrophotometrically for DNA-2-aminoacridine and for DNA-9-aminoacridine systems in 0.001M sodium chloride solution are shown in Fig. 5.4. The results of the calculations in Chapter 4 led to the conclusion that the free energy arising from dipole-dipole and dipole-polarizability interactions for intercalation of the 2-aminoacridinium ion in the

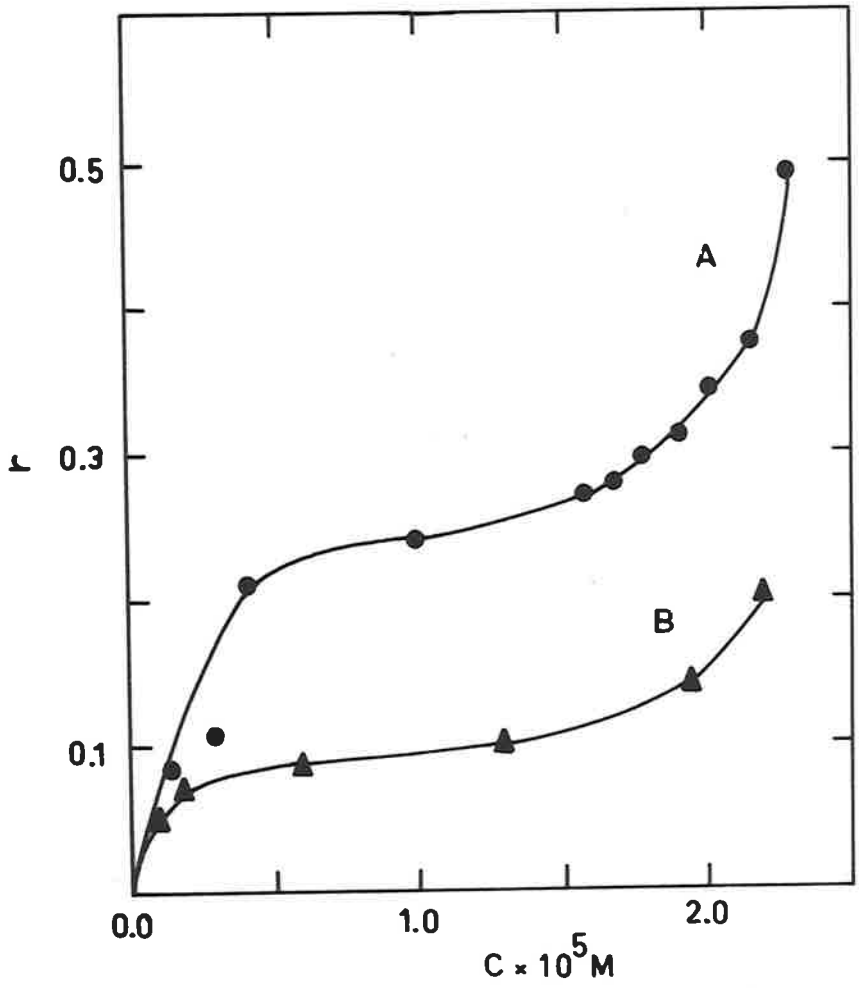

FIG. 5.4. Spectrophotometric binding curves of 9-aminoacridine (curve A) and 2-amino-acridine (curve B) on native DNA in 0.001M NaCl at 20°C.
Curve A: found at 400mμ, initial dye concentration = 2.5×10^{-5}M, average pH=6.0.
Curve B: found at 356mμ, initial dye concentration = 2.3×10^{-5}M, average pH=5.7.

DNA helix was more positive than that for intercalation of the 9-aminoacridinium ion (Table 4.2). This difference led to a more positive free energy change on intercalation of the charged form of 2-aminoacridine than of the charged form of 9-aminoacridine (see the more favourable ΔF values in Table 4.5). This implies that a higher value of r for the strong binding of 9-aminoacridine to DNA may be reached than for binding of 2-aminoacridine to DNA. This is illustrated in Fig. 5.4. However the two curves indicate that the difference in affinity of 2-aminoacridine and 9-aminoacridine for DNA is large, and is probably larger than may be accounted for by the free energy calculations. The fact that 2-aminoacridine ($pK_a = 5.88$)[17] will be about 60% ionised in a solution of pH 5.7 may account for this large difference in binding, since the uncharged 2-aminoacridine will be more weakly bound.

On the average, the pH of DNA-proflavine solutions was found to be 6.2, while Peacocke and Skerrett's experiments[5] were made at pH 6.9. However, since proflavine is fully ionised at both pH 6.2 and 6.9, and since this difference in pH has little, if any,

effect on the DNA helical structure, and, in addition, the binding curve r versus c (Fig. 5.5) found spectrophotometrically at 20°C and at pH 6.2 in this work is coincident with that found by Peacocke and Skerrett at pH 6.9 and 20°C, [5] this difference in pH has not been considered in the interpretation of the binding data.

Equilibrium dialysis studies may also be used to give the variation of r with the concentration of unbound ligand.[5] The lower two curves of Figs. 5.5, 5.6 and 5.7 for DNA-proflavine, DNA-12aminobenz[a]-acridine and DNA-7-aminobenz[c]acridine, respectively, reveal a large difference between equilibrium dialysis results and spectrophotometric results at 25°C in 0.1M sodium chloride solution. However, Peacocke and Skerrett found that the equilibrium dialysis and spectrophotometric results at 20°C coincided,[5] and concluded that the spectrum of the bound dye did not change with r in the region of 430 - 440 nm. If a solution of DNA-proflavine was heated from 20 to 25°C until equilibrium was obtained, the small amount of bound dye released would be that dye which was originally more weakly

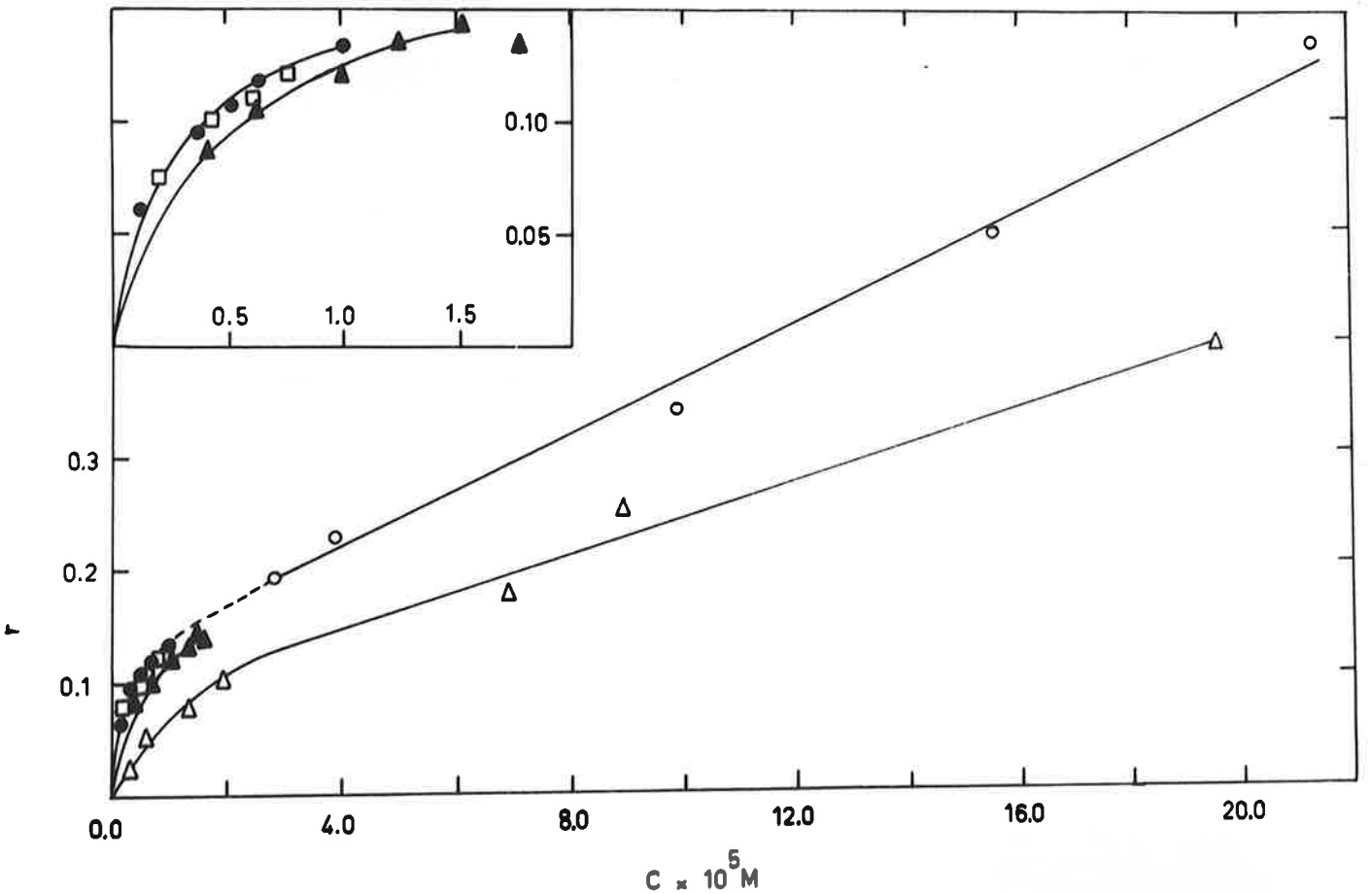

FIG. 5.5. Binding curves of proflavine on native DNA in 0.1M NaCl. Dialysis results: -o-, at 20°C (reference5); -Δ-, at 25°C (this work). Spectrophotometric results: found at 440-444 mμ: -●-, at 20°C (reference5); -□-, at 20°C (this work), initial dye concentration = 1.05×10^{-5} M; -▲-, at 25°C (this work), initial dye concentration = 2.23×10^{-5} M. The inset is drawn to a larger scale.

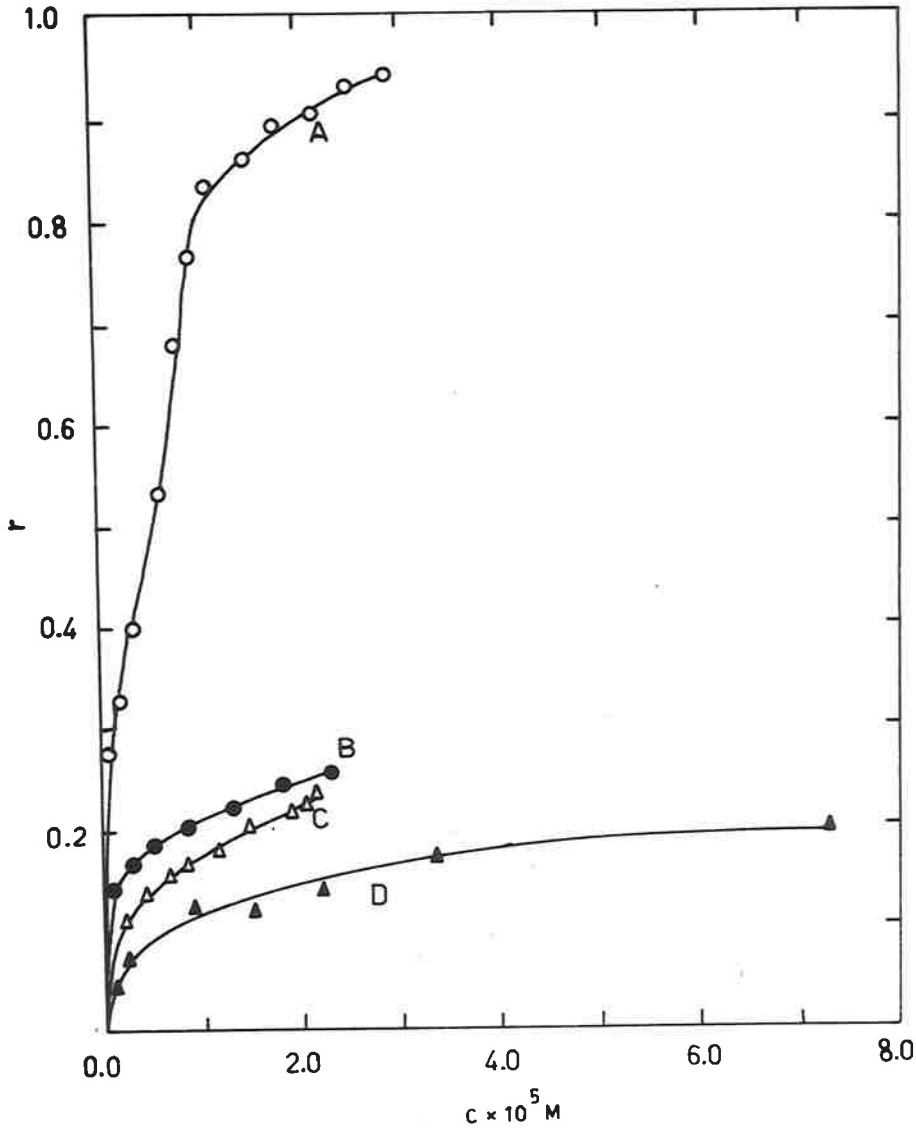

FIG. 5.6. Binding curves of 12-aminobenz[a]acridine on native calf thymus DNA.

Spectrophotometric results at 362.5 mμ: A: 0.001M NaCl, 20°C; B: 0.1M NaCl, 20°C; C: 0.1M NaCl, 25°C. The average pH for the titrations was 5.7, and initial dye concentrations were close to 3.0×10^{-5} M.

Equilibrium dialysis results: D: 0.1M NaCl, 25°C.

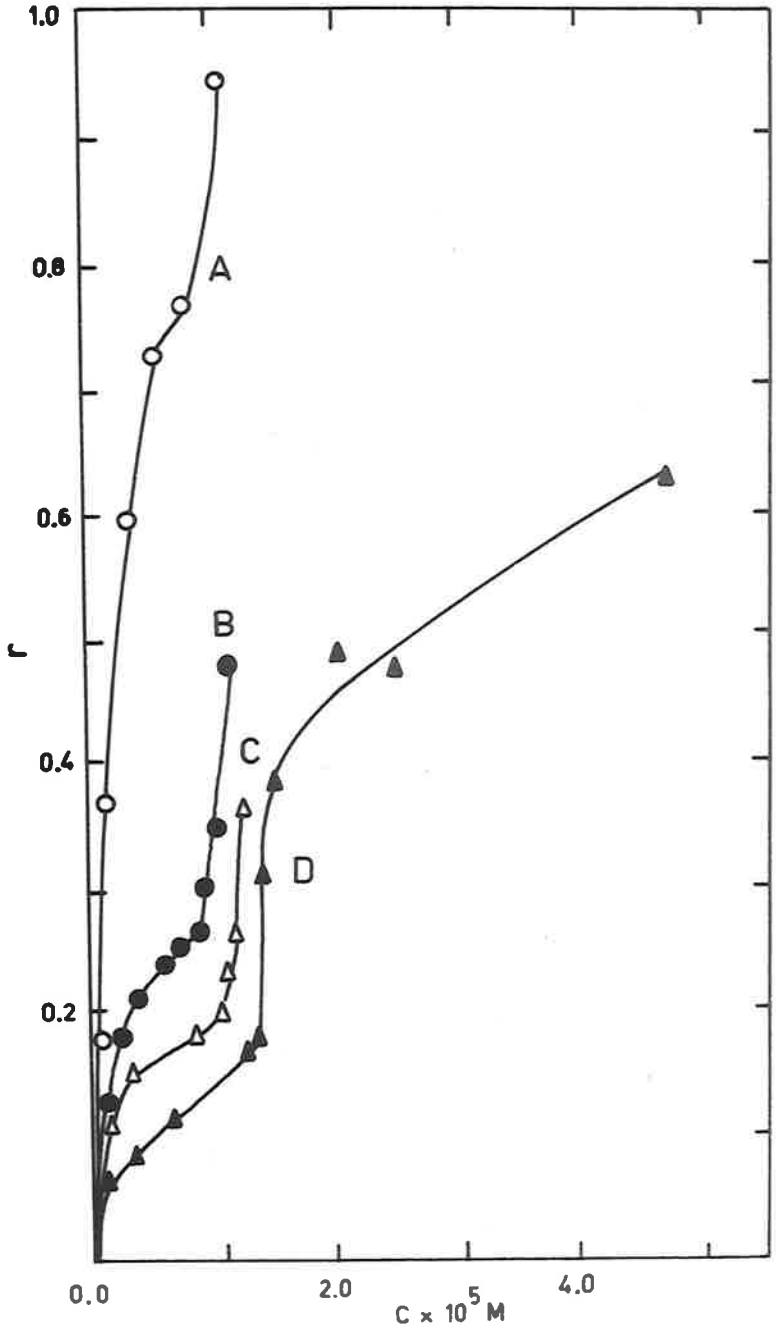

FIG. 5.7 Binding curves of 7-aminobenz[c]acridine on native calf thymus DNA.

Spectrophotometric results at 393 mμ:
A: 0.001M NaCl, 20°C; B: 0.1M NaCl, 20°C;
C: 0.1M NaCl, 25°C. The average pH for the titrations was 6.2, and initial dye concentrations were close to 1.4×10^{-5} M.
Equilibrium dialysis results: D: 0.1M NaCl, 25°C.

bound. This more weakly bound dye was interacting less with adjacent nucleotides and dye ions than the more strongly bound dye ions, and therefore the more weakly bound dye was only contributing a small amount to the overall hypochromicity and spectral change observed. Thus when the more weakly bound dye is released, the optical density of the solution does not increase in proportion to the amount of dye released. This has the effect that the observed value of r, found by spectrophotometry, for a given concentration of free dye, will be greater than that found by equilibrium dialysis. The coincidence of values by the two methods at 20°C may, in view of the above discussion, be fortuitous. These results indicate, therefore, that where a comparison of binding curves is desired, the curves must be found by the same method, wherever possible, and at the same temperature.

Comparison of the spectrophotometric curves of Figs. 5.5, 5.6 and 5.7 in 0.1M sodium chloride and at 20°C shows that the two aminobenzacridine dyes are bound to DNA by the stronger binding process to a greater extent than proflavine at the same free dye

concentrations. The free energy change, ΔF, which accompanies intercalation, is more negative for both 12-aminobenz[a]acridine and for 7-aminobenz[c]acridine than for proflavine, for some base sites and for one angle of orientation (Table 4.5). In addition, the dye-dye interactions parallel this trend (Table 4.6). The amount of dye bound to DNA by the stronger binding process is therefore expected to be higher for the two aminobenzacridines than for proflavine, and this is verified by the spectrophotometric binding curves mentioned above.

It should be noted that the additional benzene ring in the aminobenzacridines may exclude a larger number of water molecules from the vicinity of the nucleotides of the DNA helix than would proflavine, thus lowering the dielectric constant and thereby increasing the free energy of interaction of the aminobenzacridine ions with DNA. Since this will increase the differences in the ΔF values mentioned above, the interpretation to the differences in the binding curves of the two DNA-aminobenzacridine systems and of the DNA-proflavine system, (0.1M NaCl, 20°C),

of Figs. 5.6, 5.7 and 5.5, remains unaltered if the effect of the extra benzene ring is also considered.

The existence of two types of binding observed by Peacocke and Skerrett[5] may be explained only on the basis of the intercalated model. For this model, strong binding would be predicted, on the basis of the results in Table 4.4 and in Table 4.5, up to $r = 0.5$, whereas experimentally it is found that weaker binding predominates after about $r = 0.22$ for herring sperm DNA (GC content 43%).[5] When the approximations, discussed in Chapter 4 and used in the free energy calculations for the intercalated model, are taken into account the total free energy for each repeating unit will be increased (i.e. become less negative). For some repeating units this increase may give a value similar to or greater than that found for external edgewise binding for the same repeating unit (Table 4.4). The possibility then exists for a change over from intercalation to external edgewise binding at some value of $r<0.5$. The existence of two types of binding cannot be explained on the basis of external edgewise binding since the value of ΔF is the same for all binding sites (Table 4.4). The marked difference in binding sites found by Peacocke and Skerrett[5]

LIBRARY OF THE UNIVERSITY OF ANGLIA

would not be predicted on the basis of the modified version of model II of Chapter 4 in which the bound dye ions are tilted inwards towards the bases of DNA.

5.4 Effect of Ionic Strength and Temperature on the Binding Curves.

The fact that electrostatic forces play an important part in the binding of aminoacridines to DNA is well established.[5,6,18] The curves A and B of Figs. 5.6 and 5.7 correspond to 0.001M and 0.1M sodium chloride solutions, respectively, for the two DNA-aminobenzacridine systems. The effect of lowering the ionic strength is much more pronounced for the aminobenzacridines than for the aminoacridines in Fig. 5.8, indicating that electrostatic forces play a more important role in the binding of aminobenzacridines to DNA than in the binding of aminoacridines to DNA. This is also consistent with the free energy calculations discussed above.

The binding curve in 0.001M sodium chloride was also measured for 2-aminobenz[b]acridine and DNA. The value of r rose to 1.0 at very low free dye concentrations (less than 1.0×10^{-5}M), indicating that even

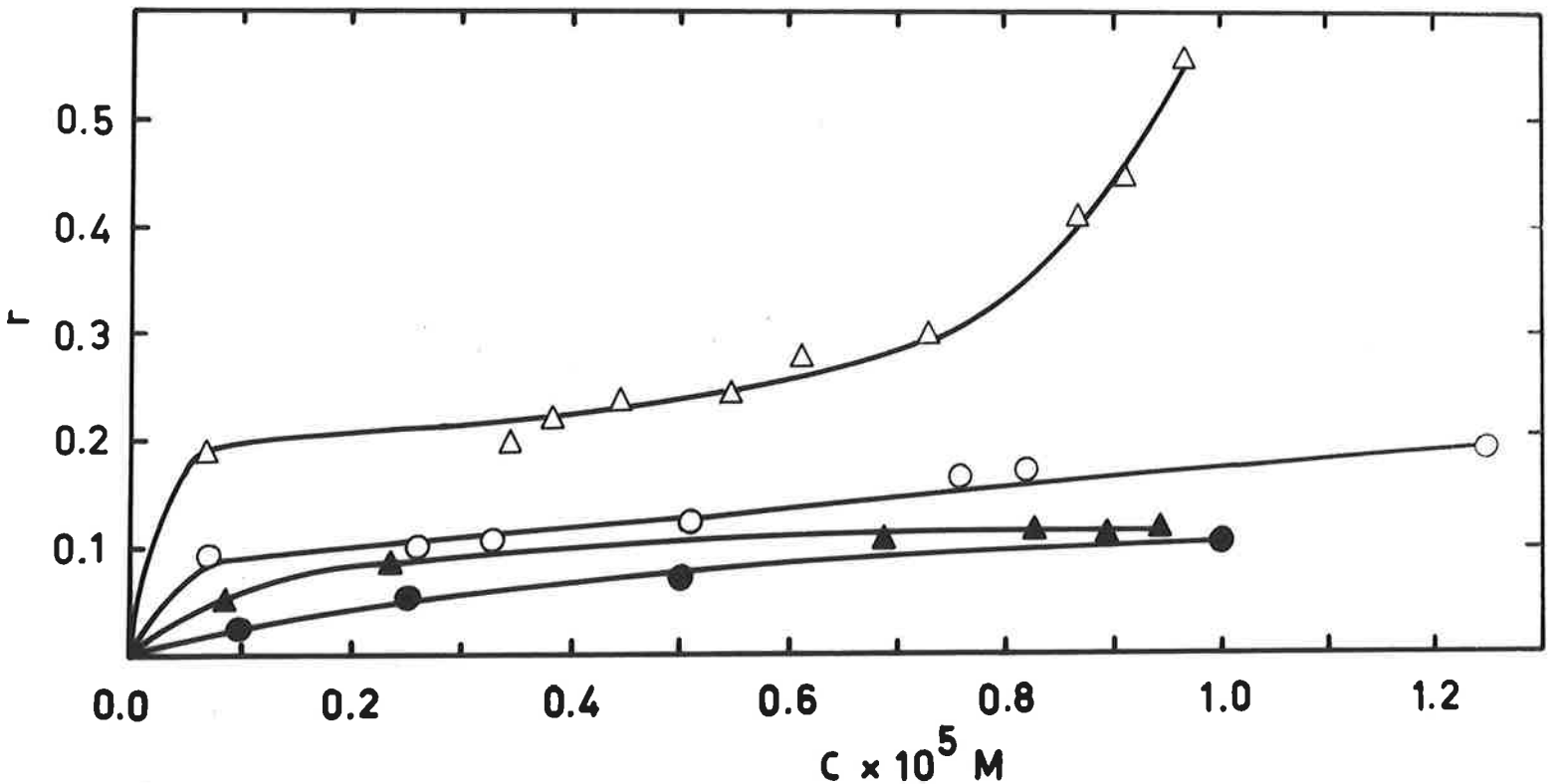

FIG. 5.8. Spectrophotometric binding curves of proflavine and 3-aminoacridine to native DNA at 20 °C with average pH values of 6.2 and 5.9, respectively.
Δ: proflavine in 0.001M NaCl at 444mμ, initial dye concentration, $c_i = 1.02 \times 10^{-5}$ M.
▲: proflavine in 0.1M NaCl at 444mμ, $c_i = 1.05 \times 10^{-5}$ M.
○: 3-aminoacridine in 0.001M NaCl at 456.6mμ, $c_i = 1.35 \times 10^{-5}$ M.
●: 3-aminoacridine in 0.1M NaCl at 456.6mμ, $c_i = 1.48 \times 10^{-5}$ M.

stronger interactions occur in this system than in, for example, the 7-aminobenz[c]acridine system. This may also be predicted on the basis of the free energy calculations in Tables 4.5 and 4.6. However, since the spectrophotometric titration was conducted at an average pH of 5.4, and the pK_a of 2-aminobenz[b]acridine is 6.1 [19], about 83% of the dye is ionised. Hence the results imply that some of the uncharged dye may also be bound to the DNA.

A pronounced temperature effect on the binding curves of DNA-proflavine systems was found by Chambron et al.[20] and this is confirmed by Fig. 5.5, for a difference in temperature of only 5°C, for both sets of binding curves. A similar effect was also found by equilibrium dialysis at 4°C and 46°C for the DNA-3-aminoacridine system. At a free dye concentration of 2.0×10^{-5}M, a difference in r from 0.16 at 4°C to 0.11 at 40°C was observed. Such temperature effects will be referred to again in Chapter 6, with reference to the thermal denaturation curves for DNA-dye systems.

5.5 Validity of Comparison of DNA-aminobenzacridine and DNA-aminoacridine Systems.

Apart from the comparison of the binding curves, no evidence has been cited to indicate that the binding processes between DNA and aminobenzacridines and DNA-aminoacridines are, in fact, similar. That the aminobenzacridines and aminoacridines do not differ in their intrinsic binding constants, k_i, when bound to DNA is shown by Fig. 5.9. The shape of the four curves of r/c versus r is similar, implying that the intrinsic binding constants which may be used to describe the binding processes involved are similar in magnitude. The differences in the binding curves of r versus c therefore arise from differences in the number of sites, n_i, available for interaction, and not from a difference in k_i in equation 5.3.

Therefore, as may be expected from the similarity in structure of the aminoacridines and the aminobenzacridines, any discussion on the binding processes involved in a DNA-aminoacridine system may also be applied to a DNA-aminobenzacridine system, provided that any additional effects which may arise

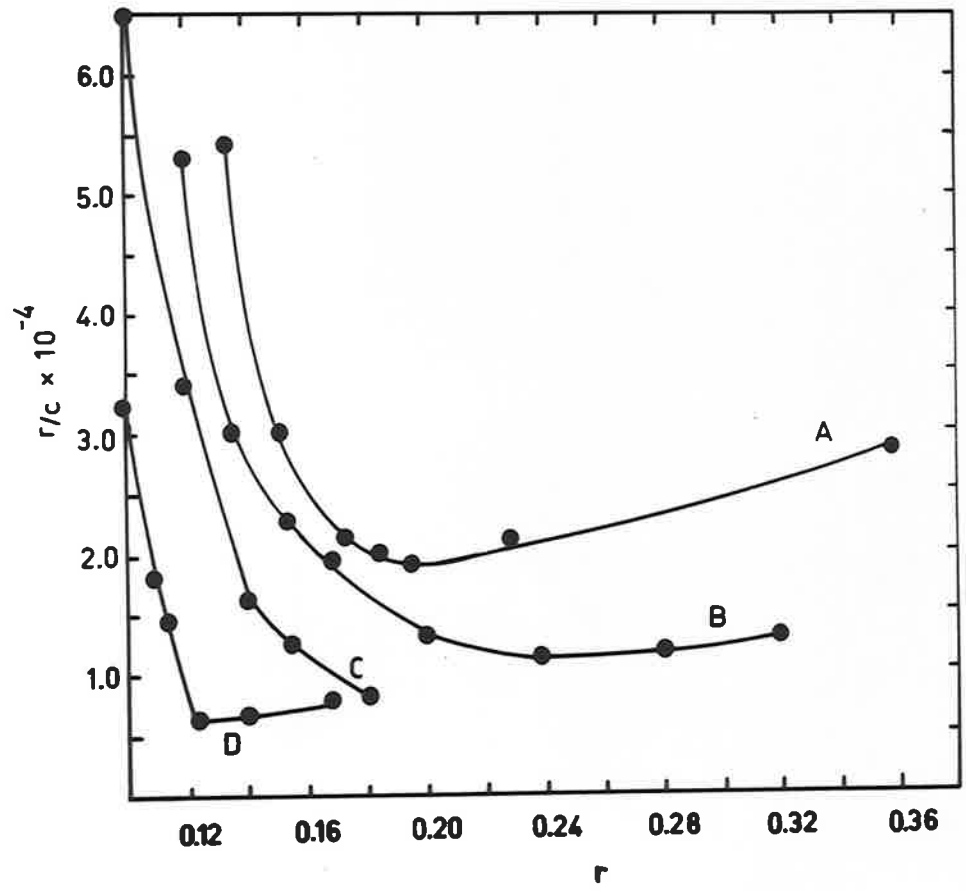

FIG. 5.9. The variation in r/c with r for various aminoacridines and aminobenzacridines in 0.1M NaCl at 25°C.

A: 7-aminobenz[c]acridine (pH=6.2)

B: 12-aminobenz[a]acridine (pH=5.7)

C: 9-aminoacridine (results from Drummond et al,[6] pH=6.9)

D: proflavine (pH=6.2)

from the differences in size and shape of the molecules are not neglected.

References.

1. Klotz, I. and Neurath, H., "The Proteins" Vol.2B, New York (1953).

2. Scatchard, G., Ann.N.Y.Acad.Sci., 51, 660 (1949).

3. Cavalieri, L. and Angelos, A., J.Am.Chem.Soc. 72, 4606 (1950).

4. Heilweil, H.G. and Van Winkle, Q., J.PhysChem. 59, 939 (1955).

5. Peacocke, A.R. and Sherrett, J.N.H., Trans.Faraday Soc. 52, 261 (1956).

6. Drummond, D.S., Simpson-Gildemeister, V.F.W. and Peacocke, A.R., Biopolymers 3,135(1965).

7. Albert, A., "The Acridines", E.Arnold and Co., London (1951).

8. Northland, F.W., De Bruyn, P.P.H. and Smith, H.H., Expt.Cell Res. 7, 201 (1954).

9. Millich, F. and Oster, G., J.Am.Chem.Soc. 81, 1357 (1959).

10. Craig, D.P. and Short, L.N., J.Chem.Soc. 419 (1945).

11. Haugen, G.R. and Melhuish, W.H., Trans.Faraday Soc. 60, 306 (1964).

12. Bradley, D.F. and Wolf, M.K., Proc.Nat.Acad.Sci., Wash. 45, 944 (1959).

13. Lawley, P.D., Biochim.Biophys.Acta 19, 328 (1956).

14. Gersch, N.F., B.Sc. Honours Report, University of Adelaide (1963).

15. Cavalieri, L.F., Roseff, M. and Rosenberg, B.H., J.Am.Chem.Soc. 78, 5242 (1956).

16. Irvin, J.L. and Irvin, E.M., J.Biol.Chem. 206, 39 (1954) and 210, 45 (1954).

17. Albert, A. and Goldacre, R., J.Chem Soc. 706 (1946).

18. Liersch, M. and Hartmann, G., Biochem.Z. 340, 390 (1964).

19. Albert, A., Rubbo, S.D. and Burvill, M.I., Brit.J. Exper.Path. 30, 159 (1949).

20. Chambron, J., Dunne, M. and Sadron, C., C.R.Acad. Sci.,Paris 258, 4867 (1964).

CHAPTER 6.

THERMAL DENATURATION OF DNA-DYE SYSTEMS.

6.1 Introduction.

The interaction of DNA with purines and pyrimidines was found to result in a lowering of the thermal denaturation temperature, T_m.[1] It was suggested[1] that this decrease in stability of the native helix of DNA may be brought about by a stronger affinity of the purines and pyrimidines for the coil form of DNA than for native DNA. This difference in affinity for denatured DNA and native DNA has now been verified.[2]

On the other hand, the hydrocarbons pyrene and benzo[a]pyrene both increased the T_m of DNA by about 6°C.[3] Furthermore, it appears that benzo[a]pyrene is solubilized to a greater extent(at 0.01M sodium chloride) in native DNA than in denatured DNA,[4,5] although this has not been found by all workers,[6] and does not apply to all hydrocarbons and steroids.[2]

Since the theory of intercalation may be used to describe the binding of polycyclic hydrocarbons to DNA, although the possibility of adsorption to the external surface of the DNA cannot be excluded,[5] it

was of considerable interest and importance for a study of the thermal denaturation of DNA-aminoacridine and DNA-aminobenzacridine systems to be undertaken. Other workers have found that the T_m of DNA in the presence of acridine orange is higher than that of native DNA alone.[7,8] An increase in T_m has also been found for DNA-proflavine systems[9] and for DNA-chloroquine systems,[10] as well as for DNA-9-aminoacridine systems.[11] Furthermore, Kleinwaechter and Kondelka[8] showed that the T_m of the DNA-acridine orange complex was dependent on the base composition of the DNA, a greater increase in T_m being observed for DNA of low GC content.

The T_m of complexes of calf thymus DNA with several aminoacridines and three aminobenzacridines in 0.001M sodium chloride solution, and two aminoacridines in 0.1M and 0.001M sodium chloride solution are reported in this chapter, and the results are discussed with reference to both the intercalated model[12,13] and the model involving external edgewise attachment of the dye to the DNA.[14,15]

6.2 Results.

The definition of T_m has been modified[16] from that usually employed, as an increase of the optical density in the temperature range 25° to about 70°C was generally observed with DNA-dye complexes. Considering curve I of Fig. 6.1 for 3-aminoacridine with DNA in 0.1M sodium chloride, which is typical, the melting curve can be clearly divided into two parts: the small increase between 25° and 80°C, AB, and the true melting region, BC. The interpretation of this behaviour is discussed later. A new melting temperature T'_m, is defined as the temperature at which 50% hyperchromicity is attained from the onset of the rapid increase of the optical density above about 70° until no further increase in optical density is recorded, i.e. in the region BC (Fig. 6.1, curve I). Extrapolation of the linear sections of the curve enable T'_m to be determined.

From the binding curves already discussed in Chapter 5, a plot of r versus T_L/T_A, where T_L and T_A are the total concentrations of dye and DNA respectively, was made. For proflavine and 3-aminoacridine, in 0.1M

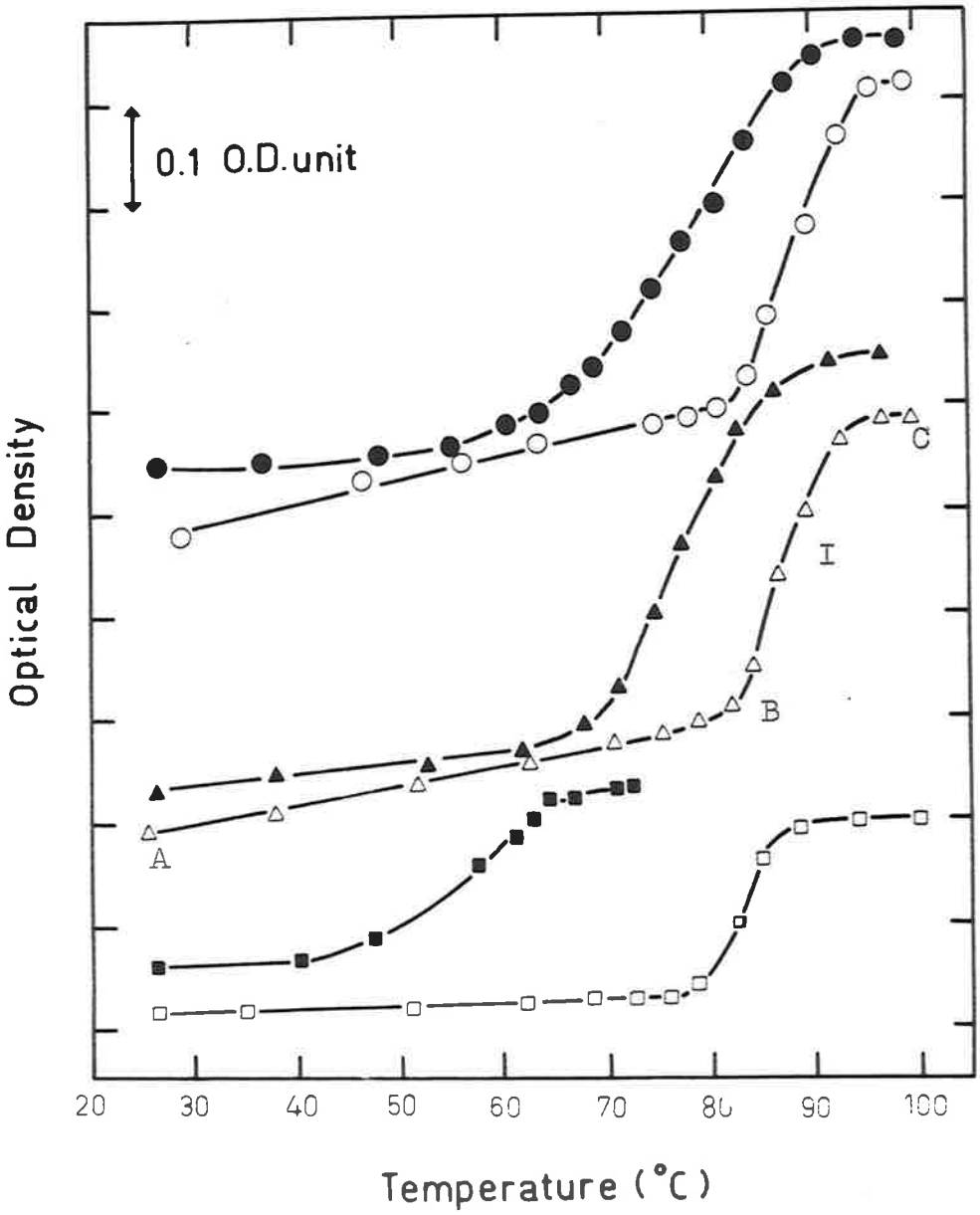

FIG. 6.1. Thermal denaturation curves for DNA and DNA-dye solutions. For the four DNA-dye solutions shown, the values of r are close to 0.13 (see text). All DNA solutions are 7.2×10^{-5} M with respect to DNA phosphorus. In the text, curve I is referred to as a typical T_m' curve, and mention is made of regions AB and BC.

-□-, DNA in 0.1M NaCl;
-Δ-, DNA-3-aminoacridine in 0.1M NaCl;
-o-, DNA-proflavine in 0.1M NaCl
-■-, DNA in 0.001M NaCl.
-▲-, DNA-3-aminoacridine in 0.001M NaCl.
-●-, DNA-proflavine in 0.001M NaCl

sodium chloride solution, the equilibrium dialysis results from Peacocke and Skerrett[17] and from this work, respectively, were used to supplement the spectrophotometric data for values of $r>0.1$ where the accuracy of the spectrophotometric method is not high. Thus the value of r could be obtained for any solution where the ratio T_L/T_A was known. This method is valid for values of $r<0.5$ and for the T_A values used here.

Typical T'_n curves obtained for DNA-proflavine and for DNA-3-aminoacridine systems at values of r close to 0.13 are shown in Fig. 6.1 (the actual values of r were: DNA-3-aminoacridine (pH = 5.9); 0.1M NaCl, 0.130; 0.001M NaCl, 0.121: DNA-proflavine (pH = 6.2); 0.1M NaCl, 0.130; 0.001M NaCl, 0.137). Several features of these curves are important and are discussed below.

(i) There is an initial increase in optical density, as typified by the region AB, curve I in Fig. 6.1, greater than that associated with the heating of native DNA, up to between 65° and 80°C. This increase is greater for 0.1M sodium chloride than for 0.001M sodium chloride solutions, for approximately the same value of r, and is larger for proflavine than for 3-aminoacridine.

(ii) The final optical density observed is usually very slightly lower than that calculated by the addition of free dye and denatured DNA optical densities. This is not shown in Fig. 6.1.

The shape of the T'_m versus T_L/T_A curves (Fig. 6.2) indicates that either the binding sites become saturated at a particular value of T_L/T_A or that further binding beyond a critical value does not affect T'_m. These curves are similar in shape to those obtained by Kleinwaechter and Koudelka[8] for acridine orange and DNA. The increase in T'_m is much larger for a given T_L/T_A (Fig. 6.2) or for a given r (Fig. 6.3) for 0.001N than for 0.1N sodium chloride solutions.

The value of T' increases rapidly with r over the range studied for 0.1N sodium chloride, but for 0.001N sodium chloride the curve flattens out at about r = 0.2 (Fig. 6.3), beyond which value Peacocke and Skerrett[17] found a decrease in binding strength for the DNA-proflavine system. This implies that some correlation exists between T'_m and strength of binding.

It is unfortunate that the curves in Fig. 6.3 cannot be extended past a value of r of about 0.15 for 0.1N

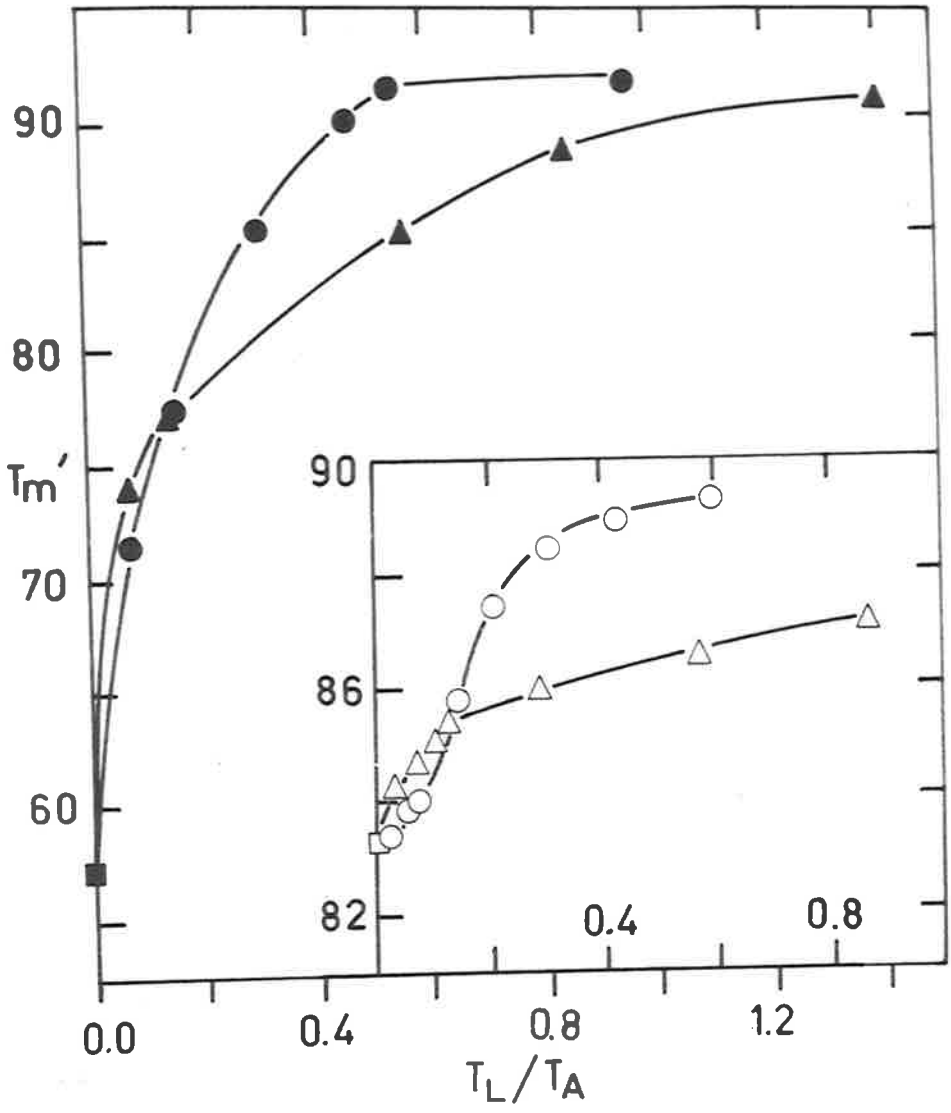

FIG. 6.2. Variation in T_m' with T_L/T_A, the ratio of total dye to total DNA phosphorus concentration for DNA-dye solutions in 0.001M NaCl. The inset refers to solutions in 0.1M NaCl. For the key to the symbols used, see the legend to Fig. 6.1.

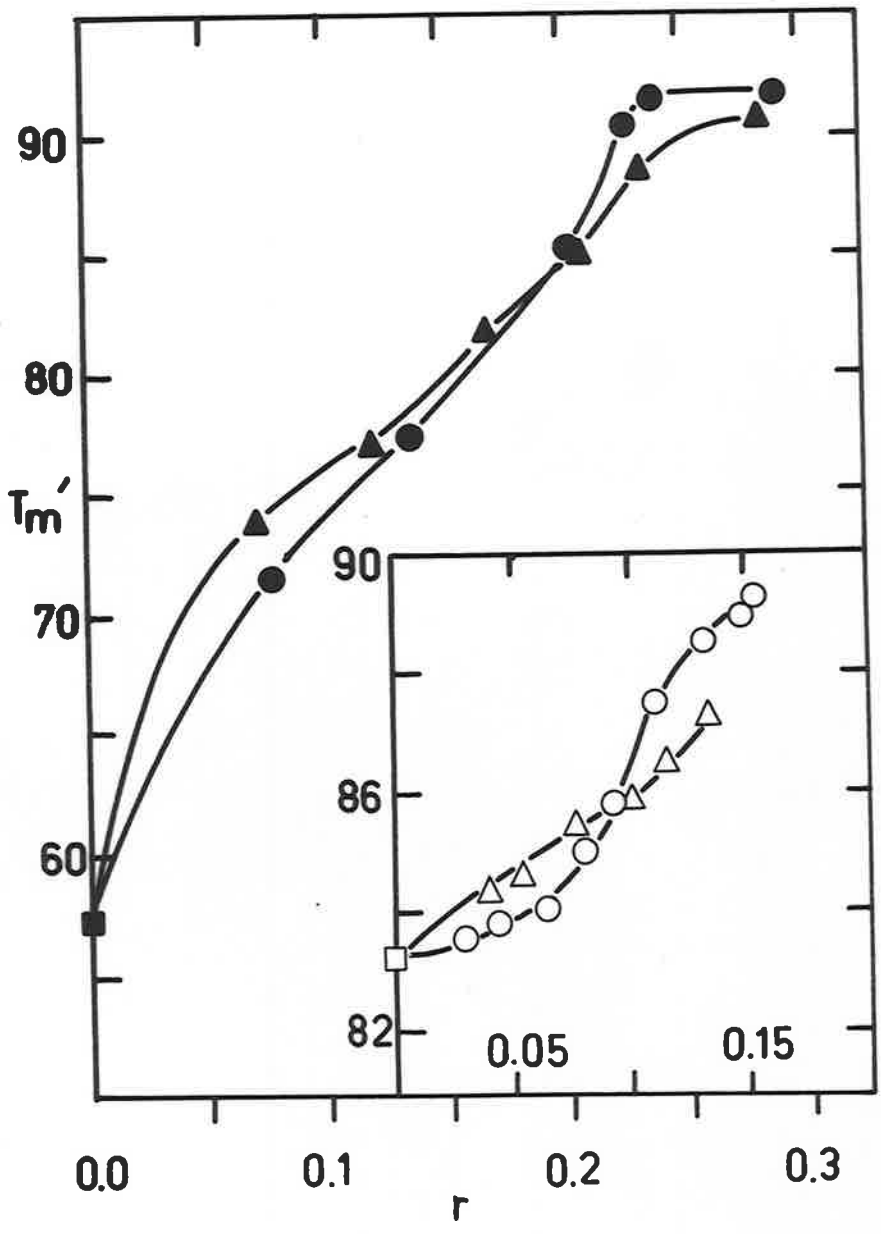

FIG. 6.3. Variation in T_m' with r for 0.001M NaCl solutions. The inset refers to solutions in 0.1M NaCl. For the key to the symbols used, see legend to Fig. 6.1.

sodium chloride. Higher values of r cannot be obtained by simple addition of dye to DNA solutions of suitable optical density range, and are obtained only by equilibrium dialysis. However, according to Peacocke and Skerrett,[17] one of the criteria for obtaining accurate values of r from equilibrium dialysis studies is a high value for the DNA concentration. If high concentrations of DNA are used, dilution of the dialysed solution is necessary for the determination of T'_m in a suitable optical density range. This process of dilution leads to a reduction of r.

The increase in T'_m with r for three aminobenzacridines and DNA and for 9-aminoacridine and DNA in 0.001N sodium chloride solution is shown in Fig. 6.4. The general shape of the curves is similar to that of the curves of Fig. 6.3 for 3-aminoacridine and proflavine and DNA.

The T'_m versus T_L/T_A^{λ} curves for DNA-2-aminoacridine and DNA-4-aminoacridine in 0.001N sodium chloride (Fig. 6.5) show the effect of varying the pH of the solution by a small amount. The values for T'_m of DNA-2-aminoacridine and DNA-4-aminoacridine systems are

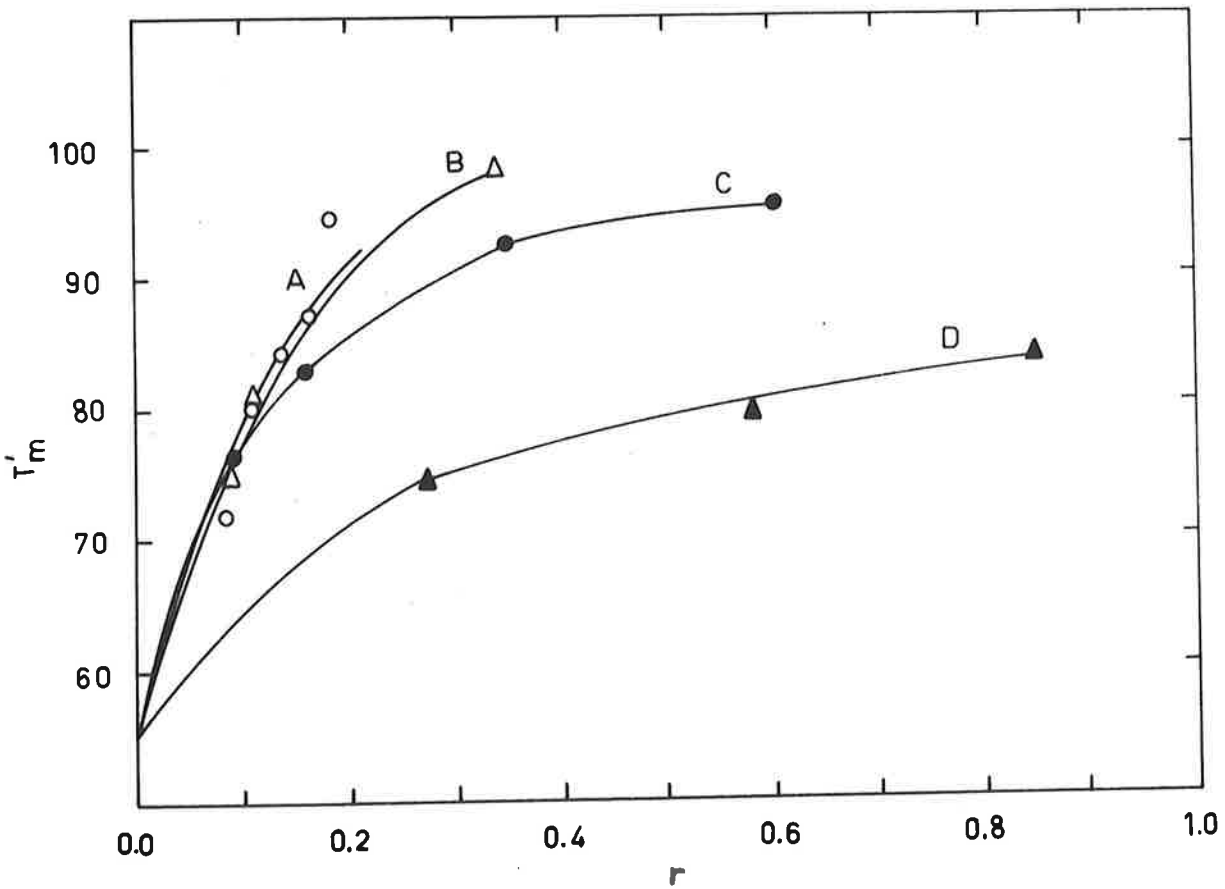

FIG. 6.4. Variation in T'_m with r for 0.001M NaCl solutions. A: DNA-9-aminoacridine (average pH = 5.8); B: DNA-7-aminobenz[c]acridine (average pH = 5.8); C: DNA-12-aminobenz[a]acridine (average pH = 5.8); D: DNA-2-aminobenz[b]-acridine (average pH = 5.9). DNA concentration = 7.2×10^{-5} M with respect to DNA phosphorus.

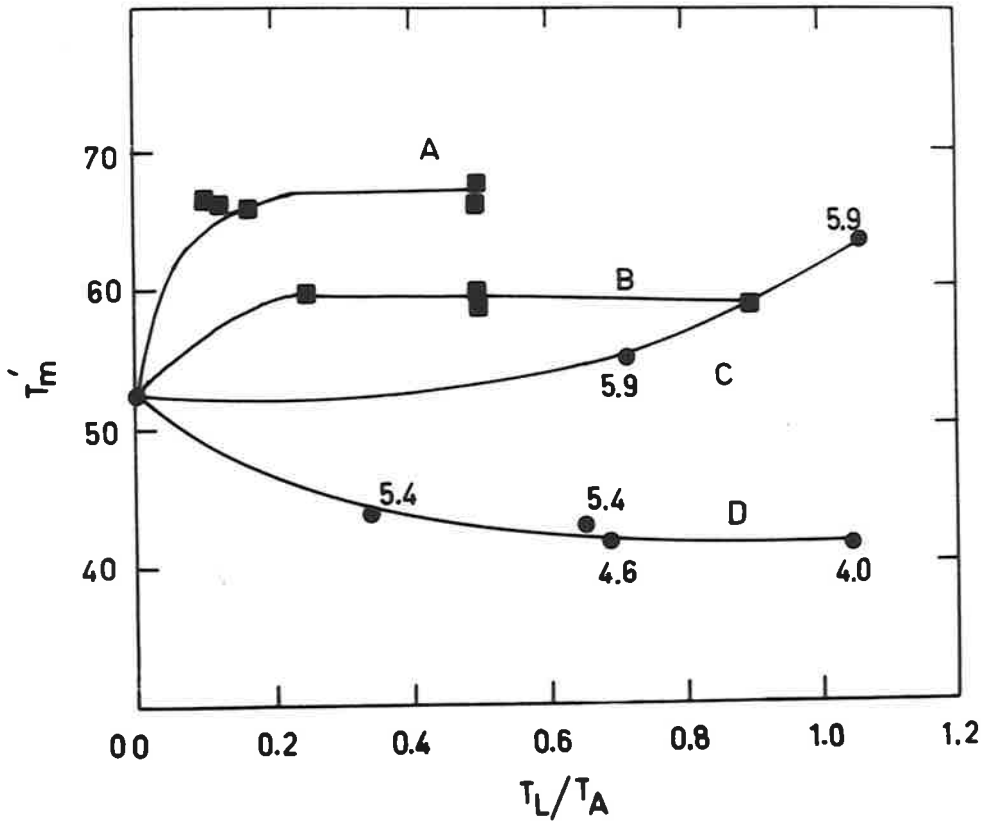

FIG. 6.5. Variation in T_m' with T_L/T_A for DNA-dye solutions in 0.001M NaCl.
A: DNA-2-aminoacridine ($5.4 \leq pH \leq 6.0$).
B: DNA-2-aminoacridine ($5.0 < pH < 5.4$).
C and D: DNA-4-aminoacridine - the pH values are indicated near each point.
For DNA concentration see Fig. 6.4.

much lower than for other DNA-aminoacridine systems (Figs. 6.3 and 6.4).

6.3 Discussion.

The initial increase in optical density as the temperature is increased in the T'_m curves (the region AB in Fig. 6.1) may be explained in terms of a decrease in dye binding with an increase in temperature. This has been confirmed for the systems DNA-proflavine[18] and for DNA-3-aminoacridine (Chapter 5) by use of equilibrium dialysis at different temperatures. Since the binding of dye to DNA is accompanied by a hypochromic effect, the release of bound dye due to an increase in temperature results in an increase in optical density. That the initial optical density increase does not account for the full hypochromic effect on the dye implies that only a small amount of the dye bound is released before the helical structure of the DNA is disrupted. This can be interpreted on the basis of either of the two models for the DNA-dye complex discussed in Chapter 4, although more easily for the intercalated model, the increase in temperature causing a removal of dye from the weaker binding sites.

In a typical T'_m determination for 0.1M sodium chloride solutions, the expected total optical density increase was 0.316, the observed was 0.305, of which 0.185 could be attributed to DNA. By 75°C (i.e. over the region AB in Fig. 6.1) an increase in optical density of only 0.060 had occurred over that at 25°C, leaving about one-half of the hypochromic effect of the dye to be accounted for in the temperature range over which the helical DNA structure is disrupted (i.e. the region BC in Fig. 6.1).

Fig. 6.1 indicates that for about the same values of r, the initial optical density increase is larger for 0.1M than for 0.001M sodium chloride solutions. This can only be interpreted on the basis of greater binding of dye at lower ionic strengths, as found by Peacocke and Skerrett.[17] At higher ionic strengths there is either more competition with Na^+ ions for the binding sites or it is more difficult for the dye ions to approach the binding sites due to shielding effects of Na^+ ions. As the temperature is increased and Brownian motion increases, the probability of a bound dye ion being displaced by a Na^+ ion is greater at

higher ionic strengths whichever model is considered. This also explains the greater increase in T'_m observed, for a given value of r, in 0.001M sodium chloride compared with 0.1M sodium chloride (Fig. 6.3).

Proflavine and 3-aminoacridine have peaks in the ultraviolet at 262mμ and 274mμ respectively. By following the helix-coil transition of the DNA-dye complex at 259 mμ the contribution of the dye to the total optical density is thus greater for proflavine than for 3-aminoacridine. Hence the initial optical density increase measured at 259 mμ is greater for proflavine than for 3-aminoacridine and does not necessarily reflect differences in binding strength.

The final optical density observed at about 100°C is often very slightly lower than that expected from the addition of the optical densities of free dye and denatured DNA. This implies that there may be slight interaction between dye and denatured DNA even at high temperatures.

The value of 40°C for T'_m predicted by Chambron *et al* [18] for the DNA-proflavine system does not agree

with the values of T_m' found in this study (Figs. 6.2 and 6.3) since T_m' is greater than that of native DNA for the DNA-proflavine complexes considered. The predicted value[18] of 40°C was based on calculations of ΔH and ΔS, the latter of which is subject to large errors since subtraction of two quantities of similar magnitude is involved. Furthermore, to find T_m from $\Delta H_2 = T\Delta S_2$, the values of ΔH_2 and ΔS_2 used were based on average values over the range 0 to 70°C. This presupposes that T_m lies in this range, which is not the case (see Figs. 6.2 and 6.3).

The curves for DNA-2-aminoacridine in Fig. 6.5 indicate that, for a pH of about 5.2, the T_m' of the system has dropped by about 7°C below that for $5.4 \leq pH \leq 6.0$. This could be attributed to a reduction in binding of dye to DNA, or to a lowering of the stability of the DNA because of the reduced pH, or to a combination of these factors. However the binding curves for 2-aminoacridine, determined at an average pH of 5.4 and 5.7, the latter of which was shown in Fig. 5.4, coincided to within $r = 0.01$ up to a free dye concentration of 1.6×10^{-5}M, with r greater for pH 5.4 than 5.7.

Since the pK_a of 2-aminoacridine is 5.88,[19] any reduction of the pH will increase the percentage of ionised dye, and thus the amount of dye bound may be expected to increase slightly with a decrease of pH. This therefore implies that the reduced T_m' increase may be attributed to the lowered stability of the DNA because of the reduced pH.

The T_m' of a native DNA solution at pH 4.9 will probably be about 16°C less than that at pH 6.0, for a 0.001M sodium chloride solution.[20] However, the reduction in T_m' for DNA-4-aminoacridine solutions is about 11°, for a pH of 4.6 and also a pH of 4.0 (Fig. 6.5). Thus the dye has increased the stability of the DNA towards thermal denaturation at pH values between 4.0 and 5.4. At a pH of 5.9, the T_m' is increased by an even larger amount. The dye is only partly ionised at this pH (since the pK_a is 4.4,[19] at pH = 5.9, the percentage ionised is about 5%, while the percentages ionised at pH values of 5.4, 4.6 and 4.0 are 9%, 39% and 71%, respectively). This suggests that some uncharged dye may also be bound at pH 5.9, to account for the increase in T_m' observed.

For curve D of Fig. 6.4, the pH was between 5.8 and 6.0. Since the pK_a of 2-aminobenz[b]acridine is 6.1,[21] about 60% of the dye is ionized. Hence either the interaction between DNA and charged 2-aminobenz[b]-acridine molecules is very strong (as already implied by the binding curve mentioned in Chapter 5 and the free energy values quoted in Tables 4.5 and 4.6), or some binding between uncharged 2-aminobenz[b]acridine molecules and DNA occurs. The experimental evidence does not distinguish between these possibilities, although it was suggested that some uncharged dye molecules may be bound to the DNA (see Section 5.4).

An increase in T_m' indicates that the stability of the native DNA-dye system has increased relative to that of the denatured DNA-dye system. This could arise through a decrease in stability of the denatured DNA-dye complex. However such a decrease is unlikely to occur since denatured DNA has been shown to bind dye.[14,22] Thus since the denatured DNA-dye system is expected to have a more negative free energy than denatured DNA, the only way in which the stability of the native DNA-dye

system can be greater than that of the denatured DNA-dye system is for a large decrease to occur in the free energy of the native DNA-dye system over that of native DNA. This decrease must be greater than the difference in free energy between the denatured DNA-dye system and denatured DNA.

Table 4.4 indicated that the free energy for both models is more negative than that of DNA alone, although that for model I is more negative than that for model IIa. The model adopted must explain the fact that many of the dye ions are released from the binding sites in the temperature range over which the DNA helical structure is disrupted (Fig. 6.1). It should be noted that dye-dye interactions between dye ions bound to the outside of the helix cannot be used alone to explain the increase in T_m°. Stone and Bradley[23] have shown that there is only a very small tendency for acridine orange ions to stack on native DNA since the stacking coefficient is only 1.25. Furthermore, the calculations presented in Table 4.3 indicated that the dye-dye interactions for model II are small, the main interactions arising from charge-dipole and charge-polarizability

forces due to the bound phosphate group. It is these forces, giving rise to the negative free energy for the native DNA-dye complex, which could give rise to an increased stability for model II.

The free energy calculations for the intercalated model indicated a dependence of the free energy of interaction on the base content of the DNA, and explained the two types of binding (see Chapter 4 and Section 5.3). However the calculations for the model involving external edgewise binding of dye to the DNA neither showed a dependence on the base content of the DNA nor explained the two types of binding. Therefore only the intercalated model will explain both the dependence on the base content of the increase in T_m of the DNA-acridine orange complex over that of DNA for different samples of DNA,[8] and the shape of the T'_m versus r curves.

The increase in T'_m is greater for the DNA-proflavine complex than for the DNA-3-aminoacridine complex at a given value of r (Fig. 6.3), indicating that the former complex is more stable than the latter relative to the denatured DNA-dye complex. The binding

curves of Chapter 5 (Fig. 5.8), also indicate that a higher value of r is reached, for which the strong mode of binding predominates, for proflavine than for 3-amino-acridine and DNA. A similar discussion may also be applied to the T'_m versus r curves, A, B and C of Fig.6.4 and their binding curves, Figs. 5.4, 5.7 and 5.6, respectively. In all of these dyes, essentially complete ionisation may be assumed since the pK_a is 2 or more units greater than the pH of the system. Furthermore, for the case of partial ionisation of dye in curve D of Fig. 6.4 and in the two upper curves of Fig. 6.5, a similar discussion to the above once again applies, with reference to the binding curve mentioned for 2-aminobenz[b]acridine in Chapter 5, and to Fig. 5.4, respectively.

References.

1. Ts'o, P.O.P., Helmkamp, G.K. and Sander, C., Proc.Nat.Acad.Sci.,Wash. 48, 686 (1962).

2. Ts'o, P.O.P. and Lu, P., Proc.Nat.Acad.Sci.,Wash. 51, 17 (1964).

3. Boyland, E. and Green, B., Proc.Biochem.Soc. 97, 14P, (1963).

4. Boyland, E., Green, B. and Lin, S-L., Biochim. Biophys.Acta 87, 653 (1964).

5. Boyland, E. and Green, B., Brit.J.Cancer 16, 507 (1962).

6. Liquori, A.M., De Lerma, B., Ascoli, F., Botré, C. and Tranciatti, M., J.Mol.Biol. 5, 521 (1962).

7. Freifelder, D., Davison, P.F. and Geiduschek, E.P., Biophys.J. 1, 389 (1961).

8. Kleinwaechter, V. and Koudelka, J., Biochim. Biophys Acta 91, 539 (1964).

9. Walker, I.O., ibid. 109, 585 (1965).

10. Cohen, S.N. and Yielding, K.L., J.Biol.Chem. 240, 3123 (1965).

11. Lerman, L.S., J.Cell.Comp.Physiol.Supp.1.64.1(1964).

12. Lerman, L.S., J.Mol.Biol. 3, 18 (1961).

13. Lerman, L.S., Proc.Nat.Acad.Sci.,Wash.49, 94 (1963).

14. Bradley, D.F. and Wolf, M.K., Ibid. 45, 944 (1959).

15. Mason, S.F. and McCaffery, A.J., Nature 204, 468 (1964).

16. Gersch, M.F. and Jordan, D.O., J.Mol.Biol. 13, 138 (1965).

17. Peacocke, A.R. and Skerrett, J.N.H., Trans.Faraday Soc. 52, 261 (1956).

18. Chambron, J., Daune, M. and Sadron, C., C.R.Acad. Sci.Paris, 258, 4867 (1964).

19. Albert, A. and Goldacre, R., J.Chem.Soc. 706 (1946).

20. Estimated from experimental results of Kelly, R.E.G. and Jordan, D.O.

21. Albert, A., Rubbo, S.D. and Burvill, M.I., Brit.J. Exper.Path. 30, 159 (1949).

22. Drummond, D.S., Simpson-Gildemeister, V.F.W. and Peacocke, A.R., Biopolymers 3, 135 (1965).

23. Stone, A.L. and Bradley, D.F., J.Am.Chem.Soc. 83, 3627 (1961).

CHAPTER 7.

VISCOSITY AND SEDIMENTATION OF DNA-DYE SYSTEMS.

7.1 Introduction.

The viscosity and sedimentation coefficient of a macromolecule in solution depend, in general, on the dimensions of the molecule, and therefore provide a means of examining any change in configuration of a macromolecule under certain conditions. For example, the viscosity of a DNA solution decreases upon treatment with high or low pH,[1] and the sedimentation coefficient decreases with decreasing electrolyte concentration.[2,3] This behaviour is caused by the transition from the more rigid helical structure of native DNA to the random coil configuration of denatured DNA, as well as by charge effects.

The intercalated model proposed[4,5] for the interaction of aminoacridines with DNA involves the extension of the native DNA helix and an increase in rigidity of regions where intercalation occurs, in addition to a reduction in mass per unit length. On the other hand, models involving external edgewise binding of the dye to the native DNA helix[6,7] give rise to no alteration in length, but a slight increase in rigidity

and an increase in mass per unit length may occur. Therefore it should be possible to distinguish between the models on the basis of viscosity and sedimentation coefficient results.

Lerman[4,5] found that acridine orange, several aminoacridines and several methylbenzacridines increased the viscosity of DNA, and also that[4] the sedimentation coefficient of DNA-proflavine systems was decreased at moderate concentrations of proflavine. Both of these effects are consistent with the intercalated model and not with a model involving only external edgewise binding of the dye to the DNA.

The aim of the work presented in this Chapter is to confirm the increase in viscosity for several DNA-aminoacridine and DNA-aminobenzacridine systems and to verify, by determining the sedimentation coefficient at several values of r, that aggregation is not responsible for the observed viscosity increase for a typical DNA-aminobenzacridine system. All of the results are quoted for known values of r, since no previous studies of the viscosities or sedimentation coefficients of these systems have been reported as functions of r. Although the results discussed do not form an exhaustive study of these two hydrodynamic

properties for the DNA- aminoacridine and DNA-aminobenzacridine systems, they emphasize the importance of studying such properties as functions of r.

7.2 Viscosity of DNA-aminoacridine and DNA-aminobenzacridine systems.

If the case of intercalation of dye is considered, the viscosity of the DNA-dye system will depend on the extension and rigidity of the DNA helix which, in turn, depend on the number of occupied intercalation sites.

Three η_{sp} versus r curves for three dyes are shown in Fig. 7.1, and it is evident that a large increase in specific viscosity occurs up to 0.1<r<0.2. After a maximum in η_{sp} has been observed, the intrinsic viscosity is seen to decrease. This decrease may be attributed to the precipitation of the DNA-dye complex from solution. In all such cases, a visible cloudiness or precipitate in the freshly dialysed solution was observed and was removed by centrifugation (see Chapter 8) before viscosity measurements were taken.

The distinct difference in the extent of increase in η_{sp} of the DNA-dye solutions for a given value of r for a given dye may be due either to a

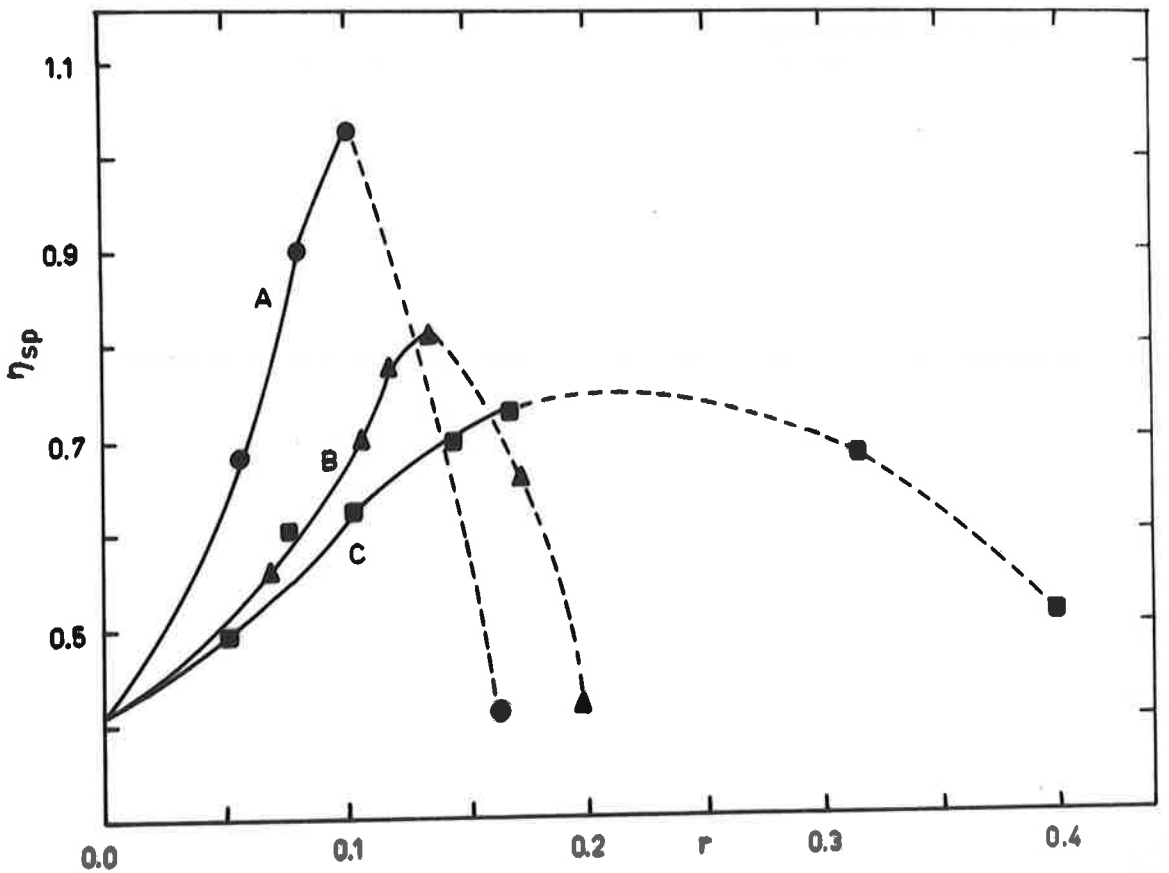

FIG. 7.1. The variation of specific viscosity, η_{sp}, with r for DNA-7-aminobenz-[c]acridine (curve A), for DNA-12-aminobenz[a]acridine (curve B) and for DNA-proflavine (curve C) in 0.1M NaCl at 25 °C.

difference in the extent of intercalation or to a difference in the rigidity of the DNA-dye complexes. The experimental results do not distinguish between these possibilities. However, a parallel between these curves and the binding curves of Chapter 5 may be noted. The relative magnitude of the maximum strong binding of Figs. 5.5, 5.6 and 5.7 correspond to the relative magnitude of the increases in η_{sp} (Fig. 7.1) for DNA-dye solutions in 0.1M sodium chloride at 25°C. This suggests that some correlation may exist between the amount of strong binding and the increase in η_{sp} observed.

For a given value of r, the viscosity curves (Fig. 7.1) are different even for the two aminobenzacridines, indicating that despite the similarities in the structure of 7-aminobenz[c]acridine and 12-aminobenz-[a]acridine, a large difference in configuration of their complexes with DNA exists. There are two possibilities; either the lower viscosity increase for DNA-12-aminobenz-[a]acridine systems results from a smaller number of intercalated ions or from a lower increase in the rigidity of the complex. A smaller number of intercalated ions could be brought about (at values of r still involving the strong binding process) by a higher (i.e. more positive) free energy of interaction for

intercalated ions than for ions bound externally to the phosphate groups, while 7-aminobenz[c]acridine has a large number of intercalated ions at the same value of r. This is possible since the total free energy of interaction of 12-aminobenz[a]acridine with DNA is, in general, more positive than that of 7-aminobenz[c]acridine with DNA for the intercalated model (see Chapter 4).

As an alternative explanation to the viscosity increase observed, it was evident in the free energy calculations of Chapter 4 that for intercalation, AT:AT sites were more favourable than GC:GC sites. The relative free energies of interaction for different dyes with these sites varied. Therefore, in a heterogeneous sample of DNA such as calf thymus DNA used in these experiments, if more sites with high free energies of interaction with one dye were adjacent to each other, then greater rigidity of the DNA-dye complex would result than for a dye whose free energies of interaction with adjacent sites were less and intercalation did not occur in adjacent sites.

The model involving external edgewise binding of the dye to the DNA will not produce any significant effect on the viscosity of DNA unless the rigidity of the DNA is greatly increased. This is unlikely as an

ion such as pinacyanol which is bound to the phosphate groups of the DNA does not increase the viscosity of DNA, but, in fact, reduces it.[4]

The phenomenon of precipitation is of interest in that it could indicate that once a certain number of sites on a DNA molecule are bound with dye, the molecule will precipitate. This would most likely occur as the molecule of DNA-dye became essentially neutralized in solution. This implies that more dye is bound to some DNA molecules than to others, and that the observed value of r is an average value of r over all DNA molecules. If this is the case, since the free energy calculations indicated a high energy of interaction with AT:AT sites, it may be anticipated that those molecules precipitated are those of high AT content, while those of high GC content remain. That only some DNA molecules, but most dye molecules are removed on precipitation is supported by the very much reduced visible absorption of the samples, tested when the overall viscosity had dropped to a little less than that of native DNA, at the same concentration as originally present in the DNA-dye system. Attempts were made to isolate the DNA (remaining with some dye in solution) by treating a DNA-7-aminobenz-[c]acridine solution, with precipitate removed, with

blotted beads of Zeocarb 225 resin, previously equilibrated with the solvent, 0.1M sodium chloride solution, to avoid pH disturbances. Lerman[4] reported to have successfully used this method for removing acridine orange from a DNA-acridine orange solution. However the method did not remove all of the bound dye (as shown by some absorption at a visible peak of the dye), indicating that the residual dye is strongly bound to the DNA. If the dye could be completely separated from the DNA, a determination of the T_m of the remaining DNA would indicate whether the DNA was AT or GC rich.

A third and possibly most likely explanation of the observed increase in viscosity may now be suggested. If this interpretation of precipitation above a certain value of r is correct, then it is evident that the difference in the value of r at which precipitation occurs for the three dyes shown in Fig. 7.1 arises because the number and type of favourable intercalation sites with a high energy of interaction differ, depending on the dye. Therefore it can be visualized that some dyes will be intercalated in many DNA molecules, whereas with other dyes, a large proportion of a few DNA molecules will be almost fully bound, at values of r where precipitation does not occur. If the viscosity of the

solution is affected to a greater extent by a few, extended and rigid DNA-dye molecules than by a larger number of partly extended and less rigid DNA-dye molecules, then the different viscosity increments observed in Fig. 7.1 may be interpreted. This implies that 7-aminobenz[c]acridine , which produces the greatest viscosity increment when bound to DNA and is the first DNA-dye complex to precipitate (Fig. 7.1), results in a smaller number of almost fully bound, extended and rigid DNA-dye molecules.

7.3 Sedimentation Coefficients of the System DNA-7-aminobenz[c]acridine.

Fig. 7.2 indicates that the sedimentation coefficient of the system DNA-7-aminobenz[c]acridine decreases in an approximately linear fashion with increasing r. It should be noted that r was chosen in the region before precipitation occurs (Fig. 7.1). However, if a small amount of precipitation did occur, the amount of DNA-dye complex in solution would be reduced, and, because of the lower DNA concentration, the sedimentation coefficient would increase slightly, if at all, and not decrease.[9] The values of $s_{20,w}$ were found at one DNA concentration, 20.8×10^{-5}M, and were

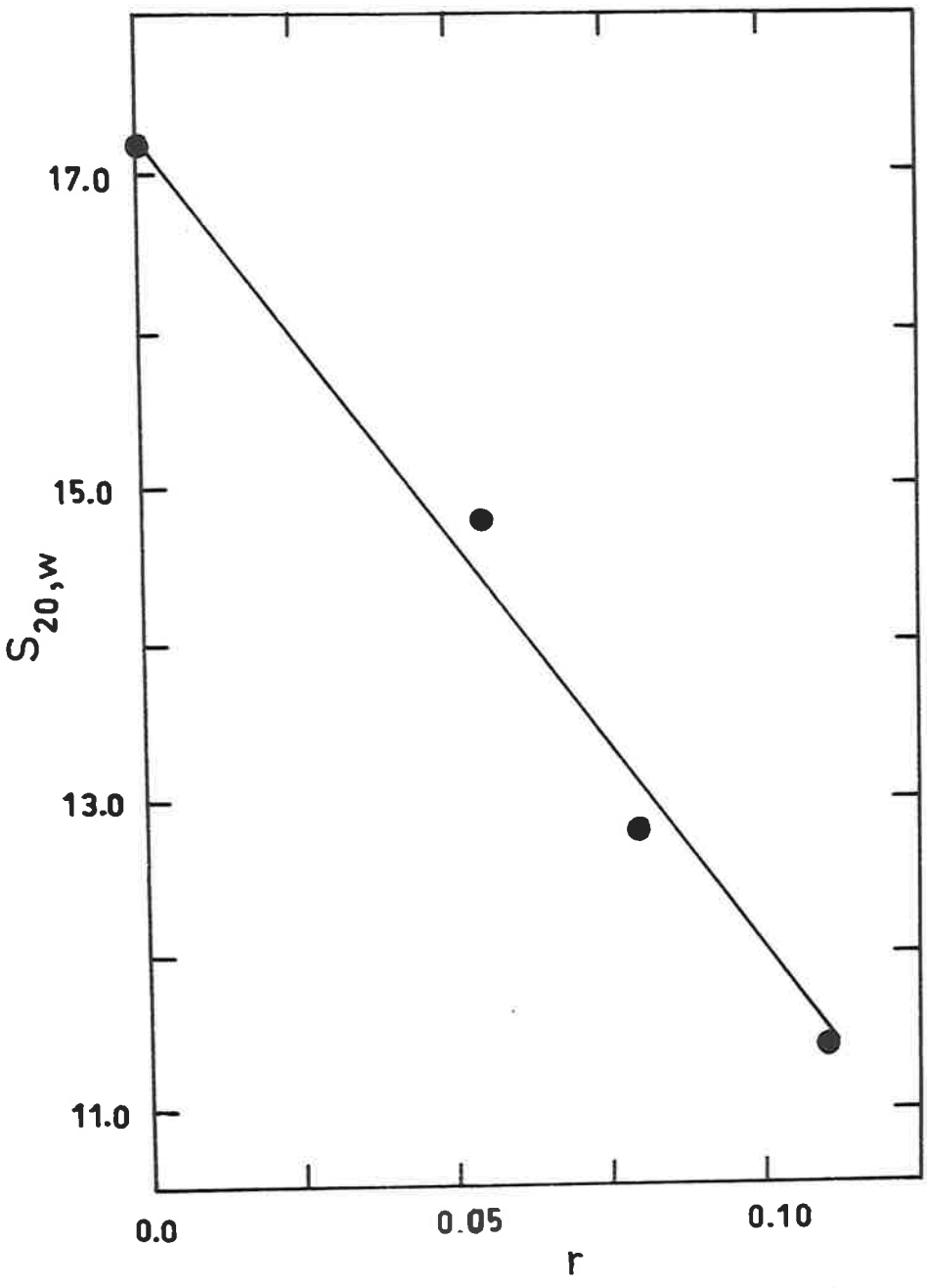

FIG. 7.2. The variation of the sedimentation coefficient, $s_{20,w}$, with r (found at 25°C) for the DNA-7-aminobenz[c]acridine system in 0.1M NaCl.

not extrapolated to zero concentration, as only the relative values of the sedimentation coefficients are of interest in the present study. The value of $s_{20,w}$ of 17.28 for DNA compares well with that of other workers at this concentration (about 0.01%), who obtain an average value of 17.58.[10]

Lerman[4] predicted that for intercalation up to r = 0.22 for proflavine, the sedimentation coefficient would be about 0.90 that of native DNA alone, and observed a decrease of this order for DNA and proflavine concentrations corresponding to a value of r of approximately 0.10. According to Lerman's interpretation of the sedimentation coefficient data of DNA-aminoacridine systems, the sedimentation coefficients of DNA-7-amino-benz[c]acridine systems would be expected to be greater than those of DNA-proflavine systems at the same values of r since the mass per unit length is greater in the former case. However, the reverse is found, since for r = 0.08 for DNA-7-aminobenz[c]acridine, $(s_{20,w})_{sol.}/(s_{20,w})_{DNA} = 0.74$.

If the above interpretation of precipitation is correct, then one possible explanation of the lower sedimentation coefficients of DNA-7-aminobenz[c]acridine systems may be put forward. The sedimentation coefficient,

s°, extrapolated to zero concentration, is given by

$$s^\circ = \frac{M(1 - \bar{v}_2\rho_0)}{6\pi\eta N \xi_f R_G} \qquad (7.1)$$

where $\bar{v}_2$ is the thermodynamic partial specific volume of the solute, ρ_0 is the density of the solvent, η is the coefficient of viscosity, N is Avogadro's number, ξ_f is the average frictional coefficient, R_G is the radius of gyration and M is the molecular weight of the macromolecule. If $\bar{v}_2$ and ξ_f are assumed to be constant for both DNA-dye systems under consideration, then

$$s^\circ \propto \frac{M}{\eta R_G} \qquad (7.2)$$

Since, from the above explanation of precipitation, the DNA-7-aminobenz[c]acridine system may have a smaller number of extended, rigid DNA-dye molecules compared with a DNA-proflavine system with a larger number of partly extended and less rigid DNA-dye molecules for a given value of r, then η (from Fig. 7.1), R_G and M will all be larger for the DNA-7-aminobenz[c]acridine system than for the DNA-proflavine system. However the difference in molecular weights of the two dyes is small compared with

the large difference in the viscosities of the two DNA-dye complexes. Therefore s° is expected to be smaller for DNA-7-aminobenz[c]acridine systems than for DNA-proflavine systems for the same value of r.

The possibility of aggregation of the DNA-dye molecules is eliminated by the lowered sedimentation coefficients, since the formation of dimers could be expected to give a sedimentation coefficient between 1.29 and 2 times that of native DNA alone.[4] Therefore aggregation cannot be used to explain the viscosity increase observed, and the above interpretations to the viscosity and sedimentation coefficient results in terms of the intercalated model may be applied.

7.4 Summary of General Conclusions of the Results and and Discussion of Chapters 4, 5, 6 and 7.

The free energy calculations of Chapter 4 show that the intercalated model is more stable than the model involving external edgewise binding for various DNA-aminoacridine and DNA-aminobenzacridine systems. The relative affinity of proflavine, for example, for base pairs of DNA was predicted to be AT:AT > AT:GC > GC:GC, in agreement with experimental evidence cited by other workers. In addition, it was possible to

predict that several differences in the affinity of various dye ions for DNA would be found. This was confirmed with the binding curves of Chapter 5, which may be interpreted in terms of the intercalated model using the free energy calculations.

The thermal denaturation temperature of DNA-aminoacridine and DNA-aminobenzacridine systems (Chapter 6) was found to increase above that of native DNA. This increase has been shown to be related to the amount of strong binding exhibited by the system in the binding curves.

The sedimentation coefficient results verified that aggregation is not responsible for the increased viscosity of the DNA-aminoacridine systems and DNA-aminobenzacridine systems over that of native DNA. The viscosity and sedimentation coefficient results (Chapter 7) were also interpreted in terms of the theory of intercalation.

Thus it is evident that the results of the free energy calculations are in conformity with the experimental results of dye binding and stability studies, and it is possible to provide satisfactory, semi-quantitative interpretations for several properties of DNA-aminoacridine and DNA-aminobenzacridine systems in terms of the intercalated model.

References.

1. Mathiesen, A.R. and Matty, S., J.Polym.Sci. 23, 759 (1957).

2. Stern, K.G. and Atlas, S.M., J.Biol.Chem. 203, 795 (1953).

3. Kahler, H.J. and Shmuk, J., J.Phys.Chem. 61, 649 (1957).

4. Lerman, L.S., J.Mol.Biol. 3, 18 (1961).

5. Lerman, L.S., Proc.Nat.Acad.Sci., Wash.49,94 (1963).

6. Bradley, D.F. and Wolf, M.K., ProcNat.Acad.Sci., Wash. 45, 944 (1959).

7. Mason, S.F. and McCaffery, A.J., Nature 204, 468 (1964).

8. Lerman, L.S., J.Cell.Comp.Physiol.Supp. 1, 64, 1 (1964).

9. Shooter, K.V. and Butler, J.A.V., Trans.Faraday Soc. 52, 738 (1956).

10. Jordan, D.O., "The Chemistry of the Nucleic Acids", Butterworths, London, p181 (1960).

CHAPTER 8.

EXPERIMENTAL TECHNIQUES.

8.1 Preparation of Samples.

Calf thymus DNA was prepared by the method of Kay, Simmons and Dounce,[1] but solutions were always made in sodium chloride solution and not in water alone to prevent partial denaturation of the DNA. The value of T_m in 0.1M sodium chloride solution was 82.7°C and the value of ε_p, 6620. These values are in agreement with those previously published for native preparations of calf thymus DNA. The value of ε_p was used for the determination of concentrations. Stock solutions of approximately 0.1% by weight of DNA were prepared in twice-distilled water and diluted with sodium chloride solution to give a final sodium chloride concentration of either 0.1M or 0.001M.

Proflavine hemisulphate (British Drug Houses Ltd., England) was recrystallized from water, after washing with dry ethanol, and dried *in vacuo* to constant weight. 3-Aminoacridine was prepared by Dr G.Chandler, of the Organic Chemistry Department, University of

Adelaide. The hydrochloride was prepared by passing dry HCl gas through a solution of the purified base in dry diethyl ether. The hydrochloride precipitated and was recovered by removal of the excess ether and dried at room temperature. Samples of both dyes, dried *in vacuo*, were used in preparing solutions by weight (to ± 0.00005 gm), and concentrations were checked by conductiometric titration; agreement was within 1%. The conductiometric titrations, with dye concentrations of approximately 10^{-4}M in twice-distilled water and 10^{-3}M ammonium hydroxide, were carried out in a specially designed micro-conductivity cell, with a capacity of about 7 mls. The cell is shown in Plate 8.1, and the tube in the foreground was used for passing a few bubbles of nitrogen through the solution for mixing purposes during the titrations.

The commercial sample of 9-aminoacridine hydrochloride (Fluka AG, Switzerland) was purified by two recrystallizations from ethanol.

The other dyes used in this work were a gift from Professor A. Albert of the Department of Medical Chemistry, the Australian National University.

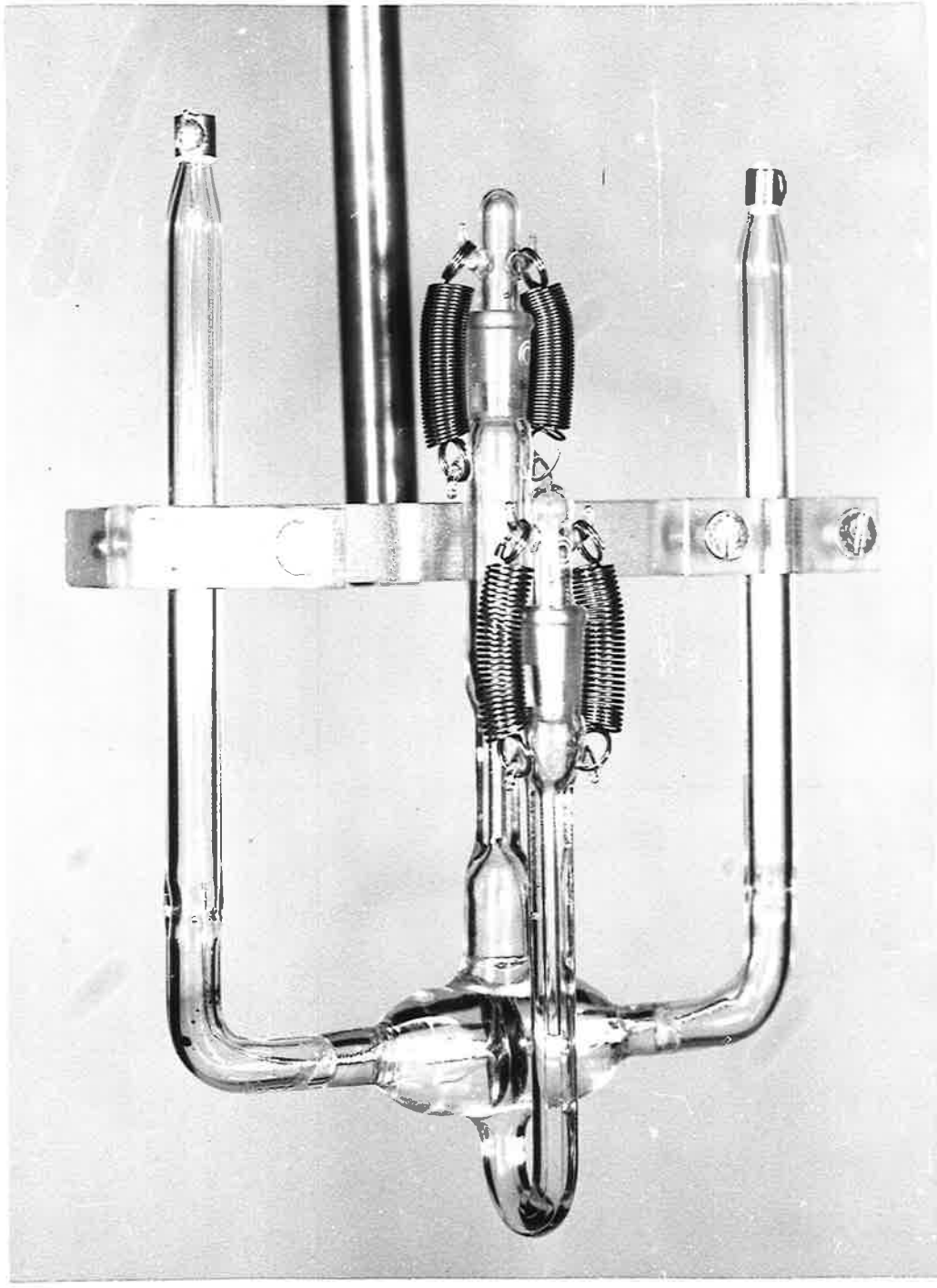

Plate 8.1. Conductivity cell used for conductiometric titrations of dyes.

The hydrochlorides of the dyes 12-aminobenz[a]acridine, 2-aminobenz[b]acridine, 7-aminobenz[c]acridine, and 2- and 4-aminoacridine were prepared by the method described above for 3-aminoacridine. The dyes were dried *in vacuo* and the solutions were prepared by weight.

Since Millich and Carter[2] found that proflavine in solution undergoes rapid photoreduction, although the other aminoacridines do not, all solutions of dyes were stored in the dark. Special precautions were necessary with 12-aminobenz[b]acridine which is very light sensitive, even in the solid form.[3] Polythene containers were used for the stock dye solutions (about 4×10^{-4}M), since these did not adsorb dye to any significant extent. Pyrex test tubes were used in the preparation of all dilute dye solutions, as it was shown that soft glass adsorbs dye to a much greater extent than does Pyrex.

8.2 Spectra and Spectrophotometric Titrations.

The spectra reported in Chapter 3 and Appendix 3, were determined with solutions prepared by weight in ethanol solution ("Univar", 99.5% purity). Before the determination of each spectrum, the 1 cm. silica cells

were thoroughly cleaned, and then rinsed with the solution under consideration.

The decrease in optical density on the addition (by weight) of small volumes of DNA solutions to dilute dye solutions contained in 1 cm. silica cells was followed at a selected λ_{max} in the visible absorption spectrum of each dye. To stir the solutions after each addition of DNA, semi-micro magnetic stirrers were made by sealing a short length of steel wire in polyethylene tubing ("Intramedic", Clay-Adams, Inc., New York; outer diameter 0.05 inches), as described by Wolf and Bradley.[4] Two or three such titrations, using a different DNA concentration each time were required before the binding curve could be found from the volume corrected optical densities by the method of Peacocke and Skerrett.[5] That this method involving successive additions of DNA to a DNA-dye solution does not affect the magnitude of the decrease in optical density is shown in Fig. 6.1. Three spectrophotometric titrations are shown for proflavine, and although each begins at a different initial DNA concentration, the curves coincide. Furthermore, the binding curve of r versus c obtained

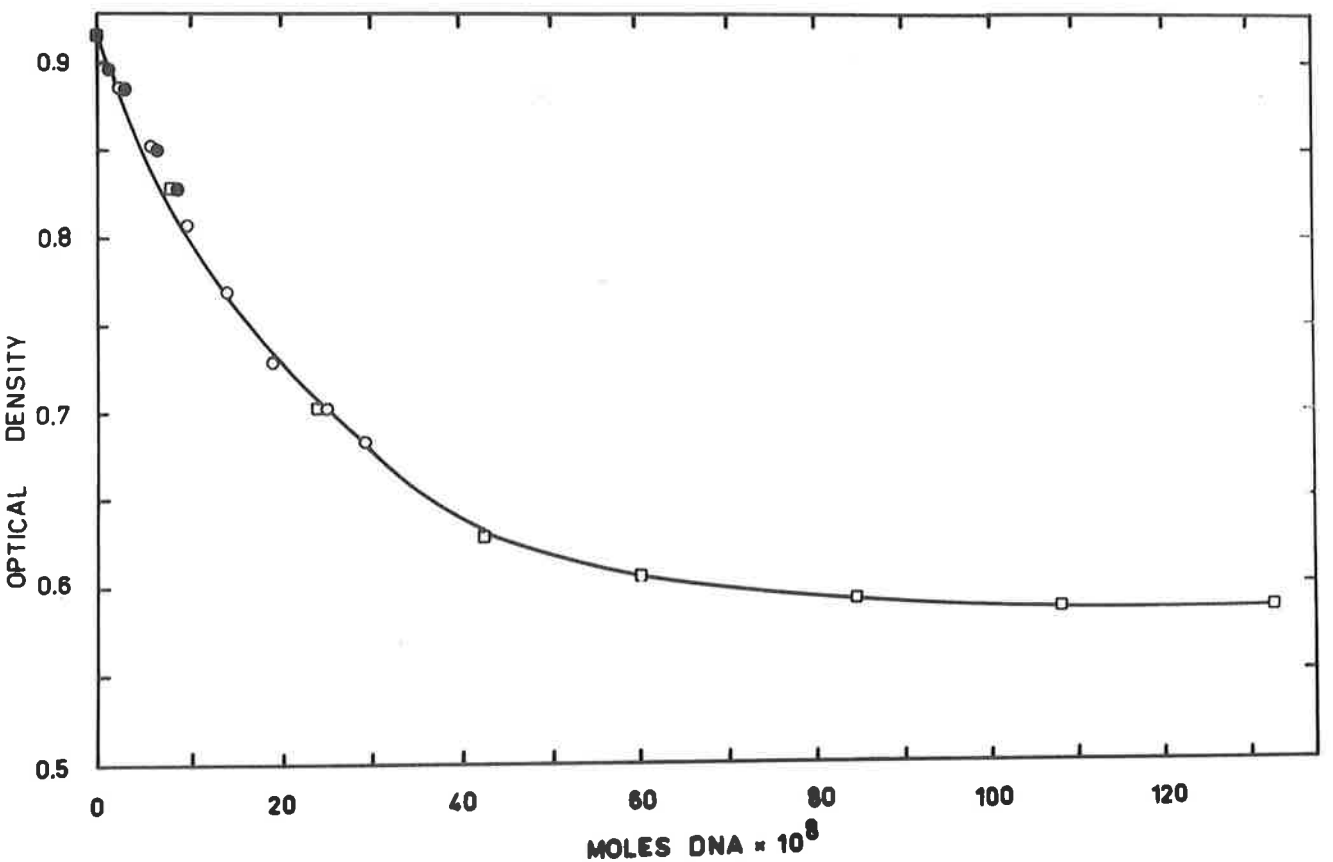

FIG. 8.1. Decrease in optical density (at 444mμ) with increasing DNA concentration for the system DNA-proflavine in 0.1M NaCl at 25°C, pH 6.2.
The initial dye concentration was 2.23×10^{-5}M.
-●-, DNA added was 5.25×10^{-5}M; -o-, DNA added was 20.8×10^{-5}M; -□-, DNA added was 107×10^{-5}M.

by this method for calf thymus DNA (GC content 42%) and proflavine at 20°C is in agreement with that obtained by Peacocke and Skerrett[5] using herring sperm DNA (GC content 43%) and proflavine at 18 - 20°C for 0.1N sodium chloride solutions. (see Fig. 5.5).

All spectra and spectrophotometric titrations reported here were found by manual use of the Gilford (Model 2000) recording spectrophotometer, with which it is possible to obtain an accuracy of ± 0.002 optical density units.

When determining the effect of DNA on the spectrum of a dye whose pK_a was sufficiently low to make pH effects significant, dye solution was added to the DNA solution so that the pH of the final solution was the minimum pH reached.

5.3 Equilibrium Dialysis.

Equilibrium dialysis was used to find the binding curves for several of the dyes, and to prepare solutions for viscosity and sedimentation measurements. The tubing (20/32 Visking; "Dexstar") was heated for 20 minutes at 80°C in 0.5% sodium bicarbonate solution

to remove any impurities, washed seven times with twice-distilled water and stored in water at 4°C.

For each determination of r, one dialysis tube was filled with 4 or 5 mls. of about 20 x 10^{-5}M DNA solution in 0.1N sodium chloride and one was filled with a similar amount of 0.1N sodium chloride solution (by weight). These were placed in two Pyrex test tubes, fitted with polythene stoppers, and containing about 4 or 5 mls. (by weight) of dye solution. The size of the test tubes and the filled dialysis tubing was such that all of the dialysis tubing was covered with dye solution and there was free movement of dye solution around the tubing. The tubes were sealed, placed in holders and shaken gently for 72 hours with the lower two thirds of the tubes in a water bath at 25.0 ± 0.002°C. On removal, the optical densities of the outside dye solutions were found either directly or after dilution, depending on the dye concentration, and the amount of dye bound to the DNA was calculated, assuming that the dialysis tubes adsorbed the same amount of dye in both cases. The equilibrium dialysis determination of r was accurate to 5% or better.

8.4 Thermal Denaturation.

For the determination of melting curves, DNA-dye solution was contained in either 10- or 2-mm. silica cells, using 0.1M sodium chloride in a matched 10-mm. cell as reference. Evaporation from the 10-mm. cells was prevented by a layer of paraffin, and from the 2-mm. cells by a layer of paraffin and a seal of Parafilm (Lindsay and Williams Ltd., London, England). The cells were placed in an electrically heated and thermostatically controlled cell holder. Temperatures close to the sample were determined using a calibrated thermocouple. The optical density at 259 mμ was found using a Unicam SP500 spectrophotometer and was corrected for increase in volume with temperature.

All DNA-dye solutions had a pH of between 5.7 and 6.2 (except where specific mention is made to the contrary). At constant sodium ion concentration, a variation of pH between 5.7 and 6.2 produces a variation of T_m of native DNA of no more than 0.5°C. [6] Hence such pH differences have been neglected in the interpretation of the T'_m values obtained.

The pH measurements were made with a Titrea

micro glass electrode (Thomas Optical and Scientific Co. Pty. Ltd., Australia). This enabled the measurement of the pH of as little as 0.5 ml. of solution.

8.5 Viscosity.

The viscosity of the DNA-dye solutions was determined at 25.0 ± 0.002°C in a specially designed low shear suspended level viscometer (shown in Plate 8.2) in which the capillary (about 1 metre of 1 mm. diameter) was wound in a spiral. The total volume of solution necessary for the operation of the viscometer was 2 mls. The average rate of shear calculated by the Kroeperlin equation was about 7 sec^{-1}. The water flow time varied between 200.13 and 200.18 sec.

The viscometer was cleaned with chromic acid and washed thoroughly with water and finally with acetone, all of these solutions being filtered through a sintered glass funnel. The viscometer was dried by attaching it to a vacuum pump.

The DNA-dye solutions for viscosity measurements were prepared by equilibrium dialysis as in Section 8.3, and then centrifuged for 1 hour at 10,000rpm

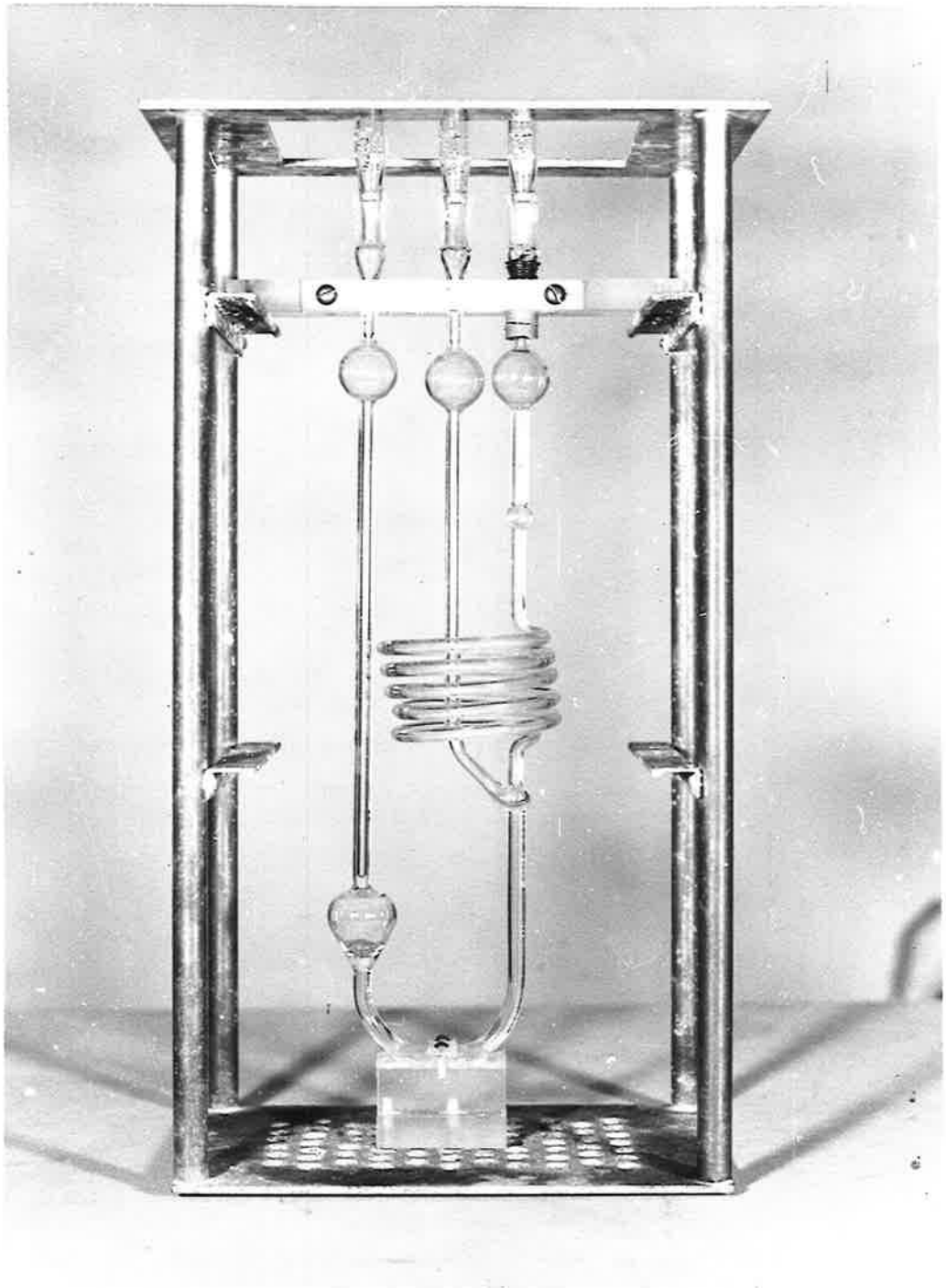

Plate 8.2. Viscometer. Note the spiral capillary and the small sizes of the bulbs.

in a Servall centrifuge before transferring to the viscometer with a long thin piece of polythene tubing ("Intramedic", Clay-Adams, Inc., New York; outer diameter 0.05 inches) attached to a syringe with a large internal diameter needle (gauge 20).

During a viscosity run the viscometer was shielded from as much light as possible, as the DNA-dye complex has been shown to be light sensitive in the case of DNA-acridine orange.[7] The flow time was found to the nearest 1/100th second with a "Hanhart" stopwatch (Dobbie Bros. Pty.Ltd., Melbourne, Australia). Flow times for each solution were repeated until three times agreed to ± 0.05 second.

Since the volume of the solution used in the viscometer is very small, care was taken that the efflux volume did not vary for successive runs. The solution was pumped into the bulb very slowly till the level in the capillary reached a certain point above the scratch mark. It was found that consistent flow times could be recorded if this procedure was followed each time.

8.6 Sedimentation Coefficients.

A Spinco model E ultracentrifuge equipped with ultraviolet optics was used to measure the sedimentation coefficients. The measurements were made at 35,600 rpm using a 12-mm aluminium wide window cell in a D rotor thermostated at 20.0 ± 0.1°C. All measurements were made in 0.1M sodium chloride, and solutions were prepared by equilibrium dialysis at 25°C as described in Section 8.3. Photographs were taken at intervals of 4 minutes and converted later to plots of concentration versus distance in the cell with a Spinco Analytrol photodensitometer with a micro-analyser attachment. From the photodensitometer tracing, the position in the cell corresponding to the 50% concentration point could be found, and from this, the sedimentation coefficient was calculated. A value of 0.55 for $\bar{v}$, the partial molar volume was assumed for both DNA[8] and for the DNA-dye complex. Although this latter value is an approximation, the conclusions of Chapter 7 will not be altered significantly.

References.

1. Kay, E.R.M., Simmons, N.S. and Dounce, A.L., J.Am.Chem.Soc. 74, 1724 (1952).

2. Millich, F. and Oster, G., ibid. 81, 1357 (1959).

3. Albert, A., personal communication (1965).

4. Wolf, M.K. and Bradley, D.F., Stain Tech. 35,44 (1960).

5. Peacocke, A.R. and Sherrett, J.N.H., Trans.Faraday Soc. 52, 261 (1956).

6. Jordan, D.O. and Kelly, R.E.G., unpublished results.

7. Freifelder, D., Davison, P.F. and Geiduschek, E.P., Biophys.J. 1, 389 (1961).

8. Doty, P., Proc.3rd Int.Nat.Cong.Biochem.,Brussels, 135 (1955).

APPENDIX 1.

STRUCTURE OF ACRIDINES AND OTHER IMPORTANT MOLECULES MENTIONED IN THE TEXT.

APPENDIX 1: STRUCTURE OF DYES AND OF OTHER MOLECULES.

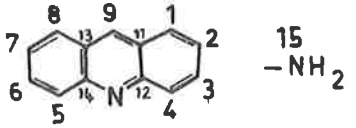

acridine

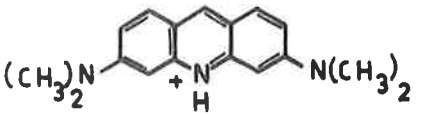

acridine orange

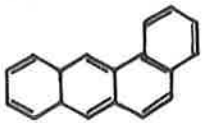

benz[a]anthracene

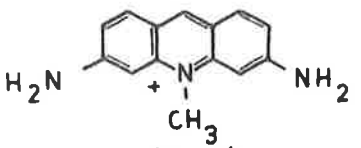

acriflavine

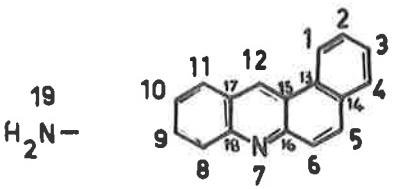

benz[a]acridine

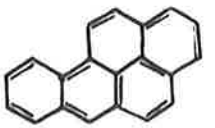

benz[a]pyrene

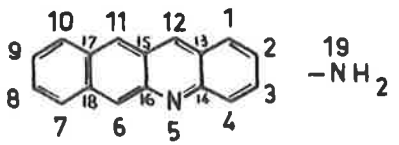

benz[b]acridine

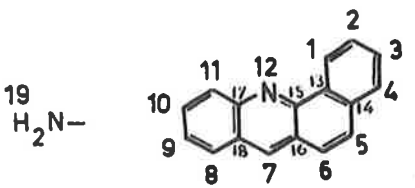

benz[c]acridine

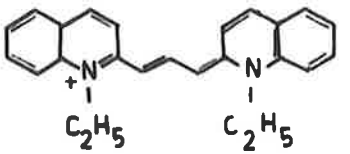

pinacyanol

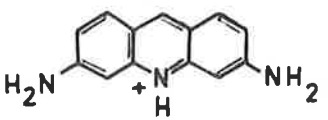

proflavine

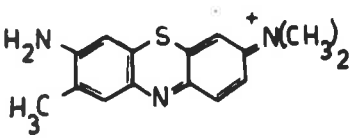

toluidine blue

pyrene

APPENDIX 2.

RESULTS OF MOLECULAR ORBITAL CALCULATIONS.

TABLE A2.1

ENERGIES OF MOLECULAR ORBITALS OF THE AMINOACRIDINIUM ION

POSITION OF AMINO GROUP				
1	2	3	4	9
0.518	0.487	0.620	0.447	0.683
0.866	0.852	0.766	0.876	1.000
1.000	1.000	1.000	1.000	1.000
1.397	1.256	1.191	1.276	1.000
1.414	1.579	1.652	1.617	1.612
1.972	1.966	1.958	1.950	2.000
2.151	2.141	2.127	2.105	2.100
2.980	2.977	2.978	2.986	2.985
-0.230	-0.176	-0.223	-0.185	-0.370
-1.000	-1.000	-1.000	-1.000	-1.000
-1.051	-1.047	-1.058	-1.052	-1.000
-1.240	-1.227	-1.180	-1.212	-1.182
-1.414	-1.452	-1.477	-1.450	-1.475
-2.024	-2.026	-2.026	-2.025	-2.000
-2.338	-2.330	-2.329	-2.334	-2.352
RESONANCE ENERGY				
3.766	3.688	3.758	3.688	3.932

TABLE A2.2

THE AMINOACRIDINIUM ION

ELECTRICAL CHARGES ON ATOMS

ATOM	POSITION OF AMINO GROUP				
	1	2	3	4	9
1	0.878	1.059	0.943	1.030	0.954
2	1.111	0.956	1.049	1.007	1.028
3	0.929	0.967	0.879	1.039	0.952
4	1.114	1.036	1.137	0.971	1.048
12	0.862	0.871	0.860	0.879	0.883
10	1.729	1.713	1.731	1.707	1.759
14	0.860	0.858	0.863	0.854	0.883
5	1.045	1.042	1.045	1.042	1.048
6	0.936	0.934	0.939	0.931	0.952
7	1.019	1.014	1.019	1.013	1.028
8	0.948	0.948	0.950	0.945	0.954
13	1.017	1.009	1.017	1.008	1.044
9	0.734	0.738	0.748	0.723	0.740
11	1.036	1.006	1.026	1.009	1.044
15	1.781	1.850	1.794	1.842	1.682

BOND ORDERS OF BONDS

BOND	POSITION OF AMINO GROUP				
	1	2	3	4	9
1-2	.630	.671	.756	.718	.701
2-3	.656	.556	.536	.616	.630
3-4	.662	.713	.619	.655	.691
4-12	.628	.593	.647	.542	.613
12-10	.403	.416	.402	.420	.377
10-14	.403	.419	.402	.423	.377
14-5	.605	.599	.606	.597	.613
5-6	.697	.703	.696	.704	.691
6-7	.615	.607	.615	.606	.630
7-8	.716	.724	.716	.725	.701
8-13	.554	.542	.553	.542	.583
13-9	.554	.579	.556	.580	.472
9-11	.624	.577	.615	.577	.472
11-1	.480	.551	.520	.536	.583
11-12	.503	.508	.491	.524	.555
13-14	.526	.513	.525	.512	.555
X-15	.469	.388	.456	.390	.597

TABLE A2.3

ENERGIES OF MOLECULAR ORBITALS OF THE AMINOBENZ(A)ACRIDINE MOLECULE

POSITION OF AMINO GROUP

1	2	3	4	5	6	8	9	10	11	12
0.447	0.428	0.462	0.419	0.403	0.365	0.358	0.454	0.405	0.384	0.390
0.533	0.639	0.569	0.570	0.634	0.667	0.696	0.611	0.706	0.666	0.675
1.000	0.822	0.844	1.000	1.000	0.865	0.834	0.862	0.766	0.854	1.000
1.000	1.126	1.105	1.000	1.000	1.166	1.104	1.000	1.085	1.135	1.000
1.285	1.186	1.240	1.347	1.194	1.211	1.318	1.331	1.263	1.238	1.235
1.450	1.492	1.475	1.385	1.435	1.412	1.396	1.427	1.485	1.469	1.386
1.610	1.592	1.580	1.589	1.726	1.612	1.627	1.605	1.563	1.560	1.765
1.851	1.907	1.911	1.866	1.809	1.913	1.839	1.904	1.918	1.882	1.781
2.243	2.237	2.241	2.255	2.229	2.198	2.250	2.239	2.237	2.245	2.198
2.538	2.525	2.524	2.532	2.543	2.550	2.537	2.525	2.524	2.535	2.563
-0.377	-0.397	-0.380	-0.390	-0.425	-0.412	-0.420	-0.401	-0.399	-0.421	-0.476
-0.792	-0.732	-0.744	-0.787	-0.759	-0.738	-0.719	-0.738	-0.716	-0.730	-0.740
-1.000	-1.034	-1.034	-1.000	-1.000	-1.040	-1.033	-1.000	-1.029	-1.036	-1.000
-1.198	-1.168	-1.180	-1.206	-1.172	-1.166	-1.186	-1.230	-1.188	-1.170	-1.179
-1.279	-1.313	-1.310	-1.271	-1.281	-1.270	-1.294	-1.275	-1.321	-1.321	-1.280
-1.501	-1.488	-1.474	-1.485	-1.541	-1.517	-1.496	-1.499	-1.483	-1.475	-1.520
-1.757	-1.778	-1.783	-1.768	-1.743	-1.772	-1.752	-1.764	-1.765	-1.754	-1.744
-2.178	-2.176	-2.177	-2.182	-2.175	-2.167	-2.189	-2.183	-2.183	-2.189	-2.171
-2.475	-2.469	-2.469	-2.473	-2.477	-2.477	-2.470	-2.467	-2.467	-2.471	-2.484

RESONANCE ENERGY

7.474	7.468	7.462	7.486	7.506	7.478	7.478	7.476	7.464	7.496	7.546

TABLE A2.4

ELECTRICAL CHARGES ON ATOMS OF THE AMINOBENZ(A)ACRIDINE MOLECULE

	POSITION OF AMINO GROUP										
	1	2	3	4	5	6	8	9	10	11	12
1	0.937	1.087	0.995	1.066	1.003	0.999	1.000	1.003	1.000	1.003	1.014
2	1.082	0.937	1.051	0.988	0.991	1.024	0.997	0.995	0.997	0.994	0.994
3	0.995	1.056	0.945	1.088	1.006	1.000	1.000	1.004	1.001	1.003	1.012
4	1.061	0.987	1.084	0.927	0.985	1.025	0.996	0.994	0.996	0.993	0.994
14	1.002	1.041	1.000	1.051	1.019	0.997	1.002	1.006	1.002	1.005	1.014
5	0.974	0.968	0.977	0.963	0.905	1.126	0.982	0.972	0.983	0.971	0.972
6	1.012	1.043	1.013	1.045	1.159	0.939	1.010	1.016	1.011	1.015	1.021
16	0.948	0.944	0.949	0.943	0.942	0.959	0.959	0.945	0.959	0.944	0.947
7	1.201	1.211	1.200	1.213	1.249	1.183	1.180	1.231	1.193	1.223	1.304
18	0.961	0.957	0.960	0.957	0.958	0.962	0.984	0.955	0.977	0.957	0.959
8	1.015	1.017	1.015	1.018	1.025	1.012	0.939	1.130	1.006	1.102	1.035
9	0.986	0.983	0.986	0.983	0.984	0.986	1.098	0.927	1.021	0.976	0.982
10	1.005	1.008	1.005	1.008	1.016	1.003	0.996	1.043	0.945	1.115	1.030
11	0.991	0.987	0.991	0.988	0.987	0.990	1.078	0.981	1.104	0.918	0.977
17	1.003	1.006	1.003	1.006	1.016	1.001	1.003	1.024	1.000	1.034	1.047
12	0.948	0.931	0.945	0.932	0.932	0.941	0.955	0.930	0.961	0.920	0.864
15	0.998	1.008	1.001	1.006	1.021	1.002	1.001	1.018	1.003	1.017	1.071
13	1.047	0.991	1.035	0.994	0.992	1.029	0.997	0.994	0.997	0.993	0.988
19	1.835	1.838	1.846	1.825	1.809	1.825	1.824	1.834	1.842	1.815	1.776

TABLE A2.5

BOND ORDERS OF BONDS IN THE AMINOBENZ(A)ACRIDINE MOLECULE

BOND	POSITION OF AMINO GROUP (X)										
	1	2	3	4	5	6	8	9	10	11	12
1-2	.633	.634	.709	.680	.693	.692	.695	.696	.695	.696	.701
2-3	.645	.574	.578	.649	.633	.627	.628	.627	.628	.627	.623
3-4	.689	.718	.643	.633	.694	.702	.701	.702	.701	.702	.704
4-14	.576	.570	.593	.529	.596	.575	.581	.580	.581	.580	.578
14-5	.495	.506	.492	.515	.447	.512	.495	.497	.495	.497	.504
5-6	.780	.772	.781	.769	.695	.711	.780	.779	.780	.780	.775
6-16	.500	.503	.498	.506	.533	.451	.499	.500	.499	.499	.504
16-7	.615	.612	.615	.611	.599	.629	.611	.608	.612	.608	.587
7-18	.577	.576	.577	.576	.570	.576	.595	.570	.584	.574	.556
18-8	.547	.547	.547	.547	.550	.547	.494	.567	.537	.551	.554
8-9	.729	.729	.729	.729	.726	.729	.664	.664	.745	.709	.721
9-10	.594	.595	.594	.595	.598	.595	.613	.540	.544	.621	.606
10-11	.730	.729	.730	.729	.725	.730	.717	.749	.670	.655	.715
11-17	.545	.547	.545	.546	.551	.545	.542	.533	.558	.493	.571
17-12	.584	.580	.583	.580	.572	.583	.583	.596	.579	.606	.512
12-15	.639	.648	.642	.646	.658	.644	.643	.634	.644	.631	.560
15-13	.460	.443	.452	.446	.439	.442	.447	.450	.447	.451	.470
13-1	.546	.613	.588	.596	.599	.601	.597	.596	.597	.595	.588
13-14	.552	.537	.540	.549	.555	.539	.546	.545	.546	.545	.539
15-16	.499	.500	.500	.500	.489	.509	.503	.507	.502	.508	.529
17-18	.496	.498	.497	.498	.501	.498	.502	.488	.491	.498	.515
X-19	.409	.404	.395	.420	.440	.416	.417	.411	.398	.431	.483

TABLE A2.6

ENERGIES OF MOLECULAR ORBITALS OF THE AMINOBENZ(B)ACRIDINE MOLECULE

POSITION OF AMINO GROUP

1	2	3	4	6	7	8	9	10	11	12
0.296	0.300	0.327	0.274	0.203	0.265	0.310	0.295	0.276	0.234	0.275
0.585	0.613	0.612	0.587	0.749	0.631	0.625	0.645	0.623	0.740	0.719
1.000	0.870	0.852	1.000	1.000	1.000	0.850	0.843	1.000	1.000	1.000
1.054	1.128	1.103	1.050	1.000	1.000	1.102	1.108	1.000	1.000	1.000
1.292	1.213	1.233	1.294	1.246	1.307	1.239	1.217	1.283	1.283	1.254
1.387	1.482	1.510	1.414	1.422	1.414	1.477	1.522	1.469	1.346	1.362
1.607	1.571	1.558	1.605	1.661	1.613	1.595	1.563	1.580	1.706	1.727
1.892	1.935	1.929	1.872	1.838	1.863	1.911	1.912	1.866	1.827	1.828
2.253	2.245	2.246	2.255	2.228	2.268	2.256	2.256	2.269	2.232	2.218
2.521	2.510	2.511	2.524	2.546	2.517	2.508	2.508	2.517	2.543	2.546
-0.279	-0.256	-0.268	-0.268	-0.312	-0.263	-0.261	-0.254	-0.269	-0.332	-0.358
-0.801	-0.769	-0.774	-0.799	-0.790	-0.818	-0.774	-0.777	-0.817	-0.788	-0.784
-1.000	-1.031	-1.033	-1.000	-1.000	-1.000	-1.033	-1.033	-1.000	-1.000	-1.000
-1.230	-1.189	-1.178	-1.222	-1.185	-1.203	-1.176	-1.184	-1.210	-1.181	-1.186
-1.289	-1.344	-1.339	-1.291	-1.285	-1.299	-1.347	-1.326	-1.283	-1.302	-1.295
-1.445	-1.432	-1.439	-1.450	-1.489	-1.450	-1.432	-1.444	-1.460	-1.472	-1.469
-1.786	-1.799	-1.801	-1.789	-1.778	-1.791	-1.804	-1.804	-1.790	-1.780	-1.781
-2.206	-2.200	-2.200	-2.205	-2.191	-2.202	-2.197	-2.197	-2.201	-2.190	-2.193
-2.452	-2.448	-2.448	-2.451	-2.463	-2.453	-2.449	-2.449	-2.453	-2.464	-2.463

RESONANCE ENERGY

7.334	7.294	7.322	7.310	7.346	7.316	7.306	7.298	7.326	7.382	7.418

TABLE A2.7

ELECTRICAL CHARGES ON ATOMS OF THE AMINOBENZ(B)ACRIDINE MOLECULE

ATOM	POSITION OF AMINO GROUP										
	1	2	3	4	6	7	8	9	10	11	12
1	0.908	1.109	0.973	1.080	0.994	0.984	0.981	0.985	0.980	0.977	0.969
2	1.124	0.946	1.040	0.997	1.002	1.006	1.011	1.006	1.011	1.020	1.041
3	0.968	1.008	0.918	1.101	0.990	0.979	0.975	0.979	0.975	0.974	0.975
4	1.111	1.008	1.141	0.939	1.010	1.017	1.022	1.017	1.022	1.030	1.045
14	0.948	0.962	0.946	0.969	0.968	0.951	0.947	0.952	0.946	0.947	0.951
5	1.250	1.205	1.259	1.189	1.175	1.207	1.232	1.211	1.229	1.265	1.350
16	0.959	0.967	0.960	0.968	0.994	0.966	0.959	0.966	0.958	0.958	0.962
6	1.041	1.023	1.043	1.019	0.908	1.005	1.073	1.018	1.063	1.172	1.071
18	0.988	0.993	0.988	0.993	1.053	1.013	0.985	1.004	0.988	0.985	0.988
7	1.009	1.004	1.009	1.004	0.984	0.929	1.130	0.995	1.100	1.035	1.015
8	0.991	0.996	0.992	0.995	1.033	1.114	0.932	1.026	0.983	0.985	0.991
9	1.007	1.003	1.007	1.002	0.994	0.993	1.037	0.943	1.122	1.040	1.015
10	0.992	0.997	0.993	0.996	1.027	1.090	0.984	1.119	0.918	0.975	0.989
17	1.007	1.003	1.008	1.002	0.998	1.003	1.019	0.999	1.029	1.061	1.019
11	0.965	0.986	0.968	0.983	1.131	1.006	0.961	1.015	0.949	0.867	0.951
15	1.010	1.002	1.010	1.001	1.001	1.001	1.010	1.002	1.010	1.041	1.040
12	0.888	0.948	0.901	0.939	0.960	0.916	0.901	0.918	0.897	0.885	0.829
13	1.030	1.001	1.020	1.004	1.000	1.003	1.009	1.004	1.009	1.022	1.059
19	1.805	1.840	1.824	1.821	1.779	1.819	1.833	1.839	1.812	1.760	1.741

TABLE A2.8

BOND ORDERS OF BONDS IN THE AMINOBENZ(B)ACRIDINE MOLECULE

BOND	POSITION OF AMINO GROUP (X)										
	1	2	3	4	6	7	8	9	10	11	12
1-2	.659	.680	.760	.726	.739	.740	.738	.740	.738	.731	.718
2-3	.616	.531	.527	.602	.584	.583	.585	.583	.585	.591	.602
3-4	.712	.753	.666	.672	.737	.738	.736	.738	.736	.732	.724
4-14	.546	.527	.563	.483	.538	.536	.538	.536	.538	.542	.550
14-5	.595	.610	.591	.622	.598	.603	.599	.603	.600	.589	.567
5-16	.564	.568	.563	.568	.599	.574	.567	.573	.568	.563	.545
16-6	.594	.592	.595	.592	.516	.581	.595	.586	.593	.597	.602
6-18	.612	.615	.612	.615	.550	.635	.607	.623	.611	.591	.604
18-7	.533	.532	.533	.532	.555	.481	.551	.522	.535	.541	.536
7-8	.739	.740	.739	.740	.727	.670	.673	.756	.719	.730	.736
8-9	.583	.581	.583	.581	.589	.603	.529	.531	.609	.596	.587
9-10	.739	.740	.739	.741	.736	.725	.758	.679	.664	.722	.734
10-17	.533	.531	.533	.531	.534	.529	.520	.544	.479	.562	.540
17-11	.613	.617	.613	.617	.606	.617	.628	.613	.640	.536	.597
11-15	.592	.584	.591	.584	.577	.583	.577	.585	.574	.508	.622
15-12	.569	.583	.572	.583	.584	.583	.590	.583	.591	.626	.499
12-13	.643	.612	.631	.616	.614	.616	.610	.615	.610	.591	.523
13-1	.478	.544	.518	.528	.531	.531	.534	.531	.534	.543	.567
13-14	.477	.472	.468	.482	.480	.478	.480	.478	.481	.488	.505
15-16	.464	.460	.462	.461	.470	.462	.458	.460	.460	.463	.477
17-18	.479	.476	.478	.476	.487	.480	.469	.471	.478	.495	.485
X-19	.441	.399	.420	.419	.464	.424	.409	.401	.433	.493	.521

TABLE A2.9

ENERGIES OF MOLECULAR ORBITALS OF THE AMINOBENZ(C)ACRIDINE MOLECULE

POSITION OF AMINO GROUP

1	2	3	4	5	6	7	8	9	10	11
0.449	0.400	0.488	0.390	0.350	0.359	0.356	0.369	0.417	0.422	0.361
0.532	0.666	0.534	0.594	0.675	0.693	0.733	0.688	0.605	0.707	0.652
1.000	0.817	0.851	1.000	1.000	0.855	1.000	0.847	0.918	0.750	0.875
1.000	1.125	1.251	1.000	1.000	1.179	1.000	1.126	1.000	1.081	1.161
1.276	1.187	1.101	1.331	1.209	1.217	1.183	1.272	1.311	1.252	1.204
1.458	1.505	1.505	1.414	1.420	1.352	1.462	1.392	1.414	1.504	1.503
1.627	1.586	1.551	1.583	1.736	1.657	1.655	1.651	1.627	1.585	1.576
1.840	1.904	1.909	1.862	1.800	1.907	1.842	1.839	1.895	1.894	1.842
2.235	2.230	2.234	2.248	2.225	2.195	2.204	2.246	2.235	2.235	2.244
2.543	2.529	2.528	2.536	2.546	2.551	2.561	2.538	2.528	2.529	2.541
-0.392	-0.404	-0.398	-0.396	-0.417	-0.425	-0.518	-0.444	-0.406	-0.422	-0.430
-0.780	-0.722	-0.729	-0.778	-0.753	-0.730	-0.700	-0.702	-0.716	-0.702	-0.709
-1.000	-1.035	-1.035	-1.000	-1.000	-1.041	-1.000	-1.031	-1.000	-1.030	-1.034
-1.177	-1.152	-1.158	-1.180	-1.154	-1.149	-1.149	-1.183	-1.222	-1.171	-1.161
-1.316	-1.351	-1.360	-1.318	-1.319	-1.313	-1.365	-1.329	-1.318	-1.355	-1.358
-1.470	-1.453	-1.435	-1.455	-1.509	-1.474	-1.437	-1.453	-1.460	-1.446	-1.436
-1.770	-1.788	-1.791	-1.778	-1.757	-1.786	-1.770	-1.763	-1.777	-1.781	-1.771
-2.183	-2.181	-2.182	-2.186	-2.179	-2.171	-2.180	-2.194	-2.187	-2.187	-2.191
-2.472	-2.466	-2.465	-2.469	-2.473	-2.475	-2.478	-2.467	-2.464	-2.464	-2.467

RESONANCE ENERGY

7.480	7.458	7.464	7.476	7.482	7.490	7.552	7.496	7.460	7.478	7.478

TABLE A2.10

ELECTRICAL CHARGES ON ATOMS OF THE AMINOBENZ(C)ACRIDINE MOLECULE

ATOM	POSITION OF AMINO GROUP										
	1	2	3	4	5	6	7	8	9	10	11
1	0.928	1.077	0.984	1.056	0.992	0.988	0.990	0.990	0.993	0.990	0.993
2	1.087	0.943	1.058	0.995	0.997	1.030	1.010	1.004	1.001	1.004	1.001
3	0.987	1.049	0.938	1.080	0.998	0.992	0.993	0.992	0.995	0.993	0.995
4	1.067	0.993	1.090	0.933	0.991	1.030	1.010	1.003	1.000	1.003	1.000
14	0.992	1.031	0.990	1.041	1.010	0.988	0.991	0.992	0.996	0.993	0.995
5	1.007	0.999	1.009	0.994	0.932	1.152	1.046	1.014	1.004	1.015	1.002
6	0.994	1.025	0.995	1.026	1.145	0.924	0.984	0.993	0.998	0.994	0.997
16	1.008	1.003	1.008	1.002	0.998	1.021	1.066	1.017	1.004	1.018	1.002
7	0.932	0.942	0.932	0.943	0.981	0.918	0.859	0.918	0.961	0.929	0.954
18	1.007	1.003	1.006	1.003	1.003	1.007	1.047	1.033	1.000	1.024	1.002
8	0.988	0.990	0.988	0.990	0.998	0.985	0.976	0.917	1.105	0.980	1.078
9	1.008	1.004	1.007	1.004	1.004	1.007	1.029	1.114	0.946	1.042	0.996
10	0.983	0.986	0.983	0.986	0.994	0.982	0.981	0.976	1.022	0.927	1.098
11	1.018	1.013	1.017	1.014	1.012	1.016	1.033	1.101	1.005	1.128	0.939
17	0.958	0.961	0.958	0.961	0.972	0.957	0.959	0.958	0.979	0.956	0.986
12	1.212	1.192	1.208	1.194	1.188	1.203	1.297	1.216	1.188	1.223	1.176
15	0.936	0.944	0.939	0.943	0.958	0.938	0.943	0.939	0.955	0.941	0.955
13	1.061	1.004	1.048	1.008	1.005	1.041	1.017	1.010	1.007	1.011	1.006
19	1.830	1.842	1.842	1.829	1.823	1.820	1.769	1.814	1.843	1.832	1.825

TABLE A2.11

BOND ORDERS OF BONDS IN THE AMINOBENZ(C)ACRIDINE MOLECULE

BOND	POSITION OF AMINO GROUP (X)										
	1	2	3	4	5	6	7	8	9	10	11
1-2	.630	.636	.712	.683	.694	.694	.699	.696	.696	.696	.696
2-3	.648	.576	.575	.647	.632	.625	.624	.627	.628	.627	.628
3-4	.686	.716	.640	.636	.695	.704	.705	.702	.701	.702	.701
4-14	.580	.572	.596	.531	.595	.573	.576	.580	.581	.580	.581
14-5	.494	.501	.491	.511	.450	.517	.505	.497	.494	.497	.495
5-6	.783	.778	.784	.774	.709	.705	.767	.780	.783	.780	.783
6-16	.495	.495	.493	.498	.513	.449	.520	.498	.494	.498	.494
16-7	.628	.626	.629	.624	.619	.643	.544	.613	.626	.616	.625
7-18	.586	.588	.586	.589	.589	.582	.514	.613	.585	.602	.589
18-8	.544	.543	.544	.542	.542	.545	.569	.490	.554	.530	.539
8-9	.730	.731	.730	.731	.731	.729	.716	.656	.672	.750	.718
9-10	.595	.594	.595	.594	.595	.596	.606	.622	.544	.540	.613
10-11	.728	.728	.728	.728	.727	.728	.720	.708	.743	.662	.664
11-17	.550	.549	.550	.549	.550	.549	.557	.553	.540	.570	.497
17-12	.571	.572	.571	.573	.571	.571	.550	.569	.579	.565	.590
12-15	.625	.634	.628	.633	.638	.631	.605	.627	.631	.627	.629
15-13	.468	.447	.459	.450	.444	.450	.457	.452	.451	.452	.451
13-1	.544	.609	.585	.592	.597	.598	.593	.595	.595	.595	.595
13-14	.549	.539	.537	.550	.553	.536	.542	.545	.545	.544	.545
15-16	.498	.502	.499	.502	.495	.507	.527	.508	.502	.507	.504
17-18	.497	.497	.498	.497	.496	.499	.515	.498	.491	.487	.502
X-19	.416	.399	.401	.416	.420	.425	.490	.432	.397	.412	.416

TABLE A2.12

ENERGIES OF MOLECULAR ORBITALS OF THE AMINOBENZ(A)ACRIDINIUM ION

POSITION OF AMINO GROUP										
1	2	3	4	5	6	8	9	10	11	12
0.447	0.512	0.492	0.461	0.535	0.446	0.454	0.564	0.489	0.506	0.637
0.777	0.755	0.745	0.781	0.778	0.747	0.712	0.759	0.721	0.717	0.745
1.000	0.871	0.882	1.000	1.000	0.909	0.920	0.868	0.894	0.921	1.000
1.000	1.142	1.117	1.000	1.000	1.166	1.115	1.000	1.103	1.147	1.000
1.298	1.214	1.290	1.355	1.196	1.216	1.374	1.348	1.337	1.376	1.246
1.586	1.529	1.475	1.469	1.625	1.592	1.512	1.559	1.563	1.471	1.489
1.732	1.847	1.861	1.792	1.760	1.773	1.710	1.699	1.641	1.629	1.781
1.975	1.975	1.974	1.972	1.978	2.001	2.066	2.108	2.131	2.146	2.067
2.358	2.333	2.333	2.357	2.343	2.305	2.292	2.286	2.284	2.283	2.295
2.982	2.981	2.981	2.981	2.984	2.992	2.991	2.983	2.982	2.984	2.990
-0.192	-0.214	-0.193	-0.212	-0.268	-0.206	-0.209	-0.235	-0.199	-0.243	-0.353
-0.791	-0.732	-0.743	-0.787	-0.759	-0.737	-0.718	-0.737	-0.716	-0.727	-0.738
-1.000	-1.031	-1.030	-1.000	-1.100	-1.036	-1.027	-1.000	-1.024	-1.028	-1.000
-1.145	-1.159	-1.162	-1.146	-1.146	-1.154	-1.153	-1.146	-1.162	-1.160	-1.146
-1.203	-1.193	-1.203	-1.206	-1.176	-1.167	-1.226	-1.232	-1.234	-1.225	-1.186
-1.498	-1.486	-1.468	-1.475	-1.539	-1.514	-1.485	-1.493	-1.479	-1.467	-1.501
-1.733	-1.759	-1.765	-1.747	-1.718	-1.747	-1.727	-1.736	-1.734	-1.723	-1.726
-I.152	-2.151	-2.152	-2.156	-2.150	-2.144	-2.170	-2.165	-2.166	-2.173	-2.153
-2.442	-2.434	-2.434	-2.439	-2.442	-2.441	-2.432	-2.430	-2.430	-2.433	-2.447
RESONANCE ENERGY										
5.482	5.490	5.472	5.508	5.570	5.466	5.464	5.520	5.462	5.532	5.672

TABLE A2.13

ELECTRICAL CHARGES ON ATOMS OF THE AMINOBENZ(A)ACRIDINIUM ION

ATOM	POSITION OF AMINO GROUP										
	1	2	3	4	5	6	8	9	10	11	12
1	0.937	1.084	0.995	1.064	1.003	0.999	1.000	1.003	1.000	1.003	1.010
2	1.067	0.922	1.035	0.974	0.980	1.007	0.980	0.982	0.981	0.981	0.986
3	0.996	1.055	0.946	1.087	1.007	1.002	1.002	1.004	1.002	1.004	1.009
4	1.044	0.970	1.068	0.910	0.972	1.005	0.977	0.980	0.978	0.979	0.985
14	1.006	1.042	1.005	1.052	1.024	1.002	1.007	1.009	1.007	1.009	1.013
5	0.902	0.900	0.905	0.894	0.848	1.043	0.904	0.912	0.907	0.909	0.931
6	1.035	1.062	1.037	1.063	1.150	0.966	1.036	1.037	1.036	1.037	1.036
16	0.824	0.826	0.825	0.825	0.837	0.836	0.826	0.835	0.830	0.831	0.859
7	1.709	1.714	1.708	1.715	1.731	1.701	1.700	1.723	1.706	1.721	1.750
18	0.868	0.868	0.867	0.869	0.879	0.865	0.896	0.870	0.888	0.872	0.888
8	1.041	1.042	1.041	1.042	1.045	1.040	0.969	1.136	1.034	1.113	1.046
9	0.944	0.944	0.943	0.944	0.952	0.941	1.049	0.889	0.982	0.939	0.957
10	1.013	1.015	1.013	1.015	1.020	1.012	1.006	1.051	0.955	1.110	1.026
11	0.957	0.956	0.956	0.957	0.963	0.954	1.039	0.952	1.066	0.888	0.960
17	1.008	1.011	1.009	1.011	1.018	1.007	1.009	1.029	1.006	1.039	1.040
12	0.778	0.773	0.773	0.776	0.804	0.762	0.772	0.785	0.783	0.773	0.764
15	1.003	1.014	1.007	1.012	1.025	1.007	1.007	1.020	1.009	1.021	1.058
13	1.032	0.977	1.019	0.980	0.981	1.012	0.981	0.981	0.982	0.981	0.981
19	1.835	1.825	1.847	1.811	1.764	1.840	1.841	1.803	1.849	1.791	1.703

TABLE A2.14

BOND ORDERS OF BONDS IN THE AMINOBENZ(A)ACRIDINIUM ION

BOND	POSITION OF AMINO GROUP (X)										
	1	2	3	4	5	6	8	9	10	11	12
1-2	.634	.627	.710	.673	.691	.693	.696	.699	.696	.699	.707
2-3	.642	.567	.575	.654	.634	.626	.626	.623	.625	.623	.617
3-4	.693	.727	.647	.628	.693	.704	.704	.707	.704	.707	.713
4-14	.568	.558	.584	.518	.595	.571	.574	.571	.574	.571	.567
14-5	.511	.531	.508	.541	.448	.520	.510	.516	.510	.516	.525
5-6	.746	.730	.747	.727	.639	.696	.749	.744	.748	.745	.743
6-16	.558	.570	.556	.573	.623	.500	.553	.559	.555	.558	.559
16-7	.435	.429	.435	.429	.413	.441	.443	.421	.439	.423	.394
7-18	.410	.406	.411	.405	.393	.416	.415	.400	.411	.400	.378
18-8	.602	.604	.602	.604	.609	.600	.544	.642	.594	.623	.612
8-9	.700	.698	.700	.698	.694	.702	.653	.623	.712	.666	.691
9-10	.612	.614	.612	.615	.621	.611	.621	.543	.560	.654	.630
10-11	.719	.717	.719	.717	.711	.720	.713	.749	.666	.632	.701
11-17	.551	.554	.551	.554	.562	.550	.544	.530	.560	.490	.584
17-12	.560	.552	.559	.552	.535	.561	.558	.592	.558	.601	.468
12-15	.616	.631	.620	.629	.658	.618	.623	.599	.622	.596	.508
15-13	.463	.444	.454	.448	.435	.444	.449	.457	.450	.458	.481
13-1	.546	.620	.588	.603	.601	.600	.597	.593	.597	.593	.582
13-14	.547	.528	.536	.539	.556	.537	.542	.539	.541	.539	.533
15-16	.526	.523	.527	.522	.498	.541	.528	.543	.529	.544	.583
17-18	.522	.526	.522	.526	.534	.521	.532	.500	.516	.513	.557
X-19	.409	.418	.394	.436	.493	.393	.391	.447	.389	.458	.572

TABLE A2.15

ENERGIES OF MOLECULAR ORBITALS OF THE AMINOBENZ(B)ACRIDINIUM ION

POSITION OF AMINO GROUP

1	2	3	4	6	7	8	9	10	11	12
0.494	0.435	0.528	0.415	0.291	0.345	0.452	0.395	0.380	0.390	0.524
0.585	0.625	0.636	0.597	0.873	0.806	0.691	0.765	0.789	0.864	0.808
1.000	0.947	0.904	1.000	1.000	1.000	0.902	0.882	1.000	1.000	1.000
1.187	1.192	1.104	1.150	1.000	1.000	1.103	1.124	1.000	1.000	1.000
1.332	1.253	1.280	1.314	1.253	1.331	1.301	1.232	1.283	1.333	1.279
1.417	1.519	1.546	1.499	1.654	1.492	1.501	1.546	1.575	1.441	1.429
1.713	1.730	1.764	1.776	1.728	1.825	1.879	1.866	1.782	1.825	1.825
2.139	2.125	2.101	2.057	1.977	1.966	1.968	1.970	1.970	1.976	2.084
2.274	2.273	2.275	2.281	2.320	2.346	2.323	2.324	2.350	2.342	2.273
2.983	2.981	2.982	2.990	2.991	2.980	2.980	2.980	2.980	2.984	2.988
-0.171	-0.119	-0.166	-0.125	-0.139	-0.121	-0.141	-0.118	-0.143	-0.219	-0.303
-0.736	-0.718	-0.728	-0.731	-0.765	-0.788	-0.732	-0.742	-0.784	-0.758	-0.737
-1.000	-1.022	-1.033	-1.000	-1.000	-1.000	-1.033	-1.032	-1.000	-1.000	-1.000
-1.195	-1.152	-1.104	-1.171	-1.103	-1.110	-1.102	-1.118	-1.113	-1.102	-1.107
-1.260	-1.305	-1.304	-1.274	-1.261	-1.294	-1.323	-1.274	-1.268	-1.295	-1.274
-1.389	-1.389	-1.408	-1.404	-1.459	-1.404	-1.389	-1.421	-1.429	-1.414	-1.414
-1.771	-1.783	-1.787	-1.778	-1.766	-1.782	-1.796	-1.795	-1.779	-1.773	-1.775
-2.192	-2.185	-2.184	-2.188	-2.169	-2.178	-2.175	-2.175	-2.177	-2.167	-2.178
-2.411	-2.407	-2.407	-2.409	-2.425	-2.416	-2.410	-2.411	-2.417	-2.428	-2.422

RESONANCE ENERGY

5.420	5.332	5.412	5.330	5.346	5.354	5.372	5.340	5.390	5.482	5.592

TABLE A2.16

ELECTRICAL CHARGES ON ATOMS OF THE AMINOBENZ(B)ACRIDINIUM ION

ATOM	POSITION OF AMINO GROUP										
	1	2	3	4	6	7	8	9	10	11	12
1	0.872	1.054	0.938	1.023	0.941	0.937	0.941	0.938	0.941	0.949	0.952
2	1.112	0.958	1.051	1.010	1.015	1.017	1.019	1.017	1.019	1.023	1.030
3	0.925	0.961	0.874	1.032	0.926	0.922	0.928	0.924	0.927	0.939	0.950
4	1.114	1.039	1.137	0.974	1.044	1.046	1.047	1.046	1.047	1.049	1.050
14	0.859	0.865	0.856	0.874	0.849	0.845	0.851	0.846	0.850	0.863	0.881
5	1.744	1.729	1.746	1.724	1.718	1.729	1.738	1.730	1.737	1.750	1.769
16	0.889	0.887	0.892	0.885	0.930	0.893	0.887	0.893	0.886	0.894	0.903
6	1.073	1.069	1.073	1.069	0.965	1.053	1.101	1.064	1.095	1.161	1.074
18	0.968	0.966	0.969	0.964	1.020	0.992	0.962	0.982	0.965	0.968	0.976
7	1.015	1.014	1.014	1.014	0.996	0.940	1.124	1.005	1.097	1.031	1.014
8	0.977	0.975	0.978	0.974	1.009	1.090	0.914	1.009	0.965	0.973	0.983
9	1.010	1.008	1.010	1.008	1.001	1.000	1.043	0.949	1.117	1.033	1.011
10	0.979	0.978	0.980	0.977	1.006	1.069	0.968	1.099	0.902	0.965	0.984
17	1.010	1.007	1.010	1.007	1.004	1.007	1.024	1.004	1.033	1.053	1.014
11	0.908	0.905	0.912	0.900	1.038	0.922	0.895	0.932	0.882	0.820	0.924
15	1.012	1.006	1.012	1.005	1.004	1.005	1.014	1.006	1.013	1.041	1.034
12	0.722	0.720	0.737	0.704	0.708	0.695	0.713	0.700	0.710	0.744	0.733
13	1.037	1.009	1.028	1.012	1.009	1.011	1.015	1.012	1.015	1.023	1.046
19	1.775	1.851	1.787	1.844	1.816	1.828	1.817	1.845	1.799	1.722	1.670

TABLE A2.17

BOND ORDERS OF BONDS IN THE AMINOBENZ(B)ACRIDINIUM ION

BOND	POSITION OF AMINO GROUP (X)										
	1	2	3	4	6	7	8	9	10	11	12
1-2	.626	.671	.757	.719	.726	.723	.719	.723	.719	.711	.700
2-3	.660	.557	.534	.616	.604	.607	.612	.608	.612	.620	.631
3-4	.657	.710	.613	.654	.703	.699	.696	.699	.696	.691	.688
4-14	.634	.596	.653	.546	.598	.603	.607	.603	.607	.612	.616
14-5	.397	.410	.396	.414	.424	.414	.404	.413	.404	.391	.372
5-16	.380	.393	.379	.397	.395	.389	.385	.389	.385	.375	.361
16-6	.669	.663	.671	.661	.589	.656	.677	.662	.675	.692	.674
6-18	.575	.580	.575	.581	.540	.594	.565	.583	.569	.541	.572
18-7	.550	.548	.550	.548	.559	.498	.579	.540	.562	.564	.550
7-8	.727	.729	.727	.729	.725	.666	.653	.743	.699	.713	.727
8-9	.593	.590	.593	.590	.591	.607	.532	.540	.627	.611	.596
9-10	.733	.735	.733	.735	.735	.724	.757	.677	.650	.711	.730
10-17	.538	.535	.538	.534	.534	.529	.520	.545	.479	.572	.544
17-11	.598	.606	.598	.606	.604	.606	.625	.603	.636	.509	.584
11-15	.602	.588	.601	.587	.578	.587	.574	.588	.572	.495	.636
15-12	.542	.567	.544	.568	.562	.564	.583	.566	.583	.637	.461
12-13	.628	.580	.619	.580	.586	.581	.569	.580	.569	.541	.469
13-1	.478	.550	.518	.534	.539	.541	.547	.542	.547	.560	.584
13-14	.500	.506	.487	.522	.508	.511	.517	.511	.517	.531	.555
15-16	.488	.479	.487	.478	.496	.483	.474	.480	.477	.471	.510
17-18	.492	.488	.492	.487	.491	.494	.476	.483	.486	.516	.500
X-19	.475	.386	.463	.387	.414	.413	.427	.394	.448	.535	.607

TABLE A2.18

ENERGIES OF MOLECULAR ORBITALS OF THE AMINOBENZ(C)ACRIDINIUM ION

POSITION OF AMINO GROUP

1	2	3	4	5	6	7	8	9	10	11
0.449	0.440	0.531	0.404	0.386	0.417	0.548	0.483	0.496	0.535	0.448
0.774	0.811	0.664	0.804	0.851	0.849	0.837	0.689	0.624	0.732	0.654
1.000	0.855	0.902	1.000	1.000	0.867	1.000	0.943	1.000	0.856	0.951
1.000	1.138	1.102	1.000	1.000	1.190	1.000	1.210	1.087	1.089	1.202
1.280	1.215	1.307	1.338	1.238	1.249	1.231	1.316	1.320	1.286	1.262
1.561	1.543	1.509	1.502	1.600	1.431	1.479	1.417	1.490	1.543	1.524
1.834	1.893	1.885	1.824	1.788	1.875	1.817	1.747	1.771	1.799	1.805
1.958	1.960	1.963	1.963	1.974	2.002	2.095	2.118	2.106	2.079	2.030
2.313	2.295	2.298	2.324	2.317	2.287	2.240	2.255	2.252	2.255	2.262
2.992	2.990	2.989	2.990	2.991	2.993	2.997	2.992	2.990	2.991	2.999
-0.226	-0.215	-0.231	-0.211	-0.219	-0.239	-0.398	-0.269	-0.218	-0.260	-0.229
-0.756	-0.705	-0.699	-0.758	-0.741	-0.717	-0.678	-0.676	-0.680	-0.680	-0.676
-1.000	-1.033	-1.034	-1.000	-1.000	-1.039	-1.000	-1.022	-1.000	-1.029	-1.024
-1.102	-1.099	-1.092	-1.101	-1.092	-1.096	-1.092	-1.159	-1.182	-1.106	-1.133
-1.283	-1.293	-1.335	-1.304	-1.280	-1.281	-1.314	-1.296	-1.287	-1.314	-1.319
-1.431	-1.422	-1.385	-1.403	-1.465	-1.414	-1.391	-1.384	-1.402	-1.407	-1.387
-1.768	-1.786	-1.789	-1.775	-1.755	-1.785	-1.770	-1.759	-1.772	-1.776	-1.769
-2.166	-2.165	-2.166	-2.169	-2.162	-2.156	-2.169	-2.185	-2.177	-2.176	-2.180
-2.429	-2.422	-2.421	-2.427	-2.431	-2.432	-2.432	-2.421	-2.418	-2.418	-2.420

RESONANCE ENERGY

5.492	5.452	5.472	5.470	5.462	5.492	5.660	5.512	5.444	5.502	5.446

TABLE A2.19

ELECTRICAL CHARGES ON ATOMS OF THE AMINOBENZ(C)ACRIDINIUM ION

ATOM	POSITION OF AMINO GROUP										
	1	2	3	4	5	6	7	8	9	10	11
1	0.903	1.054	0.960	1.032	0.967	0.965	0.975	0.967	0.966	0.968	0.966
2	1.087	0.946	1.057	0.998	1.000	1.031	1.009	1.006	1.004	1.006	1.004
3	0.969	1.027	0.918	1.061	0.978	0.974	0.982	0.975	0.975	0.976	0.974
4	1.064	0.994	1.087	0.934	0.991	1.029	1.007	1.003	1.001	1.003	1.000
14	0.974	1.011	0.972	1.021	0.991	0.969	0.980	0.976	0.976	0.976	0.975
5	1.014	1.007	1.017	1.001	0.940	1.151	1.036	1.019	1.011	1.019	1.010
6	0.981	1.009	0.981	1.011	1.129	0.910	0.977	0.980	0.982	0.981	0.981
16	1.015	1.010	1.015	1.009	1.005	1.028	1.055	1.021	1.011	1.021	1.009
7	0.769	0.759	0.766	0.762	0.793	0.749	0.757	0.764	0.774	0.776	0.762
18	1.011	1.008	1.011	1.008	1.008	1.012	1.041	1.037	1.005	1.027	1.007
8	0.955	0.953	0.955	0.954	0.960	0.952	0.958	0.886	1.065	0.950	1.038
9	1.014	1.012	1.014	1.012	1.012	1.014	1.026	1.109	0.954	1.049	1.005
10	0.943	0.940	0.943	0.941	0.948	0.940	0.956	0.937	0.980	0.887	1.048
11	1.041	1.039	1.040	1.039	1.038	1.040	1.045	1.112	1.032	1.135	0.968
17	0.869	0.865	0.868	0.866	0.875	0.865	0.883	0.872	0.887	0.869	0.894
12	1.707	1.697	1.706	1.698	1.696	1.704	1.743	1.711	1.696	1.713	1.690
15	0.804	0.806	0.806	0.804	0.821	0.807	0.846	0.814	0.811	0.817	0.807
13	1.070	1.019	1.058	1.022	1.020	1.053	1.025	1.024	1.023	1.024	1.022
19	1.811	1.844	1.826	1.829	1.829	1.808	1.697	1.789	1.849	1.802	1.841

TABLE A2.20

BOND ORDERS OF BONDS IN THE AMINOBENZ(C)ACRIDINIUM ION

BOND	POSITION OF AMINO GROUP (X)										
	1	2	3	4	5	6	7	8	9	10	11
1-2	.626	.644	.727	.691	.702	.708	.711	.706	.704	.707	.703
2-3	.652	.572	.564	.640	.625	.614	.615	.619	.622	.619	.622
3-4	.679	.717	.633	.637	.696	.710	.712	.705	.702	.705	.702
4-14	.587	.571	.603	.530	.594	.567	.570	.577	.580	.577	.580
14-5	.502	.509	.497	.520	.458	.536	.522	.510	.504	.510	.503
5-6	.780	.775	.782	.770	.709	.693	.759	.772	.779	.773	.779
6-16	.496	.497	.493	.500	.512	.449	.528	.504	.496	.504	.496
16-7	.611	.600	.611	.598	.597	.624	.491	.576	.601	.578	.602
7-18	.560	.568	.560	.569	.570	.557	.472	.611	.567	.602	.568
18-8	.551	.547	.551	.547	.547	.552	.583	.486	.556	.526	.541
8-9	.718	.722	.719	.721	.722	.718	.702	.633	.668	.752	.715
9-10	.613	.610	.613	.610	.609	.613	.629	.654	.558	.541	.620
10-11	.699	.702	.699	.702	.702	.700	.692	.667	.714	.623	.653
11-17	.604	.600	.603	.600	.599	.602	.611	.623	.592	.642	.542
17-12	.407	.415	.408	.415	.417	.410	.380	.404	.415	.403	.419
12-15	.444	.454	.446	.453	.455	.447	.408	.440	.456	.437	.461
15-13	.530	.493	.519	.497	.492	.507	.506	.500	.496	.501	.494
13-1	.523	.589	.562	.574	.579	.575	.573	.576	.578	.576	.579
13-14	.529	.527	.519	.537	.538	.519	.529	.531	.533	.530	.533
15-16	.522	.533	.524	.533	.525	.533	.586	.548	.533	.548	.532
17-18	.523	.519	.523	.519	.518	.524	.555	.510	.513	.497	.529
X-19	.439	.396	.419	.415	.413	.438	.580	.461	.389	.448	.392

TABLE A2.21

DIPOLE MOMENTS OF THE AMINOACRIDINIUM ION †

POSITION OF AMINO GROUP	μ_{π}	θ_{π}	μ_{σ}	θ_{σ}	μ_{total}	θ_{total}
1	2.16	1.993	.04	1.000	2.12	1.993
2	.88	1.380	.20	.730	.80	1.308
3	2.62	1.393	.30	.833	2.58	1.356
4	2.27	.831	.36	1.000	2.58	.853
9	3.07	.000	.04	1.000	3.03	.000

† The units of all dipole moments are Debyes. All values of θ are quoted as a fraction of π radians considering rotation from the OX axis in an anti-clockwise direction, where the positive direction of the OX axis bisects the -C-N-C- angle directed away from the ring.

TABLE A2.22

DIPOLE MOMENTS OF THE AMINOBENZ(A)ACRIDINE MOLECULE

POSITION OF AMINO GROUP	μ_{π}	θ_{π}	μ_{σ}	θ_{σ}	μ_{total}	θ_{total}
1	3.32	.126	1.63	.029	4.90	.095
2	4.94	1.913	1.72	.000	6.62	1.936
3	4.27	1.773	1.63	1.970	5.68	1.827
4	3.57	1.579	1.50	1.967	4.33	1.684
5	4.74	1.595	1.50	1.967	5.51	1.676
6	1.87	.842	1.40	.000	.92	.585
8	1.57	1.058	1.40	.000	.32	1.347
9	2.84	.370	1.50	.032	3.80	.258
10	3.34	.285	1.63	.029	4.63	.203
11	4.87	1.980	1.72	.000	6.59	1.985
12	5.37	1.987	1.72	.000	7.08	1.990

TABLE A2.23

DIPOLE MOMENTS OF THE AMINOBENZ(B)ACRIDINE MOLECULE

POSITION OF AMINO GROUP	μ_{π}	θ_{π}	μ_{σ}	θ_{σ}	μ_{total}	θ_{total}
1	5.95	1.983	1.72	.000	7.66	1.986
2	3.98	1.699	1.63	1.970	5.20	1.775
3	4.13	1.663	1.50	1.967	5.14	1.740
4	1.31	.998	1.40	.000	.08	.017
6	3.06	1.006	1.40	.000	1.66	1.011
7	1.29	1.021	1.40	.000	.13	1.789
8	3.98	.319	1.50	.032	5.05	.244
9	4.06	.302	1.63	.029	5.27	.227
10	5.91	.007	1.72	.000	7.63	.006
11	7.48	.014	1.72	.000	9.20	.011
12	7.44	1.993	1.72	.000	9.16	1.994

TABLE A2.24

DIPOLE MOMENTS OF THE AMINOBENZ(C)ACRIDINE MOLECULE

POSITION OF AMINO GROUP	μ_{π}	θ_{π}	μ_{σ}	θ_{σ}	μ_{total}	θ_{total}
1	1.53	.517	1.50	.032	2.19	.278
2	1.89	1.169	1.40	.000	.98	1.424
3	2.62	1.469	1.50	1.967	3.03	1.634
4	3.77	1.698	1.63	1.970	5.00	1.777
5	4.26	1.612	1.63	1.970	5.17	1.703
6	4.80	.068	1.72	.000	6.49	.050
7	5.64	.028	1.72	.000	7.35	.021
8	4.64	.010	1.72	.000	6.36	.007
9	3.26	.310	1.63	.029	4.48	.219
10	3.19	.412	1.50	.032	4.00	.299
11	1.78	1.029	1.40	.000	.40	1.131

TABLE A2.25

DIPOLE MOMENTS OF THE AMINOBENZ(A)ACRIDINIUM ION

POSITION OF AMINO GROUP	μ_{π}	θ_{π}	μ_{σ}	θ_{σ}	μ_{total}	θ_{total}
1	5.21	.688	.20	.730	5.41	.690
2	2.47	.686	.04	1.000	2.49	.690
3	3.24	.816	.20	1.269	3.27	.836
4	4.28	.967	.30	1.166	4.53	.979
5	4.31	1.112	.30	1.166	4.61	1.115
6	6.81	.785	.36	1.000	7.10	.795
8	5.35	.918	.36	1.000	5.70	.923
9	6.34	.714	.30	.833	6.63	.720
10	4.69	.735	.20	.730	4.89	.735
11	2.61	.602	.04	1.000	2.62	.606
12	2.98	.518	.04	1.000	2.99	.522

TABLE A2.26

DIPOLE MOMENTS OF THE AMINOBENZ(B)ACRIDINIUM ION

POSITION OF AMINO GROUP	μ_{π}	θ_{π}	μ_{σ}	θ_{σ}	μ_{total}	θ_{total}
1	6.66	1.673	.04	1.000	6.64	1.672
2	6.47	1.540	.20	1.269	6.60	1.532
3	8.41	1.497	.30	1.166	8.57	1.487
4	4.36	1.422	.36	1.000	4.46	1.397
6	6.83	1.387	.36	1.000	6.96	1.372
7	6.99	1.434	.36	1.000	7.08	1.418
8	3.07	1.566	.30	.833	2.88	1.540
9	4.59	1.551	.20	.730	4.42	1.543
10	6.53	1.681	.04	1.000	6.51	1.680
11	6.13	1.769	.04	1.000	6.10	1.767
12	6.87	1.713	.04	1.000	6.84	1.712

TABLE A2.27

DIPOLE MOMENTS OF THE AMINOBENZ(C)ACRIDINIUM ION

POSITION OF AMINO GROUP	μ_{π}	θ_{π}	μ_{σ}	θ_{σ}	μ_{total}	θ_{total}
1	5.08	.504	.30	.833	5.25	.520
2	3.68	.545	.36	1.000	3.75	.575
3	2.04	.527	.30	1.166	1.93	.573
4	2.98	.273	.20	1.269	2.77	.273
5	1.31	.338	.20	1.269	1.12	.350
6	5.97	.303	.04	1.000	5.95	.305
7	6.11	.220	.04	1.000	6.08	.221
8	5.00	.252	.04	1.000	4.97	.254
9	4.58	.431	.20	.730	4.71	.442
10	6.06	.481	.30	.833	6.20	.495
11	2.62	.633	.36	1.000	2.78	.670

APPENDIX 3.

SPECTRAL DATA AND SPECTRA OF AMINOACRIDINES AND OF AMINOBENZACRIDINES.

TABLE A 3.1 *

POSITION OF ABSORPTION MAXIMA IN ULTRAVIOLET AND VISIBLE SPECTRA AND LOG(EXTINCTION COEFFICIENT) FOR AMINOACRIDINES AND FOR AMINOBENZACRIDINES IN ETHANOL SOLUTION.

MOLECULE	CONC. ($\times 10^{5}$M)	POSITION OF PEAK λ (mμ)	ν^{-1} (cm^{-1} $\times 10^{-4}$)	LOG(E)
2-AMINOACRIDINE	2.64	240.5	4.18	4.45
	2.64	265.5	3.78	4.81
	2.64	318	3.15	3.42
	2.64	322	3.11	3.44
	2.64	338	2.96	3.57
	13.1	354.8	2.83	3.69
	13.1	421	2.38	3.71
3-AMINOACRIDINE	5.08	239	4.18	4.53
	5.08	267.5	3.75	4.76
	5.08	319	3.14	3.43
	5.08	335	2.99	3.61
	5.08	351.5	2.85	3.87
	5.08	428	2.34	3.86
4-AMINOACRIDINE	2.25	240	4.17	4.60
	2.25	273	3.66	4.52
	28.0	344	2.91	3.14
	28.0	359	2.79	3.19
	28.0	420	2.38	3.81
9-AMINOACRIDINE	6.67	253	3.95	4.58
	6.67	258.5	3.89	4.63
	6.67	263.5	3.81	4.63
	6.67	400	2.50	3.94
	6.67	422	2.37	3.81
9-AMINOBENZ(A)ACRIDINE	2.25	256	3.91	4.53
	2.25	264	3.79	4.56
	2.25	277	3.61	4.58
	2.25	298	3.36	4.66
	2.25	305	3.28	4.67
	18.7	346.5	2.89	3.74
	18.7	365.5	2.74	3.57
	18.7	419	2.39	3.96

* Data in this Table refer to spectra in Figs. A3.1-A3.12.

TABLE A3.1 (CONT.)

MOLECULE	CONC. ($\times 10^{5}$M)	POSITION OF PEAK λ (mμ)	ν^{-1} (cm^{-1}M) $\times 10^{-4}$	LOG(E)
10-AMINOBENZ(A)ACRIDINE	2.75	226	4.43	4.58
	21.0	347	2.88	3.60
	21.0	290	3.45	4.65
	21.0	416	2.40	3.83
12-AMINOBENZ(A)ACRIDINE	2.45	234	4.27	4.45
	2.45	290	3.45	4.65
	2.45	303	3.30	4.63
	2.45	375	2.67	3.82
2-AMINOBENZ(B)ACRIDINE	2.26	252.8	3.98	4.34
	2.26	285.5	3.51	5.10
	10.5	413	2.42	4.02
	10.5	492	2.03	3.81
	10.5	498	2.01	3.81
12-AMINOBENZ(B)ACRIDINE	3.29	228	4.39	4.23
	3.29	278	3.60	4.94
	3.29	332	3.01	3.62
	16.2	360	2.78	3.43
	16.2	447	2.24	4.19
	16.2	462	2.17	3.69
	16.2	478	2.09	4.94
	16.2	515	1.94	3.51
7-AMINOBENZ(C)ACRIDINE	4.12	258.8	3.89	4.49
	4.12	290.5	3.46	4.59
	4.12	305	3.28	4.68
	4.12	370	2.70	3.94
	4.12	386	2.59	4.00
	4.12	406	2.46	3.91
9-AMINOBENZ(C)ACRIDINE	4.36	259	3.86	4.55
	4.36	303	3.30	4.64
	4.36	336	2.98	3.71
	23.8	354	2.83	3.67
	23.8	403	2.48	3.77
10-AMINOBENZ(C)ACRIDINE	3.21	224	4.46	4.48
	3.21	253	3.95	4.41
	3.21	276	3.62	4.62
	3.21	291	3.44	4.66
	3.21	338	2.96	3.86
	16.9	419	2.39	3.93

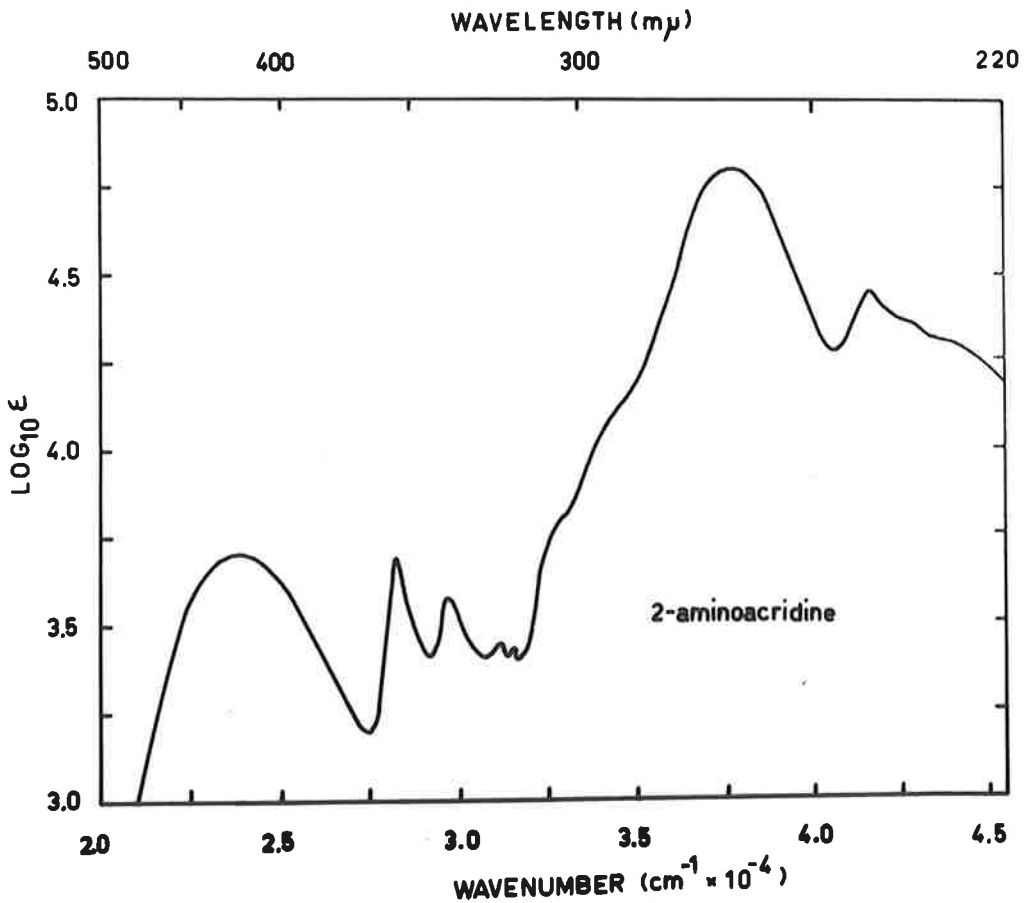

FIG. A3.1. Spectrum of 2-aminoacridine.

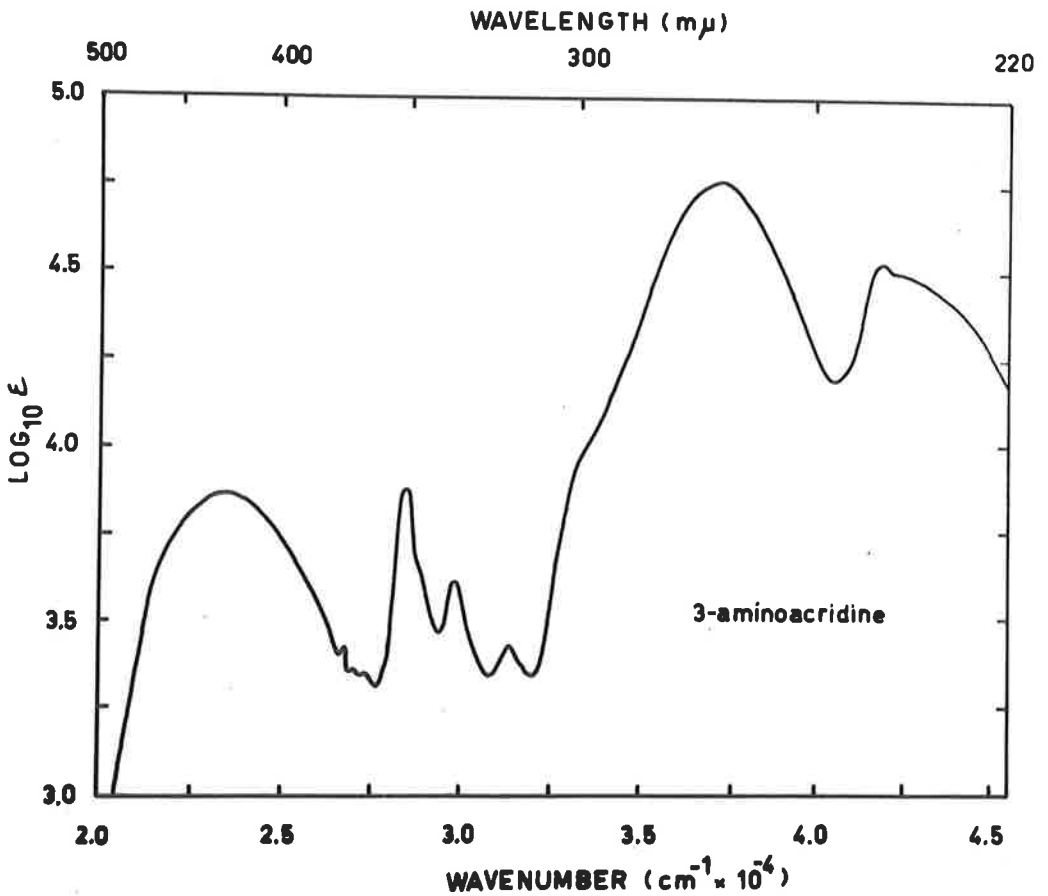

FIG. A3.2. Spectrum of 3-aminoacridine.

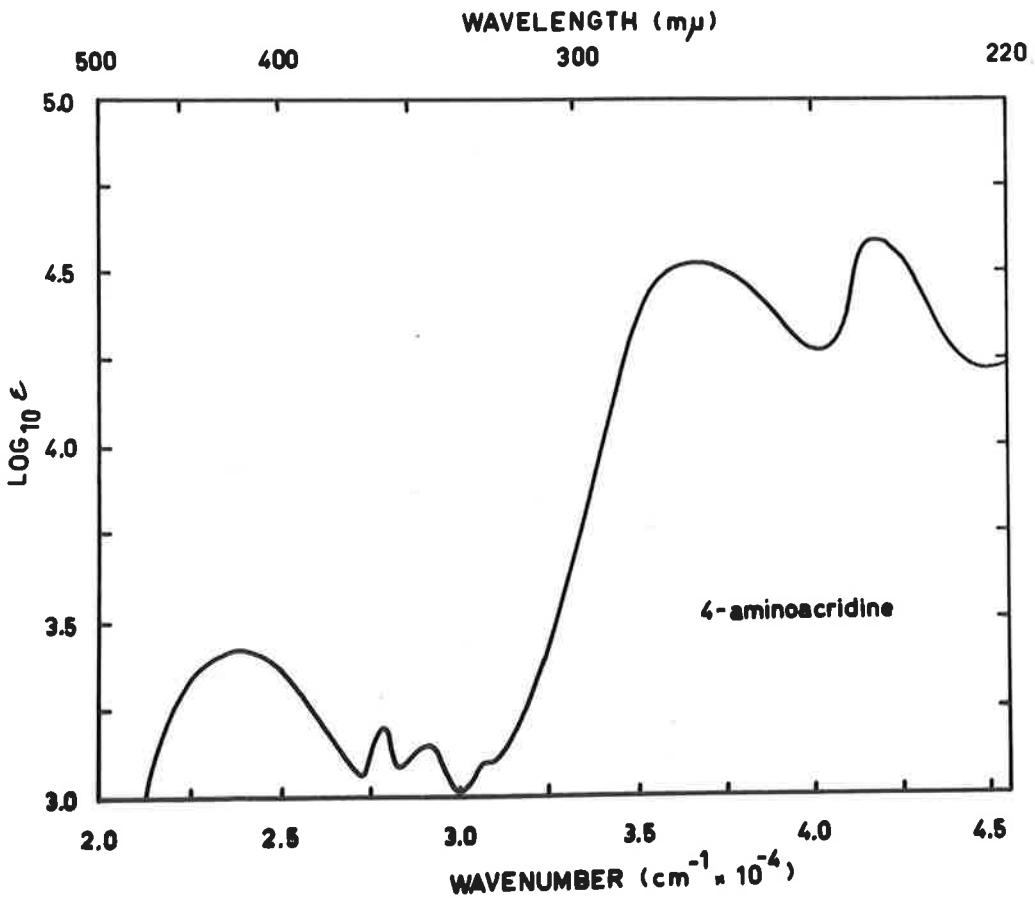

FIG. A3.3. Spectrum of 4-aminoacridine.

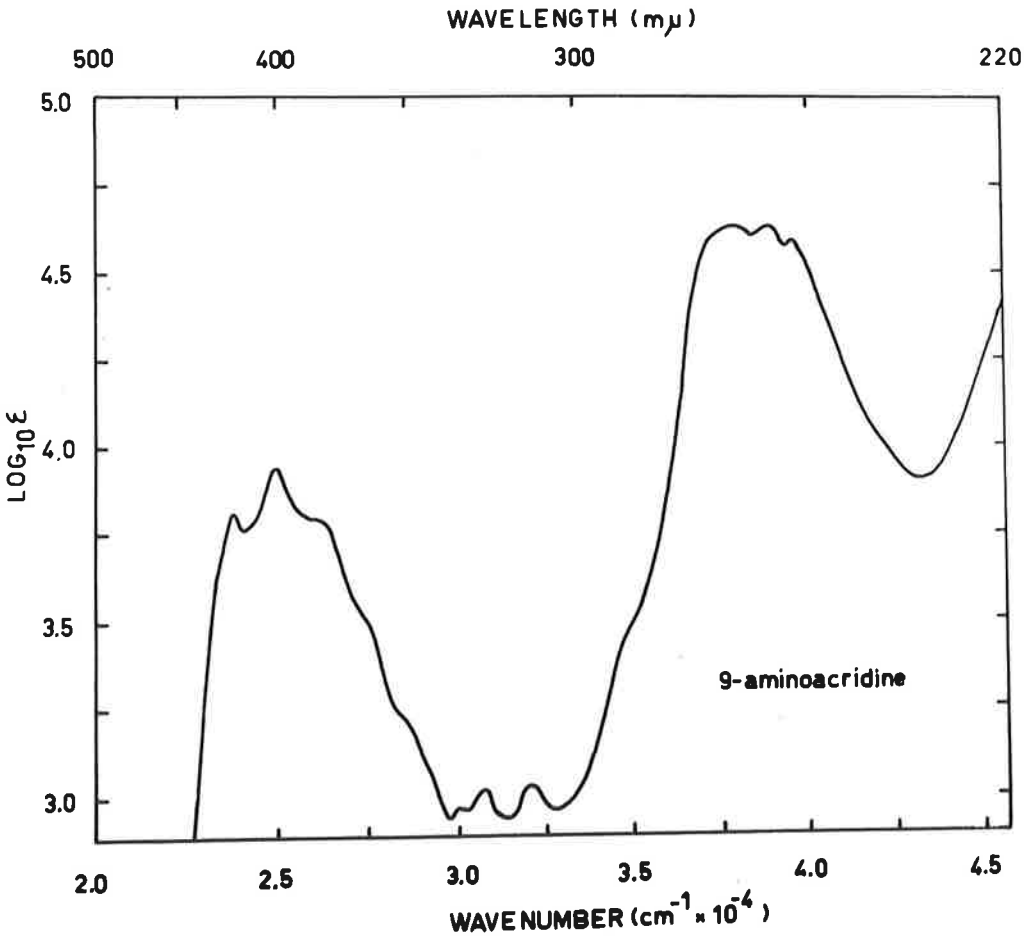

FIG. A3.4. Spectrum of 9-aminoacridine.

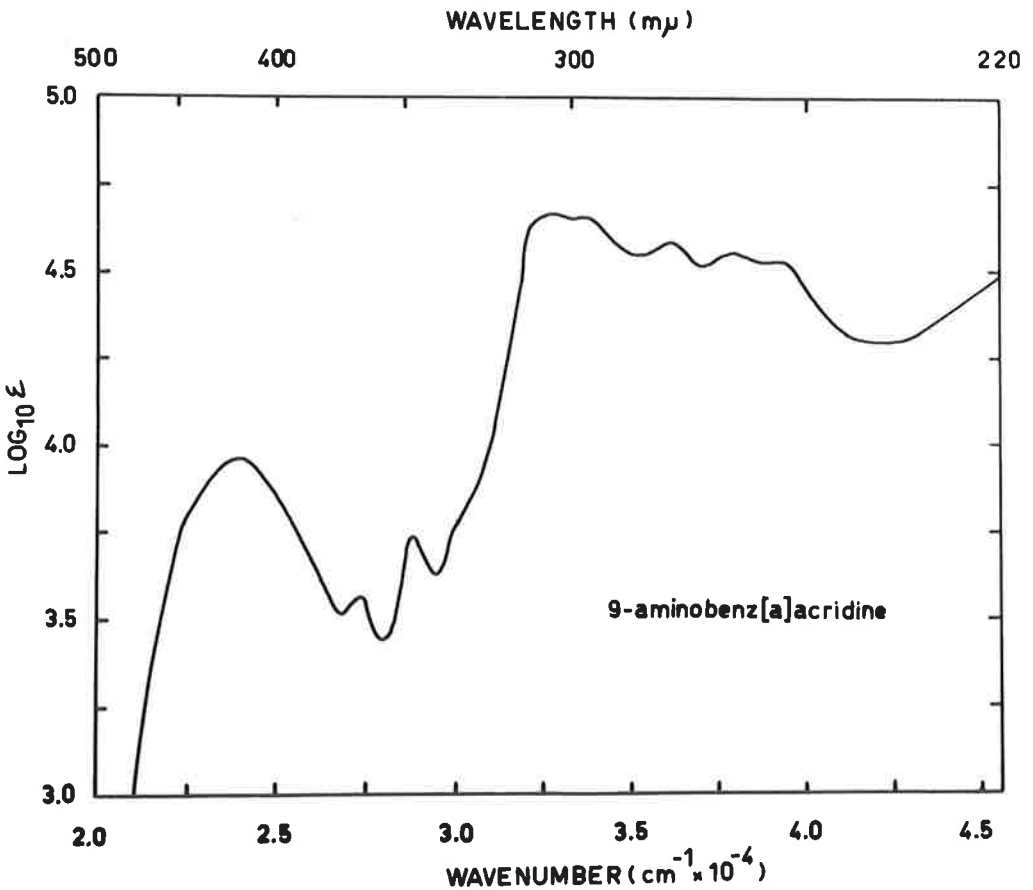

FIG. A3.5. Spectrum of 9-aminobenz[a]acridine.

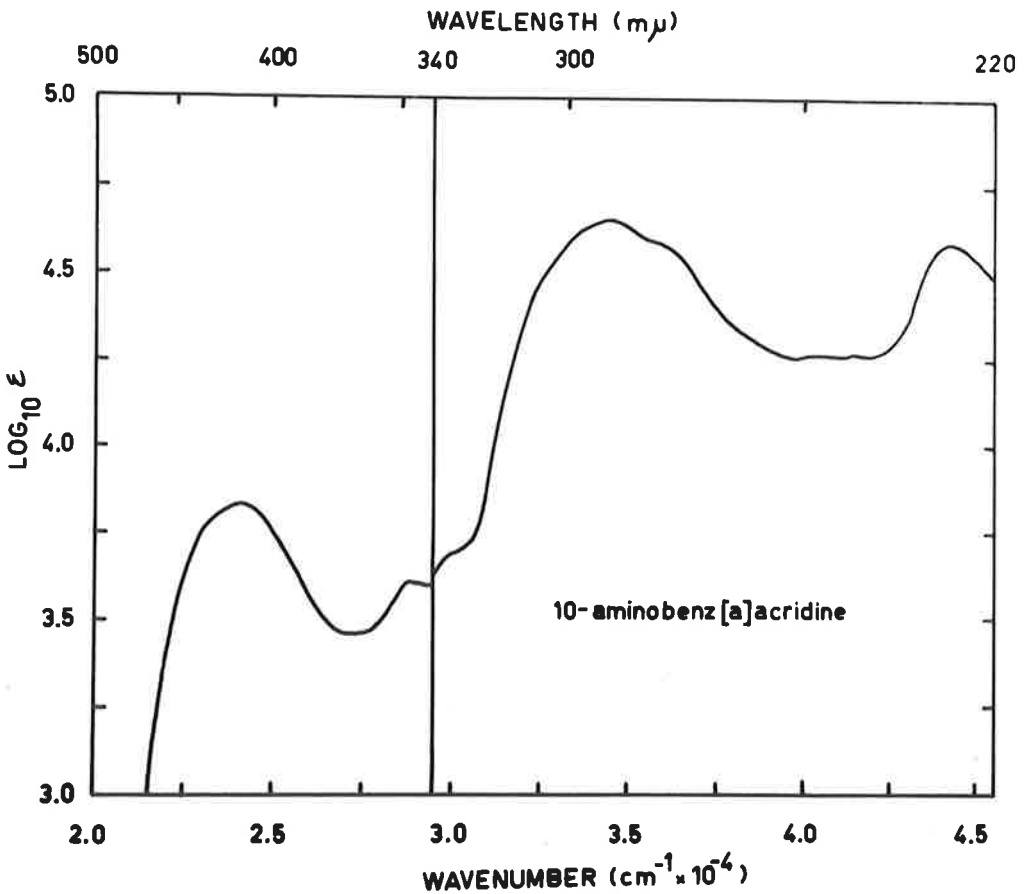

FIG. A3.6. Spectrum of 10-aminobenz[a]acridine.

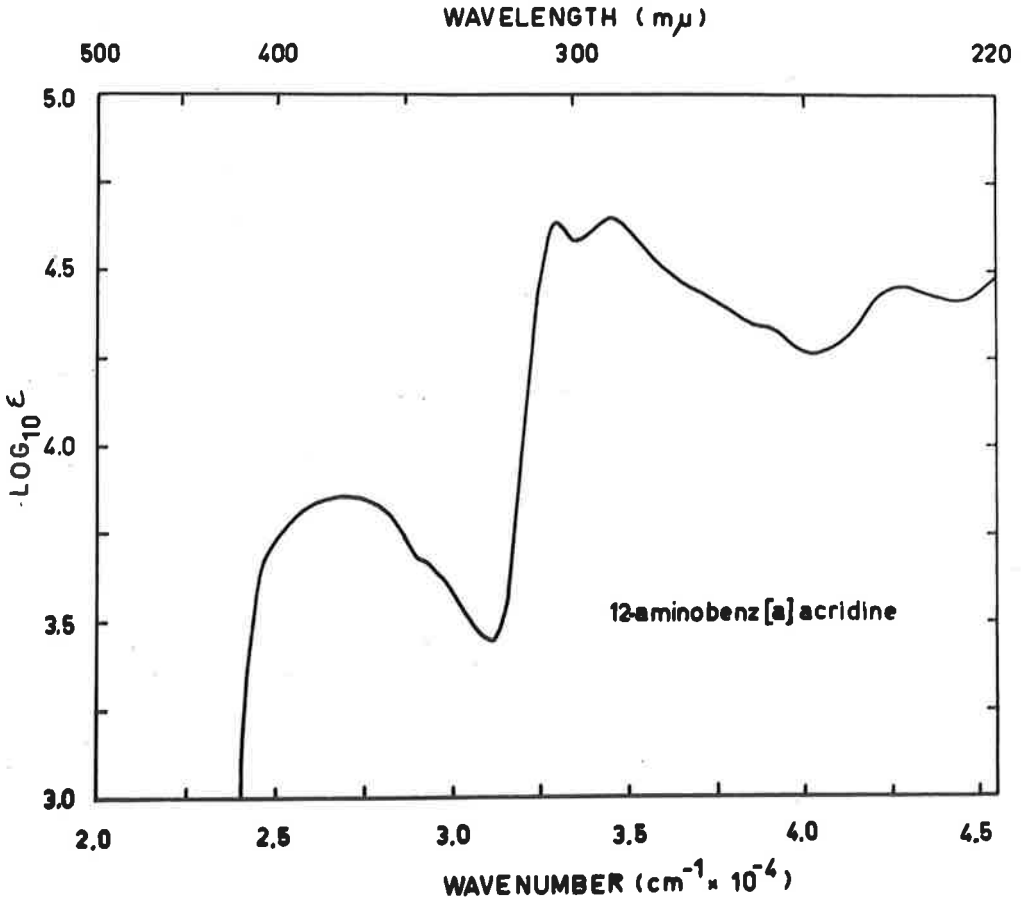

FIG. A3.7. Spectrum of 12-aminobenz[a]acridine.

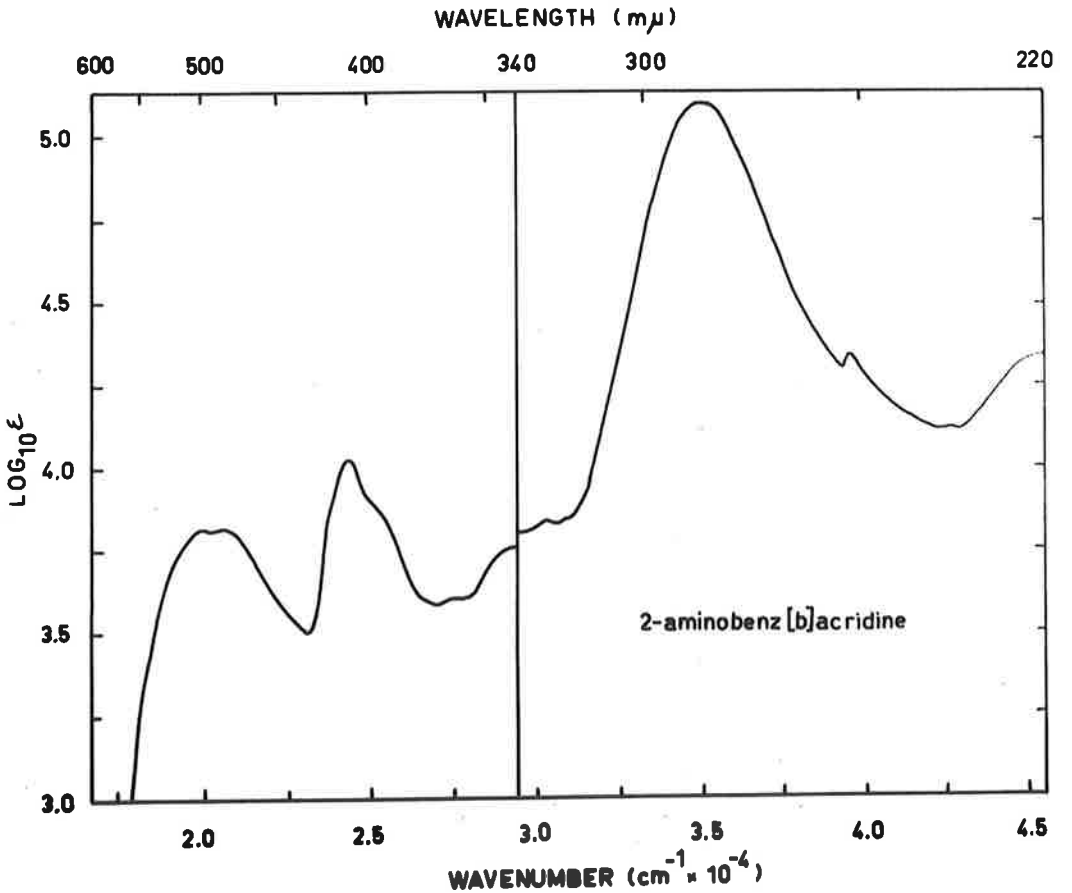

FIG. A3.8. Spectrum of 2-aminobenz[b]acridine.

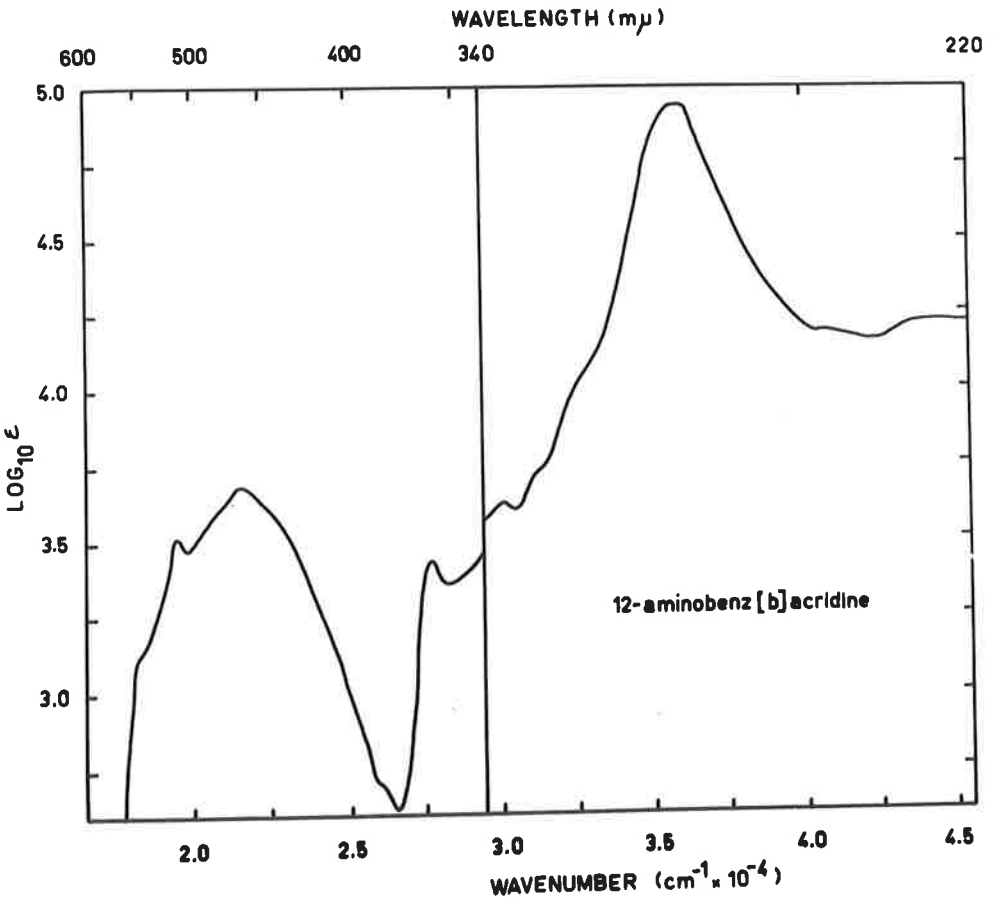

FIG. A3.9. Spectrum of 12-aminobenz[b]acridine.

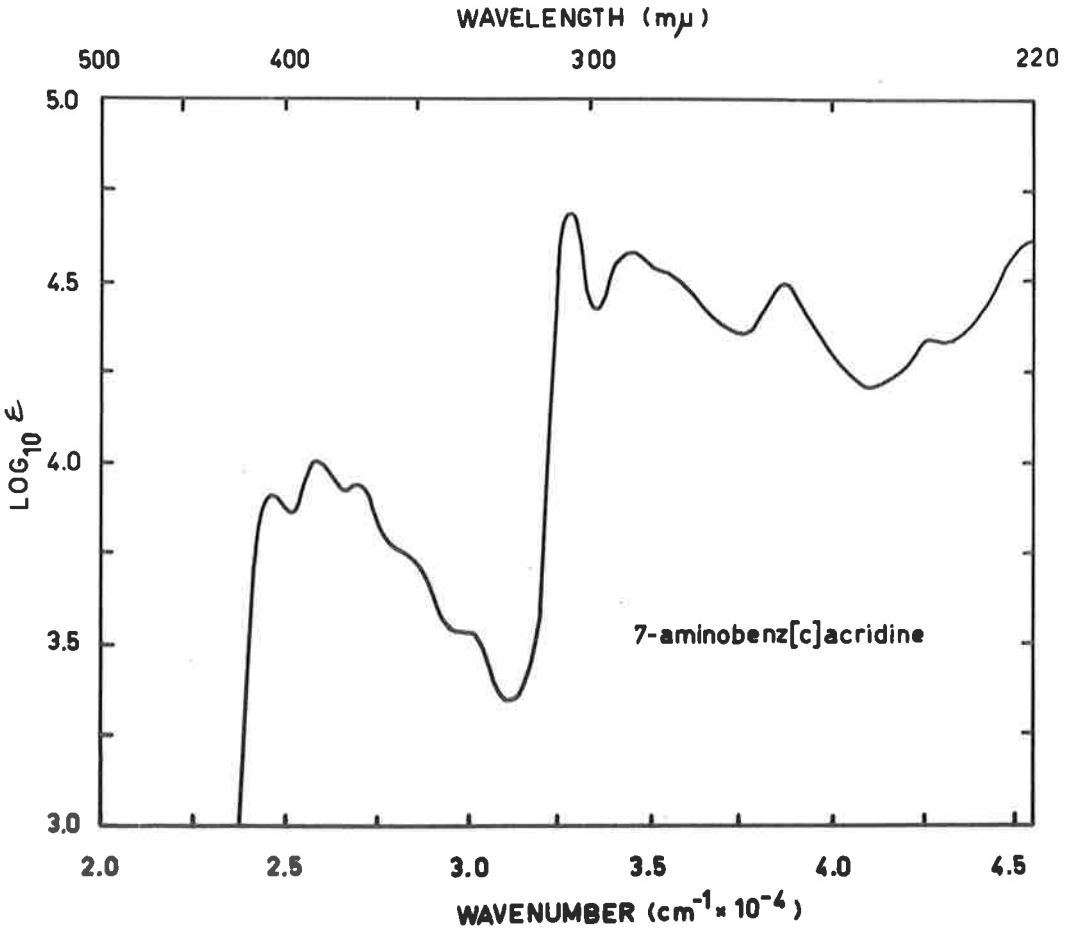

FIG. A3.10. Spectrum of 7-aminobenz[c]acridine.

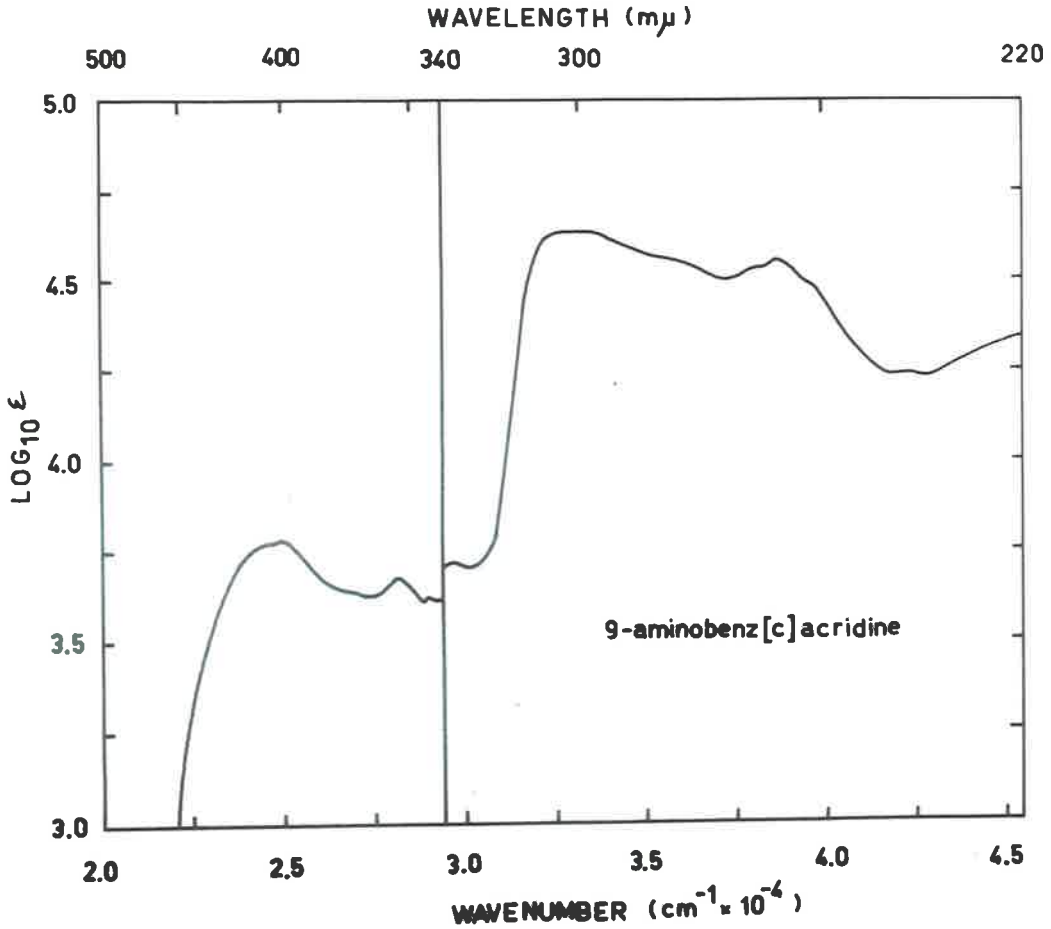

FIG. 3.11. Spectrum of 9-aminobenz[c]acridine.

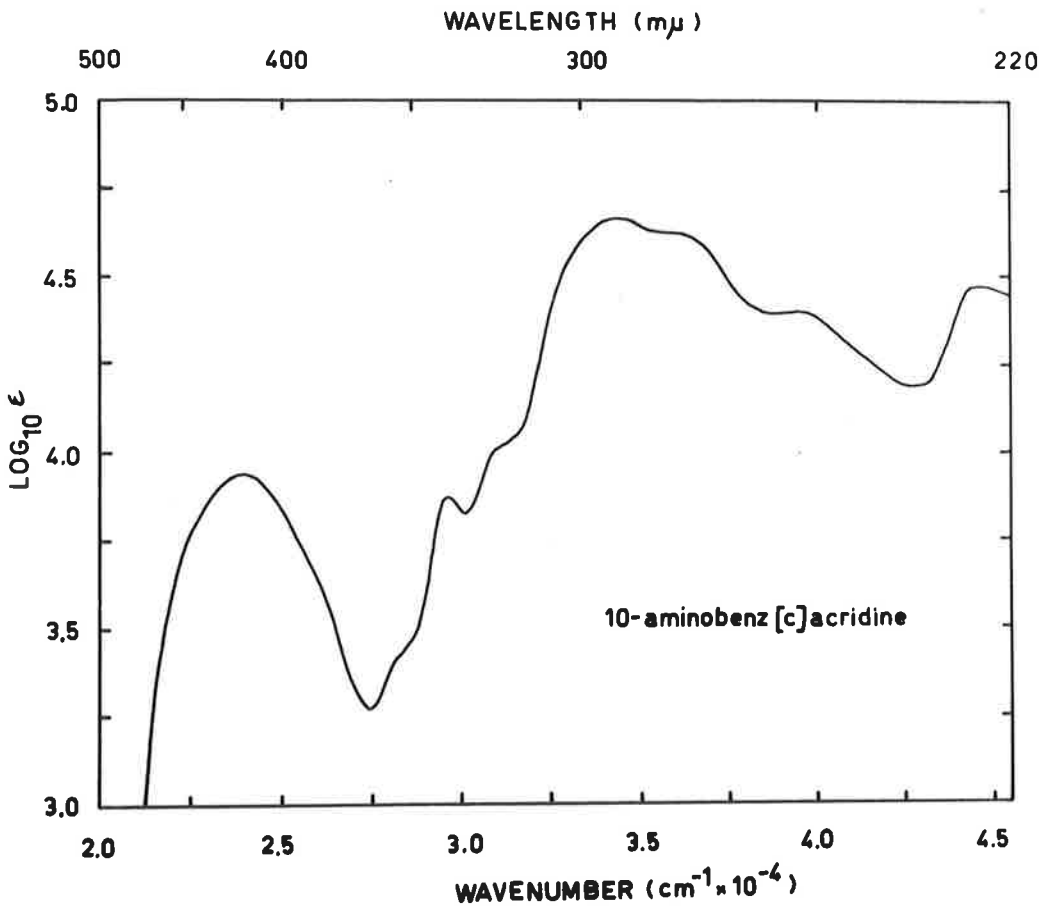

FIG. A3.12. Spectrum of 10-aminobenz[c]acridine.

APPENDIX 4.

COMPUTER PROGRAMMES

L.C.A.O. MOLECULAR ORBITAL CALCULATIONS

CENTRE OF GRAVITY COORDINATES

DIPOLE MOMENT CALCULATIONS

APPENDIX 4.

MOLECULAR ORBITAL CALCULATIONS.

This CDC 3200 computer programme computes the π-electronic charges and the net charges on the atoms of a conjugated molecule such as an aminoacridine or an aminobenzacridine molecule (or ion), and the bond orders of each bond, as well as the energies of the occupied and un-occupied molecular orbitals. An n x n symmetric matrix is first constructed for each molecule from the parameters η_{rs} and δ_r in Chapter 3. The x and y components of the π-dipole moment vector are also computed with this programme. As listed here, the programme is suitable for an aminobenzacridine molecule.

The axes adopted are shown here, and are the same for the three programmes in Appendix 4.

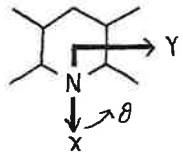

INPUT DATA.

1. Title card.
2. N is the order of the matrix.
3. OFF is the limit by which two successive iteration

steps differ before proceeding to the next step. OFF was set to be 10^{-9} for these calculations.

4. A(I,J) = A(J,I) are the values of the matrix elements in upper triangular form, starting with atom 1 in the top left hand corner of the matrix.
5. LL1 to LL6 are the numbers of the atoms at the junction of the rings. For example, for aminobenz-[b]acridine, these numbers are 13, 14, 15, 16, 17 and 18 in this order.
6. LL7 is the number of the atom to which the NH_2 group is attached.
7. CG1 and CG2 are the x and y coordinates of the centre of gravity of the molecule from the output of the Centre of Gravity Calculations programme listed below.
8. RA1(I) and RA2(I) are the x and y coordinates of the positions of the atoms, in the same order as they occur above in the matrix elements. No hydrogen atoms are included.

OUTPUT DATA-

1. Title.
2. The values of the original matrix. The numbers

appearing in the left-hand column form the diagonal.

5. Each eigen value of the matrix with its corresponding eigen vector components. The eigen values are the energies of the molecular orbitals.
4. The π-electronic charge on each atom, found by equation 3.9 (all values in order of atoms).
5. The net charge on each atom found by equation 3.10 or 3.11 (all values in order of atoms).
6. Bond orders of each bond found by equation 3.12. The values are in order of the bonds; 1-2, 2-3, etc., then LL1-LL2, LL3-LL4, LL5-LL6, LL7-LL19.
7. VD1 and VD2 are the x and y components of the π-dipole moment, to be used in the Dipole Moment Programme below.

```
C      GERSCH - MOLECULAR ORBITAL CALCULATIONS
       DIMENSIONA(20,20),S(20,20),AAA(22),B(19),RA1(19)
       DIMENSIONRA2(19)
       DIMENSION TITLE(12)
 2323  READ(60,20)TITLE
   20  FORMAT(12A6)
   44  FORMAT(1H1/1X,12A6/1H0)
       WRITE(61,44)TITLE
       READ(60,5)N,OFF
    5  FORMAT(I3,E17.9)
       DO4I=1,N
       READ(60,6)(A(I,J),J=I,N)
    6  FORMAT(20F4.1)
       WRITE(61,7)(A(I,J),J=I,N)
    7  FORMAT(/1X,20F4.1/)
       DO4J=I,N
    4  A(J,I)=A(I,J)
       READ(60,31)LL1,LL2,LL3,LL4
   31  FORMAT(6I3)
       READ(60,33)LL7
   33  FORMAT(I3)
       READ(60,37)CG1,CG2
   37  FORMAT(2F8.4)
       DO38I=1,N
   38  READ(60,39)RA1(I),RA2(I)
   39  FORMAT(2F6.2)
       AA=0.0
       AB=0.0
       AC=0.0
       AD=0.0
       AE=0.0
       AF=0.0
       AG=0.0
       AH=0.0
       AI=0.0
       AJ=0.0
       AK=0.0
       AL=0.0
       AM=0.0
       AN=0.0
       AO=0.0
       AP=0.0
       AQ=0.0
       AR=0.0
       AS=0.0
       M=22
       DO6666I=1,M
 6666  AAA(I)=0.0
       INDIC=0
```

```
      DO 1002 I=1,N
      DO 1002 J=1,N
1002  S(I,J)=0.0
      DO 1004 I=1,N
1004  S(I,I)=1.0
      SUM=0.0
      L=N-1
      DO17I=1,L
      K=I+1
      DO 17 J=K,N
   17 SUM=SUM+A(I,J)*A(I,J)
      VF=SQRTF(SUM*2.0)
      NB=1
   21 KQ=2
   22 JP=1
   23 IF(VF-ABSF(A(JP,KQ))) 24,56,56
   24 INDIC=1
      Y=-A(JP,KQ)
      ZI=0.5*(A(JP,JP)-A(KQ,KQ))
      W=Y/SQRTF(Y*Y+ZI*ZI)
      IF(ZI)29,30,30
   29 W=-W
   30 SN=W/(SQRTF(2.0*(1.0+SQRTF(1.0-W*W))))
      CS=SQRTF(1.0-SN*SN)
      IF(NB)43,43,34
   34 S(JP,JP)=CS
      S(KQ,JP)=-SN
      S(JP,KQ)=SN
      S(KQ,KQ)=CS
   43 HOLD1=A(JP,JP)*CS*CS+A(KQ,KQ)*SN*SN-2.0*A(JP,KQ)*SN*CS
      HOLD2=A(JP,JP)*SN*SN+A(KQ,KQ)*CS*CS+2.0*A(JP,KQ)*SN*CS
      DO 544 I=1,N
      D=A(I,JP)*CS-A(I,KQ)*SN
      A(I,KQ)=A(I,JP)*SN+A(I,KQ)*CS
  544 A(I,JP)=D
      IF(NB)751,751,749
  749 NB=0
      GO TO 50
  751 DO 754 I=1,N
      D=S(I,JP)*CS-S(I,KQ)*SN
      S(I,KQ)=S(I,JP)*SN+S(I,KQ)*CS
  754 S(I,JP)=D
   50 A(JP,JP)=HOLD1
      A(KQ,KQ)=HOLD2
      A(JP,KQ)=0.0
      DO 55 I=1,N
      A(JP,I)=A(I,JP)
   55 A(KQ,I)=A(I,KQ)
   56 IF(JP-KQ+1) 57,59,59
   57 JP=JP+1
```

```
      GO TO 23
   59 IF(KQ-N) 60,62,64
   60 KQ=KQ+1
      GO TO 22
   62 IF(INDIC)64,64,263
  263 INDIC=0
      GO TO 21
   64 IF(OFF-VF) 65,69,69
   65 VF=VF/10.0
      GO TO 21
   69 DO 3008 J=1,N
      WRITE(61,15)A(J,J)
      DO333I=1,N,4
      IF (N-I-3) 3071,3070,3070
 3071 IF (N-I-2) 3073,3072,3072
 3073 IF (N-I-1) 3075,3074,3074
 3070 WRITE(61,2)S(I,J),S(I+1,J),S(I+2,J),S(I+3,J)
      GO TO 333
 3072 WRITE(61,2)S(I,J),S(I+1,J),S(I+2,J)
      GO TO 333
 3074 WRITE(61,2)S(I,J),S(I+1,J)
      GO TO 333
 3075 WRITE(61,2)S(I,J)
  333 CONTINUE
      IF(A(J,J))3008,3008,555
  555 AA=AA+S(1,J)*S(1,J)
      AB=AB+S(2,J)*S(2,J)
      AC=AC+S(3,J)*S(3,J)
      AD=AD+S(4,J)*S(4,J)
      AE=AE+S(5,J)*S(5,J)
      AF=AF+S(6,J)*S(6,J)
      AG=AG+S(7,J)*S(7,J)
      AH=AH+S(8,J)*S(8,J)
      AI=AI+S(9,J)*S(9,J)
      AJ=AJ+S(10,J)*S(10,J)
      AK=AK+S(11,J)*S(11,J)
      AL=AL+S(12,J)*S(12,J)
      AM=AM+S(13,J)*S(13,J)
      AN=AN+S(14,J)*S(14,J)
      AO=AO+S(15,J)*S(15,J)
      AP=AP+S(16,J)*S(16,J)
      AQ=AQ+S(17,J)*S(17,J)
      AR=AR+S(18,J)*S(18,J)
      AS=AS+S(19,J)*S(19,J)
      AAA(1)=AAA(1)+2.*S(1,J)*S(2,J)
      AAA(2)=AAA(2)+2.*S(2,J)*S(3,J)
      AAA(3)=AAA(3)+2.*S(3,J)*S(4,J)
      AAA(4)=AAA(4)+2.*S(4,J)*S(5,J)
      AAA(5)=AAA(5)+2.*S(5,J)*S(6,J)
      AAA(6)=AAA(6)+2.*S(6,J)*S(7,J)
```

```
      AAA(7)=AAA(7)+2.*S(7,J)*S(8,J)
      AAA(8)=AAA(8)+2.*S(8,J)*S(9,J)
      AAA(9)=AAA(9)+2.*S(9,J)*S(10,J)
      AAA(10)=AAA(10)+2.*S(10,J)*S(11,J)
      AAA(11)=AAA(11)+2.*S(11,J)*S(12,J)
      AAA(12)=AAA(12)+2.*S(12,J)*S(13,J)
      AAA(13)=AAA(13)+2.*S(13,J)*S(14,J)
      AAA(14)=AAA(14)+2.*S(14,J)*S(15,J)
      AAA(15)=AAA(15)+2.*S(15,J)*S(16,J)
      AAA(16)=AAA(16)+2.*S(16,J)*S(17,J)
      AAA(17)=AAA(17)+2.*S(17,J)*S(18,J)
      AAA(18)=AAA(18)+2.*S(18,J)*S(1,J)
      AAA(19)=AAA(19)+2.*S(LL1,J)*S(LL2,J)
      AAA(20)=AAA(20)+2.*S(LL3,J)*S(LL4,J)
      AAA(21)=AAA(21)+2.*S(LL5,J)*S(LL6,J)
      AAA(22)=AAA(22)+2.*S(LL7,J)*S(19,J)
      GO TO 3008
3008  CONTINUE
      AA=2.*AA
      AB=2.*AB
      AC=2.*AC
      AD=2.*AD
      AE=2.*AE
      AF=2.*AF
      AG=2.*AG
      AH=2.*AH
      AI=2.*AI
      AJ=2.*AJ
      AK=2.*AK
      AL=2.*AL
      AM=2.*AM
      AN=2.*AN
      AO=2.*AO
      AP=2.*AP
      AQ=2.*AQ
      AR=2.*AR
      AS=2.*AS
      B(1)=AA
      B(2)=AB
      B(3)=AC
      B(4)=AD
      B(5)=AE
      B(6)=AF
      B(7)=AG
      B(8)=AH
      B(9)=AI
      B(10)=AJ
      B(11)=AK
      B(12)=AL
      B(13)=AM
```

```
      B(14)=AN
      B(15)=AO
      B(16)=AP
      B(17)=AQ
      B(18)=AR
      B(19)=AS
      WRITE(61,222)B(1),B(2),B(3),B(4),B(5)
      WRITE(61,222)B(6),B(7),B(8),B(9),B(10)
      WRITE(61,222)B(11),B(12),B(13),B(14),B(15)
      WRITE(61,222)B(16),B(17),B(18),B(19)
      NNN=N-1
      B(1)=1.0-B(1)
      B(19)=2.0-B(19)
      DO72I=2,NNN
   72 B(I)=1.0-B(I)
      WRITE(61,222)B(1),B(2),B(3),B(4),B(5)
      WRITE(61,222)B(6),B(7),B(8),B(9),B(10)
      WRITE(61,222)B(11),B(12),B(13),B(14),B(15)
      WRITE(61,222)B(16),B(17),B(18),B(19)
      WRITE(61,35)AAA(1),AAA(2),AAA(3),AAA(4)
      WRITE(61,35)AAA(5),AAA(6),AAA(7),AAA(8)
      WRITE(61,35)AAA(9),AAA(10),AAA(11),AAA(12)
      WRITE(61,35)AAA(13),AAA(14),AAA(15),AAA(16)
      WRITE(61,35)AAA(17),AAA(18),AAA(19),AAA(20)
      WRITE(61,35)AAA(21),AAA(22)
      VD1=0.0
      VD2=0.0
      DO41I=1,N
      VD1=VD1-B(I)*(RA1(I)-CG1)
   41 VD2=VD2-B(I)*(RA2(I)-CG2)
      WRITE(61,42)VD1,VD2
      GO TO 2323
    2 FORMAT(4E16.8)
   15 FORMAT(/E16.8)
  222 FORMAT(/5F9.4)
   35 FORMAT(/10XF8.4,10XF8.4,10XF8.4,10XF8.4)
   42 FORMAT(/2XF8.4,2XF8.4)
      END
```

CALCULATION OF CENTRE OF GRAVITY COORDINATES.

This IBM 1620 computer programme computes the x and y coordinates of the centre of gravity of a molecule, and arranges the atomic position coordinates of all atoms (except hydrogen atoms), originally punched in free format, in a format suitable for use directly with the CDC 3200 Molecular Orbital Calculations programme above.

INPUT DATA.

1. NAC, NPOS are identification numbers used with each set of data.
2. N is the number of atoms in the molecule, including hydrogen atoms.
3. SUMM is the molecular weight.
4. RO1(I) and RO2(I) are the x and y coordinates, respectively, of the positions of all atoms (including hydrogen atoms).
5. S(I) are the atomic weights of all atoms in the same order as in 4. above.
6. N is the number of atoms, excluding hydrogen atoms.
7. RA1(I) and RA2(I) are the x and y coordinates, respectively, of the positions of all atoms, excluding hydrogen atoms.

OUTPUT DATA.

1. MAC, MPGS as identification for each set of data.
2. CG1 and CG2 are the x and y coordinates, respectively, of the centre of gravity of the molecule.
3. RA1(I) and RA2(I), punched in format suitable for input of the Molecular Orbital Calculations programme above.

```
C      CENTRE OF GRAVITY CALCULATIONS AND COORDINATES
       DIMENSIONRO1(32),RO2(32),S(32),RA1(28),RA2(28)
 4444  FORMAT(20X13,20X13)
    6  FORMAT(2F8.4)
    3  FORMAT(2F6.2)
   98  READ,MAC,MPOS
       READ,N,SUMM
       DO4I=1,N
    4  READ,RO1(I),RO2(I),S(I)
       READ,M
       DO121I=1,M
  121  READ,RA1(I),RA2(I)
       R1=0.0
       R2=0.0
       CG1=0.0
       CG2=0.0
       DO5I=1,N
       CG1=CG1+S(I)*(RO1(I)-R1)
    5  CG2=CG2+S(I)*(RO2(I)-R2)
       CG1=CG1/SUMM
       CG2=CG2/SUMM
       PUNCH4444,MAC,MPOS
       PUNCH6,CG1,CG2
       DO2I=1,M
    2  PUNCH3,RA1(I),RA2(I)
       GOTO98
       END
```

DIPOLE MOMENT CALCULATIONS.

This IBM 1620 computer programme gives either a full listing of π-, σ- and total dipole moment components, magnitudes and angles of orientation, θ, or simply, μ_π, μ_σ and μ_{Total} with corresponding angles of orientation, as listed in Appendix 2.

INPUT DATA.

1. N is an identification number, giving a complete listing (as above) if <0, and a listing of the values of μ_π, μ_σ and μ_{Total}, and θ values if >0.
2. VD1 and VD2 are the x and y coordinates, respectively of the π-dipole moment from the output of the Molecular Orbital Calculations programme above.
3. SIG1 and SIG2 are the x and y coordinates, respectively, of the σ-dipole moment calculated using the values and methods in Chapter 3.

OUTPUT DATA.

1. If N < 0: x component, y component, magnitude and angle of orientation of each of μ_π, μ_σ and μ_{Total} in that order.
2. If N ≥ 0: magnitude and angle of each of μ_π, μ_σ and μ_{Total} in that order (see Tables in Appendix 2).

```
C       DIPOLE MOMENT CALCULATIONS
   22 FORMAT(4F8.4)
   25 FORMAT(12XF9.4,2XF9.4,2XF9.4,2XF9.4,2XF9.4,2XF9.4)
   98 READ,N
      READ,VD1,VD2,SIG1,SIG2
      SP=3.1416
      VD1=4.802*VD1
      VD2=4.802*VD2
      D=SQRTF(VD1*VD1+VD2*VD2)
      ADD=ATANF(VD2/VD1)
      IF(VD1)2,3,3
    2 IF(VD2)4,5,5
    4 ADD=(SP+ADD)/SP
      GOTO26
    5 ADD=(SP+ADD)/SP
      GOTO26
    3 IF(VD2)6,7,7
    6 ADD=(2.0*SP+ADD)/SP
      GOTO26
    7 ADD=ADD/SP
   26 SIG=SQRTF(SIG1*SIG1+SIG2*SIG2)
      SADD=ATANF(SIG2/SIG1)
      IF(SIG1)16,17,17
   16 IF(SIG2)18,19,19
   18 SADD=(SP+SADD)/SP
      GOTO27
   19 SADD=(SP+SADD)/SP
      GOTO27
   17 IF(SIG2)20,21,21
   20 SADD=(2.0*SP+SADD)/SP
      GOTO27
   21 SADD=SADD/SP
   27 FDD1=VD1+SIG1
      FDD2=VD2+SIG2
      FDD=SQRTF(FDD1*FDD1+FDD2*FDD2)
      FADD=ATANF(FDD2/FDD1)
      IF(FDD1)10,11,11
   10 IF(FDD2)12,13,13
   12 FADD=(SP+FADD)/SP
      GOTO28
   13 FADD=(SP+FADD)/SP
      GOTO28
   11 IF(FDD2)14,15,15
   14 FADD=(2.0*SP+FADD)/SP
      GOTO28
   15 FADD=FADD/SP
   28 IF(N)23,24,24
   23 PUNCH22,VD1,VD2,D,ADD
      PUNCH22,SIG1,SIG2,SIG,SADD
      PUNCH22,FDD1,FDD2,FDD,FADD
      GOTO98
   24 PUNCH25,D,ADD,SIG,SADD,FDD,FADD
      GOTO98
      END
```

APPENDIX 5.

COMPUTER PROGRAMMES FOR THE CALCULATION OF GEOMETRIC FACTORS REQUIRED FOR THE DETERMINATION OF FREE ENERGY.

PART 1: THE INTERCALATED MODEL

PART 2: THE MODEL INVOLVING EXTERNAL EDGEWISE ATTACHMENT OF DYE.

APPENDIX 5.

CALCULATION OF GEOMETRIC FACTORS: PARTS 1 AND 2.

The two IBM 1620 computer programmes listed in this Appendix compute the geometric factors $C_{i,j}$, $\theta_{i,j}$, etc., defined by equations 2.7 and 2.8 for the intercalated model (Part 1) and for the external edgewise binding model (Part 2). These geometric factors then yield the free energy values required by using equations 2.3 to 2.6 and 2.9. The programme designated 'Part 2' is also used to give the geometric factors for dye-dye interactions in the intercalated model.

CALCULATION OF GEOMETRIC FACTORS FOR INTERCALATED MODEL.

INPUT DATA

1. A(1,J) are the coordinates of centre of left-hand base.
2. A(2,J) are the coordinates of centre of right-hand base.
3. A(3,J) are the coordinates of end of the dipole moment vector of the left-hand base.
4. A(4,J) are the coordinates of end of the dipole moment vector of the right-hand base.
5. B(1,1) and B(1,2) are the coordinates of the centre of the intercalated molecule.
6. B(2,1) and B(2,2) are the coordinates of the end of the dipole moment vector of the intercalated molecule.

7. EE(I), EE and ET are factors for converting the calculated geometric factors to actual energies. (If geometric factors only are required, these above factors are set equal to 1.0)
8. N is the number of angles for which calculations are made.
9. X denotes angle, which must be in radians.

OUTPUT DATA.

1. EC(1) + EC(2) gives $F_{\mu\mu}$.
2. EC(3) + EC(4) gives F_{pp}.
3. EP + ER gives $-F_{\mu p}$.
4. G(5), G(6), G(7) and G(8) are the geometric factors which may be used to give $F_{\mu p}$.
5. G(9) and G(10) are the geometric factors which may be used to give F_L.
6. G(1) and G(2) are the geometric factors which may be used to give $F_{\mu\mu}$.
7. G(3) and G(4) are the geometric factors which may be used to give F_{pp}.
8. AC and AE are the geometric factors which may be used to give $-F_{\mu p}$.
9. X is the angle θ of Fig. 4.1, in radians.

NOTE: In the calculation of these geometric factors, the distance R_{ij} (or a power of R_{ij}) has not been included in the denominator, but was, of course, included in the calculation of the free energy terms.

```
C      GEOMETRICAL FACTORS PF-DNA GERSCH          PART 1
       DIMENSIONB(2,3),A(4,3),BA(2,3),SA(3),SB(3),SC(3)
       DIMENSIONSD(3),G(10),BB(8),BC(8)
     4 FORMAT(2XF8.4,2XF8.4,2XF8.4,2XF8.4,2XF8.4,2XF8.4,2XE13.4)
     6 FORMAT(3XF8.4,3XF8.4,3XF8.4,3XF8.4,3XF8.4)
     7 FORMAT(3XF8.4,3XF8.4,3XE13.4)
    98 READ,A(1,1),A(1,2),A(1,3),A(2,1),A(2,2),A(2,3)
       READ,A(3,1),A(3,2),A(3,3),A(4,1),A(4,2),A(4,3)
       READ,B(1,1),B(1,2),B(2,1),B(2,2)
       READ,BB(1),BB(2),BB(3),BB(4),BB(5)
       READ,BB(6),BB(7),BB(8)
       READ,BS,BT
       READ,N
       DO21I=1,N
       READ,X
       BA(1,1)=COSF(X)*B(1,1)-SINF(X)*B(1,2)
       BA(1,2)=SINF(X)*B(1,1)+COSF(X)*B(1,2)
       BA(2,1)=COSF(X)*B(2,1)-SINF(X)*B(2,2)
       BA(2,2)=SINF(X)*B(2,1)+COSF(X)*B(2,2)
       BL=2.128
       BA(1,3)=3.360
       BA(2,3)=3.360
       DA=(BA(2,1)-BA(1,1))/BL
       DB=(BA(2,2)-BA(1,2))/BL
       DO13K=1,3
       SA(K)=A(4,K)-A(1,K)
       SB(K)=A(3,K)-A(2,K)
       SC(K)=BA(1,K)-A(1,K)
    13 SD(K)=BA(1,K)-A(2,K)
       SAS=SQRTF(SA(1)*SA(1)+SA(2)*SA(2)+SA(3)*SA(3))
       SBS=SQRTF(SB(1)*SB(1)+SB(2)*SB(2)+SB(3)*SB(3))
       SCS=SQRTF(SC(1)*SC(1)+SC(2)*SC(2)+SC(3)*SC(3))
       SDS=SQRTF(SD(1)*SD(1)+SD(2)*SD(2)+SD(3)*SD(3))
       DO14K=1,3
       SA(K)=SA(K)/SAS
       SB(K)=SB(K)/SBS
       SC(K)=SC(K)/SCS
    14 SD(K)=SD(K)/SDS
       AP=DA*SA(1)+DB*SA(2)
       AB=DA*SB(1)+DB*SB(2)
       AC=SA(1)*SC(1)+SA(2)*SC(2)+SA(3)*SC(3)
       AD=DA*SC(1)+DB*SC(2)
       AE=SB(1)*SD(1)+SB(2)*SD(2)+SB(3)*SD(3)
       AG=DA*SD(1)+DB*SD(2)
       GA=(DA-3.*AD*SC(1))*(DA-3.*AD*SC(1))
       GB=(DB-3.*AD*SC(2))*(DB-3.*AD*SC(2))
       GC=(3.*AD*SC(3))*(3.*AD*SC(3))/2.
       GD=(SA(1)-3.*AC*SC(1))*(SA(1)-3.*AC*SC(1))
       GE=(SA(2)-3.*AC*SC(2))*(SA(2)-3.*AC*SC(2))
       GG=(SA(3)-3.*AC*SC(3))*(SA(3)-3.*AC*SC(3))/2.
```

```
      PA=(DA-3.*AG*SD(1))*(DA-3.*AG*SD(1))
      PB=(DB-3.*AG*SD(2))*(DB-3.*AG*SD(2))
      PC=(3.*AG*SD(3))*(3.*AG*SD(3))/2.
      PD=(SB(1)-3.*AE*SD(1))*(SB(1)-3.*AE*SD(1))
      PE=(SB(2)-3.*AE*SD(2))*(SB(2)-3.*AE*SD(2))
      PG=(SB(3)-3.*AE*SD(3))*(SB(3)-3.*AE*SD(3))/2.
      RA=(1.0-3.*SC(1)*SC(1))*(1.0-3.*SC(1)*SC(1))
      RB=(0.0-3.*SC(1)*SC(2))*(0.0-3.*SC(1)*SC(2))
      RC=(0.0-3.*SC(1)*SC(3))*(0.0-3.*SC(1)*SC(3))/2.
      RD=(0.0-3.*SC(2)*SC(1))*(0.0-3.*SC(2)*SC(1))
      RE=(1.0-3.*SC(2)*SC(2))*(1.0-3.*SC(2)*SC(2))
      RG=(0.0-3.*SC(2)*SC(3))*(0.0-3.*SC(2)*SC(3))/2.
      RP=(0.0-3.*SC(3)*SC(1))*(0.0-3.*SC(3)*SC(1))/2.
      RR=(0.0-3.*SC(3)*SC(2))*(0.0-3.*SC(3)*SC(2))/2.
      RS=(1.0-3.*SC(3)*SC(3))*(1.0-3.*SC(3)*SC(3))/4.
      TA=(1.0-3.*SD(1)*SD(1))*(1.0-3.*SD(1)*SD(1))
      TB=(0.0-3.*SD(1)*SD(2))*(0.0-3.*SD(1)*SD(2))
      TC=(0.0-3.*SD(1)*SD(3))*(0.0-3.*SD(1)*SD(3))/2.
      TD=(0.0-3.*SD(2)*SD(1))*(0.0-3.*SD(2)*SD(1))
      TE=(1.0-3.*SD(2)*SD(2))*(1.0-3.*SD(2)*SD(2))
      TG=(0.0-3.*SD(2)*SD(3))*(0.0-3.*SD(2)*SD(3))/2.
      TP=(0.0-3.*SD(3)*SD(1))*(0.0-3.*SD(3)*SD(1))/2.
      TR=(0.0-3.*SD(3)*SD(2))*(0.0-3.*SD(3)*SD(2))/2.
      TS=(1.0-3.*SD(3)*SD(3))*(1.0-3.*SD(3)*SD(3))/4.
      G(1)=AP-3.*AC*AD
      G(2)=AB-3.*AE*AG
      G(3)=SC(1)*SC(1)+SC(2)*SC(2)+SC(3)*SC(3)/2.
      G(4)=SD(1)*SD(1)+SD(2)*SD(2)+SD(3)*SD(3)/2.
      G(5)=GA+GB+GC
      G(6)=GD+GE+GG
      G(7)=PA+PB+PC
      G(8)=PD+PE+PG
      G(9)=RA+RB+RC+RD+RE+RG+RP+RR+RS
      G(10)=TA+TB+TC+TD+TE+TG+TP+TR+TS
      BC(1)=G(1)*BB(1)
      BC(2)=G(2)*BB(2)
      BC(3)=G(3)*BB(3)
      BC(4)=G(4)*BB(4)
      BC(5)=G(5)*BB(5)
      BC(6)=G(6)*BB(6)
      BC(7)=G(7)*BB(7)
      BC(8)=G(8)*BB(8)
      BR=AE*BT
      BP=AC*BS
      PUNCH4,BC(1),BC(2),BC(3),BC(4),BP,BR,X
      PUNCH6,G(5),G(6),G(7),G(8),X
      PUNCH7,G(9),G(10),X
   21 PUNCH4,G(1),G(2),G(3),G(4),AC,AE,X
      GOTO98
      END
```

CALCULATION OF GEOMETRIC FACTORS FOR EXTERNAL EDGEWISE BINDING MODEL.

INPUT DATA.

1. BA(1,3) and BA(2,3) are the z coordinates of the centre and end of the dipole moment vector of the upper of the two molecules considered.
2. B(1,1) and B(1,2) are the coordinates of the centre of the lower of the two molecules considered.
3. B(2,1) and B(2,2) are the coordinates of the end of the dipole moment vector of the lower of the two molecules considered.
4. N is the number of angles for which calculations are made.
5. X denotes the angle (in radians) which the dipole moment vector of the upper molecule makes with the dipole moment vector of the lower molecule.

OUTPUT DATA.

1. G(1) is the geometric factor which may be used to give $F_{\mu\mu}$.
2. G(3) is the geometric factor which may be used to give $F_{\mu\alpha}$.
3. G(5) and G(6) are the geometric factors which may be used to give $F_{\mu\alpha}$.

4. G(9) is the geometric factor which may be used to give F_L .
5. AC is the geometric factor which may be used to give $-F_{\rho\mu}$.
6. SCS is the distance between the centres of the interacting molecules.
7. EL is the length of the dipole moment vector and was taken as 2.128 in this programme.
8. X denotes the angle for which the calculations were made and is defined in section 5. of the input data above.

NOTE: In the calculation of these geometric factors, the distance R_{ij} (or a power of R_{ij}) has not been included in the denominator, but was, of course, included in the calculation of the free energy terms.

```
C      GEOMETRICAL FACTORS PF-DNA GERSCH          PART 2
       DIMENSIONB(2,3),A(4,3),BA(2,3),SA(3),SB(3),SC(3)
       DIMENSIONSD(3),G(10)
    4  FORMAT(2XF8.4,2XF8.4,2XF8.4,2XF8.4,2XF8.4,2XF8.4,2XE13.4)
    7  FORMAT(3XF8.4,3XF8.4,3XE13.4)
   98  READ,BA(1,3),BA(2,3)
       READ,B(1,1),B(1,2),B(2,1),B(2,2)
       READ,N
       DO21I=1,N
       READ,X
       BA(1,1)=COSF(X)*B(1,1)-SINF(X)*B(1,2)
       BA(1,2)=SINF(X)*B(1,1)+COSF(X)*B(1,2)
       BA(2,1)=COSF(X)*B(2,1)-SINF(X)*B(2,2)
       BA(2,2)=SINF(X)*B(2,1)+COSF(X)*B(2,2)
       B(1,3)=0.0
       B(2,3)=0.0
       BL=2.128
       DA=(BA(2,1)-BA(1,1))/BL
       DB=(BA(2,2)-BA(1,2))/BL
       DO13K=1,3
   13  SC(K)=BA(1,K)-B(1,K)
       SA(1)=1.0
       SA(2)=0.0
       SA(3)=0.0
       SCS=SQRTF(SC(1)*SC(1)+SC(2)*SC(2)+SC(3)*SC(3))
       DO14K=1,3
   14  SC(K)=SC(K)/SCS
       AP=DA*SA(1)+DB*SA(2)
       AC=SA(1)*SC(1)+SA(2)*SC(2)+SA(3)*SC(3)
       AD=DA*SC(1)+DB*SC(2)
       GA=(DA-3.*AD*SC(1))*(DA-3.*AD*SC(1))
       GB=(DB-3.*AD*SC(2))*(DB-3.*AD*SC(2))
       GC=(3.*AD*SC(3))*(3.*AD*SC(3))/2.
       GD=(SA(1)-3.*AC*SC(1))*(SA(1)-3.*AC*SC(1))
       GE=(SA(2)-3.*AC*SC(2))*(SA(2)-3.*AC*SC(2))
       GG=(SA(3)-3.*AC*SC(3))*(SA(3)-3.*AC*SC(3))/2.
       RA=(1.0-3.*SC(1)*SC(1))*(1.0-3.*SC(1)*SC(1))
       RB=(0.0-3.*SC(1)*SC(2))*(0.0-3.*SC(1)*SC(2))
       RC=(0.0-3.*SC(1)*SC(3))*(0.0-3.*SC(1)*SC(3))/2.
       RD=(0.0-3.*SC(2)*SC(1))*(0.0-3.*SC(2)*SC(1))
       RE=(1.0-3.*SC(2)*SC(2))*(1.0-3.*SC(2)*SC(2))
       RG=(0.0-3.*SC(2)*SC(3))*(0.0-3.*SC(2)*SC(3))/2.
       RP=(0.0-3.*SC(3)*SC(1))*(0.0-3.*SC(3)*SC(1))/2.
       RR=(0.0-3.*SC(3)*SC(2))*(0.0-3.*SC(3)*SC(2))/2.
       RS=(1.0-3.*SC(3)*SC(3))*(1.0-3.*SC(3)*SC(3))/4.
       G(1)=AP-3.*AC*AD
       G(3)=SC(1)*SC(1)+SC(2)*SC(2)+SC(3)*SC(3)/2.
       G(5)=GA+GB+GC
       G(6)=GD+GE+GG
       G(9)=RA+RB+RC+RD+RE+RG+RP+RR+RS
       PUNCH4,G(1),G(3),G(5),G(6),G(9),AC,X
   21  PUNCH7,SCS,BL,X
       GOTO98
       END
```

APPENDIX 6.

PUBLICATION.

"INTERACTION OF DNA WITH AMINOACRIDINES"

Gersch, M.F. and Jordan, D.O., J.Mol.Biol. 13, 138 (1965).

J. Mol. Biol. (1965) **13**, 138–156

Interaction of DNA with Aminoacridines

NERIDA F. GERSCH AND D. O. JORDAN

Department of Physical and Inorganic Chemistry
University of Adelaide, Adelaide, South Australia

(*Received 27 March 1965*)

The thermal denaturation of DNA–proflavine and DNA–2-aminoacridine complexes has been studied at two ionic strengths for varying ratios of dye and DNA concentrations. An increase in the thermal denaturation temperature over that of DNA alone has been found, this increase being larger for lower ionic strengths. The thermal denaturation temperature of DNA–proflavine systems is in general higher than that of DNA–2-aminoacridine systems.

Free energy calculations have been made on the basis of two models for the DNA–dye complex, the intercalated model and a model involving external edgewise attachment of the dye. The total free energy thus found is less for both models than that found by De Voe & Tinoco (1962) for native DNA. It has been shown that the observed properties of the DNA–dye complex are best explained by the intercalated model.

1. Introduction

The interaction of DNA with aminoacridines and other heterocyclic systems has been interpreted in terms of two models. In the first, intercalation of an aminoacridine molecule or ion between adjacent base pairs occurs (model I), the DNA molecule consequently extending and the original right-handed helix becoming a left-handed helix in the process (Lerman, 1961,1963). The principle forces stabilizing this model arise from charge, permanent dipole and induced dipole interactions and London forces between the aminoacridine and the neighbouring base pairs. In the second model, the aminoacridine is associated with the phosphate group on the outside of the double helix, the helix dimensions remaining essentially unchanged. As originally described by Bradley & Wolf (1959), the dye molecules were stacked perpendicularly to the helix axis, but this model has recently been refined by Mason & McCaffery (1964) who, on the basis of conclusions drawn from optical rotation measurements of streaming solutions, consider the aminoacridine to be attached through the ring NH group to a phosphate group, the heterocyclic ring being oriented at an angle of between 45 and 90° to the helix axis (model II). Electrostatic and dye–dye interactions are involved in determining the stability of this model. In the intercalated model (I), external attachment of the aminoacridine molecules, as in model II, is clearly also possible.

In this paper we present the results of calculations of the free energy of the interaction of aminoacridines with DNA according to both models I and II. The calculations are based on the methods adopted by De Voe & Tinoco (1962) for the determination of the free energy of the DNA double helix. This enables a comparison to be made of the relative stabilities of the two models, and also a prediction of the order of

preference for dye interaction with the various base pairs. On the basis of fluorescence-quenching measurements, Tubbs, Ditmars & Van Winkle (1964) have already observed that adenine–thymine sites interact more strongly with acriflavine than guanine–cytosine sites.

Experimental determinations of the melting temperature of DNA in the presence of acridine orange (Freifelder, Davison & Geiduschek, 1961; Kleinwächter & Koudelka, 1964) have shown that the value of T_m† for the dye–DNA complex is higher than that for native DNA. Furthermore, Kleinwächter & Koudelka (1964) showed that T_m for the dye–DNA complex was dependent on the base composition of the DNA, a greater increase of T_m being observed for DNA of low GC content. The T_m of complexes of calf thymus DNA with 2-aminoacridine and proflavine (2,8-diaminoacridine) at two different ionic strengths are given here and discussed with reference to the two models.

2. Materials and Methods

Calf thymus DNA was prepared by the method of Kay, Simmons & Dounce (1952), the value of T_m in 0·1 M-NaCl being 82·7°C and the value of ϵ_P, 6620; these values are in agreement with those previously published for native preparations of this DNA. The latter figure was used for the determination of concentrations. Stock solutions of approximately 0·1% by weight of DNA were prepared in twice-distilled water and diluted with NaCl solution to give a final sodium chloride concentration of either 0·1 M or 0·001 M.

Proflavine hemisulphate (British Drug Houses Ltd., England) was recrystallized from water, after washing with dry ethanol, and dried *in vacuo* to constant weight. The extinction coefficient at 444 mμ in 0·1 M-NaCl (pH 6·2) and a dye concentration of $1{\cdot}53\times10^{-5}$ M was $4{\cdot}1\times10^4$, in agreement with the value given by Haugen & Melhuish (1964). 2-Aminoacridine was prepared by Dr G. Chandler. The hydrochloride was prepared by passing dry HCl gas through a solution of the purified base in dry diethyl ether. The hydrochloride precipitated and was recovered by removal of the excess ether and dried at room temperature. The extinction coefficient was found to be $1{\cdot}2\times10^4$ at 456·6 mμ over a range of concentrations between 1·0 and $5{\cdot}0\times10^{-5}$ M in 0·1 M-NaCl (pH 5·9). Samples of both dyes, dried *in vacuo*, were used in preparing solutions by weight, and concentrations were checked by conductimetric titration; agreement was always within 1%.

All the DNA–proflavine solutions in the concentration range studied had a pH of 6·2 and those of DNA–2-aminoacridine were of 5·9. At constant sodium ion concentration, a variation of pH between 5·9 and 6·2 produces a variation in T_m of native DNA of no more than 0·1°C (Hogarth & Jordan, unpublished results). Hence such pH differences have been neglected in the interpretation of the T_m values obtained. Since Millich & Oster (1959) found that proflavine, in solution, undergoes rapid photo-reduction, although 2-aminoacridine does not, all solutions of both dyes were stored in the dark at 4°C. Polythene containers were used for the stock dye solutions (about 4×10^{-4} M), since these did not adsorb dye to any significant extent. Pyrex test tubes were used in the preparation of all dilute dye solutions, as it was shown that soft glass adsorbs dye to a much greater extent than does Pyrex.

For the determination of melting curves, DNA–dye solution was contained in either 10- or 2-mm silica cells, using 0·1 M-NaCl in a matched 10-mm cell as reference. Evaporation from the 10-mm cells was prevented by a layer of paraffin, and from the 2-mm cells by a layer of paraffin and a seal of Para-film (Lindsay & Williams Ltd., London, England). The cells were placed in an electrically heated and thermostatically controlled cell holder. Temperatures close to the sample were determined using a calibrated thermocouple. All optical density measurements were made at 259 mμ using a Unicam SP500 spectrophotometer and were corrected for increase in volume with temperature.

† Abbreviations used: T_m, the melting temperature of DNA; A, adenine; T, thymine; G, guanine; C, cytosine.

The definition of T_m has been modified from that usually employed, as an increase of the optical density in the temperature range 25 to about 70°C was generally observed with DNA–dye complexes. Considering curve I in Fig. 5 for 2-aminoacridine in 0·1 M-NaCl, which is typical, the melting curve can be clearly divided into two parts: the small increase between 25 and 80°C, AB, and the true melting region, BC. The interpretation of this behaviour is discussed later. A new melting temperature, T_m', is defined as the temperature at which 50% hyperchromicity is attained from the onset of the rapid increase of the optical density above about 70°C until no further increase in optical density is recorded, i.e. in the region BC (Fig. 5, curve I). Extrapolation of the linear sections of the curve enabled T_m' to be determined.

Dilute dye solutions were always added to dilute DNA solutions, as this procedure was found less likely to cause precipitation of the DNA–dye complex which was observed if either component was present in high concentration.

The amount of dye bound per mole of DNA phosphorus, r, was determined from spectrophotometric titrations of proflavine and 2-aminoacridine with DNA in 0·1 M- and 0·001 M-NaCl by the method described by Peacocke & Skerrett (1956), whose results for proflavine with herring sperm DNA, which differs in GC content by only 1% from calf thymus DNA, were confirmed. From these results a plot of r against T_L/T_A, where T_L and T_A are the total concentrations of dye and DNA respectively, was made. For 0·1 M-NaCl and for values of r greater than 0·1, where the accuracy of the spectrophotometric method is not high, the values of Peacocke & Skerrett (1956) obtained for proflavine using equilibrium dialysis were used. For 2-aminoacridine, at values of r greater than 0·1, equilibrium dialysis was carried out to supplement the spectrophotometric titration results for 0·1 M-NaCl. Thus the values of r could be obtained for any solution where the ratio T_L/T_A was known. This method is valid for values of r less than 0·3 and for the T_A values used here.

3. Free Energy Calculations

(a) *General principles*

The total free energy of interaction between two molecules, charged or uncharged, having permanent and induced dipole moments, is given by:

$$F_{\text{total}} = F_{ES} + F_L$$

where F_{ES} is the electrostatic free energy from interactions between charges, permanent and induced dipoles, and F_L is the London energy arising from fluctuation dipole-induced dipole interactions. F_{ES} may be considered as a total of five interactions:

$$F_{\rho\rho},\ F_{\rho\mu},\ F_{\rho\alpha},\ F_{\mu\mu},\ F_{\mu\alpha}$$

where ρ, μ and α represent charge, dipole moment and polarizability, respectively. The calculations of these interactions for the DNA–dye models have been made using similar approximations to those adopted by De Voe & Tinoco (1962). The unit vectors representing the dipole moments and polarizability components were considered to be at the geometric centre of each molecule. Quadrupole moments were not considered. The characteristic energy, $h\nu_i$, was found to be 200 kcal. mole^{-1} from experimental values of the dispersion of benzene and pyridine. The average group polarizability, α_i, was estimated to be 20 Å^3 from values of atomic refractions (Fajans, 1959). As it is not possible to measure the dipole moment of a charged molecule, the dipole moment of proflavine in the ionic form was estimated in the following way. The bond and hybrid moments used by De Voe & Tinoco (1962) for the various atoms were applied to proflavine and to acridine to give the σ moments. The π moments were

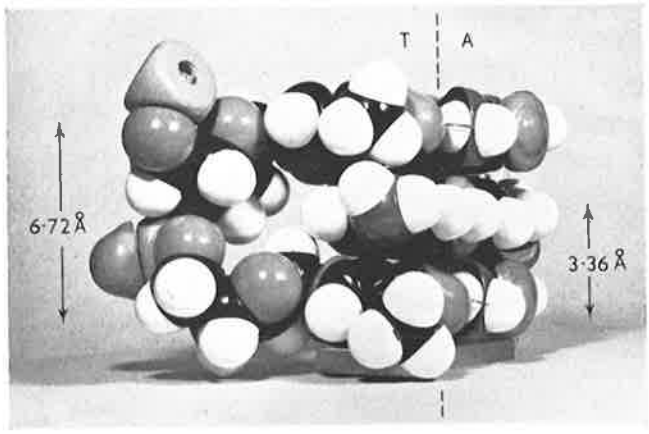

(a)

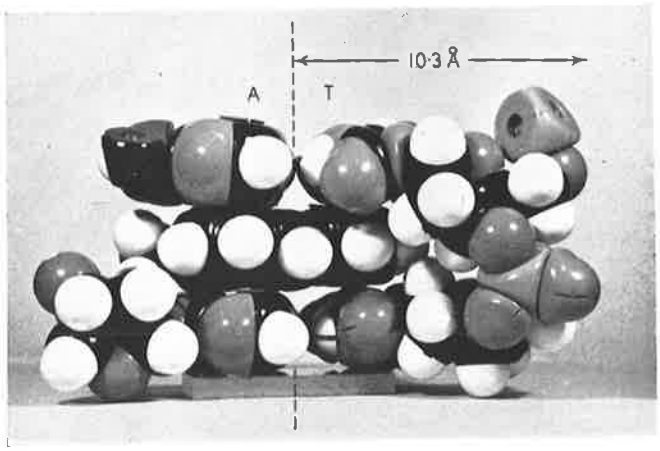

(b)

PLATE I. Relative positions of a proflavine molecule between two A–T base pairs in model I. The helix axis is represented by the broken line. (a) and (b) are two different views of the same model.

[*facing p. 141*

obtained using the electronic distribution for proflavine and acridine given by Pullman & Pullman (1963) and the method described by Daudel, Lefebvre & Moser (1959), the geometric centre of the molecule being taken as the origin. The σ and π moments so obtained were added vectorially to give a value of 4·5 D for μ_{total} for the proflavine ion. The angle which the dipole moment vector of the dye makes with the dipole moment vector of pyridine is 180°. The value of the dipole moment of acridine found by the above method is 3·4 D, somewhat higher than the experimental value of 2·1 D (Acheson, 1956).

An alternative method of calculating the σ moment described by Orgel, Cottrell, Dick & Sutton (1951) gives values for μ_{total} of 2·7 D for acridine (Pullman, 1964) and of 3·4 D for the proflavine ion. Although this method leads to a calculated value for acridine closer to the experimental value, which suggests that the value of 3·4 D for the proflavine ion may be closer to the true value than the value of 4·5 D calculated by the method of De Voe & Tinoco (1962), we have used the latter value, which probably represents an upper limit for the value of μ_{total} for the proflavine ion, to enable a comparison to be made with the results of De Voe & Tinoco (1962) for DNA. The corresponding values of μ, α and $h\nu$ for the bases of DNA were those given by De Voe & Tinoco (1962). In these calculations, no charge–charge interactions have been estimated, and $F_{\rho\rho}$ has therefore been neglected. It has been assumed that the association of gegenions with DNA and dye is such as to neutralize the charges. This would certainly be true in 0·1 M-NaCl. This assumption was, in effect, also made by De Voe & Tinoco (1962).

(b) *Intercalation of aminoacridine in DNA (model I)*

The model adopted for these calculations was that suggested by Lerman (1961). The native DNA helix (with orientations of base pairs with respect to helix and dyad axes as proposed by Langridge *et al.* (1960) in their model 3) is extended so that the distance between two adjacent base pairs is 6·72 Å and the angle between them, with a left-handed rotation, is 9° (Plate I(a)). The aminoacridine (proflavine in Plate I) is then considered to be inserted in such a way between the base pairs that the helix passes through the centre of the dye molecule (Plate I(b)). We have considered the case when one dye molecule is intercalated between each base pair and dye bonding by this mechanism is a maximum. For this situation $r = 0{\cdot}5$. In Plate I the proflavine molecule is oriented at 4·5° in a left-handed rotation about the helix axis with respect to the lower base pair. Other orientations of the dye molecule are discussed later.

The geometric factors $C_{i,j}$ and $G_{i,j}$, etc. necessary for the calculation of $F_{\rho\mu}$, $F_{\rho\alpha}$, $F_{\mu\mu}$, $F_{\mu\alpha}$ and F_{L} were calculated, using an IBM 1620 computer, at a number of angles of orientation of the dipole moment unit vector of the intercalated molecule (the angle θ in Fig. 1). Thus for proflavine, where the dipole moment vector is oriented at 180° with respect to the pyridine dipole moment vector, the possible values for θ are 175·5° and 355·5°. The former of these angles gives the positions of the molecules represented in Plate I.

Calculations have also been made for the free energy of interaction between a given dye molecule and the next intercalated dye molecule 6·72 Å above and the base pair 10·08 Å above. The free energy arising from interactions between the base pairs 6·72 Å apart in model I has not been included, since De Voe & Tinoco (1962) found that the contribution to the free energy from interactions between base pairs more than 3·36 Å apart was small.

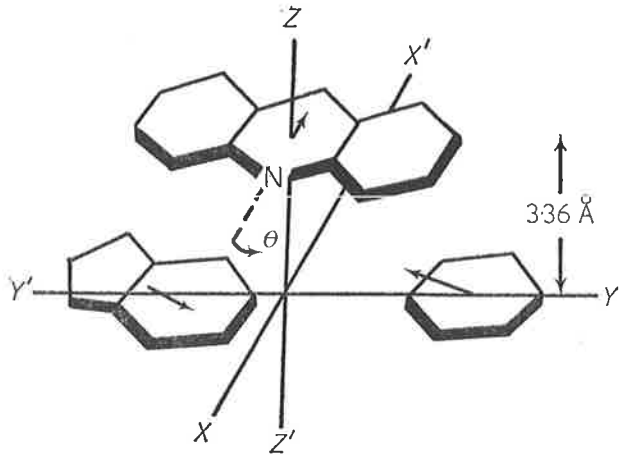

FIG. 1. Relative positions of an adenine–thymine base pair and an aminoacridine molecule, as used in the free energy calculations for the intercalated model (I). The skeletons of the molecules are shown and no amino or carboxyl groups are indicated, the ring nitrogen only of the dye being shown. The three dipole moments are represented by short arrows and are not drawn to scale.

(c) *External, edgewise binding of aminoacridine and DNA (model II)*

The model used for the calculation of the geometric factors for proflavine bound outside the helix is shown as a projection on the XY plane in Fig. 2. If both the dye molecules are oriented at the same angle to the helix axis but not perpendicular to it, as shown in Fig. 2, there will be no effect on the values of the free energy obtained provided that the angle between the dipole moment vectors remains at 36°. The energy calculations indicate that a variation in the angle of orientation of the two molecules with respect to each other within the limits imposed by the model brings about a change in F_{total} of no more than $\pm$ 0·5 kcal. per repeating unit.

Since we have considered the situation for which $r = 0{\cdot}5$ for the intercalated model (I), we have also considered only the case where $r = 0{\cdot}5$ for the external binding model (II). This has the effect, since the maximum value of r in this case is 1·0, that a dye molecule is bound to all the phosphate groups on one helix (model IIa), or, on the average, to every alternate phosphate group on both helices (model IIb). The former model (IIa) has been assumed in our calculations, since dye–dye interaction is greater for this model. However, we have also made calculations for the energy of interaction

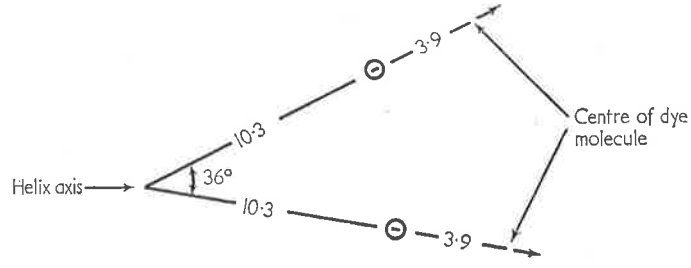

FIG. 2. Projection on the XY plane showing atomic distances used in the free energy calculations for model IIa, involving external edgewise attachment of the dye molecules to the phosphate groups. The arrows represent the dipole moment vectors of the charged dye molecules.

between a given dye molecule and the dye molecule in a plane 6·72 Å above it and with an angle of 72° between the dipole moment vectors of the two molecules as in model IIb.

The charge on the phosphate group was considered to be a point charge 10·3 Å from the helix axis, giving rise to charge–dipole and charge–polarizability interactions with the bound dye molecules. These interactions are considered for model II where the dye molecules are bound directly to the phosphate groups, whereas they are not considered for the intercalated model or for DNA alone. In model II, the sodium ion formerly associated with the phosphate has been replaced by a bound dye ion, and it is assumed that no marked change in charge distribution in the proflavine molecule, due to the negative phosphate group, occurs by induction through the bonds; and hence that the dipole moment of the charged molecule in this case is the same as that used for the intercalated model. However, for the intercalated model no values of the charge–dipole and charge–polarizability interactions have been included in F_{total}. De Voe & Tinoco (1962) made no estimate for these free energies for DNA alone. Such values cannot be calculated with accuracy, since there is a reduction of the effective charge of the phosphate groups due to gegenion association in the case of DNA and due also to intercalated dye molecules for model I.

(d) *Estimation of the effective dielectric constant, ϵ_{ij}*

In the intercalated model (I), since the dye molecules and the adjacent base pairs are effectively separated by a vacuum, we have taken ϵ_{ij} as being 1·0, as did De Voe & Tinoco (1962) for DNA. Helix solvation would reduce the contribution of the electrostatic interactions and, owing to the presence of the charged dye molecules within the helix for the intercalated model, this effect is likely to be larger than for DNA.

For external edgewise binding (model II) association of solvent molecules with bound dye molecules will occur and thereby will increase the effective dielectric constant. Rice & Nagasawa (1961) chose a value for ϵ_{ij} of 5·5 for calculations on the polymethacrylate ion, where the charge separation is 2·5 Å. This value for ϵ_{ij} and those obtained here were found from the dependence of ϵ_{ij} on the distance of a given point from an ion (Hasted, Ritson & Collie, 1948). The charge separation between the negative phosphate and the positive bound dye in the DNA–dye complex is 3·9 Å (Fig. 2). The values of 35 and 10 for ϵ_{ij} were obtained by taking the average of ϵ_r and ϵ_θ for the distance from an ion of 3·9/2 Å, using the two models described by Hasted *et al.* (1948). These are taken as limiting values for the effective dielectric constant, now denoted ϵ'_{ij}, used in the calculations of the interaction between the charge on the phosphate group and the dipole moment and polarizability of the bound dye molecule. The charge separation is about 9·0 Å between adjacent bound dye positive charges (model IIa) and a value for ϵ_{ij} of 70 was chosen. For model IIb the corresponding charge separation is 11·7 Å, and ϵ_{ij} will have a value of about 78.

(e) *Method of comparison of free energies*

For simplicity, the values of free energy for DNA and for model I are quoted for $\epsilon_{ij} = 1{\cdot}0$. Comparison of these values is possible if account is taken of the following factors:

(i) the dipole–dipole, charge–dipole, etc. interactions will be reduced to a greater extent than will the London interactions for both DNA and model I, by an increase in ϵ_{ij} due to helix solvation;

(ii) such reduction is expected to be slightly greater for model I than for DNA;

(iii) no account has been taken of the free energy required in the distortion of bond angles and alteration of bond lengths involved in the unwinding and extension of the helix to accommodate the dye molecule.

All these factors will add a positive term to the calculated free energy for model I.

The free energy values corresponding to model II can be compared with those for DNA and model I only if account is taken of the above factors. Furthermore, no account has been taken of base–solvent and dye–solvent interactions. It is evident that any such comparisons will be semi-quantitative, a more direct comparison only being possible if the calculations can be refined.

For both models the value of r adopted was 0·5, where r is the number of moles of dye bound per phosphate group. Thus for the intercalated model, all possible intercalation sites are occupied, whereas for dye bound externally, half the total binding sites are occupied.

The repeating unit for DNA is one base pair. The energy calculations for a repeating unit may be considered in one of two ways. Either one-half the sum of the eight interactions between the given base pair and that above and that below, together with the interaction energy between the bases of the given base pair, is evaluated; or the sum of the four interactions between the given base pair and that above, together with the average base pair energies of the two base pairs involved, is taken. The latter definition involves less complications when base pair sequences are taken into account and is therefore the one used here.

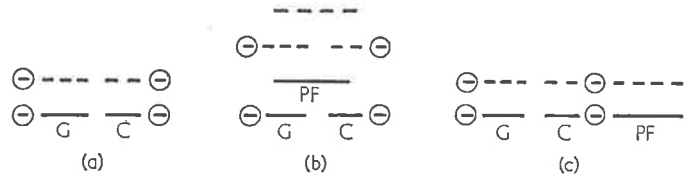

FIG. 3. A diagrammatic representation of the repeating units for (a) DNA; (b) model I; (c) model IIa. All interactions involving the molecules represented by a solid line with the molecules represented by a broken line are included in the total free energy calculations for one repeating unit. PF, proflavine.

The repeating unit for DNA is shown in Fig. 3(a). For the purpose of comparison with the results obtained here, the method of quoting the values of the total free energies for the base pairs in DNA, F_{total}, found by De Voe & Tinoco (1962) has been modified so that the free energies are quoted as kcal. per repeating unit. For example, for TA above CG, the sum of the four interactions above the CG plane, according to De Voe & Tinoco (1962), is $-18{\cdot}6$ kcal., and the average interaction of the bases of each base pair is $-1{\cdot}9$ kcal.; this gives a value of $-20{\cdot}5$ kcal. for the total free energy per repeating unit. The difference between this value and that of $-11{\cdot}2$ kcal. per 2 moles of base quoted by De Voe & Tinoco (1962) is a matter of definition only. This method of presenting F_{total} is necessary so as to permit comparison with values of F_{total} obtained for proflavine bound to DNA.

If there are n repeating units with one base pair each of the type shown in Fig. 3(a) to make up one DNA molecule, and if the same molecule is allowed to bind dye until $r = 0{\cdot}5$, then there will still be n repeating units with one base pair each, as indicated

by Fig. 3(b) and (c). Hence the free energies are quoted as kcal. per repeating unit. However, the energy per mole of repeating unit, which is found by dividing F_{total} by 2 or 3 as required, has no significance in a direct comparison of free energy. It is the total free energy of the DNA molecule as compared with that of the two different models for the DNA–dye complex which is important; but it is convenient to consider only $1/n$ of the DNA molecule or the DNA–dye complex, i.e. one repeating unit. End effects have been neglected.

4. Results

(a) *Free energy calculations*

The values of $F_{\rho\mu}$ and $F_{\rho\alpha}$ for model I are invariant with respect to rotation and magnitude of the dye dipole moment and magnitude of the dye polarizability. $F_{\mu\mu}$ is directly proportional to the dipole moment of the intercalated molecule, and F_{L} and $F_{\mu\alpha}$ are directly proportional to the polarizability of the intercalated molecule.

Figure 4 shows the variation of $F_{\mu\mu}$, $F_{\mu\alpha}$ and $F_{\mu\mu} + F_{\mu\alpha}$ with orientation of the dipole moment vector of the intercalated molecule for interaction with AT and GC base pairs. For convenience in presentation, the dipole moment of the intercalated molecule is taken as 1·0 D and α_1 as 20 Å^3. The values presented in Table 1 were

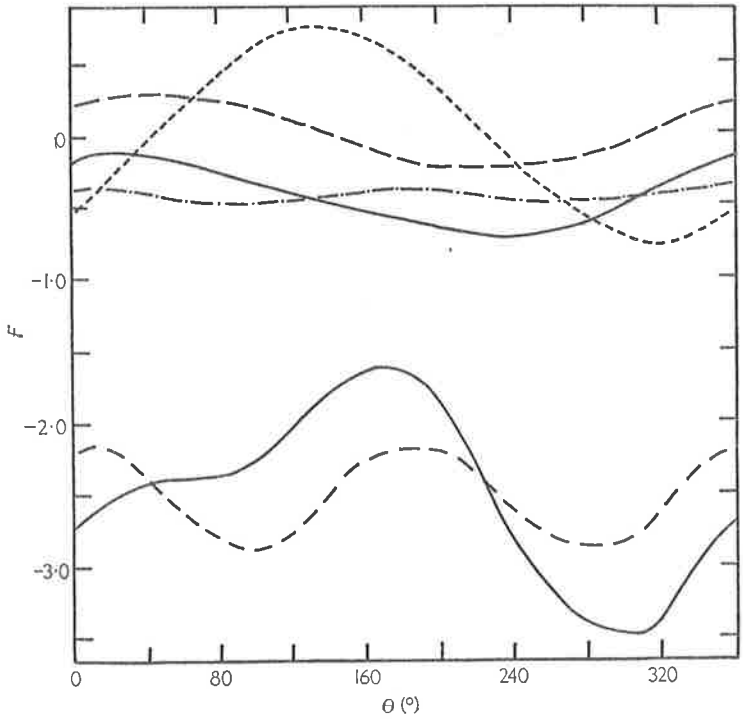

FIG. 4. F, the free energy of dipole–dipole and dipole-induced dipole interactions (in kcal. per base pair) for the intercalated model as a function of θ, the angle of orientation of the dipole moment of the intercalated molecule. The values obtained are for the intercalated molecule above *or* below the base pair indicated in parentheses.

Upper curves: $F_{\mu\mu}$ (AT), — — — —; $F_{\mu\alpha}$ (AT), —·—·—·; $F_{\mu\mu} + F_{\mu\alpha}$ (AT), ————; $F_{\mu\mu}$ (GC), – – – – –.

Lower curves: $F_{\mu\alpha}$ (GC), — — — —; $F_{\mu\mu} + F_{\mu\alpha}$ (GC),————.

TABLE 1

Calculated free energy values (in kcal. per repeating unit) for the intercalated model I ($\epsilon_{ij} = 1{\cdot}0$)

Unit	$F_{\mu\mu}$	$F_{\mu\alpha}$	F_{L}	$F_{\rho\mu}$	$F_{\rho\alpha}$	F_{total}
	(a) *Interaction of proflavine with nearest neighbour base pairs*					
G . . . C proflavine† G . . . C	5·4 (− 5·4)	− 5·6 (− 5·6)	− 13·8 (− 13·8)	− 11·8 (− 11·8)	− 16·6 (− 16·6)	− 46·3 (− 57·1)
A . . . T proflavine† A . . . T	− 1·8 (1·8)	− 2·0 (− 2·0)	− 13·8 (− 13·8)	− 26·6 (− 26·6)	− 16·6 (− 16·6)	− 60·6 (− 57·0)
C . . . G proflavine† C . . . G	4·5 (− 4·5)	− 5·2 (− 5·2)	− 13·8 (− 13·8)	− 11·8 (− 11·8)	− 16·6 (− 16·6)	− 46·8 (− 55·8)
T . . . A proflavine† T . . . A	− 1·8 (1·8)	− 2·0 (− 2·0)	− 13·8 (− 13·8)	− 26·6 (− 26·6)	− 16·6 (− 16·6)	− 60·6 (− 57·0)

The values in parentheses indicate values at $\theta = 355{\cdot}5°$.

† The proflavine molecule is considered to interact with all other molecules in the unit shown.

	(b) *Interaction of adjacent proflavine molecules*					
Proflavine† base pair Proflavine†	0·86 (− 0·86)	− 0·17 (− 0·17)	− 0·47 (− 0·47)	0·0 (0·0)	− 0·98 (− 0·98)	− 0·8 (− 2·5)

The values with and without brackets refer to angles of 171° and 351°, respectively, between dye dipole moment vectors.

† Only interactions between these two molecules are considered.

	(c) *Interaction of proflavine with base pair 10·08 Å above or below*					
Proflavine base pair dye G . . . C	0·01	− 0·01	− 0·03	− 0·65	− 0·17	− 0·9
Proflavine base pair dye A . . . T	− 0·07	0·0	− 0·03	− 1·01	− 0·17	− 1·3
Proflavine base pair dye C . . . G	0·06	− 0·01	− 0·03	− 0·65	− 0·17	− 0·8
Proflavine base pair dye T . . . A	0·0	0·0	− 0·03	− 1·01	− 0·17	− 1·2

The interactions are between proflavine and G and C, A and T, as indicated. No interactions between the bases of a given base pair are included as these are already accounted for in F_{total} in Table 1(a). The values are for $\theta = 166{\cdot}5°$ only.

Note that in Table 1 (a) and (c) rows one and three, and two and four are not identical, since the interaction depends on the relative orientation of the dipole moments of the bases of the base pairs and of the proflavine molecule.

obtained by combining the value of the dipole moment of the intercalated molecule with the values of $F_{\mu\mu}$ and $F_{\mu\alpha}$ obtained from Fig. 4 at the required angle. F_{L}, $F_{\rho\mu}$ and $F_{\rho\alpha}$ are invariant with θ.

The values of the free energies were found to be essentially the same for GC, etc. above or below the intercalated molecule. The values of the interaction free energies between the bases of AT and GC base pairs were taken as 0·2 and −3·9 kcal., as determined by De Voe & Tinoco (1962).

Table 1(a) indicates that the effect on F_{total} of a change in the dipole moment of the intercalated molecule is small, since only $F_{\mu\mu}$ and $F_{\mu\alpha}$ are affected. Values for the free energy of interaction of a dye molecule with a neighbouring intercalated dye molecule and an additional base pair are shown in Table 1(b) and (c). Since the interactions of a given proflavine molecule with the next intercalated molecule 6·72 Å above are included in the repeating unit, an additional −0·8 kcal. per repeating unit is added to the values for $\theta = 175{\cdot}5°$ in Table 1(a) to give the values of F_{total} for the intercalated model in Table 3. Also included in F_{total} is the free energy arising from the interaction of the lower base pair (the molecules represented by a solid line in Fig. 3(b)) with the dye molecule 10·08 Å above.

Liersch & Hartmann (1964) concluded that electrostatic forces were responsible for the stability of the DNA–proflavine complex, since the dissociation velocity of the complex during gel filtration on Sephadex is greatly increased by high ionic strength. The results in Table 1 show that although this is correct for model I, London forces also make a significant contribution to F_{total}. However, London forces are less important for model II (Table 2).

The calculations for the energies of interactions involved in the attachment of the dye molecule to the phosphate groups in model II show a high degree of dependence on the value of the dipole moment of the attached molecule, in direct contrast with the results for the intercalated model. The free energy arising from interactions

TABLE 2

Calculated free energy values (in kcal. per repeating unit) for external edgewise attachment of dye (model IIa)

Unit	$F_{\mu\mu}$	$F_{\mu\alpha}$	F_{L}	$F_{\rho\mu}$	$F_{\rho\alpha}$	F_{total}
⊖ Proflavine† ⊖ Proflavine†	0·06	− 0·02	− 0·10	− 3·13	− 0·48	− 0·05 ($\epsilon_{ij} = 70$)
⊖ † ⊖ Proflavine†				− 2·43	− 0·54	− 0·04 ($\epsilon_{ij} = 70$)
⊖ ⊖† Proflavine†				− 20·4	− 17·2	− 3·8 ($\epsilon_{ij} = 10$) − 1·1 ($\epsilon_{ij} = 35$)

⊖ Represents the negative phosphate group.

† Only interactions between these molecules are considered.

All values are for $\epsilon_{ij} = 1{\cdot}0$ unless stated otherwise.

between two dye molecules in model IIa is −0·05 kcal. per repeating unit; for model IIb these interactions are even smaller. The second two rows of Table 2 are, however, still applicable for model IIb.

The distance between the centre of the dye molecule and a base in model II, even if the dye molecule is tilted inwards towards a base, is between about 7·5 and 10·5 Å. The maximum free energy for the interactions between the charged dye molecule and the dipole moment and polarizability of the nearest base will be either about −0·6 or −1·0 kcal., depending on the orientation of the dye molecule and whether the base considered is A or T, or G or C, respectively. For this estimate, ϵ_{ij} was taken as 10, since although the ion distance is large, not all the volume between the bound dye and the base may be occupied by solvent molecules.

The free energy values for model IIa quoted in Table 2 are the same for all base sequences. The total free energy with the value of ϵ'_{ij} equal to 10 is −3·9 kcal. per repeating unit for model IIa and is only −0·05 kcal. per repeating unit less for model IIb, for which dye–dye interactions are not considered.

(b) *Thermal denaturation*

Typical T'_m curves obtained for DNA–proflavine and DNA–2-aminoacridine at values of r close to 0·13 are shown in Fig. 5 (the actual values of r were: DNA–2-aminoacridine, 0·1 M-NaCl, 0·130; 0·001 M-NaCl, 0·121. DNA–proflavine, 0·1 M-NaCl, 0·130; 0·001 M-NaCl, 0·137). Several features of these curves are important and are discussed below.

(i) There is an initial increase in optical density, as typified by the region AB, curve I in Fig. 5, greater than that associated with the heating of native DNA, up to between 65 and 80°C. This increase is greater for 0·1 M-NaCl solutions than for 0·001 M-NaCl solutions, for approximately the same value of r, and is larger for proflavine than for 2-aminoacridine.

(ii) The final optical density observed is usually very slightly lower than that calculated by the addition of optical densities for free dye and denatured DNA. This is not shown in Fig. 5.

The shapes of the curves of T'_m *versus* T_L/T_A (Fig. 6) indicate that either the binding sites become saturated at a particular value of T_L/T_A, or that further binding beyond a critical value does not affect T'_m. These curves are similar in shape to those obtained by Kleinwächter & Koudelka (1964) for acridine orange and DNA. The increase in T'_m is much larger for a given T_L/T_A (Fig. 6) or for a given r (Fig. 7) for 0·001 M-NaCl than for 0·1 M-NaCl.

The value of T'_m increases rapidly with r over the range studied for 0·1 M-NaCl, but for 0·001 M-NaCl the curve flattens out at about $r = 0·2$ (Fig. 7), beyond which value Peacocke & Skerrett (1956) found a decrease in binding strength. This implies that some correlation exists between T'_m and strength of binding.

It is unfortunate that the curve in Fig. 7 cannot be extended past a value of r of about 0·15 for 0·1 M-NaCl. Higher values of r cannot be obtained by simple addition of dye and DNA solutions of suitable optical density range, and are obtained only by equilibrium dialysis. However, according to Peacocke & Skerrett (1956), one of the criteria for obtaining accurate values of r from equilibrium dialysis studies is a high value for the DNA concentration. If high concentrations of DNA are used, dilution of the dialysed solution is necessary for the determination of T'_m in a suitable range of optical density. This process of dilution leads to a reduction of r.

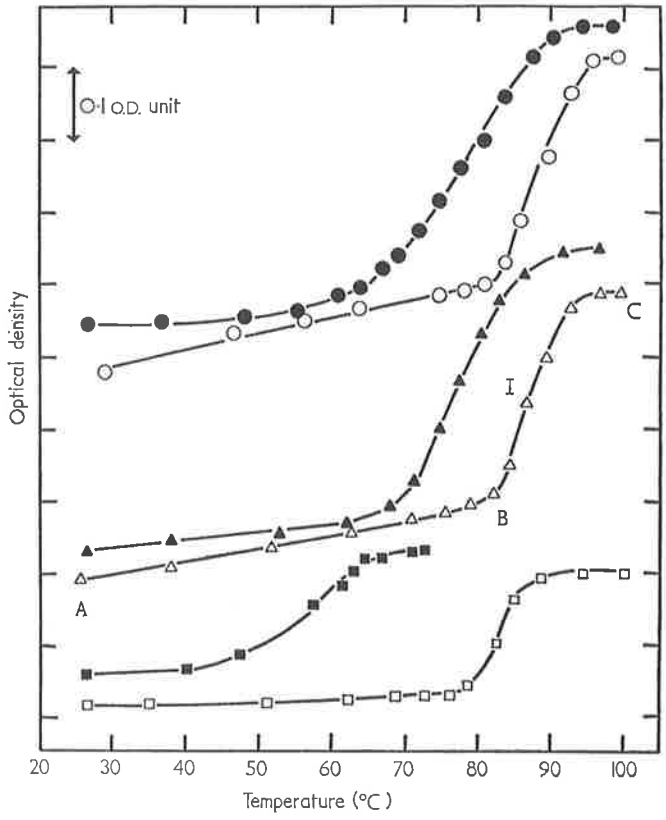

FIG. 5. Thermal denaturation curves for DNA and DNA–dye solutions. For the four DNA–dye solutions shown, the values of r are close to 0·13 (see text). All DNA solutions are $7{\cdot}2\times10^{-5}$ M with respect to DNA phosphorus. In the text, curve I is referred to as a typical T'_m curve, and mention is made of regions AB and BC.

—□—□—, DNA in 0·1 M-NaCl;
—△—△—, DNA–2-aminoacridine in 0·1 M-NaCl;
—○—○—, DNA–proflavine in 0·1 M-NaCl;
—■—■—, DNA in 0·001 M-NaCl;
—▲—▲—, DNA–2-aminoacridine in 0·001 M-NaCl;
—●—●—, DNA–proflavine in 0·001 M-NaCl.

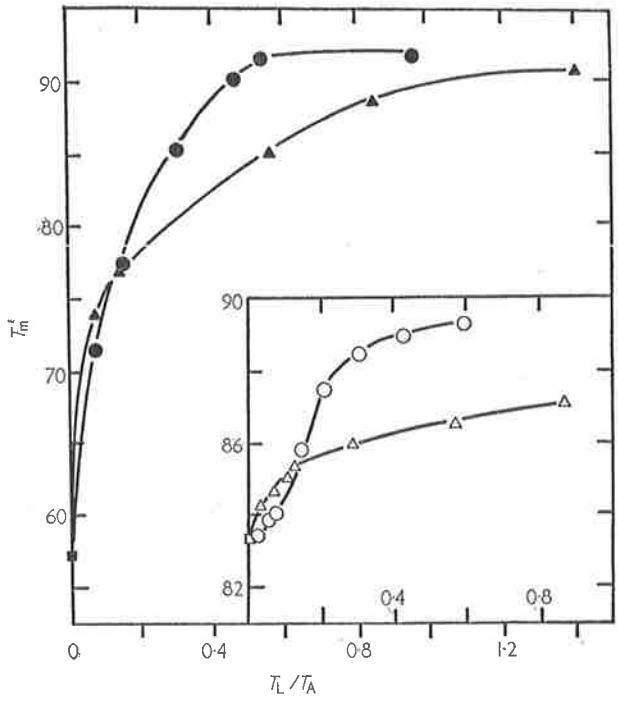

FIG. 6. Variation in T'_m with T_L/T_A, the ratio of total dye to total DNA phosphorus concentrations for DNA–dye solutions in 0·001 M-NaCl. The inset refers to solutions in 0·1 M-NaCl. For the key to the symbols used, see the legend to Fig. 5.

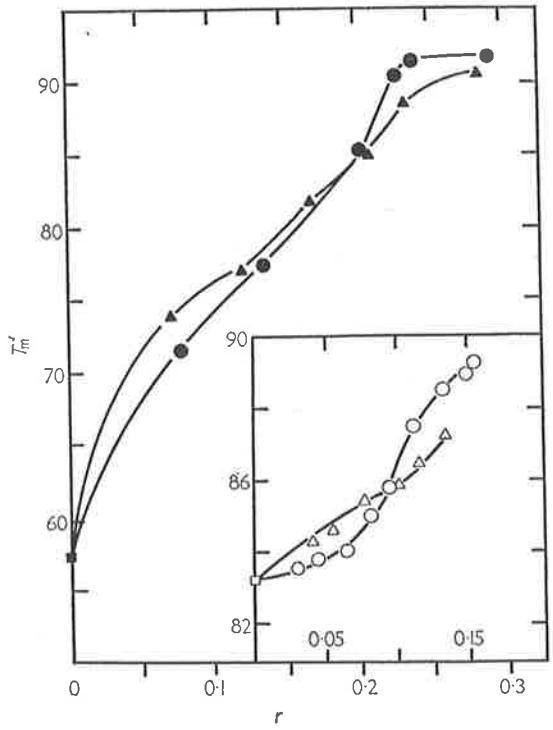

FIG. 7. Variation in T'_m with r, the amount of dye bound per mole of nucleic acid phosphorus for 0·001 M-NaCl solutions. The inset refers to solutions in 0·1 M-NaCl. For the key to the symbols used, see the legend to Fig. 5.

5. Discussion

The initial increase in optical density as the temperature is increased in the T'_m curves (region AB in Fig. 5) may be explained in terms of a decrease in dye binding with an increase in temperature. This has been confirmed for proflavine (Chambron, Daune & Sadron, 1964) and for 2-aminoacridine (Gersch & Jordan, unpublished results) by use of equilibrium dialysis at different temperatures. Since the binding of dye to DNA is accompanied by a hypochromic effect, the release of bound dye due to an increase in temperature results in an increase in optical density. That the initial optical density increase does not account for the full hypochromic effect on the dye implies that only a small amount of the dye bound is released before the helical structure of the DNA is disrupted. This can be interpreted on the basis of either of the two models, although more easily for the intercalated model I, the increase in temperature causing a removal of dye from the weaker binding sites. In a typical T'_m determination for 0·1 M-NaCl, the expected total increase in optical density was 0·316; the observed increase was 0·305, of which 0·183 could be attributed to DNA. By 75°C (i.e. over the region AB in Fig. 5) an increase in optical density of only 0·060 had occurred over that at 25°C, leaving about one-half of the hypochromic effect of the dye to be accounted for in the temperature range over which the helical DNA structure is disrupted (i.e. the region BC in Fig. 5).

Figure 5 indicates that, for about the same values of r, the initial increase in optical density is larger for 0·1 M-NaCl solutions than for 0·001 M-NaCl solutions. This can only be interpreted on the basis of a greater binding of dye at lower ionic strengths, as found by Peacocke & Skerrett (1956). At higher ionic strengths, there is either more competition with sodium ions for the binding sites, or it is more difficult for the dye ions to approach the binding sites due to shielding effects of sodium ions. As the temperature is increased and Brownian motion increases, the probability of a bound dye ion being displaced by a sodium ion is greater at higher ionic strengths whichever model is considered. This also explains the greater increase in T'_m observed, for a given value of r, in 0·001 M-NaCl compared with 0·1 M-NaCl (Fig. 7).

Proflavine and 2-aminoacridine have peaks in the ultraviolet, at 262 mμ and 274 mμ, respectively. By following the helix–coil transition of the DNA–dye complex at 259 mμ, the contribution of the dye to the total optical density is thus greater for proflavine than for 2-aminoacridine. Hence the initial increase in optical density measured at 259 mμ is greater for the former than for the latter, and does not necessarily reflect differences in binding strength.

The final optical density observed at about 100°C is often very slightly lower than that expected from the addition of the optical densities of free dye and denatured DNA. This implies that there may be slight interaction between dye and denatured DNA even at high temperatures.

The value of 40°C for T_m predicted by Chambron *et al.* (1964) for DNA–proflavine does not agree with the values of T'_m found in this study (Figs 6 and 7), since T'_m is greater than that of native DNA for both the DNA–dye complexes considered.

An increase in T'_m indicates that the stability of the native DNA–dye system has increased relative to that of the denatured DNA–dye system. This may arise through a decrease in stability of the denatured DNA–dye complex. However, such a decrease is unlikely to occur, since denatured DNA has been shown to bind dye (Bradley & Wolf, 1959). Thus, since the denatured DNA–dye system is expected to have a lower

free energy than denatured DNA, the only way in which the stability of the native DNA–dye system can be greater than that of the denatured DNA–dye system is for a large decrease to occur in the free energy of the native DNA–dye system over that of native DNA. This decrease must be greater than the difference in free energy between the denatured DNA–dye system and denatured DNA.

Table 3 indicates that the free energy for both models is less than that of DNA, although that for model I is lower than that for model II. The model adopted must explain the fact that many of the dye molecules are released from the binding sites in the temperature range over which the DNA helical structure is disrupted (Fig. 5). It should be noted that dye–dye interactions between dye molecules bound to the outside of the helix cannot be used alone to explain the increase in T'_m. Stone & Bradley (1961) have shown that there is only a very small tendency for acridine orange molecules to stack on native DNA, since the stacking coefficient is only 1·25. Furthermore, the calculations presented in Table 2 indicate that the dye–dye interactions for model II are small, the main interactions arising from charge–dipole and charge–polarizability forces due to the bound phosphate group. It is these forces, giving rise to the negative free energy for the native DNA–dye complex, which could give rise to an increased stability of model II.

The increase in T'_m is greater for the DNA–proflavine complex than for the DNA–2-aminoacridine complex at a given value of r (Fig. 7), indicating that the former complex is more stable than the latter relative to the denatured DNA–dye complex. This may arise from a difference in the dipole moment (in magnitude and direction) of the charged 2-aminoacridine molecule compared with that of the charged proflavine molecule.

The decrease in the free energy, ΔF, for the reaction

$$\text{DNA repeating unit} + \text{dye} \rightarrow \text{DNA repeating unit-dye}$$

for different base sequences for both models is given in Table 3. The result indicates that, for model I, the order of increased stabilization is AT:TA > AT:AT > TA:AT > TA:GC > AT:GC > AT:CG > GC:CG > TA:CG > GC:GC > CG:GC. Thus the base sequence with the highest free energy in DNA alone is stabilized the most in the DNA–proflavine complex. However, for model IIa and $\epsilon'_{ij} = 10$, $\Delta F = -3{\cdot}9$ kcal. per repeating unit, and does not depend on base sequence. If the bound dye molecule is tilted inwards towards a base, ΔF becomes about $-4{\cdot}5$ or $-4{\cdot}9$ kcal. per repeating unit, depending on whether the dye molecule is associated with an A or T base or a G or C base, respectively. The free energy for the modified version of model IIa therefore implies that GC sites bind dye slightly more strongly than AT sites. The experimental evidence obtained by Tubbs *et al.* (1964) from measurements of fluorescence-quenching of DNA–acriflavine solutions suggested that the relative affinity of acriflavine for possible binding sites in DNA was AT:AT > AT:GC > GC:GC, in agreement with the sequence predicted theoretically above for model I. Hence only model I can be used to explain this relative affinity of binding sites. Also, only model I will explain the dependence on base content of the increase in T_m of the DNA–acridine orange complex over that of the DNA alone for different samples of DNA (Kleinwächter & Koudelka, 1964), the increase in T_m increasing with increase of AT content.

The shape of the T'_m *versus* T_L/T_A curve (Fig. 6) and the existence of two types of binding observed by Peacocke & Skerrett (1956) can be explained only on the basis

TABLE 3

Comparison of calculated free energy values (in kcal. per repeating unit) for native DNA, model I and model IIa

Repeating unit	De Voe & Tinoco (1962) for native DNA	Proflavine intercalated, model I		External attachment of proflavine, model IIa			
	$\epsilon_{ij} = 1{\cdot}0$	$\epsilon_{ij} = 1{\cdot}0$		$\epsilon'_{ij} = 10$		$\epsilon'_{ij} = 35$	
	F_{total}	F_{total}	ΔF	F_{total}	ΔF	F_{total}	ΔF
CG GC	− 35·7	− 48·3	− 12·6	− 39·6	− 3·9	− 36·9	− 1·2
GC GC	− 19·9	− 48·0	− 28·1	− 23·8	− 3·9	− 21·1	− 1·2
TA CG	− 20·5	− 55·3	− 34·8	− 24·4	− 3·9	− 21·7	− 1·2
AT CG	− 13·7	− 55·3	− 41·6	− 17·6	− 3·9	− 14·9	− 1·2
AT GC	− 12·9	− 55·2	− 42·3	− 16·8	− 3·9	− 14·1	− 1·2
TA GC	− 12·5	− 55·2	− 42·7	− 16·4	− 3·9	− 13·7	− 1·2
GC CG	− 7·5	− 48·2	− 40·7	− 11·4	− 3·9	− 8·7	− 1·2
TA AT	− 10·6	− 62·7	− 52·1	− 14·5	− 3·9	− 11·8	− 1·2
AT AT	− 10·2	− 62·7	− 52·5	− 14·1	− 3·9	− 11·4	− 1·2
AT TA	− 3·4	− 62·6	− 59·2	− 7·3	− 3·9	− 4·6	− 1·2

The repeating unit shown is for DNA. Those for the DNA–proflavine complexes are those indicated in Fig. 3 with the appropriate base pairs. See text for explanation of the values chosen for ϵ_{ij} and for ϵ'_{ij}.

of the intercalated model I. For this model, strong binding would be predicted, on the basis of the results in Table 3, up to $r = 0{\cdot}5$, whereas experimentally it is found that weaker binding predominates after about $r = 0{\cdot}22$ for herring sperm DNA (GC content 43%) (Peacocke & Skerrett, 1956). When the approximations, discussed above, on which the calculations for the intercalated model have been made, are

taken into account, the total free energy for each repeating unit will be increased (i.e. become less negative). For some repeating units this increase may give a value similar to or greater than that found for external edgewise binding for the same repeating unit. The possibility then exists for a change-over from intercalation to external edgewise binding at some value of $r < 0{\cdot}5$. The existence of two types of binding cannot be explained on the basis of model II, since the value of ΔF is the same for all binding sites (Table 3). The marked difference in binding sites found by Peacocke & Skerrett (1956) would not be predicted on the basis of the modified version of model II in which the bound dye molecules are tilted inwards towards the bases of DNA.

The above calculations apply only to $r = 0{\cdot}5$, where all the sites suitable for intercalation have been used. Thus for $r > 0{\cdot}5$, binding to the outside of the helix must also occur. Because of the left-handed helix formed for the intercalated model (I), two dye molecules attached to the outside of the helix will be at an angle of 9° with respect to each other. The centres of the two molecules are found to be about 7 Å apart, the plane of one dye being 6·72 Å above the plane of the other. However, for native DNA with external attachment of the dye to adjacent phosphate groups on the one helix, owing to the larger angle of 36° between the two dye molecules, the distance between the centres of these molecules is 9·4 Å. The distance between the centres of two externally bound dye molecules is thus greater for native DNA than for DNA with the maximum number of intercalated dye molecules. Thus the interaction forces will be smaller for dye bound to native DNA than for dye bound externally to DNA extended by the maximum amount of intercalated dye. Furthermore, because of the greater distance in native DNA, the amount of associated water will be increased and the value of ϵ_{1j} will be larger; this will also have the effect of decreasing the interactions. However, these effects will be small, as it has already been shown (Table 2) that the contribution of dye–dye interactions to the stability of model IIa is very small.

The orientation of the dye molecule in the intercalated model (I) at 4·5° to both the adjacent base pairs (i.e. that above and that below the dye molecule, see Plate I) favours the exclusion of water molecules and hence gives the maximum interaction. Other orientations would allow water molecules to penetrate the helix; the effective dielectric constant would then be increased and the energies of interaction would become less negative.

From dye-binding studies Peacocke & Skerrett (1956) obtained a value of 8 kcal. per mole of bound dye for the standard free energy of association of herring sperm DNA and proflavine, Chambron *et al.* (1964) obtained a value of 7·4 kcal. per mole for calf thymus DNA and proflavine and our results confirm these values for calf thymus DNA and proflavine. Oster (1951) deduced a value of 9·5 kcal. per mole for the association of acriflavine and nucleic acids. From Table 3, the decrease in calculated free energy varies between $-12{\cdot}6$ and $-59{\cdot}2$ kcal. per repeating unit, depending on the base sequence for the intercalated model, and is constant at $-3{\cdot}9$ kcal. per repeating unit for external edgewise attachment of the dye molecules with $\epsilon'_{ij} = 10$. In view of the assumptions made, the agreement between the calculated and the observed values, the latter being average values over all binding sites for the particular DNA studied, is regarded as satisfactory. It is to be emphasized that any refinements to the calculations for the intercalated model are likely to make the values of the interaction energies given less negative.

A value of $-0{\cdot}065$ kcal. per mole of dye for the attraction between two bound dye molecules was found from the tendency of acridine orange molecules to stack on native DNA (Stone & Bradley, 1961) and represents an average value for this interaction. Tables 1(b) and 2 yield values of either $-0{\cdot}8$ or $-2{\cdot}5$ kcal. per mole of dye for the intercalated model (I) for the interaction between two dye molecules, depending on the relative orientations of the two molecules, and $-0{\cdot}05$ kcal. per mole for model IIa, respectively. For model IIa the agreement between the calculated and experimental values is good. However, for model I, extreme values of binding must be taken in order to compare the calculated and experimental values.

The above values calculated for the interaction between adjacent dye molecules in model I will become about $-0{\cdot}16$ or $-0{\cdot}5$ kcal. per mole of dye respectively if an average effective dielectric constant of 5 is chosen. If we consider, for example, intercalation of the dye up to $r = 0{\cdot}22$, with edgewise binding occurring at higher values of r, then for $r \leqslant 0{\cdot}22$ the free energy of interaction between two dye molecules will be $-0{\cdot}16$, or $-0{\cdot}5$ kcal. per mole of dye; but for $r = 1{\cdot}0$ it will be $-0{\cdot}072$, or $-0{\cdot}140$ kcal. per mole of dye, depending on the relative orientation of the dye molecules. Since the value of $-0{\cdot}065$ kcal. per mole of dye obtained experimentally is an average value for all methods of binding and all binding sites, the calculations indicate that the intercalated model is compatible with the experimental results. Although the intercalated model is being considered here, the free energy of interaction between two adjacent dye molecules attached externally has been taken as $-0{\cdot}05$ kcal. per mole of dye, i.e. the value for model II. However, this is not a significant approximation.

For the above experimental value for the free energy of interaction between two dye molecules bound to DNA, the value of the stacking coefficient K was taken as 1·25 (Stone & Bradley, 1961), which is an average value obtained using several samples of DNA with varying GC contents. For calf thymus DNA (GC content 42%) an average value of 1·14 was obtained for K, while for bacteriophage T4 DNA (GC content 34%) a value of 1·33 was given. The values of the free energy of interaction between two dye molecules corresponding to these values of K are $-0{\cdot}039$ and $-0{\cdot}085$ kcal. per mole of dye respectively. The significant feature of these results for the interaction between two adjacent dye molecules is that a decrease in free energy occurs with a decrease in GC content. In view of the interpretation suggested above in terms of model I for the strong mode of binding which occurs up to $r = 0{\cdot}22$ for calf thymus DNA observed by Peacocke & Skerrett (1956), it is expected that, for a given ionic strength and pH, a higher value of r will be reached before the very weak binding predominates for DNA of lower GC content. Furthermore, the average free energy of association of dye with DNA will decrease with decreasing GC content; and also, since more intercalation is possible because of the higher AT content, the experimental value for the free energy of interaction between adjacent dye molecules will include a greater contribution from interactions between two intercalated dye molecules. Thus the free energy for dye–dye interaction is expected to decrease with decreasing GC content. The above results for this free energy, calculated from values of K quoted by Stone & Bradley (1961) for samples of DNA with different GC contents support this conclusion.

We wish to thank Dr H. De Voe for data from which he and Dr I. Tinoco had calculated σ moments, Dr G. Chandler for the gift of 2-aminoacridine and the Commonwealth Scientific and Industrial Research Organisation for the award of a Senior Post-Graduate Studentship to one of us (N. F. G.)

REFERENCES

Acheson, R. M. (1956). *The Acridines*. New York: Interscience.
Bradley, D. F. & Wolf, M. K. (1959). *Proc. Nat. Acad. Sci., Wash.* **45**, 944.
Chambron, J., Daune, M. & Sadron, C. (1964). *C.R. Acad. Sci. Paris*, **258**, 4867.
Daudel, R., Lefebvre, R. & Moser, C. (1959). *Quantum Chemistry*. New York: Interscience.
De Voe, H. & Tinoco, I. (1962). *J. Mol. Biol.* **4**, 500.
Fajans, K. (1959). In *Technique of Organic Chemistry*, ed. by A. Weissberger, vol. 1, part 2, p. 1169. New York: Interscience.
Freifelder, D., Davison, P. F. & Geiduschek, E. P. (1961). *Biophys. J.* **1**, 389.
Hasted, J. B., Ritson, D. M. & Collie, C. H. (1948). *J. Chem. Phys.* **16**, 1.
Haugen, G. R. & Melhuish, W. H. (1964). *Trans. Faraday Soc.* **60**, 386.
Kay, E. R. M., Simmons, N. S. & Dounce, A. L. (1952). *J. Amer. Chem. Soc.* **74**, 1724.
Kleinwächter, V. & Koudelka, J. (1964). *Biochim. biophys. Acta*, **91**, 539.
Langridge, R., Marvin, D. A., Seeds, W. E., Wilson, H. R., Hooper, C. W. & Wilkins, M. H. F. (1960). *J. Mol. Biol.* **2**, 38.
Lerman, L. S. (1961). *J. Mol. Biol.* **3**, 18.
Lerman, L. S. (1963). *Proc. Nat. Acad. Sci., Wash.* **49**, 94.
Liersch, M. & Hartmann, G. (1964). *Biochem. Z.* **340**, 390.
Mason, S. F. & McCaffery, A. J. (1964). *Nature*, **204**, 468.
Millich, F. & Oster, G. (1959). *J. Amer. Chem. Soc.* **81**, 1357.
Orgel, L. E., Cottrell, T. L., Dick, W. & Sutton, L. (1951). *Trans. Faraday Soc.* **47**, 113.
Oster, G. (1951). *Trans. Faraday Soc.* **47**, 660.
Peacocke, A. R. & Skerrett, J. N. H. (1956). *Trans. Faraday Soc.* **52**, 261.
Pullman, B. (1964). In *Electronic Aspects of Biochemistry*, ed. by B. Pullman, p. 559. New York: Academic Press.
Pullman, B. & Pullman, A. (1963). *Quantum Biochemistry*, New York: Interscience.
Rice, S. A. & Nagasawa, M. (1961). *Polyelectrolyte Solutions*. New York: Academic Press.
Stone, A. L. & Bradley, D. F. (1961). *J. Amer. Chem. Soc.* **83**, 3627.
Tubbs, R. K., Ditmars, W. E. & Van Winkle, Q. (1964). *J. Mol. Biol.* **9**, 545.